MYOCYTE DEATH AND REGENERATION IN CARDIAC AND SKELETAL MUSCLE

GEORGINA MAY ELLISON

A thesis submitted in fulfilment of the requirements of Liverpool John Moores University for the degree of Doctor of Philosophy

JULY 2004

Dedicated to my Parents

ACKNOWLEDGMENTS

I hereby acknowledge the support of my supervisory team; Professor David F. Goldspink (Liverpool John Moores University), Dr Lip-Bun Tan (University of Leeds) and Professor Tim Cable (Liverpool John Moores University). I am particularly grateful to my Director of Studies, Professor Goldspink, for his experience and guidance throughout the 3 years.

I also acknowledge the time, help, support and guidance of Professor Bernardo Nadal-Ginard, Professor Piero Anversa and Dr. Daniele Torella, all of New York Medical College. Thank you for allowing me the valuable opportunity to visit and work in your laboratory.

This work was funded by the British Heart Foundation (PhD studentship FS/2001028/12895).

ABSTRACT

Many patients suffering from Chronic Heart Failure (CHF), exhibit sustained high levels of circulating catecholamines, through over-activation of the sympathetic system (Anker et al., 1997a). Many of these same CHF patients also experience a marked loss of their muscle bulk, which reduces their ability to move well and exercise, thereby decreasing their quality of life. As of yet there is no explanation for this phenomenon. This thesis tested the hypothesis that exposure to excess catecholamines causes significant myocyte death in both the heart and skeletal muscles. Whether this could lead to wasting of the skeletal muscles and how precisely the heart adapts to catecholamine-induced damage was determined.

Male Wistar rats were injected with 20 mmol of isoprenaline, adrenaline, or noradrenaline kg^{-1} and killed at various time points over 28 days. Apoptotic and necrotic myocyte death and myocyte regeneration were detected immunohistochemically and morphologically, and quantified using image analysis. After characterising the acute myotoxic effects of a single injection of each catecholamine, the myotoxic and hypertrophic effects of chronic administrations of isoprenaline or adrenaline (20 mmol $kg^{-1}d^{-1}$) were also investigated.

A single injection of each catecholamine induced significant ($P<0.05$) myocyte necrosis and apoptosis in both the heart and slow-twitch soleus muscle, but not the fast-twitch muscles. Through its satellite cell system, the soleus muscle completely restored its total number of fibres by 28 days. The heart compensated for catecholamine-induced myocyte death and loss through secondary myocyte hypertrophy and hyperplasia. The latter was produced by the activation and differentiation of cardiac stem-progenitor cells. The continuous infusion of the same dose of isoprenaline over 28 days caused significant myocyte death, hypertrophy and fibrosis in the heart. Both fast and slow skeletal muscles in these same rats significantly increased in weight ($P<0.05$) and this was explained by increased fibre cross-sectional areas. Chronic catecholamine exposure still caused significant fibre death: their replacement met by a continual need for cycles of regeneration, in the soleus muscle. The current work describes the injurious effects of excess catecholamines on the heart and soleus muscle. Both striated muscles repair the loss of myocytes, in order to restore functional capacity. However, when the high levels of catecholamines are sustained, muscle wasting may result due to a compromised regenerative capacity.

CONTENTS

LIST OF TABLES

LIST OF FIGURES

LIST OF FIGURES Continued...

LIST OF FIGURES Continued...

ABBREVIATIONS

Ab, Antibody

AC, adenylyl cyclase

Ad, adrenaline

AIF, apoptosis-inducing factor

AMP, 2-amino-2-methyl-1-propanol

ANOVA, analysis of variance

APAF-1, apoptotic protease-activating factor 1

α-AR, alpha-adrenergic receptor

β-AR, beta-adrenergic receptor

ATP, adenosine tri-phosphate

AV node, atrioventricular node

Bcl2, B Cell leukaemia 2

BM, bone-marrow

BMDC, bone-marrow derived cells

BrdU, Bromodeooxyuridine

BW, body weight

Ca^{2+}, calcium ions

$CaCl_2$, calcium chloride

cAMP, cyclic adenosine monophosphate

$CdCl_2$, cadmium chloride

CHF, chronic heart failure

CO, cardiac performance

$CoCl_2$, cobalt chloride

CSA, cross-sectional area

DAB, 3-3'-diaminobenzidine

DAPI, 4, 6-diamidino-2-phenylindole

DNA, deoxyribonucleic acid

dp/dt_{max}, systolic contraction

dp/dt_{min}, diastolic relaxation

dUTP, biotin-16-deoxyuridine triphosphate

EDL, Extensor digitorum longus

EGFP, enhanced green fluorescent protein

ERK, extracellular related kinase

FADD, Fas-associated death domain

FGF, Fibroblast growth factor

FHL1, four-and-a-half LIM domain protein-1

FITC, Fluorescein isothiocyanate

GFP, green fluorescent protein

G_s, stimulatory G protein

G_i, inhibitory G protein

H&E, haematoxylin and eosin

HF, heart failure

HGF/SF, Hepatocyte growth factor/scatter factor

HRP, Horse radish peroxidase

IGF 1 and II, Insulin-like growth factors I and II

IgG/M, Immunoglobulin G/M

i.p., Intraperitoneal

IP3R, inositol 1,4,5-trisphosphate receptors

ISO, isoprenaline

kDa, Kilo daltons

LV, left ventricular

LVEDP, LV-end diastolic pressure

MAPK, mitogen activated protein kinase

MDR1, multi drug resistance 1

mdx, Genetic deletion of dystrophin gene

MEF2D, myogenic enhancer factor 2D

MGF, Mechano-growth factor

MHC, myosin heavy chain

mmol, Millimolar

mg, milligram

µm, micrometer

µg, microgram

mRNA, messenger ribonucleic acid

NAd, noradrenaline

NHE1, Na^+-H^+ exchanger 1

NH_4S, ammonium sulphide

nitro-BT, nitroblue tetrazolium

PBS, Phosphate buffered saline

PKA, Protein Kinase A

PLB, phospholamban

RyR, ryanodine receptor

ROS, reactive oxygen species

s.c., Subcutaneous

Sca-1, stem cell antigen 1

SD, Standard deviation

SEM, Standard error of the mean

SERCA, SR Ca^{2+} reuptake pump

SP, side population

SR, sarcoplasmic reticulum

SSC, salted sodium citrate

TGF-β, transforming growth factor beta

TRITC, Rhodamine isothiocyanate

TUNEL, Terminal deoxynucleotidyl transferase mediated dUTP nick end labelling

UCP2, uncoupling protein 2

PUBLICATIONS

Ellison, G. M., Torella, D., Goldspink, D. F., Rota, M., Whang, B., Kajstura, J., Anversa, P., Nadal-Ginard, B. Cardiac Primitive Cell Activation and Myocyte Regeneration Have a Key Role in the Ventricular Remodeling of the Damaged Myocardium. (Abstract) Circulation Supplement. In press, October 2004.

Ellison, G. Tan, L-B and Goldspink, D.F. (2003) Injury and repair of skeletal muscle exposed to excess catecholamines. *Journal of Muscle Research and Cell Motility*, **24**, 367.

Ellison, G., Tan, L. B., Cable, N. T. and Goldspink, D. F. (2003) Skeletal muscle regeneration following catecholamine-induced injury. *Journal of Physiology*, **548.P**, 69P.

Ellison, G., Cox, H., Goldspink, D. F., Burniston, J., Clark, W. and Tan, L. B. (2002) The synthetic catecholamine, isoprenaline, induces apoptosis and necrosis in the soleus muscle of the rat. *Journal of Physiology*, **543.P**, 100P.

Goldspink, D. F., Burniston, J. G., Ellison, G. M., Clark, W. A. and Tan, L-B. (2004). Catecholamine-induced apoptosis and necrosis in cardiac and skeletal myocytes of the rat *in vivo*: the same or separate death pathways. *Experimental Physiology*, **89**, 407-416.

Torella, D., Leosco, D., Curcio, A., Ellison, G. M., LiVolti, G., Torella, M., Russo, V. G., Rengo, F., Indolfi, C. and Chiariello, M. (2004) Aging exacerbates negative remodeling and impairs endothelial regeneration after balloon injury. *American Journal of Physiology*. In Press.

1.0 INTRODUCTION

1.1 Heart Failure and Adrenergic Activity

Heart failure (HF) is a major public health problem in western society. A staggering 2.7 million people are estimated to be living with coronary heart disease in the UK – a number that is rising year on year. This year almost one in eight people - or 12% - have been diagnosed with a disease of the heart or circulatory system. In 1989 this was just 7%. Despite 30 years in decline, the UK death rate from heart failure is still one of the highest in Western Europe – only Finland and Ireland have slightly higher rates. A working man is more than twice as likely to die from heart disease in the UK than in Italy. The UK death rate is also higher than most other developed countries, including the USA, Australia and Japan (British Heart Foundation Statistics, 2004).

Heart failure is a complex clinical syndrome that can result from any structural or functional cardiac disorder that impairs the ability of the ventricle to fill with, or eject blood. Coronary artery disease is the underlying cause of HF in approximately two-thirds of patients with left ventricular systolic dysfunction (Hunt et al., 2001). The remainder have non-ischemic causes of systolic dysfunction and may have an identifiable cause e.g. hypertension, valvular disease, myocardial toxins, or myocarditis or may have no discernible cause, e.g. idiopathic dilated cardiomyopathy (Hunt et al., 2001).

Left ventricular (LV) dysfunction begins with some injury to the myocardium and is usually a progressive process, even in the absence of a new identifiable insult to the myocardium. The principal manifestation of such progression is a process known as remodelling, which occurs in association with homeostatic attempts to decrease wall stress through increases in wall thickness. This ultimately results in a change in the geometry of the left ventricle such that the chamber dilates, hypertrophies, and becomes more spherical. The process of cardiac remodelling generally precedes the development of symptoms, occasionally by months or even years. The process of

remodelling continues after the appearance of symptoms and may contribute importantly to worsening of symptoms despite treatment.

It has been established that many patients suffering from Chronic Heart Failure (CHF) exhibit sustained high levels of circulating catecholamines through over activation of the sympathetic system (Anker et al., 1997a). Subsequently, this plays an important role in the progression of heart failure, with the severity of the disease increasing in proportion with the level of catecholamines (Francis et al., 1990; Packer, 1992), or vice versa.

Regulation by the sympathetic nervous system constitutes an important modulator of cardiac function. More specifically, the catecholamines, adrenaline and noradrenaline, perform hormonal and transmitter functions to regulate and control cardiac performance and metabolism, and re-direct systemic blood flow, substrate mobilisation and utilisation. All regions of the heart are innervated by sympathetic nerves to varying degrees. The density of β-adrenoceptors (AR) in a single myocardial cell is much higher than that of α_1-receptors, and the effects of catecholamines during normal functioning of the heart are mediated mainly by β-AR stimulation (Hiraoka, 2002).

The β_1-AR constitutes approximately 80% of the cardiac β-AR complement (Freedman and Lefkowitz, 2004). Like the β_2-AR (with 54% overall homology), the β_1-AR is a seven-membrane–spanning receptor, with three extracellular polypeptide sequences ("loops") connecting the transmembrane helices. With their intracellular domains, the β-ARs couple to the stimulatory heterotrimeric GTP-binding protein (Gs). Activation of the β_1-AR requires a specific receptor conformation; one that is stabilized by the agonist and the binding of certain immunoglobulin Gs (IgGs) to the second extracellular loop (Jahns et al., 2004). The seven-membrane-spanning β_1-AR is stimulated by the physiological agonists, catecholamines. The receptor site is highly stereo-specific, the best fit among catecholamines being isoprenaline (ISO), a synthetic catecholamine, rather than adrenaline (Ad) and noradrenaline (NAd).

More specifically, in the case of β_1 receptors, the order of agonist activity is ISO > Ad = NAd, whereas for β_2 receptors the order is ISO > Ad > NAd (Opie, 2001).

The stimulated β_1-AR then activates the heterotrimeric G_s, which dissociates into its G_s and G_i substituents. The G_s activates both adenyl cyclase (AC), which catalyses cyclic adenosine monophosphate (cAMP) formation, and the L-type calcium channel, which then permits calcium ions (Ca^{2+}) to enter the cardiomyocyte through the sarcolemma of the T tubule. These Ca^{2+} ions release more Ca^{2+} from the sarcoplasmic reticulum (SR) to increase cytosolic Ca^{2+} and to activate troponin C. On a slower time scale, this Ca^{2+} can also promote cardiomyocyte apoptosis by activating Ca^{2+}/calmodulin kinase II (Katz, 2001). The cAMP produced by AC activates Protein Kinase A (PKA), which subsequently phosphorylates numerous substrates important to sarcoplasmic Ca^{2+} regulation: the L-type Ca^{2+} channel, the ryanodine receptor (RyR) and phospholamban (PLB). Taken as a whole, there is greater and more rapid rise of intracellular free Ca^{2+} concentration, increased calcium-troponin C interaction with de-inhibition of tropomyosin effect of actin-myosin interaction, and increased rate and number of cross bridges interacting with increased myosin ATPase activity (Opie, 2001). Activation of G_s can also increase L-type Ca^{2+} channel currents directly. The increase in cytosolic Ca^{2+} concentration during a contraction is immediately followed by Ca^{2+} removal, resulting in de-activation of the contractile machinery and muscle relaxation. Cytosolic Ca^{2+} is pumped back into the SR by SR Ca^{2+}-ATPase (SERCA2). These sequences of events are illustrated in Figure 1.1. The net effect of this activity in the short term is to augment sarcoplasmic Ca^{2+} and contractility, but in the long term this activity engenders cardiomyocyte toxicity (Freedman and Lefkowitz, 2004).

Overall, the major effects of catecholamines on cardiac function mainly exerted through the β_1 receptor sub-type (Cui et al., 1996) are an increase in heart rate (chronotrophic effect) and force of contraction (inotropic), caused by enhanced myosin ATPase activity and increased activation of troponin C. There is also an increased rate of relaxation and acceleration of impulse conduction (dromotrophic

effect) through the AV node. The increased rate of relaxation is mediated by the phosphorylation of PLB which controls the rate of re-uptake of Ca^{2+} into the SR through SERCA2 (Opie, 2001).

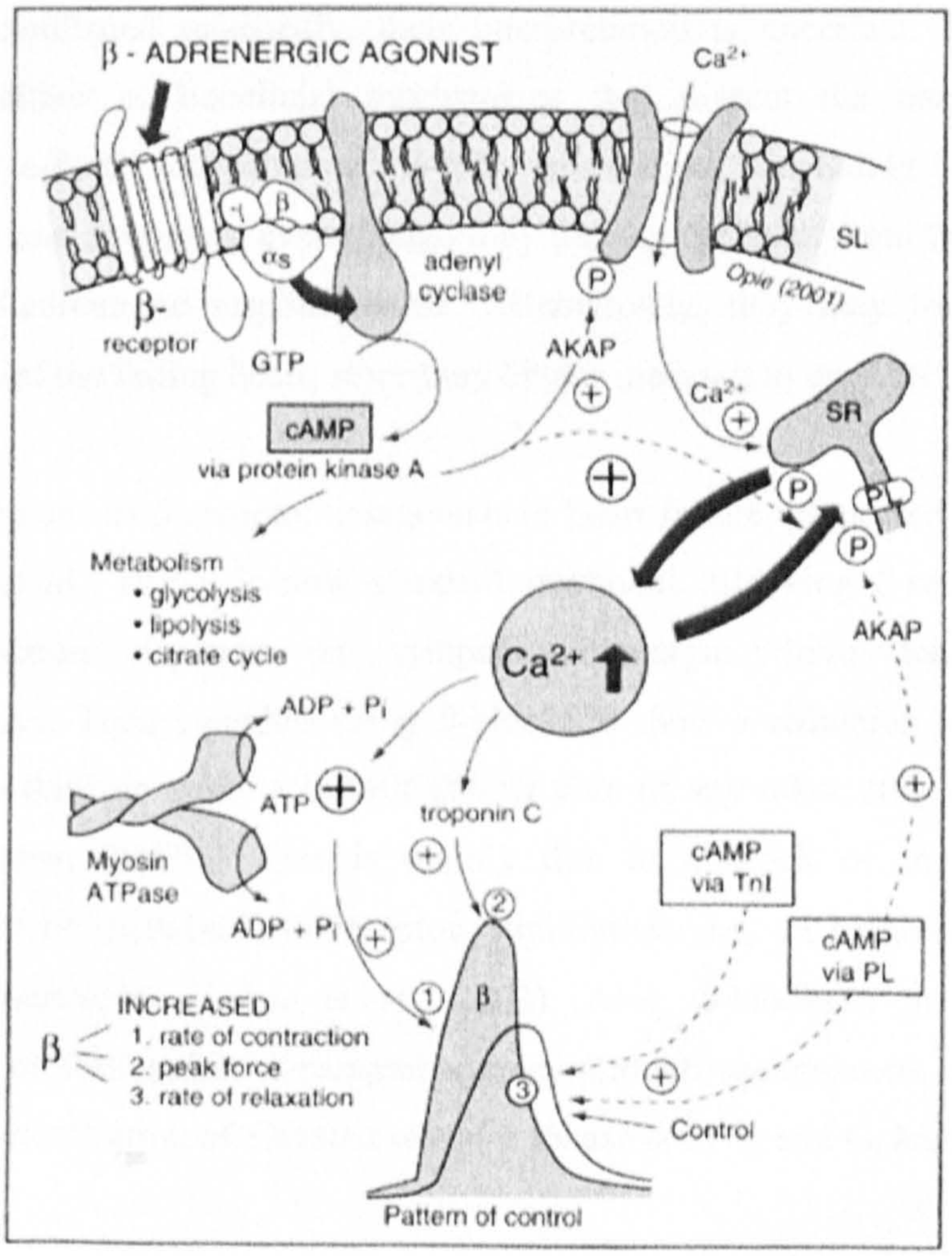

Figure 1.1 Signal systems involved in the effects of β-adrenergic stimulation (Opie, 2001).

The β-AR system plays a major role in heart failure with studies showing alterations of the cardiac β-receptor system in failing hearts (Lohse et al., 2003). Engelhardt et al. (1996) reported a reduction of the β_1 subtype and it's mRNA by up to 50%, which was correlated to severity of the disease, while the β_2-receptor levels remained unchanged. It is not clear why down-regulation in heart failure is specific

for the β_1 subtype. The remaining β-receptors are desensitised and are uncoupled from Gs, via increased activity of the receptor kinases (Ungerer et al., 2003). Heart failure-induced elevated catecholamine levels are most likely the cause of all these alterations that functionally limit the contractile reserve. Even though these changes have been confirmed repeatedly, their interpretation is uncertain. They can be interpreted either as beneficial mechanisms that protect the heart from the detrimental effects of chronic β-AR stimulation, including arrhythmias, hypertrophy, and apoptosis, even though they deprive the heart from the benefits of short-term β-adrenergic responsiveness. Alternatively, they may lead to further deterioration of the failing heart, since they hinder the heart to meet its demands.

Clinically, the use of β-receptor antagonists in heart failure, pioneered in the 1970s (Waagstein et al., 1975), is now standard treatment. Blocking β-receptors when cardiac function depends on sympatho-adrenergic drive long appeared counterintuitive. Today, studies using β-blockade show a reduction in the risk of death by one-third or more; a benefit greater than of any other drug used in heart failure (Bristow, 2000). This is mainly due to a block of the detrimental consequences of sustained β_1-receptor stimulation, i.e. arrhythmia, apoptosis, necrosis, hypertrophy (Lohse et al., 2003). Also, β-blockade may cause re-sensitisation of the cardiac β-receptor system through upregulation of β-receptor levels and normalisation of elevated receptor kinase activity and G_i levels (Lowes et al., 2002).

1.2 Catecholamine Cardiotoxicity

For many years it has been established that excess catecholamines are cardio-toxic, directly damaging the heart (Rona et al., 1959; Todd et al., 1980; Benjamin et al., 1989; Teerlink et al., 1994; Heap et al., 1996; Shizukuda et al., 1998; Xi et al., 2000; Goldspink et al., 2004). In the early study conducted by Rona et al. (1959) it was reported that isoprenaline was capable of producing both gross and microscopic myocardial necrosis (most frequently found in the apex) to otherwise normal rats. Accordingly, the amount of necrosis depended on the dose of isoprenaline

administered (Rona et al., 1959). Benjamin et al. (1989) also found that a single subcutaneous injection of isoprenaline to rats resulted in the appearance of necrotic myocytes. This damage was largely confined to the subendocardial region of the heart and increased from 3 to 24 hours after administration. Similarly, Xi et al. (2000) reported the development of lesions, characterised by degraded cardiomyocytes and infiltrating cells, in the subendocardium of hearts administered 10 mg of isoprenaline kg^{-1}. This region of injury increased in a time dependent manner, from 3 to 16 hours after the isoprenaline injection. Furthermore, apoptotic myocytes were detected 8 hours following isoprenaline injection (Xi et al., 2000). In support of these findings, Shizukuda et al. (1998) reported significant apoptosis of cardiomyocytes in the hearts of rats 12 hours after treatment with 400μg $kg^{-1}h^{-1}$ isoprenaline and this persisted up to 7 days of treatment. More specifically, Communal et al. (1998) reported that noradrenaline stimulated apoptosis in adult rat ventricular myocytes when exposed for 24 hours *in vitro*. This cell death was mediated through the activation of the β-adrenergic pathway and protein kinase A, as this effect was completely blocked by the β-adrenergic antagonist propranolol (Communal et al., 1998). More recently, *in vitro* work has been reported describing the anti-apoptotic effects of β_2-AR stimulation (Kang and Izumo, 2003).

Teerlink et al. (1994) investigated the adaptation of the heart, i.e. in terms of LV remodelling, to graded myocardial injury in the presence of a patent coronary circulation. These workers found that isoprenaline caused significant necrosis, increased LV-end diastolic pressure (LVEDP), myocardial hypertrophy, decreased the ratio of LV mass to volume, increased wall stress, ventricular dilation and altered the pressure-volume relation (LV contraction and relaxation) (Teerlink et al., 1994). Subsequently, these changes correlated with increased dose and time after isoprenaline shock. It was concluded that isoprenaline-induced myocardial necrosis resulted in enlargement of the LV cavity that is out of proportion to mass, similar to that observed after discrete myocardial infarction (Teerlink et al., 1994).

The mechanisms and pathways by which elevated catecholamines become cardiotoxic and cause progressive heart failure are controversial. The most popular theory is that alteration of the sarcolemma by catecholamine-induced cardiac injury, leads to myocardial calcium (Ca^{2+}) overload. This results in myofilament overstimulation, increased contractile force and oxygen requirement, and excessive ATP breakdown; all contributing to cardiomyocyte injury (Rona, 1985). Supporting this view, Mann et al. (1992) found that catecholamine cardiotoxicity is a result of cAMP-mediated Ca^{2+} overload.

Defective Ca^{2+} handling has been implicated in many pathological conditions. In Ca^{2+}-driven cell death, the Ca^{2+} storage status of the endoplasmic reticulum and the levels of cytoplasmic free Ca^{2+} are proposed as the main determinants of cell fate. The spatial organization of Ca^{2+} release channels, ryanodine receptors (RyR2 and RyR1 in the heart and skeletal muscle, respectively), or inositol 1, 4 ,5-trisphosphate receptors (IP3R) appears to be of key importance in determining cellular fate. RyRs are large homotetrameric channels (molecular mass, 2.3 MDa) that mediate Ca^{2+} release from SR in skeletal and cardiac muscle. Increased density of IP3R and RyR triggers cell death (Jayaraman and Marks, 1997; George et al., 2003), and the finding that both IP3R and RyR can directly sense cytoplasmic and luminal Ca^{2+} environments (Xu and Meissner, 1998; Koizumi et al., 1999) suggests that Ca^{2+} itself is a key transducer in the activation of programmed cell death. Marx et al. (2003) have reported that in failing human hearts, there is PKA-hyperphosphorylation of the RyR2 receptor, resulting in defective channel function and excitation coupling, in turn contributing to cardiac dysfunction. Furthermore, infusion of isoprenaline resulted in PKA phosphorylation of RyR2 in the rat, indicating that systemic catecholamines can activate phosphorylation of RyR2 *in vivo*, and therefore this could play a role in catecholamine cardiotoxicity (Reiken et al., 2003).

Several other indirect mechanisms may contribute to the development of myocardial injury from catecholamines. These include mobilisation of free fatty acids

(Kjekshus, 1975), increased intracellular acidity (Mosinger et al., 1997), increased platelet aggregation (Hoak et al., 1969), inefficient O_2 utilisation (Horak and Opie, 1983), and hindrance of coronary circulation (Handsforth, 1962). Interestingly, another factor which may be responsible for catecholamine-induced myocardial injury relates to the oxidative products of catecholamines and the subsequent generation of free radicals (Yunge et al., 1989; Rupp et al., 1994). These could damage cell membranes and other structures. Therefore, it could be that it is not catecholamines *per se*, but their oxidation products which cause cardiac injury. It is obvious that the development of myocardial injury from catecholamines is multi-factorial, but which mechanism predominates has yet to be ascertained.

It has become apparent that many CHF patients also experience a marked loss of muscle bulk. Through the loss of this metabolically important tissue, there is a decreased tolerance to exercise, thereby decreasing the patient's quality of life. The metabolic impact also potentially increases their risk of death (Anker et al., 1997b). As yet there is no explanation for this loss of muscle bulk. Chronic Heart Failure patients exhibit a greater proportion of type II fibres (fast), decreased oxidative enzymes and subsequent decreased exercise capacity and fatigue resistance (Minotti et al., 1991; Drexler et al., 1992). These changes are mainly due to the inactivity of these patients. When muscles become smaller and weaker, they become susceptible to injury (McArdle et al., 2002).

Anker et al. (1997a) found that cachexia, of which muscle wasting is an important factor, was strongly associated with the hormonal changes that accompany CHF. They (1997a) reported that CHF patients who also exhibited signs of cachexia had sustained higher than normal levels of noradrenaline (x 3) and adrenaline (x 5), when compared to normal and non-cachexic CHF patients. Furthermore, noradrenaline was found to correlate independently with wasting in CHF. Subsequently, Anker et al. (1997b) reported wasting as an independent risk factor for mortality in CHF. It is conceivable that sustained elevated catecholamines, instead of boosting cardiac performance (i.e. CO), may induce cumulative myocyte

damage and loss in both cardiac and skeletal muscles, leading to a generalised, rather than cardiac specific, myopathy (Opasich et al., 1999).

Our laboratory and others have found a direct effect of catecholamines on skeletal muscle. Heap et al., (1996) found necrosis in both the subendocardial region of the heart and in the soleus muscle of rats administered a minimum of 5mg of isoprenaline kg^{-1}. Data from our laboratory agree with these findings. We have recently shown in normal rats that acute exposure to high levels of isoprenaline causes myocyte death in both the heart and the skeletal muscles, via a combination of necrosis and apoptosis (Ng et al., 2002; Ellison et al., 2002; 2003; Goldspink et al., 2004). Such cell death and the ability or otherwise to regenerate them, will inevitably affect muscle function.

1.3 Chronic β-AR Stimulation

Chronic β-AR stimulation results in cardiac hypertrophy and desensitization and/or downregulation of the β-receptors (Kudej et al., 1997; Morisco et al., 2001). Furthermore, enhanced β-adrenergic signalling through over-expression of upstream adrenergic signalling effectors, i.e. $G_{s\alpha}$, β1-AR or β_2-AR, in transgenic mice results in either normal or increased cardiac function in young adult animals, but the development of cardiomyopathy with age (Vatner et al., 1999; Engelhardt et al., 2001). This is characterized by reduced LV function (Engelhardt et al., 2001; 2002), LV hypertrophy and chamber dilation (Engelhardt et al., 1999; 2002), fibrosis (Engelhardt et al., 2001; 2002), and apoptosis (Geng et al., 1999).

The mechanisms underlying these detrimental changes have been extensively investigated. Engelhardt et al. (2001) reported that abnormal Ca^{2+} transients in cardiomyocytes were responsible for early contractile dysfunction, i.e. before the appearance of interstitial fibrosis and cardiomyocyte hypertrophy, and this was due to decreased expression of the SR protein, junctin (Engelhardt et al., 2001). Junctin plays an important role in sarcoplasmic calcium handling by mediating the binding of calsequestrin to RyR.

In another study Engelhardt et al. (2002) identified the importance of the cardiac Na^+-H^+ exchanger 1 (NHE1) in the detrimental effects of β-adrenergic stimulation during the progression of heart failure. Compared with wild-type controls, Engelhardt et al. (2002) found a 140% and 30% increase in NHE1 mRNA and protein levels respectively, in hearts of 5 month old β_1-receptor over-expressed transgenic mice. Furthermore, the treatment of β_1-receptor transgenic mice with selective NHE1 inhibitor, cariporide, completely prevented LV fibrosis, reduced cardiomyocyte hypertrophy by 88% and completely inhibited the impairment of LV systolic contraction (dp/dt_{max}) and relaxation (dp/dt_{min}). The mechanisms of how NHE1 exerts its detrimental effects are currently unknown. However, it is postulated that an increased sodium load could be involved in inducing hypertrophy, with increased intracellular sodium being exchanged for Ca^{2+} via the cardiac Na^+-Ca^+ exchanger. The resulting increase in Ca^{2+} during diastole might exert several deleterious effects, including activation of protein kinase C and Ca^{2+}-dependent transcription factors. This concept is supported by the earlier finding of altered intracellular Ca^{2+} handling in β_1-AR transgenic mice (Engelhardt et al., 2001). More recently, in further support of this mechanism, Engelhardt et al. (2004) reported that altered calcium handling is critical for the detrimental effects of β1-adrenergic signalling. This was shown by deleting the principal inhibitor of SR Ca^{2+} uptake, phospholamban (PLB) in β_1-AR transgenic mice. Phospholamban knockout (PLB$^{-/-}$) β_1-adrenergic receptor transgenic mice showed enhanced survival, less cardiac hypertrophy and fibrosis, and improved cardiac function. The latter was demonstrated by a preservation of LV systolic pressure, improved LV congestion (normalized LVEDP), LV contractility (dp/dt_{max}) and diastolic function (dp/dt_{min}).

Engelhardt et al. (2004) also showed a faster decay of intracellular Ca^{2+} transients in β_1-adrenergic receptor PLB$^{-/-}$ transgenic mice, when compared to β_1-AR transgenic mice or wild-type controls. Subsequently, diastolic Ca^{2+} levels and Ca^{2+} load were significantly decreased in β_1-AR PLB$^{-/-}$ transgenic mice. These findings are supported by Iwanaga et al. (2004) who found that the inhibition of PLB in rats after

myocardial infarction with gene therapy prevented the progression of heart failure by improving cardiac function and preventing fibrosis (Iwanaga et al., 2004).

As with over-expression of β-receptors, it is well documented that over-expression of G-protein receptors results in chronically enhanced β-AR signalling and either normal or increased cardiac function in young adult animals, but the development of cardiomyopathy with age (Iwase et al., 1997). Furthermore, β-AR blockade with propranolol prevented the development of cardiomyopathy (Asai et al., 1999). This was shown through the prevention of cardiac dilation and the decline in LV function, whilst also arresting myocyte hypertrophy, fibrosis and apoptosis. Consequently, premature mortality, usually seen in this transgenic animal model, was abolished (Asai et al., 1999). More recently, the cellular mechanisms of β-AR blockade were found to be related to alterations in mitogen-activated protein kinases (Karoor et al., 2004). Karoor and colleagues (2004) found that in $G_{s\alpha}$ over-expressed mice, there were significant increases in phospho-kinase levels of p38 MAP kinase, $p70^{S6K}$, ERK, Akt and JNK up to 15-20 months. However, following treatment with propranolol for 5 weeks there was a reversal in the levels and activities of these phospho-kinases, which are involved in the growth and death of cardiomyocytes (Karoor et al., 2004). Furthermore, Gaussin et al. (2003) found a role for uncoupling protein 2 (UCP2), a protein involved in the control of mitochondrial membrane potential, and four-and-a-half LIM domain protein-1 (FHL1) for causing cardiomyopathy in mice over expressing $G_{s\alpha}$. However, β-AR blockade treatment reversed the cardiomyopathy and suppressed the increased expression of UCP2 and FHL1 (Gaussin et al., 2003).

Caution should be exercised when interpreting these findings as signalling mechanisms caused by agonist stimulation and those by receptor over-expression might not be identical.

Increases in catecholamine stimulation have been implicated as a causative factor in the development of cardiomyopathy (Dash et al., 2001). Using over-expression of

PLB transgenic mice Dash et al. (2001) reported that, as expected, there was initially a mild depression of ventricular contractility. Basal PLB phosphorylation was found to be substantially higher in transgenic mice, to relieve the inhibitory effects of PLB on SR function. The phosphorylation of PLB is mediated predominantly by β-adrenergic drive and when the transgenic mice were treated with propanolol it resulted in a significant depression in contraction rate and a prolonging of the relaxation phase, whereas no changes in contractile parameters were found in wild-type littermates. Subsequently, there were reductions in cardiac noradrenaline, adrenaline and dopamine levels in the transgenic mice. Plasma noradrenaline levels however were elevated, reflecting a compensatory increased adrenergic drive in order to relieve the inhibitory effects of PLB (Dash et al., 2001).

With aging, these over-expressing PLB mice developed cardiomyopathy exhibited by deterioration in LV function, dilated LV chambers as well as extensive interstitial fibrosis and myocyte hypertrophy. Aged transgenic mice also displayed a desensitised adenylyl cyclase response to isoprenaline, which was independent of any alterations in β-receptor density. This decreased β-adrenergic response may have precluded adequate compensatory phosphorylation of PLB and thereby depressed myocardial function (Dash et al., 2001).

These findings suggest an interaction between increased PLB expression and an enhanced sympathetic drive to attenuate its inhibitory effects. Over time this hyper-adrenergic compensatory mechanism, seems to progress to a maladaptive one leading to cardiomyopathy. Therefore, it was concluded that increases in catecholamine stimulation, in the absence of pre-existing heart failure, could be a primary causative factor in the development of cardiomyopathy and early mortality (Dash et al., 2001).

In further support of chronic catecholamine exposure resulting in cardiomyopathy, Benjamin et al. (1989) found that daily doses of isoprenaline, administered to rats for 10 days induced additional myocardial necrosis, cardiac hypertrophy and

significant fibrosis. In support of these findings, more recently Schlaich et al. (2003) found that LV hypertrophy was associated with increased sympathetic activity, and more specifically noradrenaline release was related to the development of LV hypertrophy.

It has also been reported that the reason why myocardial $G_{s\alpha}$ over-expressed transgenic mice develop cardiomyopathy is because they lack the protective desensitisation mechanisms against catecholamines and sympathetic stimulation (Vatner et al., 1998). This further suggests a link between increases in catecholamines and the development of cardiomyopathy.

Chronic exposure to catecholamines has also been shown to have hypertrophic effects on skeletal muscles. Ishii et al. (1998) reported that 5mg of isoprenaline $kg^{-1}d^{-1}$ for up to 2 weeks induced hypertrophy to the fibres of the orbicularis oculi and stapedius muscles and improved muscle fibre function in rats. More recently, Kumar et al. (2003) reported that 1.5mg of isoprenaline kg^{-1}, administered orally for 120 days resulted in an increased body weight in growing chicks. This increased body weight was largely due to skeletal and cardiac muscle hypertrophy.

In support of these findings it has been shown that the chronic administration of the β_2-AR agonist, fenoterol, for 4 weeks reversed the wasting and restored muscle mass and strength in the extensor digitorum longus and soleus muscles of aged rats (Ryall et al., 2003). This was specific to increases in muscle fibre cross-sectional areas. However, the authors also reported detrimental effects of hypertrophy in the heart (Ryall et al., 2003). Extreme over-expression of β_2-ARs in the heart (140-fold increase) has been shown to cause cardiac hypertrophy (Dorn et al., 1999). Furthermore, the anabolic effects of clenbuterol, a β_2 agonist, have also been investigated (Choo et al., 1992). However, it has been reported that high doses of clenbuterol can have detrimental effects on skeletal and cardiac muscle, causing myocyte necrosis in both muscles (Burniston et al., 2002).

1.4 Cell Death: Necrosis and Apoptosis

Numerous studies have documented that myocyte death is an important variable in the development of ventricular dysfunction and failure in ischemic and idiopathic dilated cardiomyopathy, long-term systemic hypertension, and during myocardial ageing in animals and humans (Anversa, 2000). On the other hand, skeletal muscle fibre death has been described as a pathogenetic mechanism of several neuromuscular disorders and muscular dystrophies (Primeau et al., 2002).

Apoptosis and necrosis (Figure 1.2) are presently recognised as the major types of physiological and pathological cell death. Apoptosis is a tightly regulated cell deletion process that differs morphologically and biochemically from necrotic cell death. Through the cell death pathway of oncosis followed by necrosis, there is a significant initial net increase in cytoplasmic Ca^{2+} (either by stimulating the uptake of extracellular calcium or by facilitating the release of Ca^{2+} stores from the endoplasmic reticulum) and swelling of the cell and mitochondria (oncosis), followed by membrane rupture and leakage of contents to the exterior. Cells suffer necrotic death when exposed to extreme environmental insults. Necrosis has been considered generally to be a chaotic decadence process that affects the inevitable demise of cells otherwise not destined to die (Syntichaki and Tavernarakis, 2002). Necrosis can be identified morphologically and from a standard haematoxylin and eosin (H&E) stain, dead necrotic cells appear completely demised with disrupted sarcolemmal membranes and pale cytoplasmic staining. Another method for the detection of necrosis involves the use of the large myosin antibody (Nolan et al., 1983; Benjamin et al., 1989; Kajstura et al., 1996; Goldspink et al., 2004). This antibody is considered one of the most selective markers of necrotic myocytes due to its permeabilisation through leaky disrupted membranes and its specific binding to myosin once inside.

The onset of apoptosis is characterised by shrinkage of the cell and the nucleus as well as condensation of nuclear chromatin into sharply delineated masses (Saraste and Pulkki, 2000). Later on, the nucleus progressively condenses and breaks up (i.e.

karyorrhexis). The cell detaches from the surrounding tissue and its outlines become convoluted and form extensions. Apoptotic budding is a process whereby these extensions separate and the plasma membrane seals to form a separate membrane around the detached solid cellular material. These apoptotic bodies are crowded with closely packed cellular organelles and fragments of nucleus. The fine structures, including membranes and mitochondria, are well preserved inside the bodies. The apoptotic bodies are rapidly phagocytosed into neighbouring cells, including macrophages and parenchymal cells. Apoptotic bodies can be recognised inside these cells, but eventually they become degraded (Saraste and Pulkki, 2000). If the fragmented cell is not phagocytosed it will undergo degradation which resembles necrosis and has been called secondary necrosis (Kerr et al., 1994).

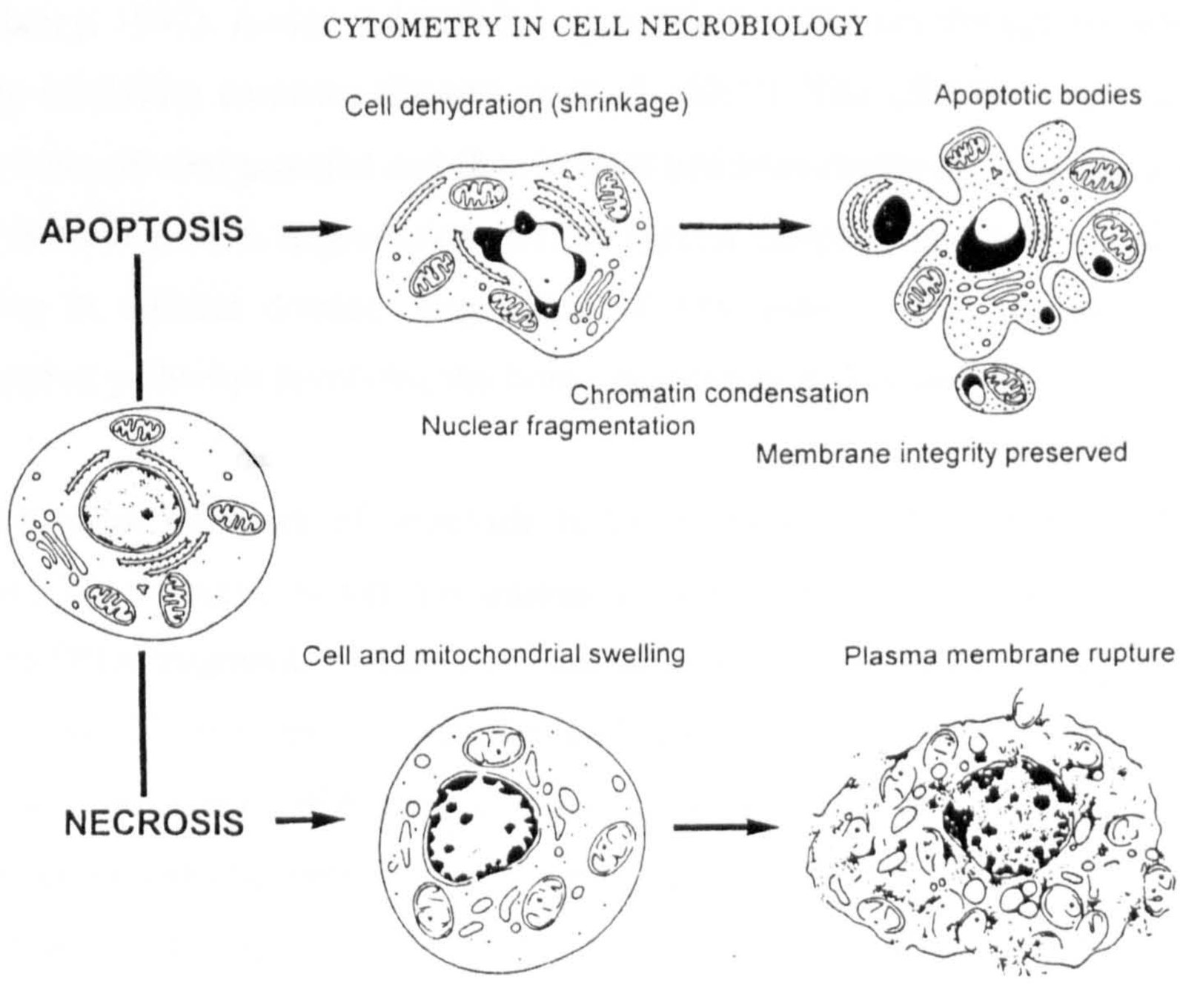

Figure 1.2 Cell death pathways: necrosis and apoptosis (Darzynkiewicz et al., 1997).

The first molecular evidence of apoptotic cell death/survival machinery comes in the form of the Bcl2 gene. Numerous death signals and death receptors (including Tumor Necrosis Factor) and many growth factors culminate on a pathway regulated by pro-apoptotic (e.g. Bax, Bad) and anti-apoptotic members of the Bcl2 family (e.g. Bcl2, BclX) (Satler et al., 1997). Relative balances of the two classes of Bcl2 proteins affect interaction of adaptor proteins, such as apoptotic protease-activating factor 1 (APAF-1) and Fas-associated death domain (FADD) with caspase enzymes (Chou et al., 1998), which are initially inactive but become activated on interaction with proteins such as APAF-1. Specifically, caspases are activated during apoptosis in a self-amplifying cascade. Activation of the upstream caspases, such as caspases 2, 8, 9 and 10, by pro-apoptotic signals leads to proteolytic activation of the downstream or effector caspases 3, 6 and 7. Caspase activation often leads to a feedback loop resulting in amplification of cell death signals (Nicholson and Thornberry, 1997). A class of inhibitor apoptosis proteins are thought to function in part by inhibiting caspases (Deveraux et al., 1997). The effector caspases finally cleave a set of vital proteins and thus initiate and execute the apoptotic degradation phase including DNA degradation and the typical morphologic features, ultimately resulting in cellular demise. Regulation of cell death is also mediated through overlapping pathways involving the tumor suppressor p53 (Clarke et al., 1993).

A biochemical hallmark of apoptosis is the degradation of DNA by endogenous DNases. These enzymes cut the internucleosomal regions of DNA into double-stranded DNA fragments of 180–200 base pairs which contain blunt ends as well as single base 3′ overhangs (Didenko and Hornsby, 1996). With the terminal transferase mediated DNA nick end labelling (TUNEL) assay, cells containing DNA strand breaks become visible in light microscopic analysis. The validity of the TUNEL assay as a method to detect apoptosis has however been questioned (Kanoh et al., 1999), as DNA damage is not a unique feature of apoptosis, but can occur in necrosis and during repair of reversibly damaged DNA.

An alternative approach to study the presence of apoptosis is to demonstrate the activation of downstream caspases (Boatwright and Salvesen, 2003). These can be detected using cleavage-site-specific antibodies that detect only the cleaved and active forms of caspase substrates. They can be applied to detect apoptotic cells in tissue sections by light microscopy.

Several studies have provided evidence of caspase activation in cardiomyocyte death. Active forms of caspases 2, 3 and 7 are generated in the ischemic–reperfused myocardium (Holly et al., 1999). Moreover, activated form of caspase 3 has been shown to co-localise with the TUNEL-positive cardiomyocytes in ischemic–reperfused myocardium (Black et al., 1998).

In summary, both acute and chronic exposure of catecholamines have a detrimental effect on the heart causing necrosis, apoptosis, hypertrophy, fibrosis and impaired function. Patients with CHF exhibit sustained high levels of catecholamines, due to over-activation of sympathetic drive. It is possible that this elevation in circulating catecholamines could be related to the muscle wasting seen in some of these patients. The effects of catecholamines on skeletal muscle are much less well documented. There is however evidence to suggest that they can cause cell death, as well as having anabolic effects of promoting muscle growth and hypertrophy.

1.5 Skeletal Muscle Regeneration

Under normal circumstances mammalian adult skeletal muscle is a stable tissue with very little turnover of its fibre number and nuclei (Decary et al., 1997). In normal rat muscle, it is estimated that no more than 1-2% of myonuclei are replaced every week (Schmalbruch and Lewis, 2000).

It has been known for many years that skeletal muscle has a remarkable capacity for rapid and extensive regeneration after injuries resulting in partial or complete damage to muscle fibres (Bodine-Fowler, 1994). Muscle regeneration is characterized by two phases; a degenerative phase, followed by a regenerative

phase. The kinetics and amplitude of each phase varies according to the extent of the injury and the specific muscles injured. The process of regeneration can be studied in a controlled and reproducible way, using animal models of muscle injury. The easiest way to induce damage is through the use of myotoxins, such as bupivacaine (Hill et al., 2003) or notexin (Harris et al., 1975). Harris *et al.* (1975) investigated the pathological responses of rat skeletal muscle to a single injection of a toxin isolated from the venom of the Australian tiger snake. They found that 12-24hr following intramuscular injection the muscles underwent degenerative necrosis, accompanied by oedema and the infiltration of lymphocytes, polymorphs and phagocytic macrophages. Factors released by the injured muscle activated the inflammatory cells residing within the muscle, which in turn provided the chemotactic signals to circulating inflammatory cells (Tidball, 1995). Three days after injecting the venom, Harris et al. (1975) reported that the muscle oedema had subsided and the necrotic fibres had been completely destroyed by phagocytic cells. Such muscle degeneration is followed by the activation of a repair process. In order to provide a sufficient source of new myonuclei for muscle repair, there is an expansion of myogenic cells (satellite cells) through cellular proliferation.

Harris et al. (1975) found the existence of myoblasts or myogenic cells (i.e. derived from satellite cells) 3 days post-injury. After 5 days the myoblasts had differentiated and fused to form new myotubes. Myotubes then developed or grew into histochemically distinct muscle fibre types which were evident 7 days following the injection of the toxin. In muscle cross sections, the morphological characteristics of newly formed muscle fibres are small and angulated, expressing embryonic/developmental forms of MHC and possessing centralized nuclei (Williams et al., 2001). In the animal model of muscle damage using the snake venom, the whole regenerative process was complete, with full restoration of the injured muscle fibres, 21 days following injection of the venom. The regenerated muscle was morphologically and functionally indistinguishable from normal un-damaged muscle (Harris et al., 1975). This is a 'typical' example of how skeletal

muscles can regenerate new fibres following injury and is as much as *bona fide* embryonic myogenesis (Charge and Rudnicki, 2004).

Essential aspects of the muscle regeneration process are revascularisation, re-innervation and reconstitution of the extracelluar matrix and muscle fibre basal lamina. Whalen *et al.* (1990) reported that if re-innervation of the regenerating muscle was allowed to occur, then there was complete restoration of muscle fibres in the rat soleus muscle 28 days following injection of snake venom toxin. However, if the muscle was denervated (and hence functionally inactive) at the time of toxin injection, although the early stages of regeneration took place the regenerating fibres failed to increase in size. Instead, they showed significant atrophy or less growth, relative to the size of the regenerating fibres in normally innervated muscles. Furthermore, adult slow myosin was the exclusive form in innervated regenerating fibres, but adult fast myosin was the predominant isoform in denervated muscle once its damaged fibres were regenerated (Whalen et al., 1990). Hence, the pattern of contractility affects the type of MHC expressed. Another critical factor that influences the rapid and complete regeneration of fibres is the availability of a viable population of satellite cells.

1.6 Muscle Satellite Cells

The remarkable ability of skeletal muscle to regenerate following injury, as well as adapt to physiological demands such as growth and exercise training, is largely attributed to a small population of dormant cells, called satellite cells. These are resident in adult skeletal muscle and were first described by Mauro (1961).

Satellite cells are small, self-renewing, undifferentiated mononuclear cells located between the basal lamina and plasma membrane of skeletal muscle fibres (Figure 1.3). Therefore, they have the defining characteristic of a continuous surrounding basal lamina (Carlson and Faulkner, 1983). While mitotically quiescent they express proteins, such as c-met receptor tyrosine kinase, m-cadherin, Pax7 and myocyte

nuclear factor (Irintchev et al., 1994; Cornelison and Wold, 1997; Seale et al., 2000; Garry et al., 1997).

When activated in response to fibre damage and degeneration, the satellite cells re-enter the cell cycle and also express myogenic factors such as MyoD, myogenin, MRF-4 and myf-5 (Cusella-De Angelis et al., 1992; Grounds et al., 1992; Koishi et al., 1995; Cornelison and Wold, 1997; Dupont-Versteegden et al., 1998). From the ensuing proliferation, differentiation and fusion of active satellite cells new multi-nucleate myofibres emerge to replace the degenerating ones. Alternatively, if a fibre has been damaged in part, satellite cells fuse with the ends of existing damaged fibres, repairing the fibre by creating continuity between the damaged ends (Figure 1.4). Therefore, under normal circumstances the total number of fibres should be fully preserved.

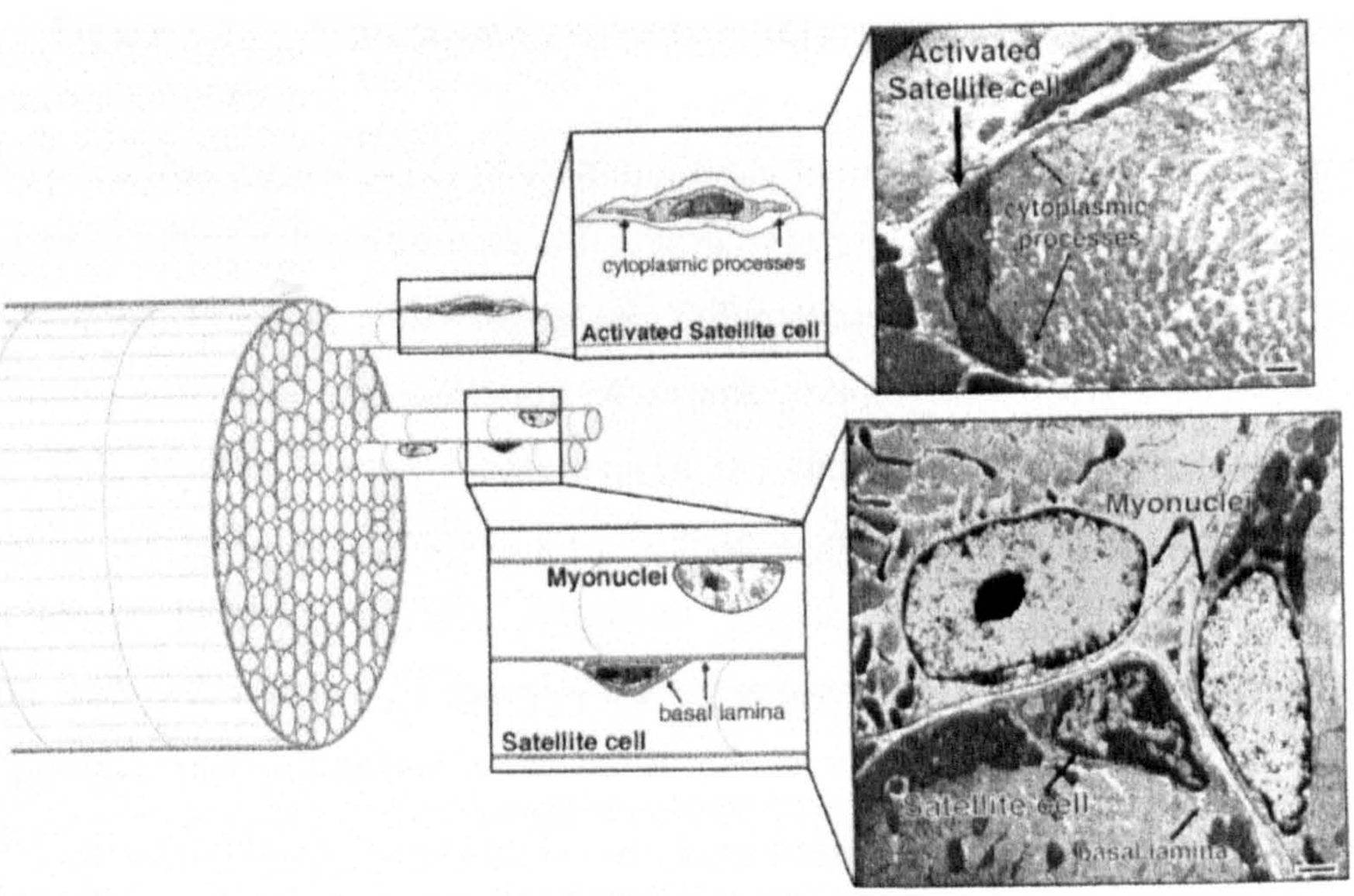

Figure 1.3 The location of satellite cells in the muscle fibre (Hawke and Garry, 2001).

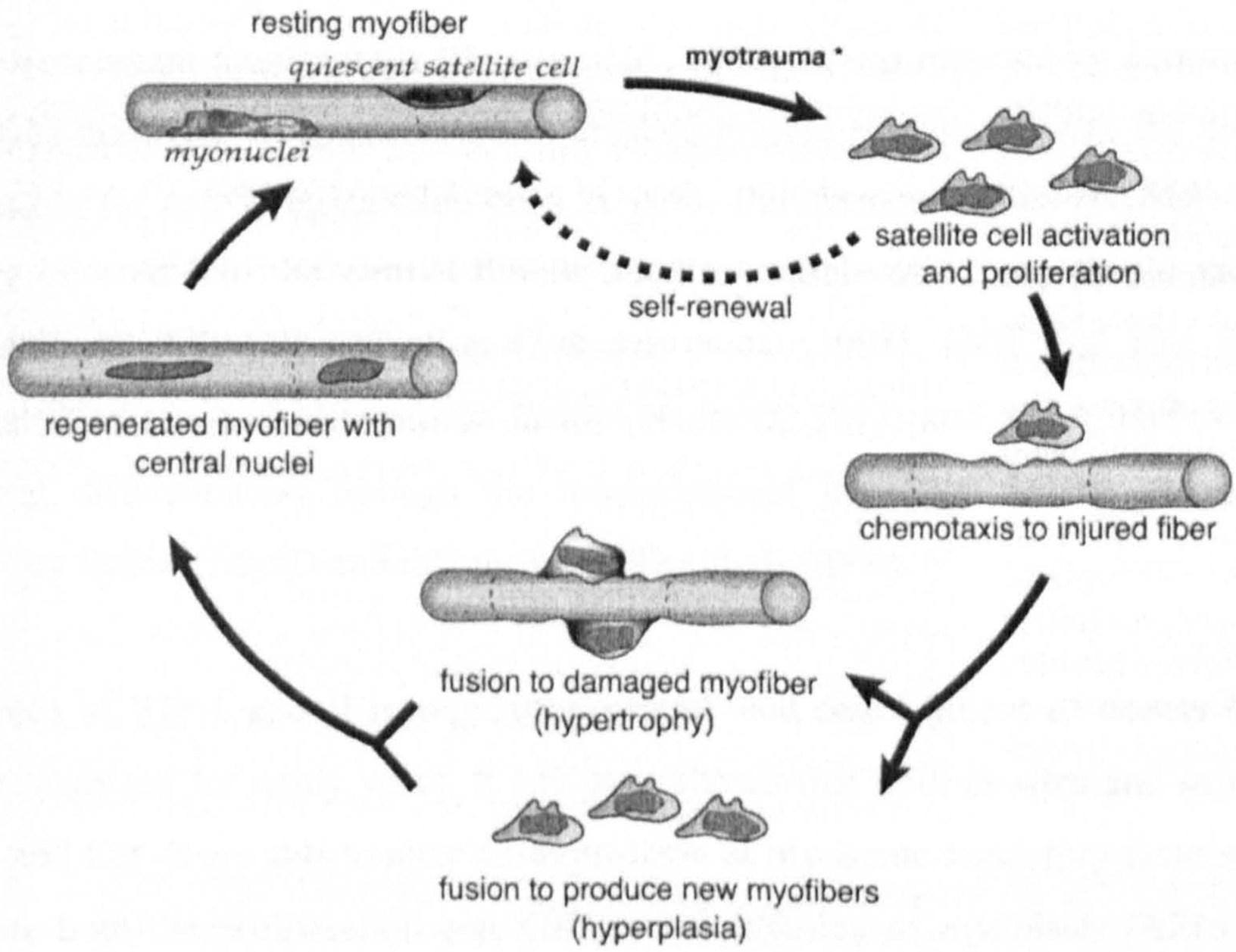

Figure 1.4 Satellite cell response to injury (Hawke and Garry, 2001)

Bischoff (1985) first found that muscle regeneration is initiated by the release of an endogenous mitogen from traumatised, crushed adult muscle. It is now accepted that the activation, ensuring proliferation and differentiation of satellite cells, requires the timely, controlled up-regulation of muscle transcription factors and specific genes. This process is mainly governed by the endocrine and paracrine/autocrine regulatory mechanisms of various growth factors. In particular, Hepatocyte growth factor/scatter factor (HGF/SF); Fibroblast growth factors (FGFs); Insulin-like growth factors 1 and II (IGF-1 and II), Mechano-growth factor (MGF; Hill et al., 2003) and the TGF-β family (Charge and Rudnicki, 2004).

Hepatocyte growth factor/scatter factor elicits mitogenic, motogenic and morphogenic activities during development and tissue regeneration (Zarnegar and Michalopoulos, 1995). It has been found that the role of HGF in muscle regeneration is most important in the early phase of the repair process, and it

appears to act directly on muscle satellite cells due to the expression of its receptor c-met in quiescent satellite cells (Bottaro et al., 1991). It was reported by Tatsumi et al. (1998) that HGF/SF was present in crushed muscle extract and was the factor responsible for activating satellite cells *in vitro*. Furthermore, when HGF/SF was directly injected into the normal tibialis anterior muscle of 12 month old rats it stimulated satellite cell activation (Tatsumi et al., 1998). HGF has also been implicated as a potent chemotactic factor (Bischoff, 1997) and as an inhibitor of myoblast differentiation through the transcriptional inhibition of the myogenic regulatory factors, MyoD and myogenin (Miller et al., 2000).

The roles of IGF-1 and II in regulating growth and development of tissues have been recognized for many years. It has been shown that both *in vitro* and *in vivo*, IGF-1 and IGF-II are able to alter the expression of myogenic regulatory factors and promote both the proliferation and differentiation/fusion of myoblasts (Allen and Boxhorn, 1989; Chakravarthy et al., 2000; Rabinovsky et al., 2003). Also, IGF-1 and IGF-II levels are upregulated in skeletal muscle undergoing regeneration (Hill et al., 2003a, b). Subsequently, increasing the levels of IGF-1 leads to increases in hypertrophy and muscle mass due to augmentation of muscle protein and DNA contents (Musaro et al., 2001). The hypertrophic effects of IGF-1 have also been attributed to the activation of satellite cells and their proliferation to provide more myonuclei (Barton-Davis et al., 1999; Hill et al., 2003a, b).

Recently, another factor has been implicated in the activation of satellite cells and is known as Mechano-growth factor (MGF). It was first discovered by Goldspink et al. (1992), and is a splice variant derived from the IGF-1 factor, although its sequence is different from the systemic IGF-1 produced by the liver. MGF is expressed in mechanically overloaded muscle and has been shown to be involved in tissue repair and adaptation, in particular muscle hypertrophy (Goldspink, 2001). Hill et al. (2003a, b) induced local muscle damage in rats with either an injection of bupivacaine, a local anaesthetic which induces muscle fibre necrosis, or by a combination of stretch and electrical stimulation. It was found that the expression of

MGF mRNA was maximal as early as 1 day following stretch and stimulation and peaked 4 days following bupivacaine injection. These message levels then begun to decrease once regeneration and fusion of myoblasts had begun. Interestingly, the mRNA and protein levels of M-cadherin and MyoD (i.e. markers of quiescent and activated satellite cells) peaked at 4-7 days following both types of injury. In marked contrast, the expression of mRNA for IGF-1Ea peaked much later, at ~12 days after inducing the injury. IGF-1Ea is an isoform of IGF-1 in muscle and is similar to the hepatic endocrine type of IGF-1. These data suggest an individual role for MGF in initiating the proliferation and differentiation of satellite cells, as it precedes M-cadherin and MyoD expression (Hill et al., 2003a, b). In support of these data, stable transfection of cells in culture with MGF was shown to stimulate myoblast proliferation and suppress differentiation (Yang and Goldspink, 2002).

Satellite cell number is dependent on muscle fibre type and age. The satellite cell content differs between muscle fibre types. The percentage of satellite cells in rat adult slow soleus muscle is 2- to 3-fold higher (11%) than in the fast tibialis anterior muscle (4%) (Schmalbruch and Hellhammer, 1977). The regulatory mechanisms behind these differences were identified as an increased density of satellite cells in association with the proximity of capillaries and myonuclei; capillaries being greater in the slow muscle (Schmalbruch and Hellhammer, 1977). Therefore, the increased number of satellite cells in the soleus muscle is understandable as slow-oxidative muscles are characterized by their increased capillary density when compared to fast-glycolytic muscles. In another study, more satellite cells were also observed at the motor neuron junctions (Wokke et al., 1989). Renault et al. (2002) reported a decrease in the number of satellite cells, expressed as a proportion of myonuclei, in biceps brachii and masseter muscle biopsies derived from older humans. That is 1.5% in ~75 years-olds, when compared to 5% in younger adults (~23 years old). Therefore, the important characteristic of self-renewal by satellite cells (Schultz, 1996) may be compromised with age.

It has been shown that aged muscles display a lower adaptive and regenerative capacity (Grounds, 1998; Blough and Lindermann, 2000) caused by a decrease in satellite cell numbers and proliferative cell potential with ageing (Schultz and Lipton, 1982). However, not all studies are in agreement (Decary et al., 1997; Putman et al., 2001). Whether the age-related decrease in satellite cell number affects the regenerative capacity of skeletal muscle has been more recently investigated with cells in culture. Decary et al. (1997) showed that satellite cells isolated from muscles of aged human subjects are still able to make about 15 divisions, which is enough to repair muscle damage. Furthermore, Putman et al. (2001) reported that the satellite cells and satellite cell progeny of ageing rats are not compromised and possess an unaltered capacity to contribute to the adaptive response of 50 days of chronic low-frequency electrical stimulation. Therefore, it was concluded that although the number of satellite cells decreased with age, the proliferative potential is not greatly affected. This suggests that the ability of skeletal muscle fibres to adapt, or regenerate, is maintained throughout life.

The situation would be remarkably different however if the proliferation of the satellite cells were to be highly solicited, as observed in muscular dystrophies (Decary et al., 2000). In support of this, Reimann *et al.* (2000) proposed that the failure to regenerate fibres in dystrophic muscle was due to exhaustion of the proliferative potential of the satellite cell pool and the continual need for satellite cell proliferation and fibre repair. This 'exhaustion' of the satellite cells ability to proliferate results in incomplete restoration of the muscle fibre numbers and significant muscle atrophy and wasting.

Sadeh et al. (1985) found that the weekly administration of bupivacaine for 6 months resulted in marked variability in terms of fibre size and atrophy, extensive fibre splitting, numerous internal nuclei and many 'whorled' fibres. These findings suggest that chronic exposure to bupivacaine results in incomplete fibre regeneration after several cycles of degeneration-regeneration.

One mechanism which has been suggested to control this limited proliferation, or mitotic clock, is the shortening of the telomeric sequences. It was found that in the quadriceps muscles there was only a very small decrease in the length of the telomeric DNA with increasing age. However, a dramatic decrease in telomeric DNA length was observed in the muscles of children with muscular dystrophy (Decary et al., 2000). This progressive loss of DNA could eventually destabilise telomere structure, leading to chromosome modifications (Counter et al., 1992) and triggering the entry of cells into a senescent programme (Torella et al., 2004). Therefore, the more cell divisions a satellite cell undergoes (i.e. as a result of the continual repair of chronic muscle damage) the resulting outcome is cellular senescence and consequent impaired skeletal muscle regeneration.

Until recently, the muscle satellite cell was presumed to be the sole source of myonuclei in muscle repair. However due to the recent findings of multipotential stem cells in various adult tissues, the view that tissue-specific stem cells are pre-determined to a specific tissue lineage has been challenged.

Ferrari et al. (1998) transplanted genetically marked ($LacZ^+$) bone-marrow (BM) derived cells (BMDC) into immuno-deficient mice. It was found that these cells migrated into areas of irradiation-induced muscle degeneration. Here, they underwent myogenic differentiation and participated in the regeneration of new fibres (Ferrari et al., 1998). However, the contribution of BM-derived progenitors to muscle regeneration was minimal. Nonetheless, these cells appeared to be recruited as a result of the inflammatory signals originating from the degenerating tissue, as they accessed the damaged tissue through the circulation (Ferrari et al., 1998). Furthermore, it was suggested that BM cells could serve as a reservoir of progenitors for muscle tissue, and that under conditions of extended damage these progenitors might expand or maintain the pool of resident, more differentiated, muscle-forming precursors (Ferrari et al., 1998). With this view, the ability of the skeletal muscle to regenerate, even after periods of chronic degeneration-

regeneration when the muscle satellite cell pool has become exhausted, would never be compromised.

These findings of Ferrari et al. (1998) have been more recently supported by LeBarge and Blau (2002). In this excellent study, it was found that green fluorescent protein (GFP) labelled BMDCs became satellite cells, occupying the muscle stem cell niche, when transplanted following irradiation-induced damage. Also, these BMDC satellite cells gave rise to new fibres, a contribution to as many as 3.5% muscle fibres following subsequent exercise-induced damage (LeBarge and Blau, 2002). Furthermore, this contribution of new multinucleated fibres from BMDCs was much greater than that reported by Ferrari et al. (1998). Therefore, the frequency of conversion of BMDCs into the myogenic lineage could be related to the conditions or extent of the muscle damage. Furthermore, there may be differences among different skeletal muscle types and the incorporation of BMDCs (Brazelton et al., 2003).

There is strong evidence for the presence of progenitor cells with myogenic potential, other than satellite cells, within skeletal muscle (Asakura et al., 2001; Seale et al., 2000; Jankowski et al., 2002; Blaveri et al., 1999; Gussoni et al., 1999; DeAngelis et al., 1999; Qu-Petersen et al., 2002; McKinney-Freeman et al., 2002; Torrente et al., 2001). Asakura et al. (2001) identified a novel stem cell population which they named side population (SP) cells within skeletal muscle. These cells expressed the haematopoietic stem cell marker, Sca-1, but were negative for markers of satellite cells. They possessed the ability to differentiate into haematopoietic cells, satellite cells and skeletal muscle following transplantation (Asakura et al., 2001). Therefore, SP cells may be satellite cell progenitors capable of direct myogenic fusion. SP cells were also present in the muscles of Pax7 null mice, which lack satellite cells (Seale et al., 2000). Taken together, these findings suggest that SP and satellite cells represent distinct cellular populations within skeletal muscle.

It has been shown that when $Sca1^+$ and $CD34^+$ muscle-derived stem cells expressing the LacZ gene, were injected into the arterial circulation of the hindlimb of *mdx* mice, the late passage $Sca1^+/CD34^+$ cells adhered to the endothelium (Torrente et al., 2001). However, following muscle and blood vessel damage they were able to migrate from the blood vessels into host muscle tissues, and participate in the formation of muscle fibres. This was evidenced by the presence of ~12% β-galactosidase positive fibres, 48 hours after their intra-arterial injection followed by damage to the tibialis anterior muscle (Torrente et al., 2001). These data would suggest that there are bi-potential (both haemopoietic and muscle lineage) stem cells present within the vasculature that may be activated to enter the myogenic lineage when the muscle receives extensive damage. However, it should not be excluded that these cells, like SP cells, could also represent progenitors of satellite cells. Regardless of this, it was concluded that these cells may prevent irreversible pathological damage and thus signals governing their migration need to be investigated further (Torrente et al., 2001).

To summarise, upon injury skeletal muscle possesses the ability to regenerate damaged fibres and this is due to its resident satellite cells. However, considerable evidence now exists to suggest that other 'stem' cells (e.g. SP cells) are resident in skeletal muscle and these potentially originate from the bloodstream. The replicative potential of satellite cells diminishes following repetitive recruitment of the cells into the cell cycle, i.e. following chronic bouts of degeneration-regeneration. Whether the ability of the muscle to regenerate is ever completely compromised could be due to the presence of SP and other cells, e.g. BMDCs, that can also give rise to skeletal muscle fibres. These recent advances may offer an attractive means of cellular therapy for muscular dystrophy.

1.7 Cardiac Regeneration

Over many decades the accepted paradigm has been that the heart is a post-mitotic organ without any regenerative capacity. Under this opinion, cardiac homeostasis is stagnant, cell renewal is non-existent and the cardiomyocytes are as old as the individual. Now it is believed that myocyte death and regeneration are part of the normal homeostasis of the heart. It was previously believed that hypertrophy was the only form of myocyte growth in the heart. However now, in addition to myocyte hypertrophy, it is thought that new myocyte generation predominates over cell death and contributes significantly to the normal growth of the heart into adulthood (Nadal-Ginard et al., 2003). This is supported by the detection of myocytes undergoing mitosis in the hearts of normal rat (Overy and Priest, 1966), mice (Anversa and Kajstura, 1998) and humans (Kajstura et al., 1998). Consequently, DNA synthesis persists in adult cardiomyocytes (Anversa and Kajstura, 1998). However, these data have been questioned.

In many species cardiac myocytes become multinucleated and exhibit polyploidy (Anversa and Kajstura, 1998). So, some investigators dismissed the mitoses as examples of multinucleation with karyokinesis but without cytokinesis. However, myocytes undergoing true cytokinesis have been identified (Kajstura et al., 1998; Beltrami et al., 2001). Also, it has been reported that there is no increase in the number of multinucleated myocytes after puberty in hearts of both animals and man (Anversa and Olivetti, 2002). Therefore, if the DNA-replicating myocytes underwent karyokinesis without cytokinesis, there would be an increase in the number of multi-nucleated myocytes with age, which is not the case

Another cause for dispute against the existence of myocyte replication and cardiac regeneration is the use of Bromodeooxyuridine (BrdU) as a marker for DNA synthesis, cell division and replication. Its use has sparked continued criticism due to its incorporation into DNA during DNA repair. BrdU is therefore not considered a selective marker of cell replication. However, Ki-67, a nuclear antigen which is expressed in all stages of the cell cycle (except G_0) and is not involved in DNA

repair, has also been detected in myocytes, indicating cell cycling (Beltrami et al., 2001; Anversa et al., 2002; Quaini et al., 2002; Urbanek et al., 2003). Furthermore, with the increased access to highly specialised equipment, i.e. confocal microscopy, analysis can be carried out with greater precision and accuracy than was previously the case. This is undoubtedly another reason why many investigators were unable to reach similar conclusions regarding this area of research.

The strongest argument in favour of new myocyte formation in the adult heart is that there is an increase in myocyte number between birth and young adulthood in both animals and humans (Anversa and Olivetti, 2002). Furthermore, the increase in cardiac mass seen over this maturational time period cannot solely be accounted for by myocyte hypertrophy (Anversa and Olivetti, 2002). Also, the increase in myocyte numbers in the adult heart is an under estimation due to concurrent cell death seen with maturation (Anversa and Olivetti, 2002). The finding of myocyte cell death in the adult heart further supports the concept of cardiac regeneration, because if myocyte renewal did not take place then the cardiomyocytes would simply disappear within a few decades of life (Nadal-Ginard et al., 2003).

It has been shown that cell death, through both necrosis and apoptosis, occurs in the normal heart. Hence, subsequently the number of myocytes will decrease with age (Anversa et al., 1990; Kajstura et al., 1996; Anversa and Olivetti, 2002). Kajstura et al. (1996) found that apoptotic and necrotic myocyte death occurs in the hearts of 3, 7, 12, 16 and 24 month old Fisher 344 rats. Furthermore, the incidence of cell death increased with age and this was associated with ventricular dysfunction and failure, at 16 and 24 months of age (Kajstura et al., 1996). Therefore, myocyte cell death constitutes an important determinant of the ageing process, participating in the occurrence of ventricular dysfunction and failure in the 'old' heart (Kajstura et al., 1996). Together with the occurrence of cell death there is myocyte regeneration, identified by nuclear mitotic division with BrdU labelling (Anversa and Kajstura, 1998). This process of regeneration partially counteracts the death of cells seen with

ageing. Hence, there is ongoing cell death and regeneration throughout the entire life span.

Cell death has been shown to correlate with the size of the cell and the level of cellular senescence (Brenner et al., 1998). It has been shown that large myocytes are older, do not react to growth stimuli and are prone to activate the cell death pathway. In contrast, smaller cells are younger, possess the ability to undergo hypertrophy and are less susceptible to cell death. Also, the smaller cells have been formed more recently and can still undergo a limited number of divisions before withdrawing from the cell cycle (Nadal-Ginard et al., 2003). This concept is supported further by the findings that young adult rats that have been subjected to a myocardial infarction, possess small replicating myocytes 7 days post infarction (Nadal-Ginard et al., 2003).

1.7.1 Myocyte Hyperplasia and Pathological Conditions of the Heart

The level of cell renewal increases significantly under a variety conditions. Studies which have been carried out on both humans (Kajstura et al., 1998; Beltrami et al., 2001; Urbanek et al., 2003) and animals (Anversa and Kajstura, 1998) have provided evidence that myocyte replication occurs under physiological and pathological conditions of the heart (Anversa and Nadal-Ginard, 2002). In the male human heart suffering from advanced chronic ischaemic cardiomyopathy, the measured incidence of myocyte cell death by apoptosis and necrosis (at a given time point) are 0.18% and 1.2%, respectively. Using these data, the diseased heart could not continue to function in the absence of new myocyte formation. It has been found that myocyte regeneration is an important contributor to the maintenance of cardiac mass under these physiological and pathological conditions of the heart (Nadal-Ginard et al., 2003).

The magnitude of haemodynamic stress may be the main determinant of whether cellular hypertrophy or hyperplasia is initiated in the pathological heart (Anversa and Kajstura, 1998). It has been shown that a gradual or moderate increase in

cardiac workload ensures that myocyte hypertrophy predominates (Anversa et al., 1978). In contrast, a severe increase in workload, whether acute or chronic in nature, results in myocyte DNA synthesis, mitosis and proliferation in both animals and humans (Kajstura et al., 1994; Anversa and Kajstura, 1998; Kajstura et al., 1998; Beltrami et al., 2001; Urbanek et al., 2003).

Anversa and Kajstura (1998) have shown the presence of DNA replication and mitotic divisions in myocytes of the decompensated post-infarcted rat heart. Subsequently, it was documented that the number of nuclei per cell does not change in the failing heart of rats (Anversa et al., 1990), verifying that increases in the number of myocyte nuclei must correspond to increases in myocyte number. In an excellent study by Kajstura et al. (1998) it was reported that in humans 882 x 10^3 and 760 x 10^3 myocytes were undergoing mitosis in the entire ventricular myocardium affected by ischaemic or idiopathic dilated cardiomyopathies, respectively. These figures compare with 81.2 x 10^3 myocytes undergoing mitosis in normal control hearts. More recently, Beltrami et al. (2001) found that in infarcted human hearts there was an increase in Ki-67 expression in myocyte nuclei in regions adjacent to and distant from, the infarcted area. Also, events characteristic of cell division, e.g. the formation of mitotic spindles and contractile rings, karyokinesis and cytokinesis, were identified. This further demonstrates that there is myocyte proliferation in the viable myocardium after a myocardial infarction (Beltrami et al., 2001). It should however be noted that the replicating myocytes are not detectable in the infarcted area, making regeneration in this area impossible (Anversa et al., 2002).

With pressure-volume overload there is also evidence of myocyte regeneration. Urbanek et al. (2003) reported that in human aortic stenosis there is an increase in cardiac mass, resulting from a combination of myocyte hypertrophy and hyperplasia (Urbanek et al., 2003). These findings challenge the 'heart weight theory' that suggests that cell replication is secondary to exhausted myocyte hypertrophy (Nadal-Ginard et al., 2003). Therefore, evidence does exist which suggests that the

heart has the capability to replicate myocytes, which contributes to the formation of new muscle mass. However, where do these new cycling myocytes come from?

The cycling cells could come from 2 possible sources; i) cells which are resident within the heart, i.e. cardiac stem cells, or ii) systemic cells, i.e. BM-derived stem cells which continuously colonise the myocardium and contribute to myocyte renewal (Nadal-Ginard et al., 2003). It has previously been shown that BMDCs can give rise to new myocytes either when injected into, or stimulated to 'home to', the heart by cytokine administration following a myocardial infarction (Orlic et al., 2001a, b).

In a study performed by Quaini et al. (2002) human sex-mismatched heart transplants were performed. When a female heart was transplanted into a male host, this led to the findings that host cells homed to the transplanted heart and they could be identified by the presence of the Y chromosome (Quaini et al., 2002). They showed that 9%, 10%, and 7% of myocytes, smooth muscle, and endothelial cells, respectively possessed the Y chromosome. Furthermore, 17%, 14%, and 16% of these male (Y chromosome) myocytes, smooth muscle and endothelial cells, respectively, were replicating as identified by labelling with Ki-67.

The study also reported cells expressing c-kit, MDR1 or Sca-1 in the atria and left ventricle, of which 12-16% of these cells contained the Y chromosome. These particular markers identify stem cells, but are not exclusive to this population of cells. These particular cells were undifferentiated and were negative for markers of BMDCs, e.g. CD45. They were also negative for markers of differentiated myocytes (e.g. sarcomeric α-actin), endothelial cells (e.g. CD31, Factor VIII and vimentin), smooth muscle cells (e.g. smooth muscle α-actin and desmin) and fibroblasts (e.g. vimentin) (Quaini et al., 2002). These primitive cells were also present in control hearts, but at lower percentages.

To identify the cells involved in the generation of new myocytes, the transcription factors MEF2D and GATA4 were recognised in Y-chromosome bearing cells, showing that these cells were committed to myocyte differentiation. Also, the intermediate filament protein, nestin, was identified indicating a more advanced stage of myocyte differentiation (Quaini et al., 2002). Therefore, this study showed that undifferentiated, primitive cells expressing surface stem cell-related antigens (c-kit, MDR1, Sca-1) are present in both control hearts and in female transplanted hearts into male recipients. Because some of these cells were Y chromosome-positive, they must have translocated from the host into the atria and ventricles of the grafted heart. Once there, they lose the marker properties of stem cells, proliferate, acquire their mature phenotype, and subsequently give rise to myocytes, coronary arterioles and capillaries (Quaini et al., 2002).

This study does not however identify the source of these primitive cells that lead to the cardiac chimerism. It is possible that circulating haematopoietic stem cells from the recipient could have translocated to the implanted heart. Although Quaini et al. (2002) found that cells expressing c-kit, MDR1 or Sca-1 were negative for markers of bone marrow differentiation, it is still possible that stem cells were mobilised from the bone marrow and reached and infiltrated the transplanted heart (Quaini et al., 2002).

Interestingly, the same study did identify a high number of undifferentiated, primitive cells in the transplanted heart that were negative for the Y chromosome. This suggests that groups of primitive cells may reside in the heart, and are able to multiply and acquire cardiac cell lineages. This is supported by the presence of cycling myocytes (Ki-67 positive), which were present in the female heart but were Y chromosome negative (Quaini et al., 2002).

Although the study of Quaini et al. (2002) failed to identify the origin of these primitive cells, it is significant that it provides clear proof of new myocyte formation in the adult heart and that there are 'stem-like' cells which are able to

differentiate into the 3 types of cell (myocyte, smooth muscle and endothelial cell) within the heart (Nadal-Ginard et al., 2003). But can these primitive cells be termed 'cardiac stem cells'?

Beltrami et al. (2003) recently reported the existence of Lin^- $c\text{-}kit^{pos}$ cells (Lin^- is a blood lineage marker; c-kit a stem cell marker) in the rat myocardium, with the properties of cardiac stem cells. These cells are negative for myocyte (α-sarcomeric actin, cardiac myosin, myosin, desmin, α-cardiac actinin and connexin 43), endothelial cell (Von Willebrand factor, CD31 and vimentin), smooth muscle cell (α-smooth muscle actin and desmin), and fibroblast (fibronectin, procollagen I and vimentin) cytoplasmic proteins.

Beltrami et al. (2003) identified one Lin^- $c\text{-}kit^{pos}$ cell for approximately every 10^4 myocytes. Also, all of the detected $c\text{-}kit^{pos}$ cells were negative for CD45 and the endothelial/haematopoietic progenitor marker CD34. The Lin^- $c\text{-}kit^{pos}$ cells were found in small clusters in the interstitium between well-differentiated myocytes. In agreement with Quaini et al. (2002), many of these Lin^- $c\text{-}kit^{pos}$ cells expressed Ki-67 (indicative of a cycling cell), and the transcriptions factors GATA-4 and MEF2, indicative of cells at the early stages of cardiac myogenic differentiation. Also, there were small amounts of sarcomeric proteins in their cytoplasm. This is strong evidence of their cardiac myogenic potential and fate (Beltrami et al., 2003).

This study also established a precursor-product relationship. Lin^- $c\text{-}kit^{pos}$ cells were isolated from the rat myocardium and then injected into an ischaemic heart bringing about the formation of new blood vessels and myocytes, with the characteristics of young cells, encompassing ~70% of the entire ventricle just 20 days after the infarction (Beltrami et al., 2003). Following *in vitro* and *in vivo* testing, Beltrami et al. (2003) reported that the cardiac Lin^- $c\text{-}kit^{pos}$ cells were self renewing, clonogenic and multi-potent, giving rise to 3 different cardiogenic cell lineages; myocytes, endothelial cells and smooth muscle cells.

Beltrami et al. (2003) found that stem cell implantation into the area bordering the infarct resulted in a reduced infarct size, cavity dilation and diastolic stress, while increasing wall thickness, ejection fraction and improving end-diastolic pressure and dP/dt, an indicator of contractility. Also, Beltrami et al. (2003) reported that the myocytes produced by the cardiac Lin^{-} $c\text{-}kit^{pos}$ cells were structurally and functionally competent when their contractile parameters (time-to-peak shortening; peak shortening and velocity of shortening) were compared with the spared myocytes *in vitro*. Therefore, Lin^{-} $c\text{-}kit^{pos}$ cells are able to generate *bona fide* cardiac myocytes, which are functionally and structurally similar to the spared myocytes (Beltrami et al., 2003). Subsequently, the new myocardial cells improved the overall function of the heart due to the complete differentiation of the isolated Lin^{-} $c\text{-}kit^{pos}$ cells into myocytes. Interestingly, the injected cells were attracted to the ischaemic zone, as it was shown that regenerating cells (i.e. BrdU positive) were located in the necrotic area and not the spared, surrounding viable myocardium even though the cells were injected at the border between the ischaemic and healthy myocardium (Beltrami et al., 2003).

This excellent study by Beltrami et al. (2003) clearly shows the presence of undifferentiated cells in the adult heart, which could potentially be cardiac stem cells. However, whether these cells reside in the heart or continuously colonise the heart via the circulation still remains an unanswered question. Both possibilities may be correct. The isolated Lin^{-} $c\text{-}kit^{pos}$ cells were negative for markers of bone marrow (CD45) and endothelial/haematopoietic progenitor marker CD34, suggesting that if they did reach the myocardium from the circulation they may have resided in the myocardium for long enough to adopt the myocardial specific phenotype (Beltrami et al., 2003). But perhaps the most important point is that they actually exist and that new myocyte formation does occur in the heart.

1.7.2 Cellular Therapy

Although the full process of cellular renewal exists in the myocardium, by itself the heart appears to be unable to reconstitute all the lost myocardium after coronary artery occlusion. Therefore, a number of protocols involving cell therapies have been investigated in both animals and humans, in an attempt to replace lost myocytes with autologous or heterologous contractile cells injected into, or around, the necrotic infarcted area (Nadal-Ginard et al., 2003).

Many investigations have focused on different types of cells, including embryonic stem cells (Behfar et al., 2002; Mummery et al., 2003), skeletal myoblasts (Tambara et al., 2003; Thompson et al., 2003), bone marrow and haemopoietic (Orlic et al., 2001a, b; Yeh et al., 2003), or cardiac stem cells (Beltrami et al., 2003) in attempts to find the best type and source of cell to reconstitute the myocardium and improve function following myocardial damage. However, research into this particular area of cardiovascular medicine is in its early stages. Only a few clinical trials have been conducted thus far (Menasche et al., 2003; Perin et al., 2003; Kang et al., 2004). These have reported improvement in cardiac function, of which the mechanism remains uncertain, but it has been difficult to demonstrate long term benefit. Also, there are reported negative side effects (Menasche et al., 2003; Kang et al., 2004). These may be related to the type of cells that have been used. One problem with injecting skeletal myoblasts is the differentiation of these cells into myotubes and skeletal muscle fibres, but not cardiomyocytes. These fail to create gap junctions, due to lack of connexin 43, with existing cardiomyocytes and hence electromechanical coupling is unlikely. Furthermore, this could contribute to the serious adverse event of ventricular arrhythmias reported in some patients (Menasche et al., 2003). The use of primary fetal or neonatal cardiac myocytes, or cell lines derived from embryonic stem cells, proposes to be an attractive alternative. However, due to the difficulty in obtaining sufficient cells in order to make a functional difference, as well as consequent problems with histocompatibility and immuno-suppression, this approach has also proved to be far from ideal. It is important to state that this field of biomedical research is a long way

from identifying the most appropriate intervention to help remodel and repair, and hence improve the performance, of the infarcted heart. Also, in recognising the detrimental consequences of such cell therapy procedures.

Some investigators have not been able to replicate other peoples' findings and disagree on the transdifferentiation of BMDCs into cardiomyocytes in the infarcted area, as reported specifically by Orlic et al. (2001a, b) and others (Laflamme et al., 2002; Deb et al., 2003), when injected into the myocardium (Murry et al., 2004; Balsam et al., 2004; Nygren et al., 2004). To follow haematopoietic cell fate, Murry et al. (2004) used cardiomyocyte-restricted (MHC-nLAC and MHC-enhanced green fluorescent protein (EGFP)) and ubiquitously expressed (β-actin-EGFP) reporter transgenes. They reported no transdifferentiation of these cells into cardiomyocytes when injected into infarcted mouse hearts. Similar results were reported by Balsam et al. (2004). These workers showed that haematopoietic stem cells from transgenic mice, and expressing GFP, did not transdifferentiate into cardiomyocytes when injected directly into ischaemic myocardium, as evidenced by these GFP^+ cells failing to express cardiac-specific tissue markers. Furthermore, they found no evidence of myocardial regeneration from blood-borne partner-derived cells when using GFP^+-GFP^- parabiotic mice (Balsam et al., 2004). There are certain technical problems within both studies which could explain why they failed to replicate strongly accepted scientific evidence. In particular, it is not certain that Murry et al. (2004) were successful in the actual injection of the BMDCs into the infarcted region of the myocardium. Furthermore, the extent of the infarct may determine whether regeneration takes place and Murry et al. (2004) caused considerably less damage than that in previous studies. The use of a parabiotic mice model in the Balsam et al. (2004) study is non-physiological, and bears no relevance to real life situations. The resolution of image analysis in both studies was poor, therefore detection of newly formed cardiomyocytes, previously found using high resolution confocal microscopy, could have been missed. Finally, and most importantly, both studies failed to screen for markers of myocyte proliferation (ki67 or BrdU), which

would undoubtedly represent regenerative processes if occurring in the myocardium.

Both studies (Murry et al., 2004; Balsam et al., 2004) suggested that previous investigations which had reported the transdifferentiation of BMDCs into cardiomyocytes were probably not due to transdifferentiation, but as a result of cell fusion with existing myocytes. Using BMDCs which were GFP^+ and endogenous cardiomyocytes carrying the LacZ transgene, Nygren et al. (2004) recently reported the low frequency existence of bone-marrow derived cardiomyocytes outside the infarcted myocardium, which were derived exclusively through cell fusion following BMDC transplantation. This was evidenced by X-gal precipitate within the cytoplasm of the GFP^+ cardiomyocytes. Furthermore, bone-marrow derived cardiomyocytes were typically bi-nucleated when stained with Hoechst 33342 (Nygren et al., 2004).

It should be noted that these above studies question the use of BMDCs to successfully reconstitute myocardium after an infarct. The identification and use of cardiac stem cells to generate new myocardium has never been disputed and their existence has been confirmed by three different groups (Beltrami et al., 2003; Oh et al., 2003; Matsuura et al., 2003). Beltrami et al. (2003) reported that the regenerating myocytes found in rat myocardium after transplantation of cardiac stem cells into the bordering regions of an infarct, was not the result of cell fusion between injected cells and spared myocytes. Five reasons conclusively argue against cell fusion in this study. First, the number of new myocytes that was generated was greater than the number of injected cells, which in addition also gave rise to smooth muscle and endothelial cells. Second, the myocardial infarct resulted in very few surviving, spared myocytes in this area, leaving no fusion partners. Third, no small myocytes (BrdU or GFP^+) were found in the spared myocardium, where differentiated fusion partners were in abundance. Fourth, the newly formed myocytes in this study were smaller than the fully differentiated myocytes, indicating their immature nature. The product of cell fusion would lead to myocytes

being as large as the differentiated partner. Finally, regenerating myocytes had a 2n DNA content and not the 4n expected for fusion products.

Strategies to increase and improve the differentiation of cardiac stem cells into myocytes following injury are areas of ongoing investigation. The ultimate aim is the endogenous promotion of their migration and activation, as opposed to the injection of these cells into the myocardium after infarction. Interestingly, it has been shown that cardiac stem cells express c-met, the selective receptor of HGF, and that HGF promotes cardiac stem cell migration (Chimenti et al., 2002). Indeed, local injections of HGF and IGF-1 aid the repair of infarcted hearts in mice, with the numbers of viable cardiac stem cells increasing in the border zone, the infarct and the remote surviving portion of the wall. This results in myocyte regeneration two weeks later, with the new myocardium containing parenchymal cells and coronary vessels consisting of resistance arterioles and capillaries (Chimenti et al., 2002).

In summary, there is clear evidence that the heart is not a terminally differentiated organ and cell death and new myocyte formation is involved in the normal homeostasis of the heart. Furthermore, the heart has cardiac stem-progenitor cells supporting myocyte regeneration. The level of cell replication, renewal and hypertrophy increases under a variety of physiological and pathological conditions, thereby contributing to the formation of new muscle mass. With ischaemic heart disease these processes are restricted to the remaining viable myocardium and the border regions around the infarct. Therefore, the concept of stem cell therapy has become an attractive intervention for repairing the injured myocardium to maintain or improve cardiac function. However, the efficacy of such therapies still has to be established.

1.8 Cardiac vs. Skeletal Muscle

As this thesis focuses on the cell death and regeneration in skeletal and cardiac muscle, the similarities and differences between these 2 muscles will now be discussed. Fundamentally, 3 types of muscle tissue exist: (1) skeletal (2) cardiac and (3) smooth muscle.

The basic contractile cells of skeletal muscle are the muscle fibres. These are individually surrounded by connective tissue (endomysium) and grouped into bundles by perimysium to form a skeletal muscle (Charge and Rudnicki, 2004) (Figure 1.5). Muscle fibres express different characteristic protein molecules, principally different myosin heavy (MHC) and light chain isoforms and levels of metabolic enzymes (creatine kinase; succinate dehydrogenase). Myosin heavy chains are the molecules primarily responsible, together with actin, for cross bridge formation and the contraction of muscle fibres. MHCs are composed of two major domains. One, a rod that with another rod of MHC forms a α-helical coil, making up the principal component of thick filament. The other domain, a head that binds to actin, has actin-catalysed ATPase activity, and works in a ratchet fashion along the thin filament to bring about contraction and shortening of the muscle (Hughes et al.,1993).

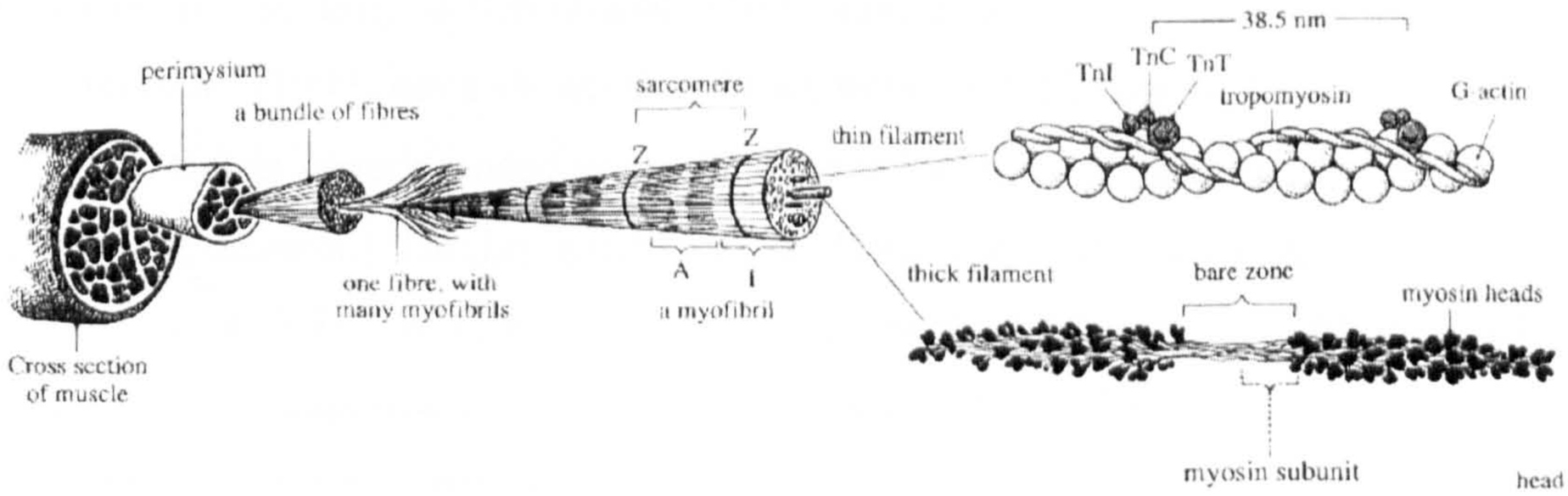

Figure 1.5 Skeletal muscle structure (Goldspink and Cox, 1997).

Individual adult skeletal muscles are composed of a mixture of muscle fibres with different physiological properties due, in part, to the presence of different MHC isoforms and ATPase activities. The activity of the ATPase determines the rate of splitting ATP and hence velocity of shortening. Also, ATPase activity can be used to histochemically distinguish different fibre types. Fibre types within skeletal muscles range from slow-contracting/fatigue resistant types to fast contracting/easily-fatigued types. It is generally accepted that slow fibres have a low ATPase activity, while fast fibres have higher ATPase activities (Jones and Round, 1990). The proportion of each fibre type within a muscle determines its overall contractile properties. For example, the soleus muscle is termed a slow-twitch muscle, due to its high proportion of fibres expressing the slow type I MHC isoform. In contrast, the fast contracting tibialis anterior muscle is composed predominantly of fast type IIa and IIb MHC isoforms. Therefore, there are 3 major fibres types: slow (Type I, SO) fast-oxidative (Type IIa, FOG) and fast-glycolytic (Type IIb, FG). Their general characteristics, and how these compare to cardiac muscle cells, are outlined in Table 1.1.

Different MHC isoforms are expressed during development as muscle fibres are formed (via myoblast fusion), grow and then reach their adult status. Initially, an embryonic MHC is expressed. The expression of this isoform then declines and is replaced by a neonatal MHC isoform before the temporal expression of the adult isoforms in the fully differentiated adult muscle fibre (Schiaffino et al., 1989). Hughes *et al.* (1993) have shown that the expression of fibre-type specific isoforms, i.e. slow/fast is superimposed upon the expression of stage-specific isoforms (e.g. embryonic/neonatal). Hughes and associates (1993) reported the onset of expression of three slow MHC isoforms during development of humans and the rat. These findings were supported by the work of Narusawa *et al.* (1987), who found that the slow MHC isoform, normally expressed in the adult soleus, was expressed along with embryonic MHC in primary generation myotubes of limb muscles in the 16 day old rat foetus. In this multi-gene family, the order of the gene on the chromosome determines their sequential expression. Tonic innervation is required

for slow isoform expression in skeletal muscle. Notably, the slow skeletal muscle isoform is identical to the β-cardiac MHC isoform.

Table 1.1 Characteristics of the 3 major skeletal muscle fibre types (Type I, SO; Type IIa, FOG; Type IIb, FG) and cardiac muscle cells.

	Type I	Type IIa	Type IIb	Cardiac
Morphology				
Location and number of nuclei	Peripheral and multi-nucleated			Central and single, bi- or tri-nucleated
Colour	Red	White/Red	White	Red
Fibre diameter	Small	Intermediate	Large	Very small
Capillaries	High	Intermediate	Low	High
Mitochondria	High	Intermediate	Low	High
Biochemistry				
Myoglobin	High	Intermediate	Low	High
Myosin ATPase	Low	High	High	Low
Glycolytic capacity	Low	High	High	Low
Oxidative capacity	High	Medium/High	Low	High
Function				
Speed of contraction	Slow, voluntary control	Fast, voluntary control	Fast, voluntary control	Very slow, autonomic control
Fatigability	Low	Moderate/High	High	Low

Mitochondria, abundant in cardiac and slow muscle fibres, contain a number of pro- (cytochrome c and apoptosis-inducing factor (AIF)) and anti-apoptotic molecules (Bcl2), the expression or release of which can determine cell fate. This release can

be triggered by a variety of external stimuli and appears to be regulated by the Bcl-2 family of proteins associating with the inner and/or outer membranes of the mitochondrion. Second, mitochondria produce reactive oxygen species (ROS). These ROS produced in mitochondria in proportion to tissue oxygen utilization, have both direct effects on cell death, as well as indirect effects via the activation of transcription factors. These promote the selective transcription of genes which are implicated in regulating the formation of the permeability transition pore, and the subsequent release of cytochrome c and AIF. Thus, the combination of mitochondrial content as well as the high respiration rate could make cardiac muscle and slow skeletal muscle particularly susceptible to apoptosis via the mitochondrial pathway (Primeau et al., 2002).

Another important feature that cardiac muscle cells and slow muscle fibres have in common is the presence of the PLB (Simmerman and Jones, 1998). In cardiac and slow skeletal muscle SR, but not in fast skeletal muscle SR, the Ca^{2+}-ATPase (SERCA2) is subject to regulation by PLB, an intrinsic SR protein that is naturally co-expressed with SERCA2 (and not SERCA1) isoform (Simmerman and Jones, 1998). It is widely recognised that dephospho-phospholamban inhibits Ca^{2+}-ATPase function through physical interaction with the enzyme, and dissociation of the two proteins upon phosphorylation of PLB by PKA relieves the inhibition. The differences between the cardiac and slow, compared with fast, muscle fibres for the presence of PLB could have implications for initiating cell death in these different muscles, considering that Ca^{2+} overload is the underlying mechanism for catecholamine-induced cardiomyocyte death (Mann et al., 1992).

As previously discussed it is now apparent that, like skeletal muscle, the heart is not a post-mitotic organ. It possesses the capacity to form new myocytes. This is brought about by the activation and ensuring proliferation and differentiation of the resident stem cells, present in both tissues.

As outlined above there are several similarities and differences between skeletal and cardiac muscle, in terms of contractile, metabolic and regenerative properties. Overall, the slow contracting type I skeletal muscle fibres are similar to cardiac muscle cells, whereas faster fibres differ. The present study questions whether the 2 different types of muscle tissue will respond in the same way to the effects of catecholamines. More precisely, due to the close relationship between slow skeletal muscle fibres and cardiac muscle, will this mean that they will react differently when compared to the fast skeletal muscles? Furthermore, are the effects of catecholamines specific for a population of cells, i.e. differentiated cells or progenitor cells, if the latter then perhaps impairing the capacity of regeneration in each tissue? Overall, the following questions are asked: Is the cellular response to catecholamines the same in skeletal muscle as it is in the heart, and is the effect specific to mature or immature cells?

Aims and Objectives

1. To examine the effects of acute catecholamine exposure on skeletal muscle, in terms of cell death and the time course and sequence of events in the regeneration process, including the involvement of satellite cells and MGF in this process.
2. To investigate the effects of acute catecholamine exposure on the heart, in terms of cell death and the adaptation of the heart, in terms of cellular renewal and hypertrophy and the functional consequences.
3. To examine the effects of chronic catecholamine exposure on skeletal muscle, in terms of cell death and consequent regeneration, and the adaptation of skeletal muscle through fibre hypertrophy and growth.
4. To investigate the effects of chronic catecholamine exposure on the heart, in terms of myocyte death, fibrosis and hypertrophy.

2.0 METHODS

2.1 Fibre Death and Skeletal Muscle Regeneration

2.1.1 Animals and husbandry

Male, Wistar rats (264 ± 22g) derived from a conventional colony at John Moores University were housed under controlled conditions of 25°C, 50% relative humidity and a 12 hr light (6:00 – 18:00) and 12 hr dark cycle, with water and food (containing 18.5% protein) available *ad libitum*. All experimental procedures were carried out under the British Home Office Animal (Scientific Procedures) Act 1986.

2.1.2 Experimental design

Time course of catecholamine-induced damage

Muscle damage was induced by a single, subcutaneous injection of isoprenaline at a dose of 20 mmol kg^{-1} (i.e. 5 mg kg^{-1}). Rats were killed 3, 9, 12, 18, 24, 48 or 72 hrs following this administration of isoprenaline. Additionally the natural catecholamines, adrenaline and noradrenaline, were also investigated for closer relevance to sporting activities as well as medical conditions. In these experiments rats were only killed 18 hrs after equimolar 20 mmol kg^{-1} (6.7 mg kg^{-1}) subcutaneous injections.

Control groups of rats (n=5) were run along side the experimental groups, and received an equivalent volume (~0.3ml) of the saline vehicle only, without any of the synthetic or natural catecholamine.

Fibre regeneration and the time course of the regenerative process

Figure 2.1 shows a schematic representation of the experimental design. Animals were randomly divided into groups of n = 5 for each time point. Each animal was administered a single injection of either 20 mmol of isoprenaline kg^{-1} or adrenaline kg^{-1} at day zero. This dose has been shown in our lab (Ellison et al., 2002) to cause significant necrosis and apoptosis in the soleus muscle.

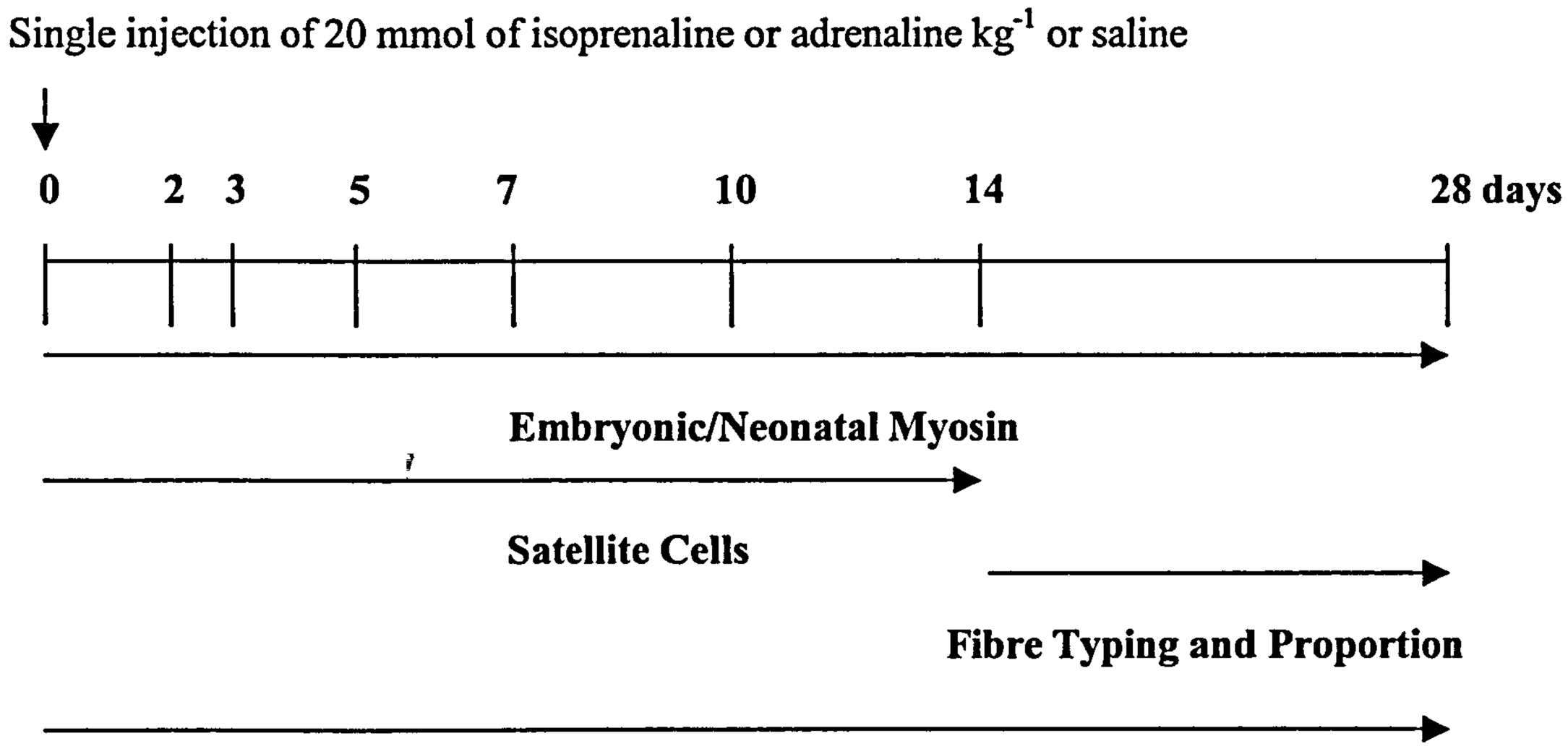

Figure 2.1 Schematic representation of the time course of the regenerative process.

Regenerating fibres were detected using an embryonic/neonatal antibody (Ab), following fibre damage (necrosis and/or apoptosis) induced by either isoprenaline or adrenaline administration. Changes in fibre type proportions and number (based on myosin ATPase/SDH staining) following regeneration were also studied. Possible developmental changes in both fibre number and type could conceivably occur over the 28 day duration of these studies. It was important to verify or exclude this possibility by examining control (non-damaged) muscle between 0 and 28 days.

The regeneration of skeletal muscle following catecholamine-induced injury was monitored by killing animals at specified time points over 28 days (Figure 2.1).

Continuous infusion of catecholamines

Chronic delivery of either isoprenaline, adrenaline or saline was facilitated using osmotic mini-pumps (i.e. Alzet Model 2002 delivering 0.5µl/hr, or 2004 delivering 0.25µl/hr; Charles River, UK). These were implanted subcutaneously in the dorsal region via a small interscapular incision using sterile surgical technique, while the animals were under light isoflurane anaesthesia. Isoprenaline bitartrate or adrenaline hydrochloride (Sigma, Poole, UK) was prepared in 0.9% sodium chloride (pH 5.5) at a concentration calculated to deliver 20 mmol $kg^{-1}d^{-1}$ during either a 5, 7, 14 or 28 day infusion period (n=20, 5 per group). Sham-operated (Placebo) rats received pumps filled with 0.9% sodium chloride for 7, 14 and 28 days (n=15, 5 per group).

All rats were killed by cervical dislocation and the heart, soleus, diaphragm, tibialis anterior and plantaris muscles isolated. To establish whether continuous exposure of catecholamines had caused hypertrophic growth in the heart and skeletal muscles, the weights of the heart and each skeletal muscle were recorded for each animal. For the heart, the atria were dissected from the ventricles and the ventricles mounted on cork discs apex uppermost. Cross-sectional samples taken from the mid-belly region of each skeletal muscle were mounted on cork discs and supported by a piece of liver. Longitudinal samples were also mounted on cork discs for each muscle. Tissues were embedded in optimal cutting temperature compound, immediately snap frozen in super-cooled isopentane and stored at -80°C. These were subsequently cryo-sectioned at 5µm (Leica, CM3050S), mounted on microscope slides and stored at -20°C until analysed, as described below.

2.1.3 Analytical procedures

Detection of fibre necrosis and apoptosis

Necrosis

Myocyte or fibre specific necrotic damage was detected using a mouse anti-myosin monoclonal Ab *in vivo* (Benjamin et al., 1989; Kajstura et al., 1996; Goldspink et al., 2004). All animals received 1 mg of the anti-myosin Ab kg^{-1} intraperitoneally (i.p.) 1h prior to either the saline vehicle (control), isoprenaline, adrenaline or noradrenaline injection. Significant levels of the Ab have been shown to remain in the circulation for up to 72 hours (Benjamin et al., 1989), i.e. well within the time frame of these experiments. Once introduced into the circulation, this Ab only permeates the disrupted membrane of necrotic myocytes and is too large to pass into viable myocytes. Once inside the necrotic myocyte or fibre it binds to myosin heavy chain where it can be visualised. It is therefore an excellent, highly sensitive and selective method for detecting myocyte necrosis. This Ab is not commercially available and was obtained through collaboration with Prof. W. A. Clark (Michael Reese Hospital, Chicago, USA). It is therefore an 'in house' method. Due to limited availability of the myosin Ab, it was only injected into the 18 hr group. This time point has been shown previously within our laboratory to cause significant cardiomyocyte and muscle fibre specific necrosis in the soleus muscle (Goldspink et al., 2004).

For the continuous infusion of catecholamines, 12 animals received 1 mg of the anti-myosin Ab kg^{-1} intraperitoneally 24 hrs prior to being killed. These animals were n=3 for the 7 day adrenaline, isoprenaline or sham-operated group and n=3 from the 14 day isoprenaline group.

Cellular apoptosis

Apoptosis was detected *in vitro* on 5μm serial cryo-sections. A rabbit anti-caspase 3 1°Ab (1:200 dilution; R&D systems, Abingdon, UK) was used to detect the activated caspase 3 enzyme. Sections were incubated for 1 hour at 37°C. This enzyme is only activated in apoptotic cells (Saraste and Pulkki, 2000). A positive

control for apoptosis, using sections of lactating mammary glands (Majno and Joris, 1995) was run along side all experimental sections, in order to ascertain antibody specificity, accuracy and reliability of the staining protocol on a day to day basis.

Immunofluorescence

For the time course of catecholamine-induced damage, the anti-myosin 1°Ab and caspase 3 1°Ab were detected in turn using immunofluorescence on the same sections. Sections were incubated for 1 hour at 37°C with fluorescin anti-mouse conjugated 2°Ab (1:200 dilution) and Texas red anti-rabbit conjugated 2°Ab (1:50 dilution; Vector Labs, Peterborough, UK) to visualise necrosis (stained green) and apoptosis (stained red), respectively. Sections were examined under a fluorescent microscope (Nikon E1000) and digitised using a 12-bit cooled digital camera (DVC 1312C).

Standard histochemistry

For the continuous infusion of catecholamines, the anti-myosin Ab was detected using a rabbit anti-mouse horseradish peroxidase-conjugated (HRP) 2°Ab (1 hour at 37°C; 1:200 dilution; Dako) and caspase 3 Ab was detected using a goat anti-rabbit HRP-conjugated 2°Ab (1 hour at 37°C; 1:200 dilution; Vector Labs). The chromogen 3, 3-diaminobenzidine (DAB) (Sigma) and Nova red (Vector Labs) were used to visualise the necrotic and apoptotic cardiomyocytes, respectively. Sections were then counterstained with haematoxylin and permanently mounted before being examined by light microscopy. Negative controls were run in parallel with the experimental slides, these were exposed to the same procedure, but the 2°Abs were omitted.

Quantification

For the time course of catecholamine-induced damage, the number of fibres in the skeletal muscles that were damaged via either necrosis and/or apoptosis were counted (~800 fibres in total) in 4 randomly chosen fields of whole cross-sections of the muscle belly, using image analysis (Lucia G) (x100 magnification). Results

were expressed as the percentage of damaged fibres relative to the total number counted.

For the heart, percent apoptosis (i.e. percent area of positive staining in field of view) was determined using image analysis on 6 randomised fields of view (x 100 magnification) around the LV lumen of heart, and specifically at 2.2 mm from the apex. This method is semi-quantitative and allowed some limited interaction by the operator. Work in our laboratory has shown previously that the peak necrotic and apoptotic damage is localised 2.2mm from the apex along the longitudinal axis and within the sub-endocardium (Goldspink et al., 2004).

For the continuous infusion of catecholamines, the numbers of fibres damaged via either necrosis or/and apoptosis in the skeletal muscles were counted in the entire cross-sections of the muscle belly using image analysis (x100 magnification). Results were expressed as the number and percentage of damaged fibres in the whole soleus.

In the heart, percent necrosis or apoptosis was determined for the entire cross section of the heart at 2.2 mm from the apex, using x100 magnification (~50 fields). Measured fields were selected using a motorized microscope stage which had been programmed to move across the entire cross section. The mean value of all fields quantified for each animal was calculated.

Detection of fibre types

Histochemical staining

The principle is to identify different isoforms of the enzyme, myosin ATPase, by marking the sites of myosin ATPase activity in the muscle fibres. The first stage of the procedure consists of pre-incubating the muscle sections at either an acid or alkali pH. Generally, fast myosins are inactivated at acid pH (between pH 4.3 to 4.6) and slow myosins are inactivated at an alkaline pH, of around pH 9.4. Having inactivated the enzyme activity in one set of fibres during the pre-incubation, the

remaining ATPase activity can be detected by incubating the section with ATP substrate and an excess of calcium at pH 9.4. The inorganic phosphate which is liberated from the ATP couples with calcium to produce a colourless precipitate of calcium phosphate, which is insoluble at this alkaline pH. The section is then placed in a solution of cobalt chloride, and the calcium phosphate precipitate is replaced by cobalt phosphate. After adding ammonium sulphide, the phosphate is replaced, leaving cobalt sulphide a highly visible black-brownish precipitate and marking the sites of myosin ATPase in the muscle fibres. This can then be visualised using light microscopy.

Acid (pH 4.35) and alkaline (pH 10.4) pre-incubation conditions were used to detect 3 fibre types, and the staining methods were based on that described previously by Guth and Samaha (1970). Following pre-incubation for either 30 min or 15 min for acid or alkaline, respectively, the sections were rinsed in solution consisting of 18 mM $CaCl_2$ in 100 mM Tris buffer at pH 7.8 for 2 x 1 min. Sections were then incubated for 15 min at 37°C in a medium containing 2.7 mM ATP, 50 mM KCl, 18 mM $CaCl_2$ in 100 mM 2-amino-2-methyl-1-propanol (AMP) buffer, at pH 9.4. Following incubation with the substrate, slides were washed 3-times in 1% $CaCl_2$, and then placed in a 2% solution of cobalt chloride ($CoCl_2$) for 3 min. Sections were then washed 4-times in an alkaline solution (100mM AMP buffer, pH 9.4) before being placed in a 1% solution of ammonium sulphide (NH_4S) to develop the colour. Sections were finally washed under running tap water, dehydrated, cleared and mounted.

Acid pre-incubation results in the identification of 3 fibre types: type I stain as positive, dark staining fibres, type IIa stain as pale (negative) fibres and type IIb as intermediate staining fibres (Figure 2.2). According to Ranatunga *et al.* (1990), the contraction characteristics of a muscle, i.e. the shortening-velocity and force-velocity relationships closely correlate with the muscle's histochemically-determined fibre type composition. The contraction speed is either faster or slower if more type II or type I fibres predominate within the muscle, respectively.

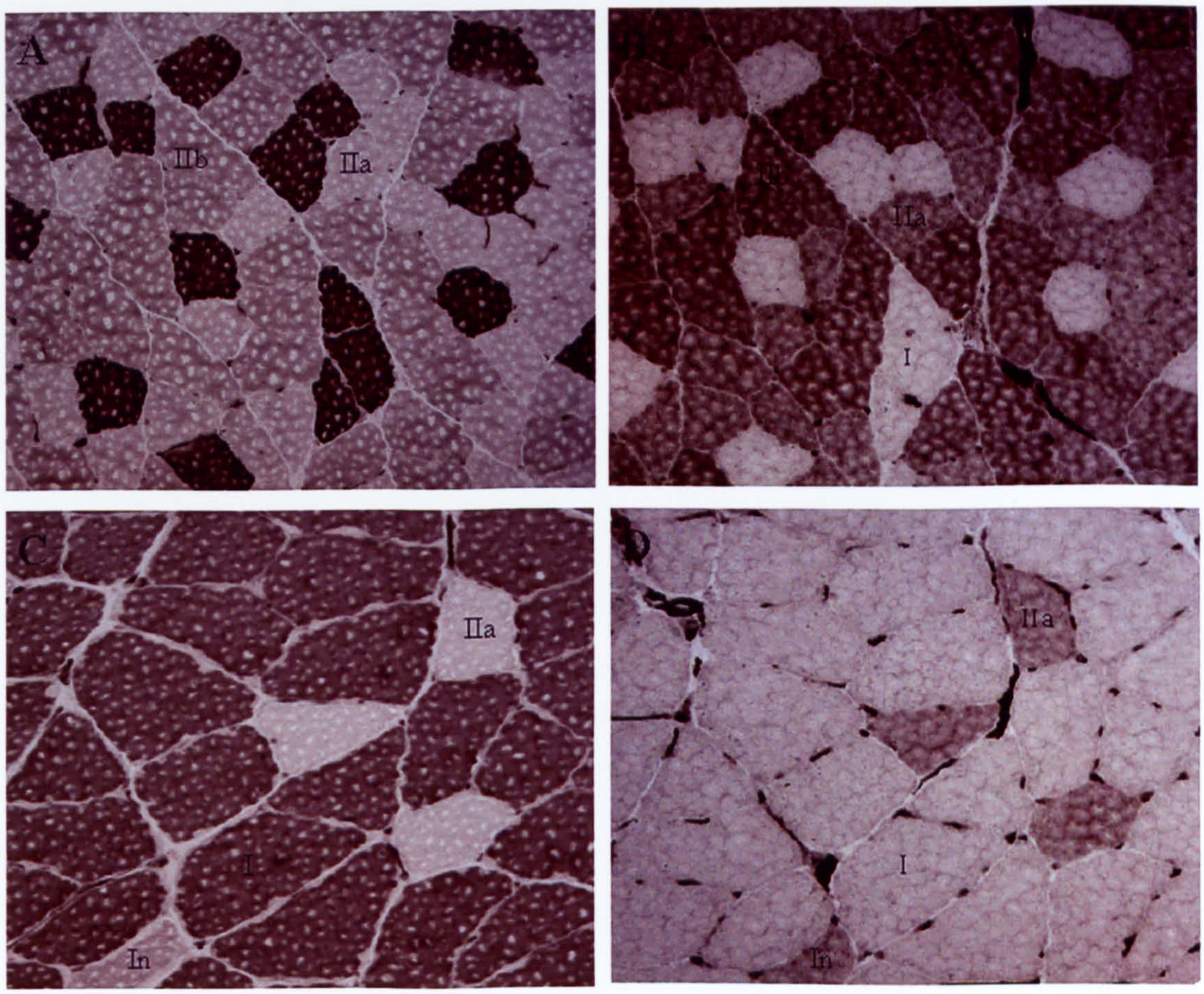

Figure 2.2 Myosin ATPase stain.

Serial cross-sections of the myosin ATPase stain following acid (pH 4.35) (A and C) or alkali (pH 10.4) (B and D) pre-incubation for the plantaris (A and B) and soleus (C and D) muscles. Acid pre-incubation (pH 4.35) results in the identification of 3 fibre types. Type I (dark), type IIa (pale) and type IIb (light brown) for the plantaris muscle (A). The soleus muscle (C) does not contain type IIb fibres but it does contain an intermediate fibre (In) which stains a colour intermediate between type IIa and type I. Alkali pre-incubation (pH 10.4) (B and D) results in the identification of 2 fibre types. Type I (pale) and type II (dark). No discrimination can be made between type IIa and IIb with this stain.

The soleus muscle contains predominantly type I fibres and a minor component of type IIa fibres (Schiaffino et al., 1989). Also found in the soleus are some lighter brown staining fibres that have been classified as intermediate or type IIc fibres (Figure 2.2). The latter possess myosin ATPase activity that is intermediate between type I (positive) and type IIa (negative) (Brooke and Kaiser, 1974).

Alkaline pre-incubation to inactivate slow myosin ATPase activities is the reverse of acid pre-incubation. However, there is no differentiation between the two fast fibre types, IIa and IIb. Therefore, type I fibres appear negatively stained (very pale) and type II fibres positively dark stained (Figure 2.2).

Immunohistochemical staining

To complement the histochemical procedures, more sensitive identification of slow or fast fibres was achieved using selective antibodies against either slow or fast MHC. More specifically, monoclonal anti-slow-twitch and anti-fast-twitch antibodies (Sigma), which are highly specific for the slow or fast MHC of adult skeletal muscle, were used.

Initially, a titration assay was performed in order to determine the optimal working dilution for each Ab against rat skeletal muscles. Table 2.1 shows the dilutions that were assayed and the semi-quantitative staining intensities observed in the muscle fibres. The soleus and tibialis anterior muscles were used specifically in the assay due to their slow and fast contractile properties, respectively.

A working dilution of 1:500 was chosen for both the anti-slow and anti-fast MHC antibodies in relation to quality and intensity of staining and cost. Thereafter, muscle sections were incubated overnight at 4°C with 1:500 dilution of 1°Ab in 5% normal serum and PBS, in a Sequenza staining/histology unit (Thermo Shandon, Basingstoke, UK). The secondary Ab (2°Ab) used was a rabbit anti-mouse conjugated with HRP (1:100 dilution) (Dako, Glostrup, Denmark). The chromogen,

Nova Red (Vector Labs), was used to visualise the slow or fast fibres. The sections were examined under a light microscope.

Table 2.1 Immunohistochemical staining of skeletal muscle.

Titration Assay to determine optimal working dilution for anti-slow and anti-fast MHC antibodies. + denotes poor reactivity, + + + denotes strong reactivity.

	Soleus		Tibialis anterior	
Ab Dilution	**Anti-slow**	**Anti-fast**	**Anti-slow**	**Anti-fast**
1:1000	+	+	+	+
1:500	+++	+++	+++	+++
1:200	+++	+++	+++	+++
1:100	+++	+++	+++	+++

Succinate dehydrogenase (SDH)

Succinate dehydrogenase is an enzymatic component of the inner mitochondrial membrane and is involved in the transfer of hydrogen ions along the oxidative pathway (electron transport chain) of the Krebs cycle.

Succinate dehydrogenase serves as a marker enzyme of aerobic end-oxidation and can be used to classify a fibre's metabolic characteristics (Nemeth and Pette, 1981). By measuring the activity of SDH within a muscle, an idea of the number of mitochondria present and the muscle's oxidative capacity can be obtained.

The staining procedure works by using sodium succinate as a substrate, which is oxidised by SDH. Upon adding an artificial hydrogen ion (H^+) acceptor, e.g. nitroblue tetrazolium (nitro-BT), nitro-BT is reduced producing a blue precipitate. The method used was a modification of those described by Nachlas *et al.* (1957) and Nemeth and Pette (1981). The intensity of the reaction, characterises the metabolism

of the fibre; the higher the oxidative capacity and hence SDH activity, the greater the staining intensity.

The slides were incubated in a solution consisting of 0.67 M Sodium Dihydrogen Orthophosphate, 0.67 M DiSodium Hydrogen Orthophosphate and 0.2M Sodium Succinate at pH 7.0. Nitro-BT (0.1mM) was added and slides were incubated for 1 hr at 37°C. After incubation, slides were fixed in 10% formal saline, washed in phosphate buffered saline (PBS), before being dehydrated, cleared and mounted.

The amount of SDH enzyme activity is different in different fibre types, and this determines staining intensity. Type I and IIa fibres stain positive (blue), whereas type IIb fibres usually stain negative (Figure 2.3). However, it has been found previously that some type IIb fibres can stain positively, such that a poor correlation can exist between the myosin type II identified subgroups (as obtained from the myosin ATPase stain) and the metabolic subgroups (Nemeth and Pette, 1981). These findings suggest that the myosin-based classification system alone may not always be a reliable indicator of the metabolic characteristics of type II fibres. Hence, in the study by Nemeth and Pette (1981), SDH staining was used in conjunction with the myosin ATPase stain for effective fibre typing and classification.

To obtain the proportions of fast and slow fibre types within the soleus muscle, using image analysis (x100 magnification), fibres in the entire cross section at the muscle belly were counted and the percentage of each fibre type calculated.

Newly regenerating fibres

Regenerating fibres were detected using an anti-mouse MHC (developmental) 1°Ab (Novacastra Laboratories, Newcastle, UK). This Ab recognises a MHC present during embryonic and neonatal stages of development in skeletal muscle. The same MHC is re-expressed during regeneration of new muscle fibres (Ecob-Prince et al., 1989; Williams et al., 2001).

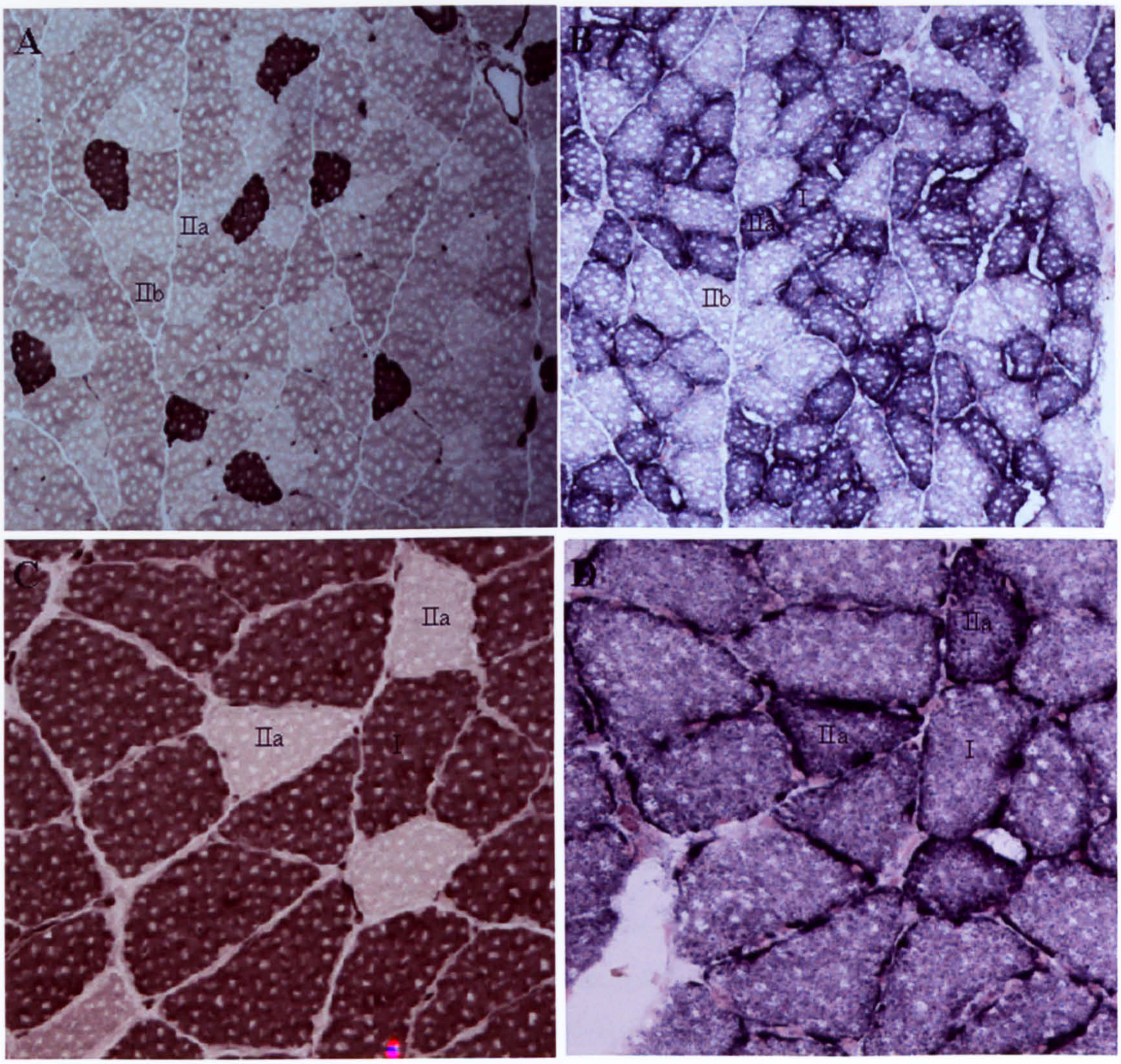

Figure 2.3 Myosin ATPase and SDH stain.

Serial cross sections of the myosin ATPase stain (acid pre-incubation) (A and C) and the SDH stain (B and D) for the plantaris (A and B) and soleus (C and D) muscles. The SDH stain results in the identification of type I and IIa fibres staining as dark blue, exhibiting high levels of SDH enzyme activity, and type IIb fibres staining as light blue, exhibiting low levels of SDH activity and thus low oxidative capacity (B and D).

To detect these newly regenerating fibres, muscle sections were incubated with the 1°Ab (1:20 dilution) either for 1 hr at 37°C, or overnight at 4°C in a Sequenza staining/histology unit. The 2°Ab used was a rabbit anti-mouse, conjugated with HRP (1:200 dilution; Dako). The chromogen DAB (Sigma) was used to visualise the regenerating fibres. Positive control tissue, obtained from 7 day-old rat limb muscles, was stained along side these experimental muscles in order to test antibody specificity, and the accuracy and reliability of this staining protocol. Negative controls were also processed alongside the experimental slides, these were not exposed to the 2°Ab. Stained sections were examined under the light microscope (x100 magnification). Image analysis was used to count both the total number of regenerating fibres (i.e. positive for embryonic/neonatal myosin) and viable adult fibres in whole cross sections derived from the muscle belly. The number of animals for these determinations were n=9 for saline control and n=5 for 2, 3, 5, 7, 10, 14 and 28 days.

Satellite cells

In order to identify satellite cells throughout the stages of skeletal muscle regeneration (1 to 14 days), sections were stained for protein markers of quiescent (c-met) or activated, proliferating and differentiating (the myogenic transcription factor - MyoD) satellite cells (Cornelison and Wold, 1997).

Double immunofluorescence was performed on sections. Sections were exposed overnight at 4°C to a 1°Ab against c-met (1:50 dilution; rabbit polyclonal, Santa Cruz, Autogen Bioclear, UK). Anti-rabbit Texas Red (1:100 dilution; Vector Labs) conjugated 2°Ab was used to detect the 1°Ab, after incubation for 1 hr at 37°C. Sections were then exposed to MyoD (1:50 dilution; mouse monoclonal, Dako) 1°Ab for 2 hr at 37°C. This 1°Ab was detected using Fluorescein (FITC)-conjugated donkey anti-mouse IgG (1:100 dilution; Jackson Immunochemicals, Strathtec, UK). Nuclei were counterstained with the DNA binding dye, 4, 6-diamidino-2-phenylindole (DAPI, Sigma) at 1µg/ml and sections mounted in Vectashield and

viewed under a fluorescence microscope. BrdU incorporated satellite cells were also labelled to identify proliferating satellite cells – see description of technique later.

Mechano-growth factor (MGF)

It has recently been documented that the expression of mRNA for MGF, a splice variant of the IGF-1 gene, is associated with the activation of satellite cells following injury to skeletal muscle (Hill et al., 2003; Hill and Goldspink, 2003). To examine the role of MGF, if any, in the catecholamine-induced damage and repair, the protein expression of MGF in the heart and skeletal muscle was detected using a rabbit polyclonal anti-MGF Ab, kindly gifted by Prof. Geoffrey Goldspink (University College, London). Using immunofluorescence, sections were exposed to the MGF 1°Ab (1:400 dilution) overnight at 4°C. In turn, the MGF 1°Ab was detected using an anti-rabbit fluorescein 2°Ab (1:200 dilution; Vector Labs) after incubation for 1 hour at 37°C. Nuclei were counterstained with DAPI (1μg/ml). Sections were mounted in Vectashield and viewed under a fluorescence microscope (x200 magnification). The number of MGF positive nuclei in 4 randomised fields across the entire cross section of each skeletal muscle were quantified using image analysis. Results were expressed as the percentage of MGF positive nuclei relative to the total number of nuclei (DAPI positive). For the heart, percent MGF expression (percent area of positive staining) was determined using image analysis on 6 randomised fields of view (x 200 magnification) taken from around the LV lumen of heart, at 2.2 mm from the apex. The number of animals for these determinations were n=5 for 3, 9, 12, 18, 24, 48, 72 hours and saline control.

Growth and hypertrophy

To determine whether continuous infusion of catecholamines for 28 days caused significant growth and hypertrophy, the cross sectional areas of 100 muscle fibres at the belly of each soleus muscle were measured on an image analyser at x100 magnification. The number of animals for these determinations were n=5 for 28 days after isoprenaline, adrenaline and placebo saline infusion.

Fibrosis

To establish whether continuous exposure of catecholamines caused significant myocardial fibrosis, sections of the heart and soleus muscle were stained with Sirius red, by the method previously described by Sweat et al. (1964). Serial sections were fixed in 10% formalin in PBS for 20 min. After washing in distilled water for 5 min, sections were incubated at room temperature for 30 min in 0.1% Fast Blue RR in Magnesium Borate buffer at pH 9 (Sigma). Then sections were washed in distilled water before incubation at room temperature for 10 min in 0.1% Sirius red in saturated picric acid (Sigma). Sections were further washed in distilled water before they were dehydrated, cleared and mounted. In this protocol, connective tissue (mainly collagen) stains red and myocytes yellow/orange.

Semi-quantitative evaluation of the amount of myocardial connective tissue was carried out using image analysis (x100 magnification). Percent collagen (percent area of positive staining) was determined in the entire cross section of the heart at 2.2 mm from the apex and in the entire cross section at the muscle belly of the soleus. The number of animals for these determinations were n=5 at 14 days for isoprenaline, adrenaline, saline placebo infusion and zero day control.

2.2 Cardiomyocyte Death and Regeneration

2.2.1 Animals and husbandry

Experiments were performed on 25 Male Wistar rats (Charles River, UK) weighing 336 ± 18g up to 14 days following a single 5mg injection of isoprenaline kg^{-1}. Another group of 5 animals received a single injection of saline and acted as the control rats. Animals were housed under controlled conditions of 25°C, 50% relative humidity and a 12 hr light (6:00 – 18:00) and 12 hr dark cycle, with water and food available *ad libitum*. All animals were injected (i.p.) with 50 mg of bromodeoxyuridine (BrdU) kg^{-1} twice daily until they were killed. Experiments were approved by the New York Medical College.

2.2.2 Cardiac haemodynamics

For haemodynamics measurements, rats were anaesthetised with 30% chloral hydrate (i.e. 400 mg/kg body weight) administered i.p. A Millar microtip pressure transducer (Houston, Texas, USA), connected to a chart recorder, was advanced into the LV cavity through the right carotid artery. This facilitated evaluation of LV end-diastolic and end-systolic pressures, developed pressure and $^{+}dP/dt$ (contraction) and $^{-}dP/dt$ (relaxation) in the closed chest preparation (Torella et al., 2004). The number of animals for these determinations were n=5 at 1, 3, 6, 14 days and saline vehicle controls.

After completion of the haemodynamic measurements, the abdominal aorta was cannulated and the heart arrested in diastole using cadmium chloride ($CdCl_2$). Then the myocardium was perfused with 10% buffered formalin (Orlic et al., 2001a; Orlic et al., 2001b; Beltrami et al., 2003).

The isolated hearts were cut into right and left ventricles, and right and left atria. After being weighed, the long axis of the LV was measured before it was sectioned into 3, i.e. apical, mid and basal regions. Anatomical measurements were taken using the mid region of the LV. From these measurements chamber diameter was calculated by combining the lateral (LD) and anterior-posterior (A-PD) diameters and dividing by 2. LV Chamber volume was determined through the following equation, where LVlgaxis denotes the measurement taken of the LV long axis:

Chamber volume = 4/3*π*LD/2*A-PD/2*LVlgaxis/2 (Anversa and Olivetti, 2002)

Free wall thickness was calculated by dividing free wall area by free wall length. Septum thickness was calculated by dividing septum wall area by septum wall length. After anatomical measurements were taken, samples were embedded in paraffin, cut into 5µm sections on a cryotome and mounted on microscope slides. The LV was sectioned at 2.2 mm from the apex, as this distance has been shown previously to exhibit peak necrosis and apoptosis along the longitudinal axis

(Goldspink et al., 2004). The soleus muscles in these animals were also isolated and fixed in 10% buffered formalin, before being paraffin embedded, cryo-sectioned into 5μm sections and mounted on microscope slides.

2.2.3 Morphometric analysis

The quantitative estimation of the ventricular myocardium requires the application of morphometric methods. Using two-dimensional samples, i.e. tissue sections, and a superimposed grid of test points and line segments, the three-dimensional volume, surface area, number and length of recognizable components through the process of counting can be determined (Anversa and Olivetti, 2002). The population of cells of any given cell type distributed within a tissue may be considered in general terms to be a group of individual compartments existing in a spatial volume (Anversa and Olivetti, 2002). Sections of the LV were stained with H&E. The sub-endocardial, mid-wall and sub-epicardial layers of the LV wall were analysed. Sections were examined at x1000 magnification with a morphometric reticle containing 42 sampling points to determine the area fraction of viable myocytes, dead myocytes and interstitial cells in the myocardium (Anversa and Olivetti, 2002). Cells were classified as dead if they displayed disrupted sarcolemmal membranes and pale cytoplasmic staining, implicating focal necrosis.

The area fraction, A_A, is the fraction of all the points that lie over these cell profiles, P_P, i.e. if 36 of the sampling points lie over viable myocytes, then 34/42 would give an area fraction of 86%:

$$A_A = P_P$$

Conversion of the morphometric area measurements, A_A, to their three-dimensional counterparts is accomplished by stereologic formulas. For any component its volume fraction, V_V, volume per unit volume, is directly equal to its area fraction:

$$V_V = A_A = P_P$$

The sampling error was kept below 10% by counting at least 100 of each cell type (viable myocytes, dead myocytes, and interstitial cells) for each LV layer (sub-endocardium, mid-wall and sub-epicardium). If this number could not be achieved then the entire area of each layer was measured (Anversa and Olivetti, 2002).

The total number of myocytes in the LV, N_T, is evaluated through knowledge of the absolute volume of myocytes V_T. The quantity of V_T was obtained by first calculating the **LV volume** (volume of LV muscle mass) which is determined by dividing the weight of the LV by the specific gravity of muscle tissue, 1.06g/ml (Mendez and Keys, 1960), and then multiplying by the volume fraction of myocytes, V_V:

$$V_T = \text{LV volume} * V_V$$

The myocyte volume, V_C, was determined through measuring ~100 myocyte diameters (**MD**) across the nucleus, in the sub-endocardium with image analysis (Olivetti et al., 1997), and assuming a spherical cross-section (πr^2) and a length, of 100μm. The calculation of myocyte volume poses as a potential limitation of the present methods as the myocyte length is an assumed variable (100μm). This is limiting in the calculation of myocyte volume, as alterations in myocyte growth could occur through changes in both cross-sectional area and length:

$$V_C = \pi * ((MD/2)^2) * 100$$

Thus, the total number of myocytes, N_T (Anversa and Olivetti, 2002), is derived from:

$$N_T = V_T / V_C$$

These determinations were n=5 at 1, 3, 6, 14 days and saline vehicle controls.

2.2.4 Apoptotic cell death

Terminal deoxynucleotidyl Transferase (TdT) assay

Nuclei with all forms of damaged DNA have a high concentration of 3'hydroxyl ends that are a substitute for TdT (Gavrieli et al., 1992). TdT can extend the 3' base of single stranded DNA and overhanging, blunt and recessed 3'bases of double-stranded DNA (Didenko, 2003).

For the reaction of available DNA 3'hydroxyls with TdT, myocardial sections were incubated with a solution containing 100 units/ml of TdT, 2.5 mM cobalt chloride, 0.2 M potassium cacodylate, 24 mM TRIS/HCl, pH 7.2 and 0.5 nM biotin-16-deoxyuridine triphosphate (dUTP) (Roche, Indianapolis, IN) for 30 minutes at 37°C in an humidified chamber. Sections were then incubated in staining buffer containing 4 x salted sodium citrate (SSC) and non-fat dried milk for 30 minutes at room temperature. Then sections were exposed to staining buffer containing, 5µg/ml of fluorescein isothiocyanate-Extravidin (Sigma). Nuclei were counterstained with DAPI and sections were mounted in Vectashield and viewed under a fluorescence microscope. Positive and negative controls were included in the protocol to confirm the specificity of the methods. As a positive control, myocardial sections were treated with DNase I to induce enzymatically the formation of DNA strand breaks. This tissue was treated with this enzyme for 15 minutes at 37°C and after washing in PBS, the TdT assay was performed. Negative controls consisted of incubating tissue sections in which the DNA strand breaks had been enzymatically formed, as described above, but omitting biotin-16-dUTP or TdT from the procedure. This was also carried out on experimental heart sections, where DNA strand breaks had been identified.

In order to determine the fraction of myocyte nuclei labelled by dUTP, the number of dUTP positive myocyte nuclei in each layer of the LV wall (sub-endocardium mid-wall and sub-epicardium) were counted in each 5µm section (x1000 magnification). The number of myocyte nuclei per unit area of tissue was determined by counting the number of myocyte nuclei in an average of 60 fields,

0.6mm^2, so the numerical density of myocyte nuclei in each myocardial area was obtained. By combining these data with the preceding estimations of dUTP labelled myocyte nuclei per unit area of myocardium, the percentage of apoptotic myocyte nuclei was determined (Olivetti et al., 1996). These determinations were n=5 at 1, 3, 14 days and saline vehicle controls.

2.2.5 Immunohistochemistry

Myocyte cytoplasm

Myocyte cytoplasm was labelled by an antibody against α-sarcomeric actin (1:50 dilution; clone 5C5, Sigma) for 2hrs at 37°C and this was detected with Rhodamine (TRITC)-conjugated donkey anti-mouse IgM 2°Ab (1:100 dilution; Jackson Immunochemicals, West Grove, PA). Sections were incubated with 2°Ab for 1 hr at 37°C. Nuclei were counterstained with DAPI. Sections were mounted in Vectashield and viewed under a fluorescence microscope.

Cardiac stem cells

Cardiac stem cells (CSCs) were identified by employing an antibody against the stem cell marker c-kit (Beltrami et al., 2003). Sections were incubated for 2 hr at 37°C with mouse anti-human c-kit (1:50 dilution; DAKO, Carpinteria, CA). The c-kit Ab was detected using a Rhodamine (TRITC)-conjugated donkey anti-mouse 2°Ab (1:100 dilution; Jackson Immunochemicals). Nuclei were counterstained with DAPI. Sections were mounted in Vectashield and viewed under a fluorescence microscope.

Cardiac stem cells were quantified using image analysis. The number of c-kit positive cells was counted for a total of 3 sections of the LV at x1000 magnification. The areas of these 5μm cross sections were then measured using image analysis and the number of c-kit positive cells present was expressed per unit area (Torella et al., 2004). These determinations were n=5 at 1, 3, 6, 14 days and saline vehicle controls.

Cardiac stem cell progeny

To recognize the committed progeny of CSCs, an antibody against a transcription factor expressed early in the myocyte lineage, i.e. GATA4, was used in conjunction with c-kit staining (as described above) on the same section. Sections were stained with an anti-rabbit GATA4 Ab (1:100 dilution; Santa Cruz Biotechnology, Santa Cruz, CA) overnight at 4°C (Urbanek et al., 2003). This 1°Ab was then detected with donkey anti-rabbit FITC (1:200 dilution; Jackson Immunochemicals). Nuclei were counterstained with DAPI. Sections were mounted in Vectashield and viewed under a fluorescence microscope.

Proliferating cardiac stem cells

An antibody against Ki67, a nuclear antigen expressed on all proliferating cells during late G1, S, M and G2 phases of the cell cycle (Novocastra, Newcastle, UK) was employed to identify proliferating CSCs. Sections were incubated overnight at 4°C with Ki67 Ab (1:30 dilution). This in turn was detected using an anti-rabbit FITC (1:100 dilution; Jackson Immunochemicals). Sections were then stained for c-kit (as previously described). Nuclei were counterstained with DAPI. Sections were mounted in Vectashield and viewed under a fluorescence microscope.

Macrophages

To determine the presence and extent of the inflammatory reaction following catecholamine-induced cardiomyocyte damage, tissue sections were incubated with a monoclonal antibody against myeloid cells (CD68; clone ED1; Serotec, Oxford, UK). The antigen is expressed by the majority of tissue macrophages and weakly by blood granulocytes. Sections were incubated overnight at 4°C with mouse anti-rat CD68 (1:50 dilution) and this was recognized with FITC (1:100 dilution). Myocyte cytoplasm was labelled as previously described, using the anti-α-sarcomeric actin antibody. Nuclei were stained with DAPI, before sections were mounted in Vectashield and viewed under a fluorescent microscope.

Myocyte proliferation

Tissue sections were incubated with an antibody against BrdU (1:50 dilution; Roche) for 45 minutes at 37°C. This antibody was detected with an anti-mouse IgG FITC (1:100 dilution; Jackson Immunochemicals). Myocyte cytoplasm was labelled with anti-α–sarcomeric actin (as previously described), after the BrdU detection procedure and nuclei stained by DAPI. The samples were viewed under a fluorescent microscope.

The fraction of myocytes labelled by BrdU was measured (x1000 magnification) by counting a total of 1500 cardiomyocytes for each layer of the LV wall (sub-endocardium, mid-wall and sub-epicardium), across a total of 4 cross sections from each animal. The number of newly formed cardiomyocytes (i.e. BrdU positive) per 1500 cardiomyocytes was expressed as a percent fraction. To determine any changes in the size of the newly formed myocytes with time, the myocyte diameter of the first 10 newly formed myocytes were measured in the sub-endocardium, using image analysis. These determinations were n=5 at 3, 6, 14 days and saline vehicle control.

To complement the identification of a newly formed cardiomyocyte with BrdU labelling, the antibody against Ki67 (Novocastra) was also employed to identify cycling myocytes. Sections were incubated overnight at 4°C with Ki67 Ab (1:30 dilution), and this was detected using an anti-rabbit FITC (Jackson Immunochemicals). Myocyte cytoplasm was labelled using the anti-α–sarcomeric actin antibody, as previously described and nuclei counterstained with DAPI. Sections were mounted in Vectashield and viewed under a fluorescence microscope.

2.3 Statistical Analysis

Results are presented as either Mean ± SD or Mean ± SEM. Significance between 2 groups was determined by Student's t test and in multiple comparisons by the analysis of variance (ANOVA). Tukey's Honestly Significant Difference (HSD) *post hoc* analysis was used to locate the differences. However, if any of the data

violated the homogeneity of variance, an assumption of ANOVA, the non-parametric equivalent, Kruskal-Wallis test, was employed and 2-Sample Mann-Whitney tests used as follow tests to identify where the differences lay (Altman, 1991). Significance was set at $P<0.05$.

3.0 RESULTS

3.1 Histochemical and immunohistochemical staining procedures to establish fibre type profiles.

Sections of soleus, plantaris and tibialis anterior muscles were pre-treated with an acid incubation prior to staining for myosin ATPase (Figure 3.1 A-C, respectively). This procedure demonstrated 3 fibre types:- dark brown (type I fibres), light brown (type IIb fibres) and pale/clear (type IIa fibres). These criteria apply to the tibialis anterior and the plantaris muscles. However, the soleus muscle contains predominantly type I fibres and a minority of type IIa components (Schiaffino et al., 1989). The lighter brown staining fibres found in the soleus have been classified as intermediate fibres or type IIc, their myosin ATPase activity being placed in between that of type I (dark brown) and type IIa (pale/clear) (Brooke and Kaiser, 1974).

This standard myosin ATPase staining procedure was confirmed by the use of monoclonal antibodies. The slow anti-myosin antibody was specific for the slow MHC of skeletal muscle (type I fibres). In contrast, the anti-myosin (fast) antibody was specific towards the fast isomyosin molecules in skeletal muscle but could not distinguish between types IIa and type IIb fibres. Figures 3.2 (A-C), 3.3 (A-C) and 3.4 (A-C) show serial sections for the myosin ATPase (acid pre-incubation) stain (A), slow MHC antibody stain (B) and fast MHC antibody stain (C) for the soleus, plantaris and tibialis anterior muscles, respectively.

These procedures allow fibre types to be identified with confidence within adult skeletal muscles. Furthermore, any fibre type transition which may occur during the regenerative process in skeletal muscle can be identified.

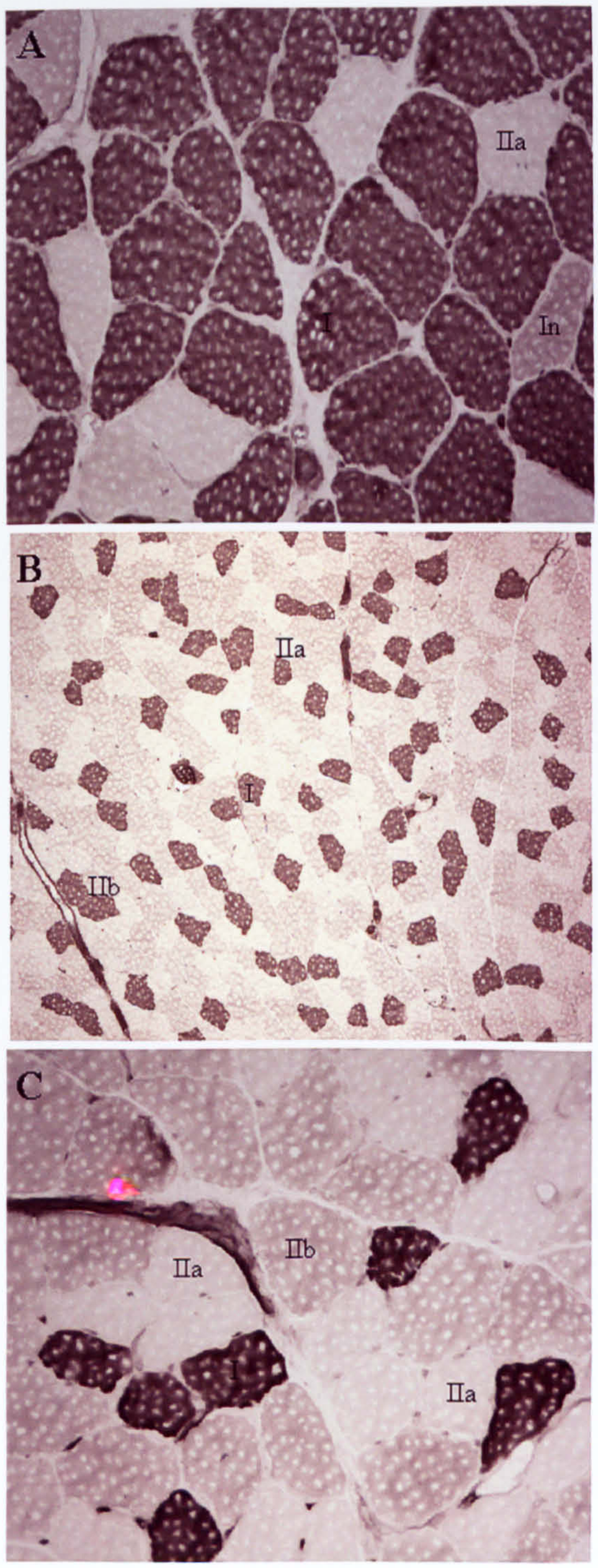

Figure 3.1 Fibre type profiles.

Transverse sections of the soleus (A), plantaris (B) and tibialis anterior (C) muscle were stained for myosin ATPase (acid pH 4.35) to identify the different fibre types; Type I-slow (I), Intermediate (In), Type IIa-fast oxidative (IIa) and Type IIb-fast glycolytic (IIb) (x200 magnification, except B which is x100).

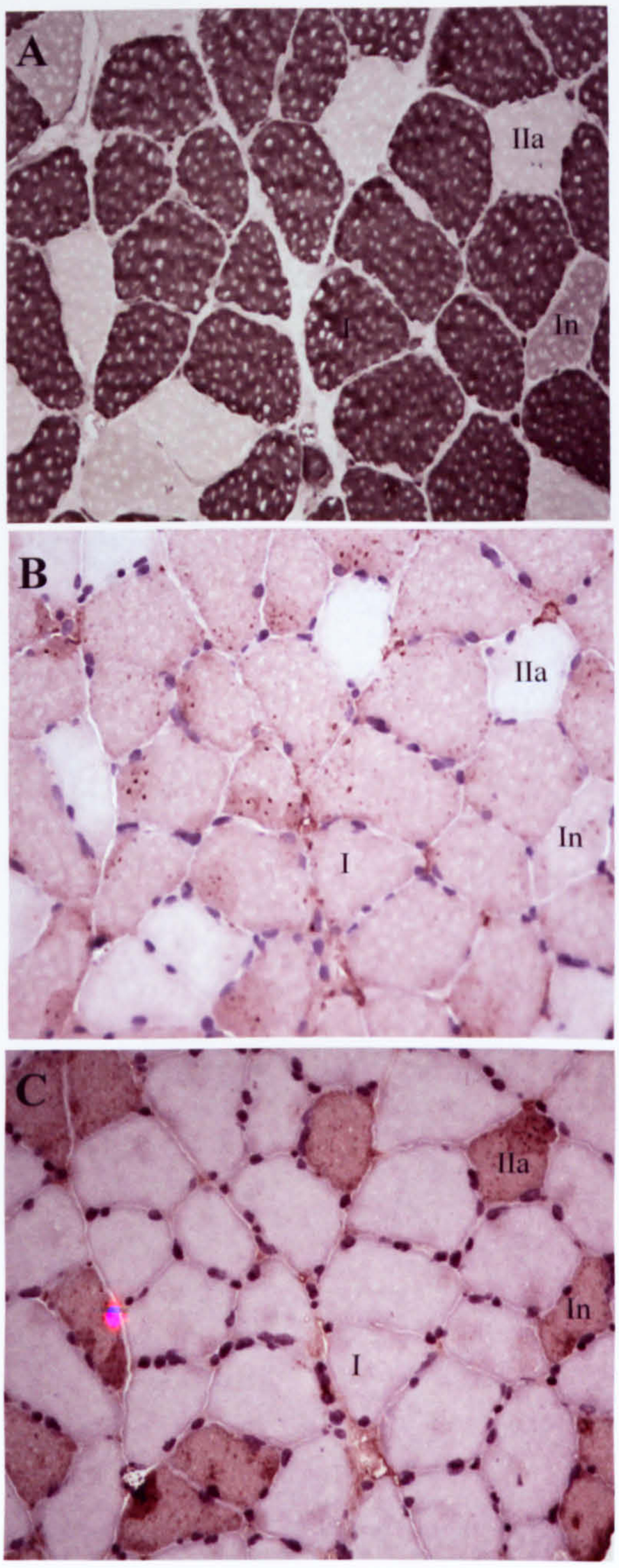

Figure 3.2 Specificity of the histochemical and immunohistochemical staining procedures showing the fibre type profile of the soleus muscle.

Myosin ATPase (acid pH 4.35) stain (A); the slow myosin heavy chain antibody (B) clearly interacts with slow (I) and partially with intermediate (In) fibres, but not fast (IIa). Conversely, the fast myosin heavy chain antibody (C) reacts with type IIa and In, but not type I (all x200 magnification).

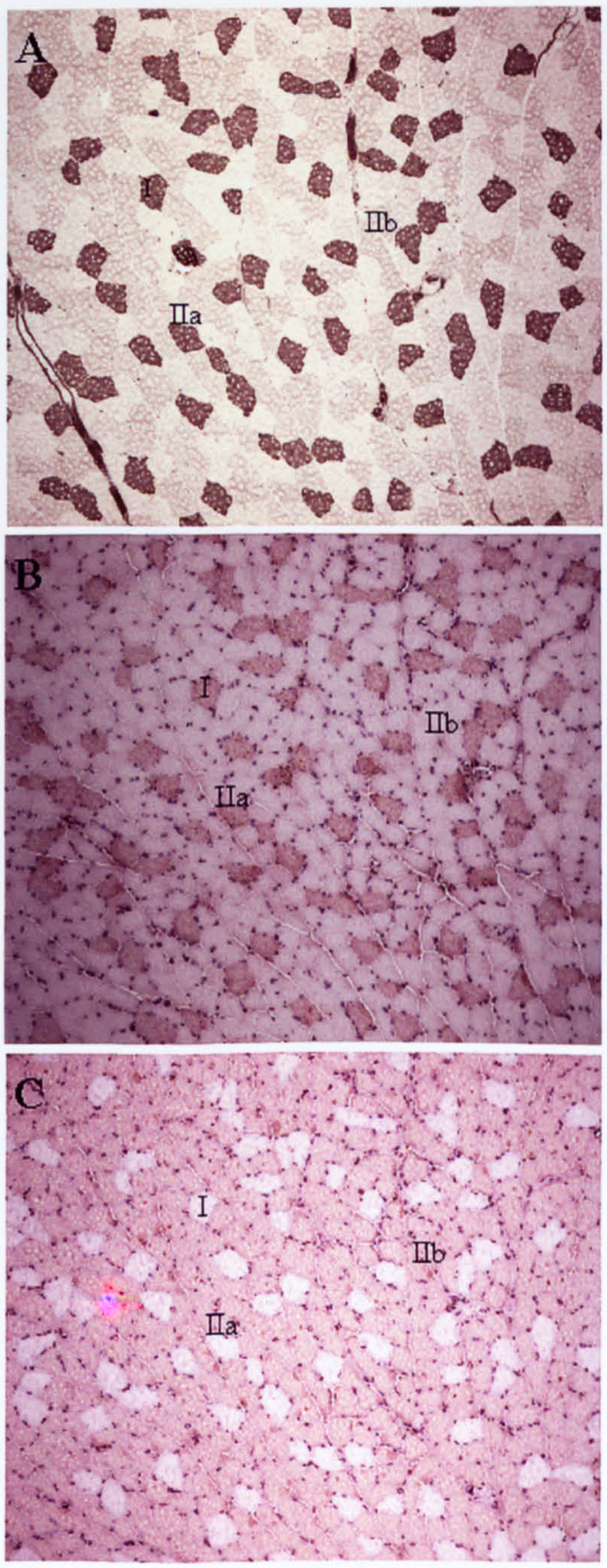

Figure 3.3 Specificity of the histochemical and immunohistochemical staining procedures showing the fibre type profile of the plantaris muscle.

Myosin ATPase (acid pH 4.35) stain (A); the slow myosin heavy chain antibody (B) clearly interacts with slow (I) fibres, but not fast (IIa or IIb). Conversely, the fast myosin heavy chain antibody (C) reacts with both type IIa and IIb, but not type I (all x100 magnification).

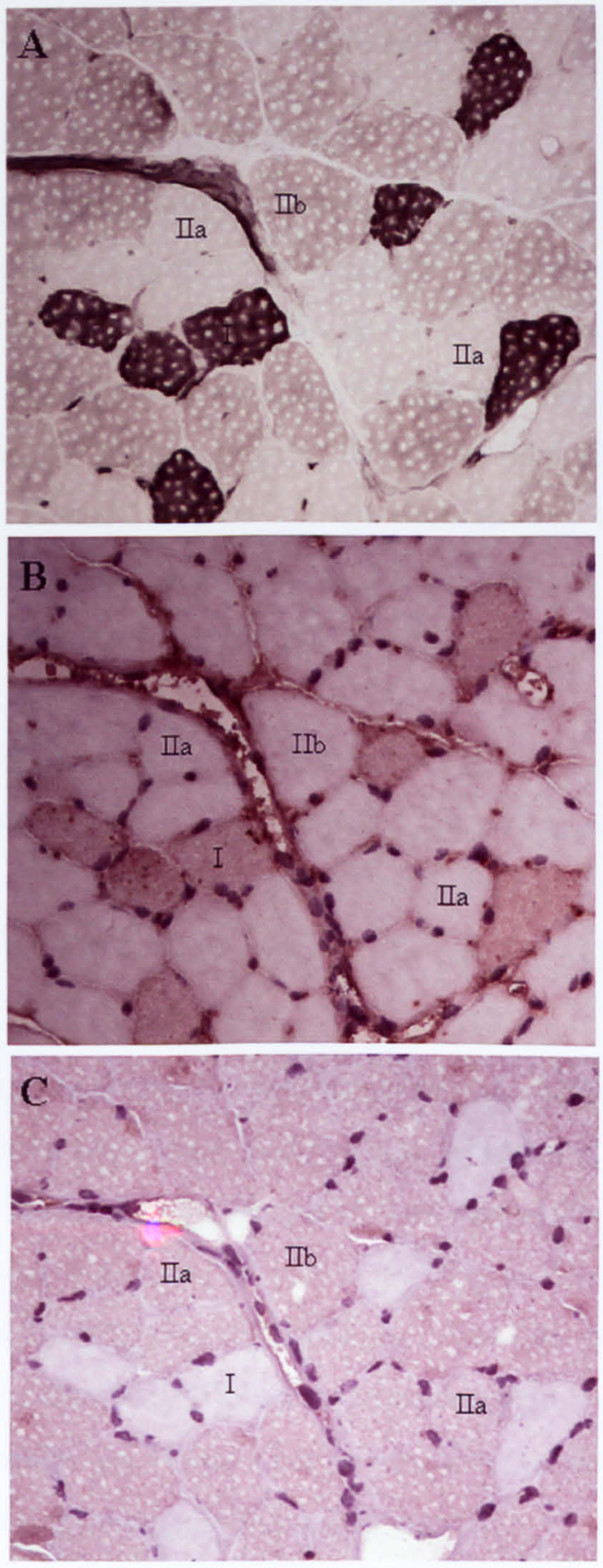

Figure 3.4 Specificity of the histochemical and immunohistochemical staining procedures showing the fibre type profile of the tibialis anterior muscle.

Myosin ATPase (acid pH 4.35) stain (A); the slow myosin heavy chain antibody (B) clearly interacts with slow (I) fibres, but not fast (IIa or IIb). Conversely, the fast myosin heavy chain antibody (C) reacts with both type IIa and IIb, but not type I (all x200 magnification).

3.2 Catecholamine-induced damage

The soleus, plantaris, tibialis anterior and diaphragm muscles from the saline control group showed no signs of fibre necrosis or apoptosis, i.e. a baseline of zero damage. Throughout all the experiments using 20 mmol of isoprenaline, adrenaline or noradrenaline kg^{-1}, no damage was ever found in the plantaris, tibialis anterior or diaphragm muscles at any time point. In marked contrast, the heart and soleus muscles, of the same animals, showed severe damage and cell death, via both necrosis and apoptosis, in response to a single injection of either 20 mmol of isoprenaline, adrenaline or noradrenaline (Figures 3.5; 3.6; 3.7; 3.8).

Cardiomyocyte apoptosis was evident between 3 and 72 hours, peaking at 3 hours and decreasing thereafter (Figure 3.7) following the isoprenaline administration. This peak at 3 hours (2.5 ± 1%), was significantly different ($P<0.001$) from the amounts of apoptosis found in saline controls and all other time points (Figure 3.7).

In contrast to the heart, catecholamine-induced apoptosis and necrosis in the soleus muscle has only recently been described by our laboratory and warrants more intensive study. In the soleus muscle, fibre apoptosis was also evident from 3 to 24 hours, and this increased with time (Figure 3.8). The peak amount of apoptosis occurred at 24 hours (4 ± 1%), some 21 hours later than that seen in the heart, and this was significantly greater ($P<0.05$) than that found in saline control samples, and at 3, 9, 12, 48 and 72 hours. By 48 and 72 hours the amount of apoptosis had fallen to zero, i.e. equivalent to saline control tissue (Figure 3.8).

A single injection of either 20 mmol kg^{-1} of the natural catecholamines adrenaline or noradrenaline, similarly caused severe fibre necrosis and apoptosis in the soleus muscle (Figure 3.9). Examples of this type of damage are shown in Figure 3.5 (C and D).

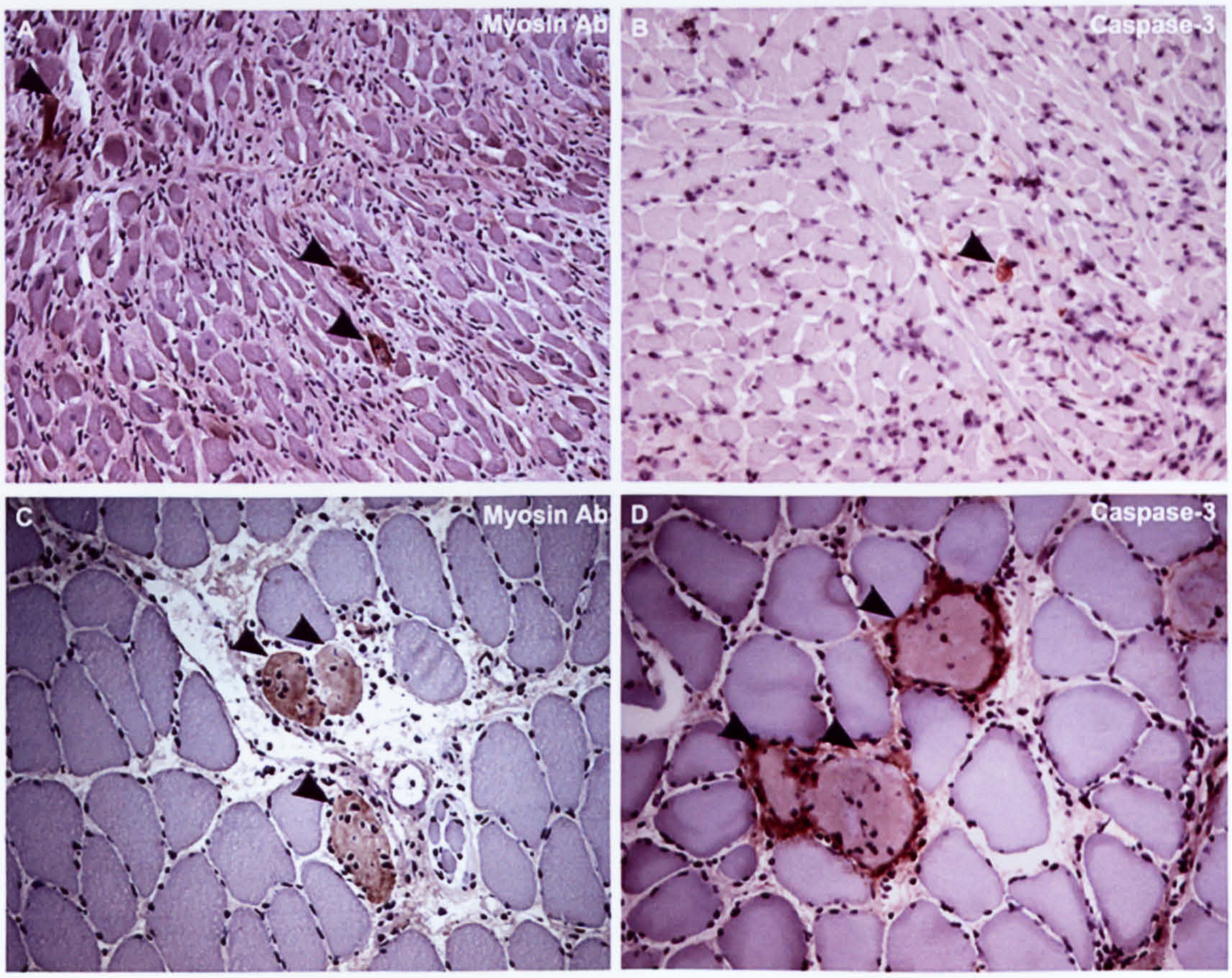

Figure 3.5 Catecholamine-induced necrosis and apoptosis in the heart and soleus muscle.

Necrotic (containing myosin Ab) and apoptotic (caspase-3 labelled) myocytes were identified in transverse sections of the heart (A and B) and soleus (C and D). For necrosis (A and C) the myosin Ab was detected using a rabbit anti-mouse HRP-conjugated 2°Ab. Necrotic myocytes were visualised using DAB (brown; arrowheads). For apoptosis (B and D; arrowheads) sections were exposed to caspase-3 1°Ab, before incubation with a goat anti-rabbit HRP-conjugated 2°Ab. Apoptotic myocytes were visualised using Nova red (red; arrowheads). All sections were counterstained with haematoxylin (all x200 magnification).

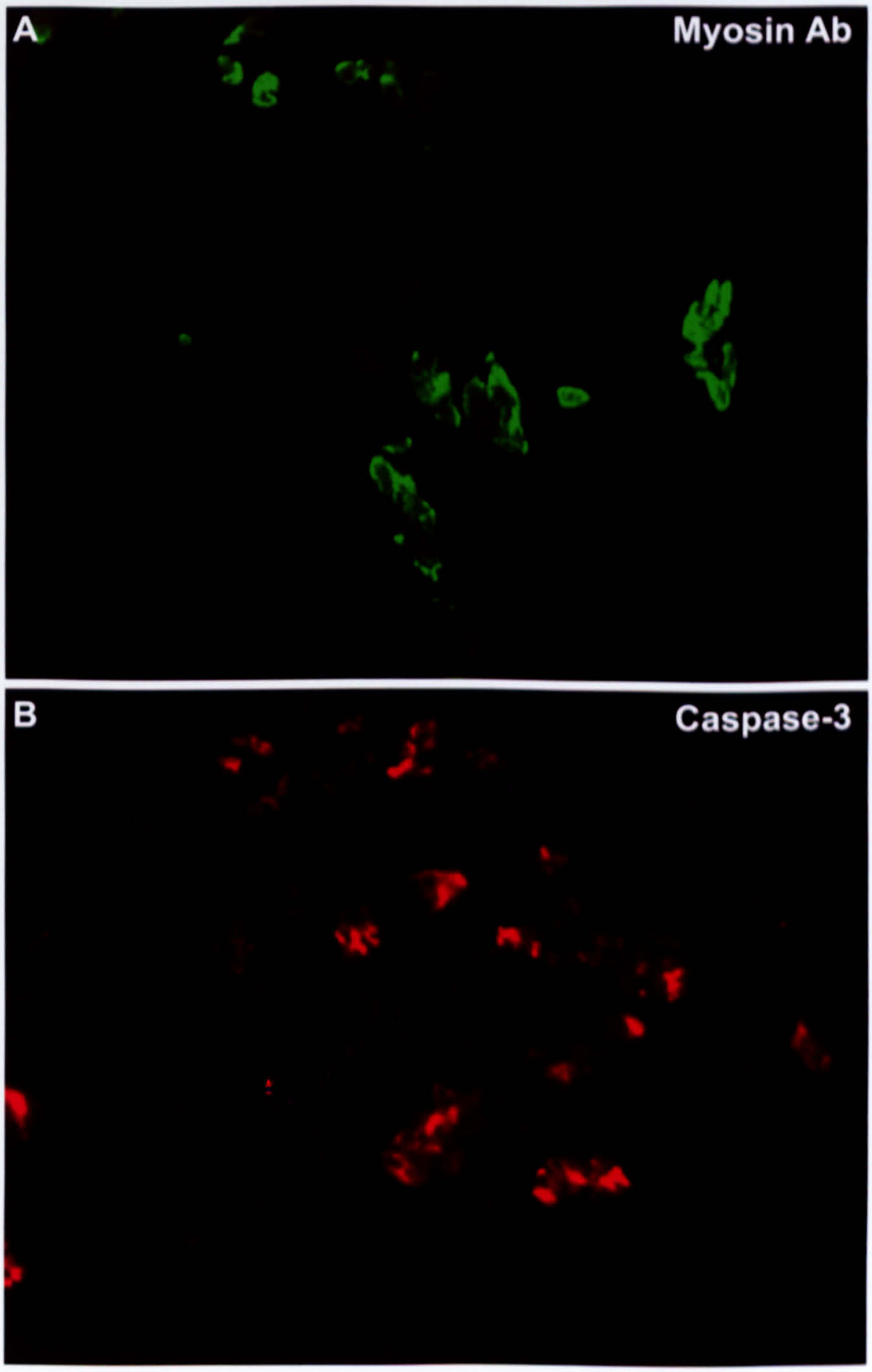

Figure 3.6 Immunofluorescence staining of necrosis and apoptosis in the heart.

Transverse sections of the heart were exposed to a caspase-3 Ab, before being stained with fluorescein and Texas red 2°Abs to detect necrotic-myosin antibody labelled (green, A) and apoptotic-caspase-3 labelled (red, B) cardiomyocytes respectively, after catecholamine administration (x200 magnification).

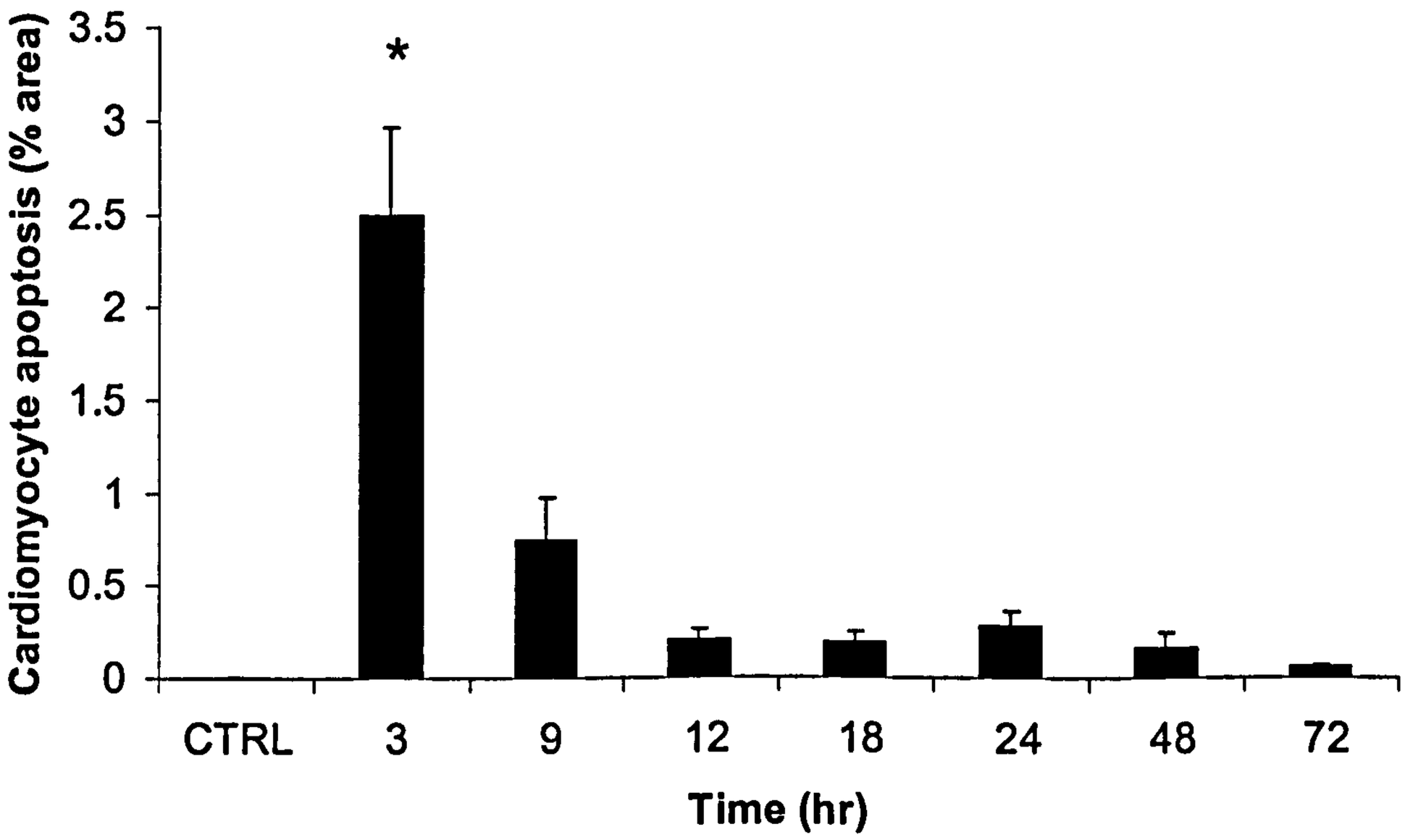

Figure 3.7 Time course of catecholamine-induced apoptosis in the heart. Cardiomyocyte apoptosis (caspase-3 labelled) in response to a single injection (s.c.) of 20 mmol of isoprenaline kg^{-1}. No apoptosis was found in the control muscles (CTRL) receiving saline vehicle only. However, caspase-3 labelled myocytes, quantified as the percentage area, were evident after 3 hours. Results are Mean ± SEM for n=5 and *denotes significant difference ($P<0.001$) from CTRL and all other time points.

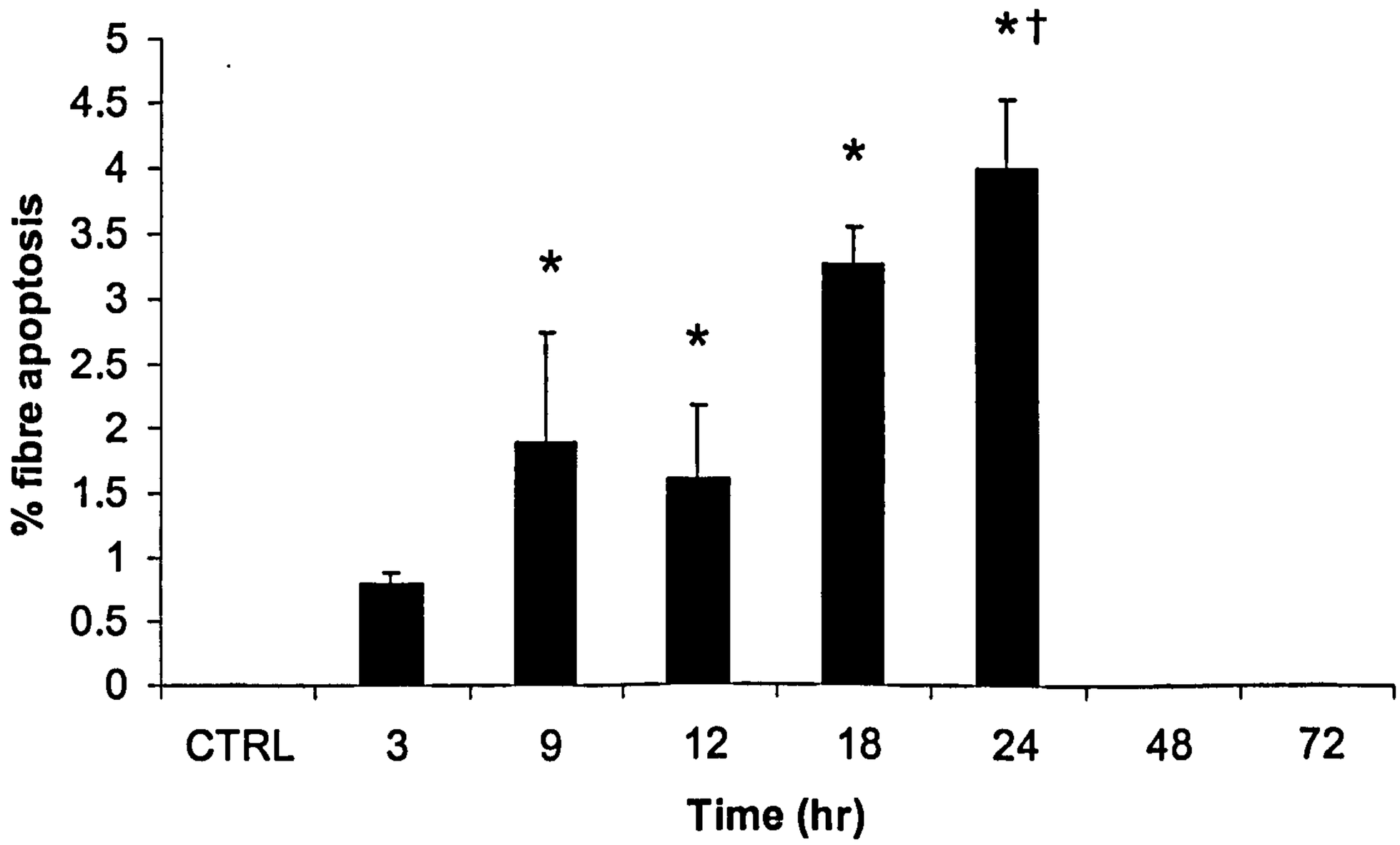

Figure 3.8 Time course of catecholamine-induced apoptosis in the soleus muscle.

Fibre apoptosis (caspase-3 labelled) in response to a single injection (s.c.) of 20 mmol of isoprenaline kg^{-1}. No apoptosis was found in the control muscles (CTRL) receiving saline vehicle only. However, caspase-3 labelled fibres, quantified as percent number of fibres counted in the soleus, were evident after 3 hours. Results are Mean ± SEM for n=5, with *denoting significant differences ($P<0.05$) from CTRL, 48 and 72 hours. † denotes significant difference ($P<0.05$) from 3, 9 and 12 hours.

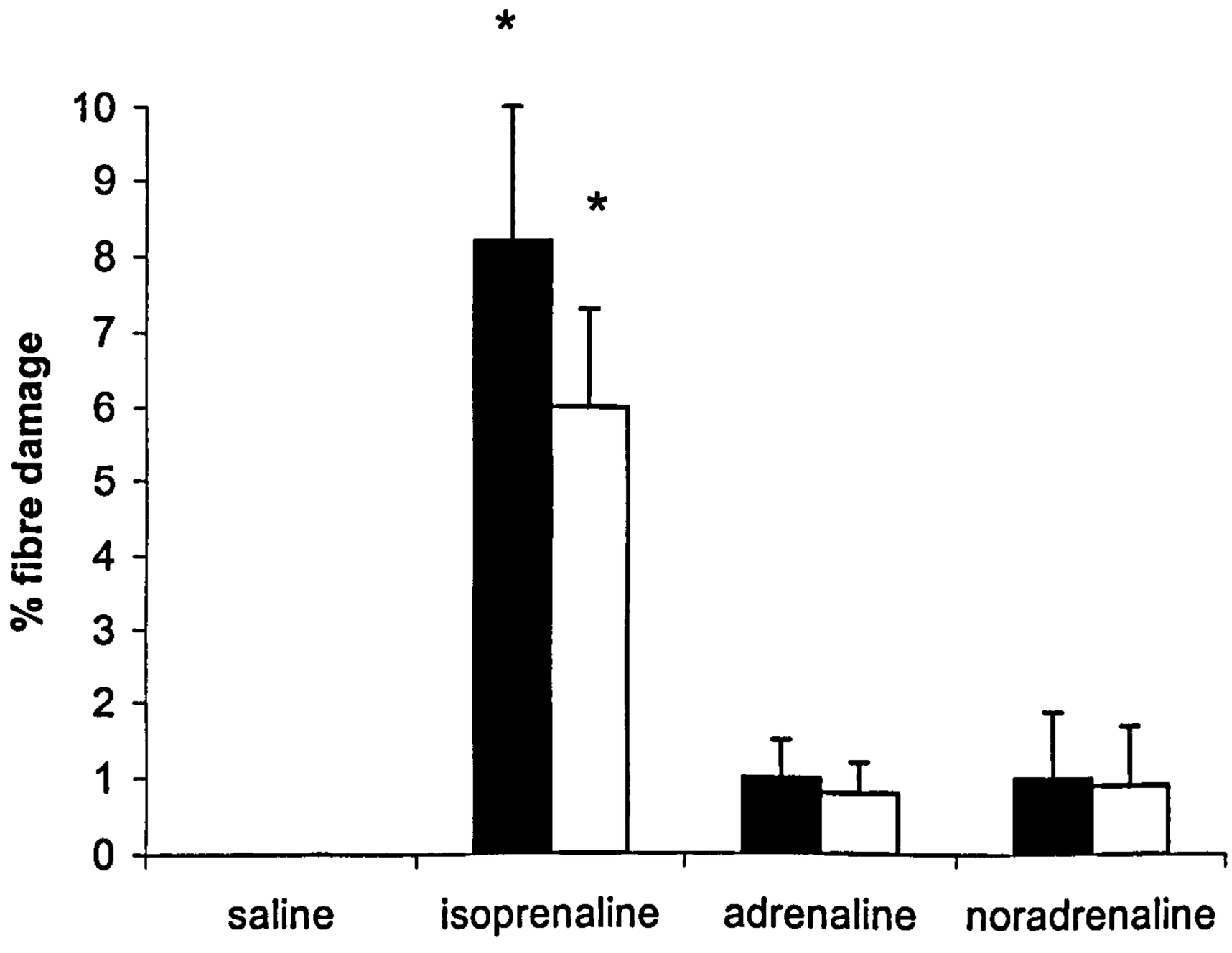

Figure 3.9 Catecholamine-induced fibre necrosis and apoptosis.

Myocyte necrosis (anti-myosin labelled) and apoptosis (caspase-3 labelled) in the soleus muscle 18hr following either a single injection (s.c.) of 20 mmol of isoprenaline, adrenaline or noradrenaline kg^{-1}. Fibre specific necrosis (■) and apoptosis (□) were quantified as percent number of fibres counted in the soleus. No necrosis or apoptosis was found in the control muscles receiving saline vehicle only. Results are Mean ± SEM for n=5-9 and *denotes significant difference ($P<0.01$) between isoprenaline vs. saline, adrenaline or noradrenaline treatments.

While each natural catecholamine induced similar amounts of necrosis and apoptosis (Figure 3.9), the total number of necrotic and apoptotic fibres was significantly greater ($P<0.01$) in response to isoprenaline, than in the saline controls, adrenaline or noradrenaline treated soleus muscles (Figure 3.9).

Other recent studies in our laboratory have suggested substantial similarities in the time of onset, threshold dose and optimal amounts of necrosis and apoptosis in the soleus in response to a single 20 mmol injection of isoprenaline kg^{-1}(Goldspink et al., 2004). This raises the question as to whether necrosis and apoptosis are two distinct processes. To investigate this in greater depth, both necrotic (myosin antibody labelled) and apoptotic (caspase-3 labelled) fibres can be identified on the same section using double immunofluorescence. Hence, using this approach the possibility of cellular co-localisation could be investigated.

The percent of damaged fibres in the soleus muscle that were either apoptotic, necrotic or exhibited co-localisation for both processes were counted from 4 random fields of view (~800 fibres). After exposure to the isoprenaline 521 injured fibres were counted. None (0%) of the fibres were purely apoptotic, while 377 (72%) fibres exhibited co-localisation (i.e. both apoptotic and necrotic) and 144 (28%) fibres were found to be purely necrotic. Figure 3.10 shows double immunofluorescent stained fibres in the soleus muscle. Hence, many fibres exhibit co-localisation for both necrosis and apoptosis, following a 20 mmol injection of isoprenaline.

After adrenaline-induced damage, 76 injured fibres were counted. Similarly, none (0%) of these fibres were purely apoptotic, 58 (76%) exhibited co-localisation of both death pathways, and 18 (24%) of the fibres were necrotic only. After noradrenaline administration, 66 injured fibres were counted. None (0%) were

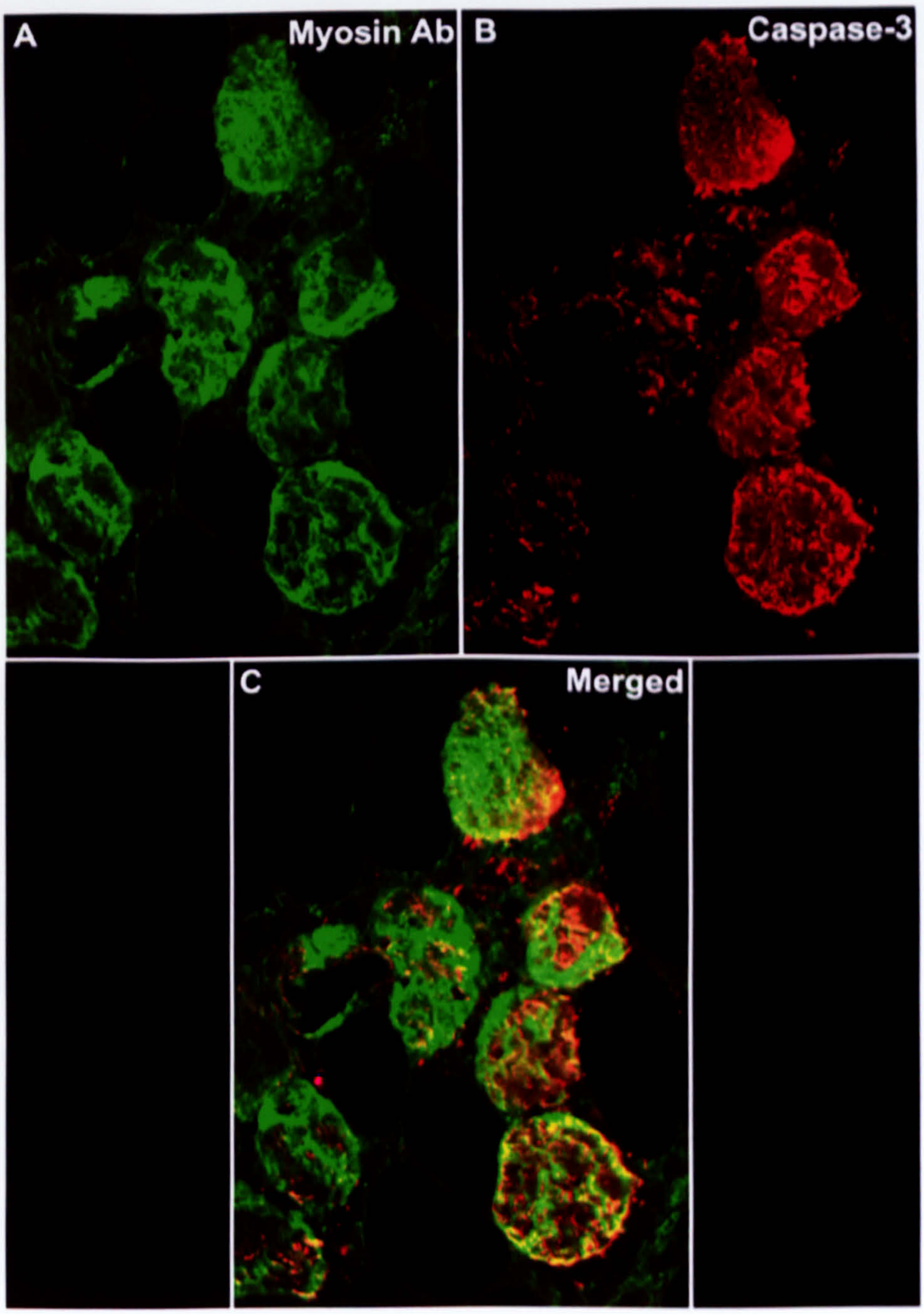

Figure 3.10 Co-localisation of catecholamine-induced fibre necrosis and apoptosis.

Transverse sections were stained with fluorescein and Texas red to show necrotic-myosin antibody labelled (green, A) and apoptotic-caspase-3 labelled (red, B) fibres, 18 hours after 20 mmol of either isoprenaline, adrenaline or noradrenaline kg^{-1}. When the images are merged (C), any co-labelling within the same fibres becomes apparent.

purely apoptotic, 57 (86%) exhibited co-localisation being labelled for both apoptosis and necrosis, and 9 (14%) fibres were found to be purely necrotic. Therefore, all apoptotic fibres found in the soleus muscle following an injection of either isoprenaline, adrenaline or noradrenaline were also found to be labelled as necrotic.

Key points:

1. Acute catecholamine exposure causes significant fibre apoptosis and necrosis to the predominantly slow-twitch soleus muscle, but not the other predominantly fast muscles.

2. Apoptotic fibre death is co-localised with necrotic fibre death, in the same muscle fibres in the soleus.

3.3 Fibre regeneration and the time course of the regenerative process

3.3.1 Time course of the regenerative process

The normal soleus muscles from 250 ± 7g rats contains on average 2653 ± 111 fibres. Because of the necrotic and apoptotic cell death, the total number of fibres in the entire soleus muscle initially decreased following a single injection of isoprenaline. A significant ($P<0.05$) loss of ~500 fibres (23%) occurred between day 0 (2653 ± 111) and day 5 (2196 ± 145) after the isoprenaline administration. By day 7, the total number of fibres begun to increase, and by day 28 the number was almost the same as at day 0 (Figure 3.11). The effects of equimolar amounts of adrenaline were less severe (see Figure 3.9). Hence, the trend of changes in fibre numbers after adrenaline (Figure 3.12) was less dramatic than for isoprenaline. Consequently, the number of normal fibres in the soleus muscle following a single injection of adrenaline was not statistically different at any point over the 28 days (Figure 3.12).

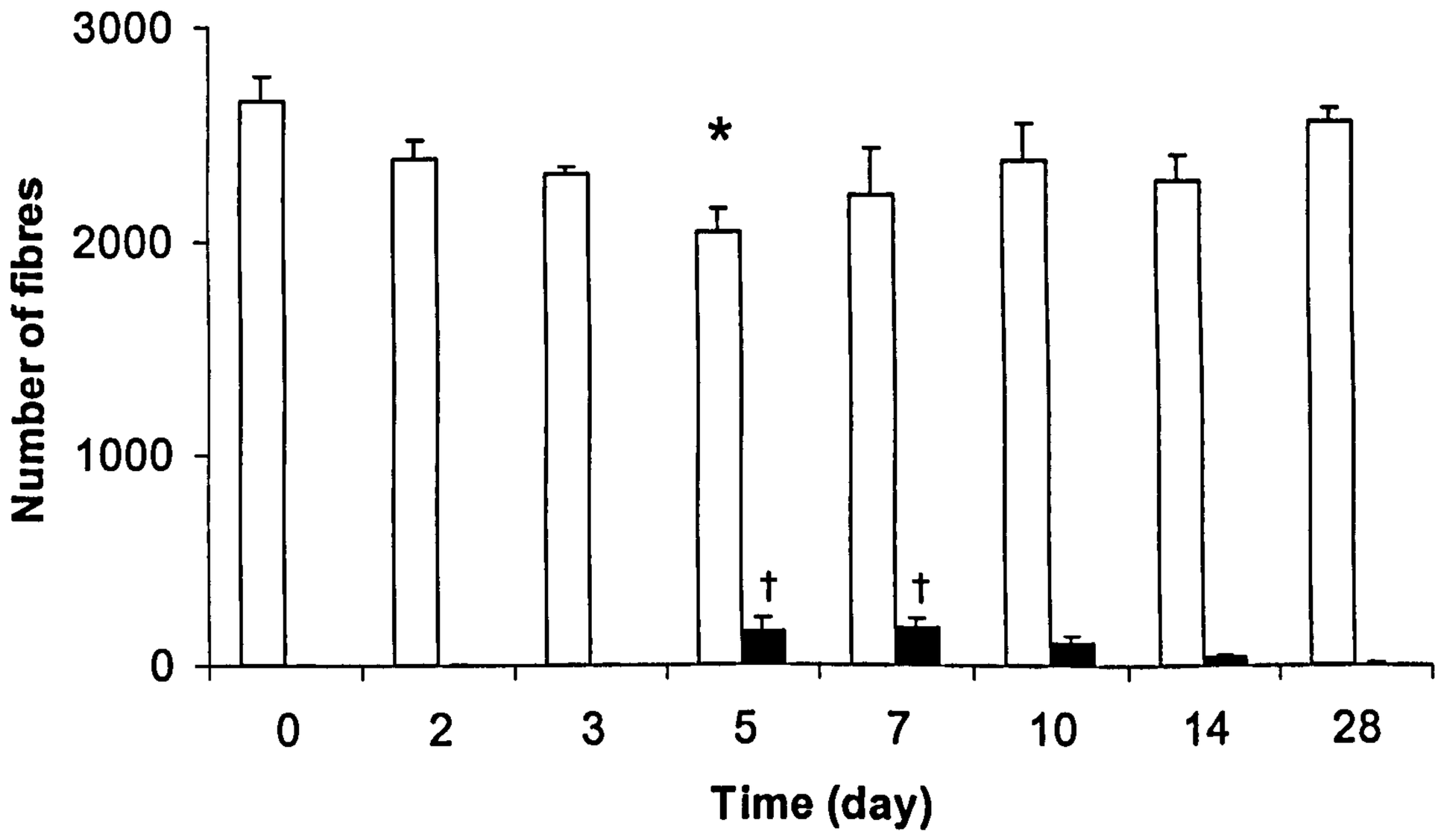

Figure 3.11 Time course of fibre regeneration in the soleus muscle after synthetic catecholamine administration.

Number of normal fibres (□) and newly-formed regenerating fibres (■) following a single injection (s.c.) of 20 mmol of isoprenaline kg^{-1}. Results are Mean ± SEM for n=5-9. *denotes significant difference ($P<0.05$) from 0 day control. †denotes significant differences ($P<0.05$) from 0 (control), 2, 3 and 28 days.

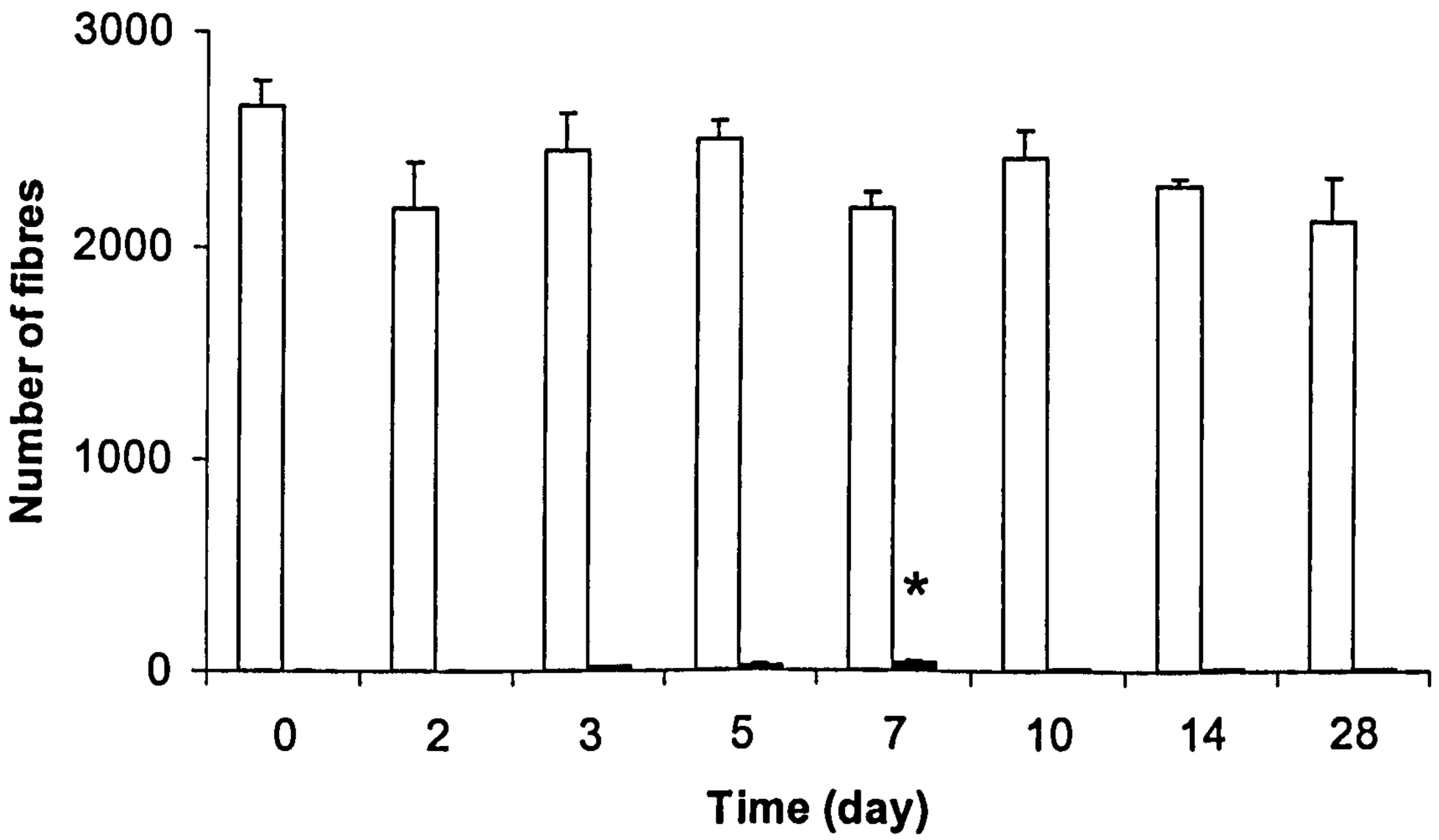

Figure 3.12 Time course of fibre regeneration in the soleus muscle after natural catecholamine administration.

Number of normal fibres (□) and newly-formed regenerating fibres (■) following a single injection (s.c.) of 20 mmol of adrenaline kg^{-1}. Results are Mean ± SEM for n=5-9. *denotes significant differences ($P<0.05$) from 0 (control), 2 and 28 days.

Following catecholamine-induced injury, there was an increase in the number of mononucleated cells within the extracellular space and connective tissue (Figure 3.13 B). These cells probably consisted of both inflammatory and myogenic cells, involved in the removal of necrotic debris and repair and regeneration of new muscle fibres, respectively. Phagocytosis of necrotic fibres appeared to be almost complete by 3 days. Cells that are thought to be immature myotubes could be seen after 3 days (Figure 3.13 C). At this stage the adrenaline group exhibited 16 ± 2 regenerating fibres within the population of normal fibres in the soleus muscle. These fibres were small, angulated and stained positively for embryonic/neonatal myosin and as a consequence were classified as regenerating fibres (Figure 3.13 D).

The isoprenaline-treated muscles started to exhibit regenerating fibres later than the adrenaline group, these becoming evident by day 5. These regenerating fibres represented 6% ($P<0.05$) and 1% (157 ± 66 fibres, compared with 20 ± 8 fibres) of the total number of fibres in the whole soleus 5 days (Figures 3.11; 3.12) after isoprenaline and adrenaline administration, respectively. Seven days after catecholamine-induced injury more regenerating fibres were evident within the soleus muscle. These now accounted for 8% and 2% (176 ± 45 fibres; 42 ± 16 fibres) of the total number of fibres in the entire soleus following isoprenaline and adrenaline administration, respectively and were significantly different ($P<0.05$) from days 0 (control), 2 and 28 (Figures 3.11; 3.12).

The soleus muscles obtained 10 days post-isoprenaline showed evidence of fibre splitting within a few individual muscle fibres (Figure 3.13 F). Despite this, by day 10 the number of regenerating fibres had decreased to 4% (105 ± 30) and 0.4% (11 ± 2) in the isoprenaline and adrenaline groups, respectively. This trend continued and by 14 days there was only 38 ± 12 regenerating fibres, representing only 1.4% ± 0.7 of the total number for the isoprenaline group (Figure 3.11). By this stage there was also an increase in the number of centralised nuclei within muscle fibres (Figure 3.13 G). This is a characteristic common to newly regenerated fibres prior to

Figure 3.13 Degenerative and regenerative changes in the soleus muscle after catecholamine-induced injury.

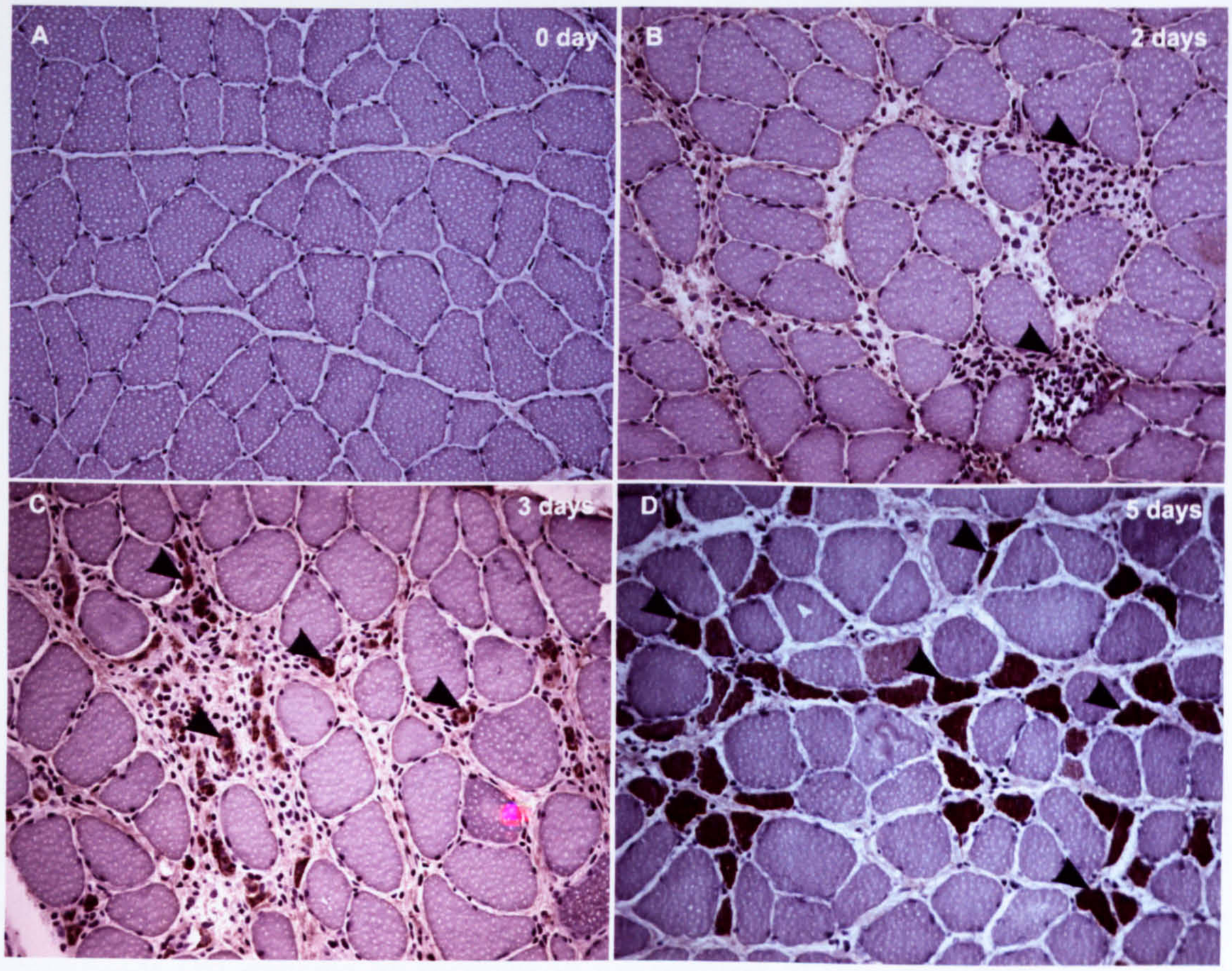

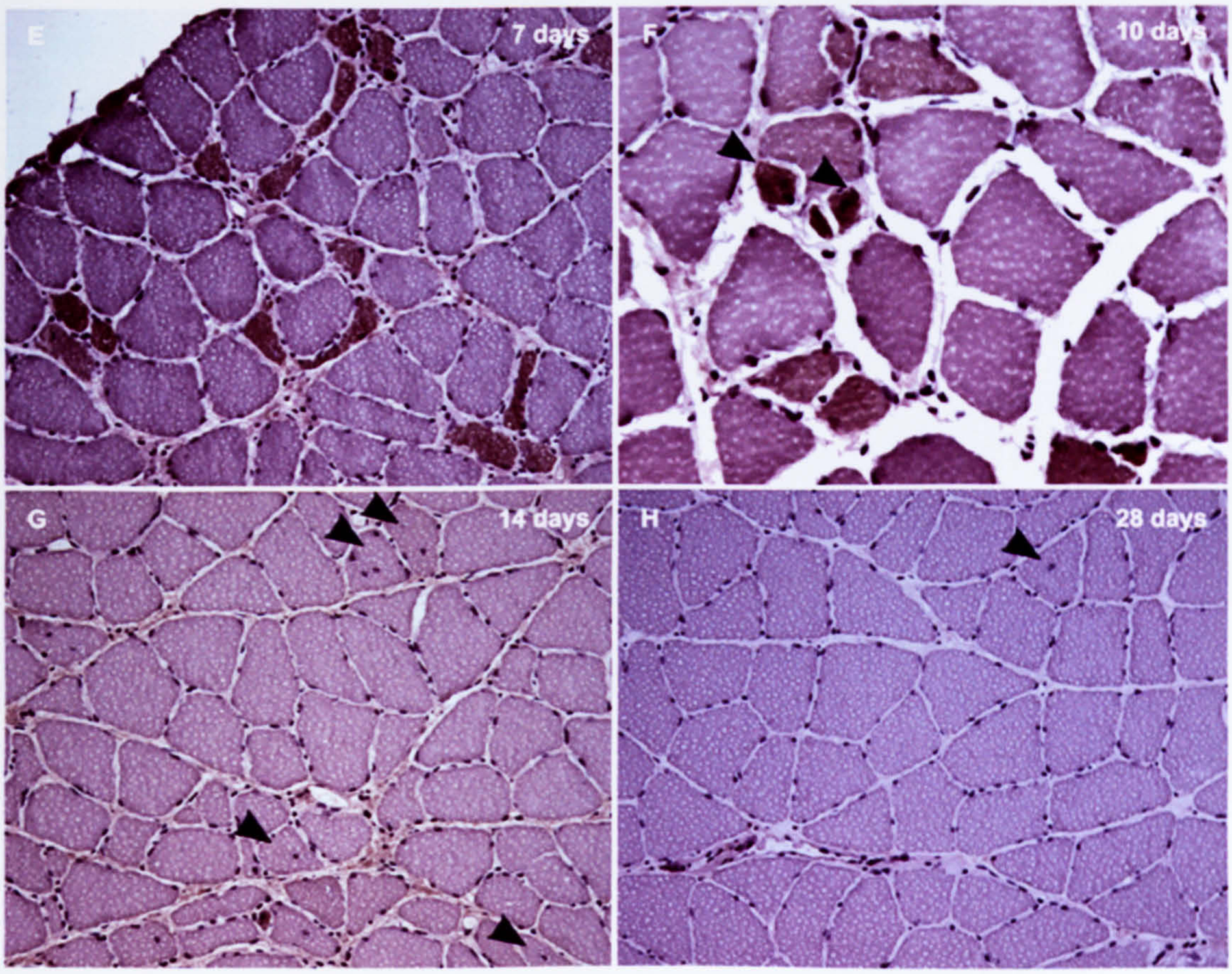

Transverse sections were stained with embryonic/neonatal 1°Ab during regeneration, following catecholamine-induced fibre damage. A, zero time control; B, 2 days; C, 3 days; D, 5 days; E, 7 days; F, 10 days; G, 14 days and H, 28 days after catecholamine injection (all x200 magnification, except F which is x400). The arrowheads (B) indicate an increase in the number of mononucleated cells within the extracellular space after 2 days. Arrowheads (C) indicate the emergence of immature myotubes after 3 days. Arrowheads (D) indicate small, angulated regenerating (embryonic/neonatal MHC positive) fibres at 5 days. Arrowheads (F) indicate fibres growing within basement membranes of another fibre after 10 days. The arrowheads (G and H) indicate newly regenerated fibres with characteristic centralized nuclei after 14 and 28 days.

their re-innervation (Palmer and Rudnicki, 2002). In the adrenaline group, by 14 days the number of regenerating fibres was minimal (8 ± 1), suggesting that regeneration was almost complete (Figure 3.12). Total regeneration of the soleus muscle in the isoprenaline group was almost complete after 28 days, with only 0.2% (5 ± 2 fibres in the entire soleus) of the fibres staining for embryonic/neonatal myosin (Figure 3.11). Indeed, by day 28 after either the injection of isoprenaline or adrenaline the soleus muscle looked normal. At this time there were very few regenerating fibres or those with centralized nuclei (Figure 3.13 H), with the complete restoration of the muscle's total fibre number (Figure 3.11: Figure 3.12).

Although the total number of fibres was fully restored by 28 days, this itself says nothing about the properties of the newly regenerated fibres, i.e. whether slow- or fast-twitch, and whether the fibre type profile of the soleus had changed as a consequence. To investigate whether there was any transitional changes in the fibre type proportions during regeneration, a myosin ATPase stain was carried out and the different fibre types quantified at 14 and 28 days. There was a significant decrease ($P<0.05$) in the number of type IIa (0.04%) and intermediate (0.3%) fibres 14 days after the isoprenaline injection, compared to zero time (7% type IIa; 3% intermediate). At day 14 all fibres in the soleus were type 1 (99.7%) (Figure 3.14). By 28 days the fibre type proportion had returned to the normal complement of 91% type I, 7% type IIa and 2% intermediate (Figure 3.14).

3.3.2 Data from control muscles

Fibre type proportions of the rat soleus muscle change during development and with age (Caccia et al., 1979). Since these experiments were conducted over a period of 28 days, it was necessary to ascertain whether any developmental changes had occurred in the soleus muscle of growing (250g) rats. This was a safeguard to check that any such normal developmental changes did not affect the accuracy of the experimental results. The total number of fibres and proportion of fibre types in these normal control soleus muscles at 28 days (Figure 3.15) were almost identical

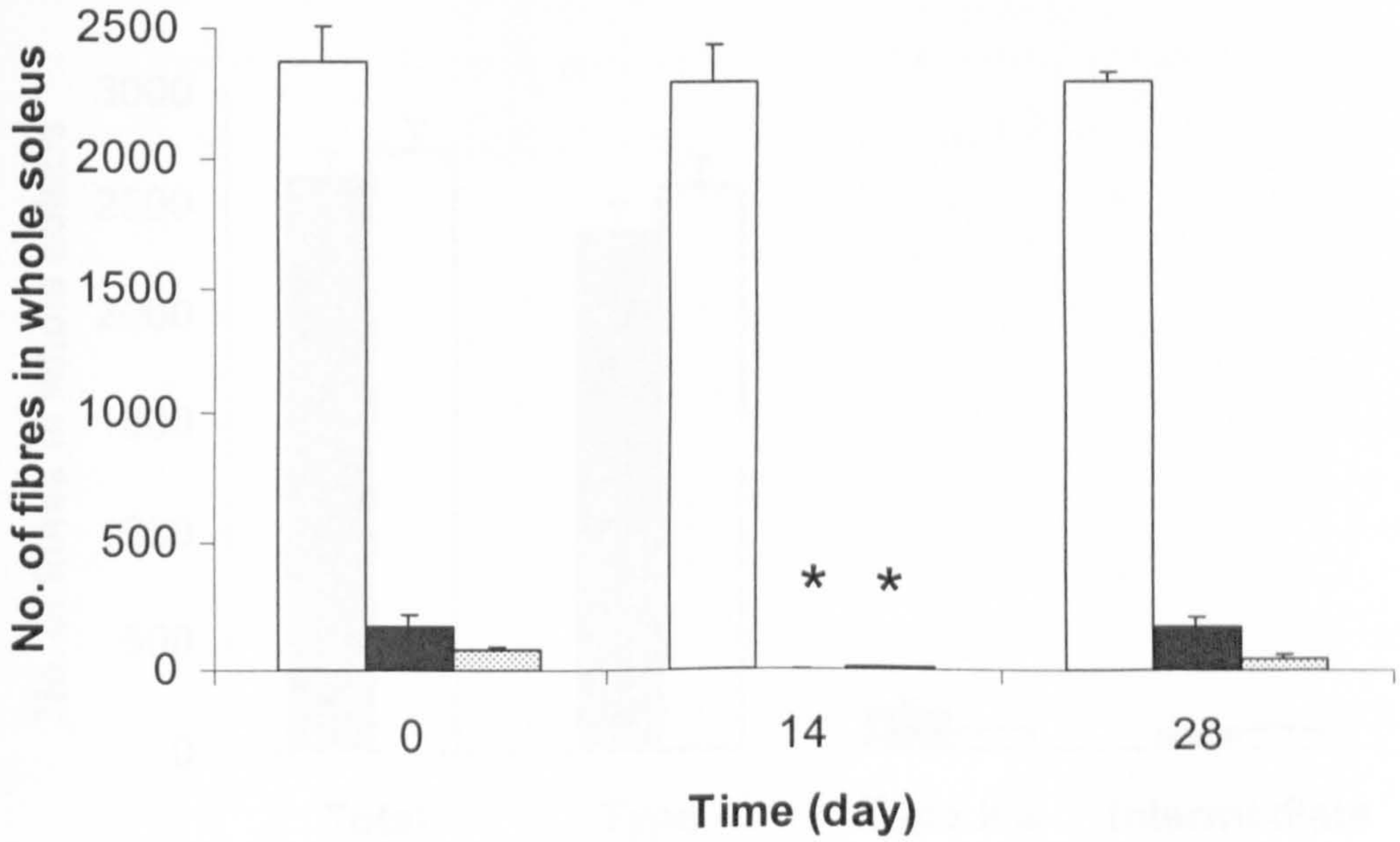

Figure 3.14 Fibre type proportions in the recovering soleus muscle.

Soleus muscle sections were stained for myosin ATPase 14 and 28 days after a single injection (s.c) of 20 mmol of isoprenaline kg^{-1}. Results are Mean ± SEM for n=5-9. Fibre types are indicated by Type I (□), Type IIa (■) and Intermediate (⊡).

*denotes significant decreases ($P<0.05$) in the number of type IIa and intermediate fibres, compared to both 0 day control and 28 days.

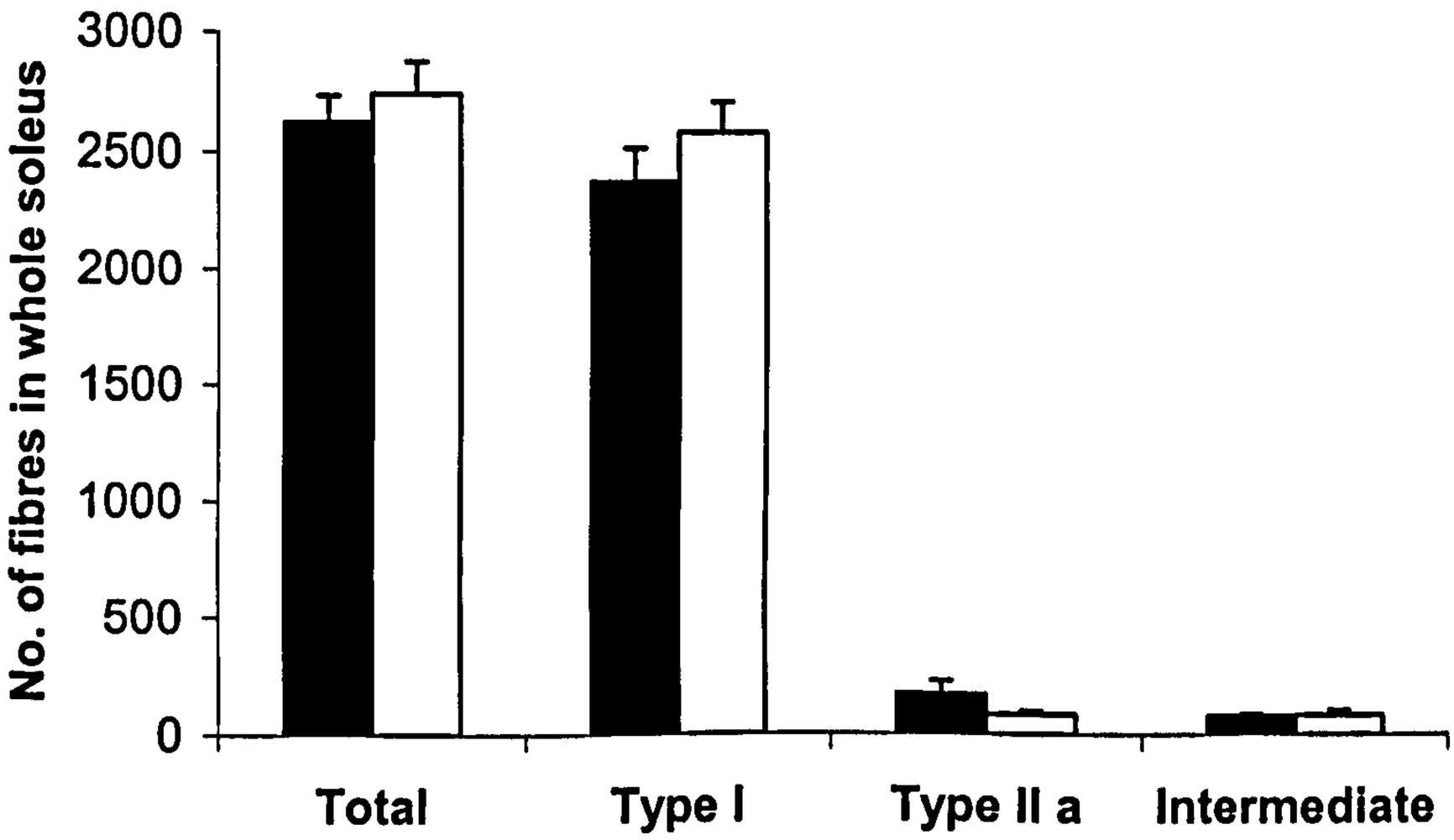

Figure 3.15 Total number, and fibre type proportions, in the normal soleus muscle.

Type I, IIa and intermediate fibres are shown for the soleus muscle during normal development in growing 250g male rats at zero time (■) and 28 days later (□). Results are Mean ± SEM, with n=5.

to those at day 0 and 28 in the experimental groups (Figure 3.14), with no significant differences. These precautionary findings indicate that no significant developmental changes had occurred in the soleus muscle during this stage of life. These findings also indicate that no additional control muscles were necessary for any of the time points throughout the time course of regeneration.

3.3.3 Satellite cells

Satellite cells, or dormant myoblasts, reside within skeletal muscle. These stem cells are involved in the regeneration of fibres following injury, and can be identified using specific antibodies. This was done on 5μm sections of the soleus muscle. The tyrosine kinase receptor, c-met is known to be expressed on satellite cells (Cornelison and Wold, 1997). Such c-met positive cells were found in the sections of soleus muscle (Figure 3.16 A and B) within the areas of inflammatory response (Figure 3.16B), and specifically 2 and 3 days after catecholamine-induced injury. Using double immunofluorescent staining, it was possible to demonstrate that some of these c-met positive cells had incorporated BrdU, which is indicative of satellite cell activation and re-entry into the cell cycle (Figure 3.16 C). Subsequently, some c-met positive cells co-expressed the myogenic transcription factor, MyoD in their nuclei (Figure 3.16 D). This is indicative of satellite cell proliferation and differentiation into the skeletal muscle lineage, thereby ensuring regeneration of lost fibres.

3.3.4 Mechano-growth factor (MGF) expression

This splice variant of IGF-1 is thought to be involved in stimulating satellite cell activation, proliferation and fusion (Hill and Goldspink, 2003; Hill et al., 2003). Catecholamine-induced damage to the soleus muscle was shown to have a marked effect on MGF expression (Figures 3.17; 3.18). Examples of MGF stained nuclei in the soleus muscle are shown in Figure 3.17. MGF expression increased throughout the 72 hour experimental period following isoprenaline injection. At 3 hours, 26% of the nuclei in the soleus muscle were MGF positive (Figure 3.18). Thereafter,

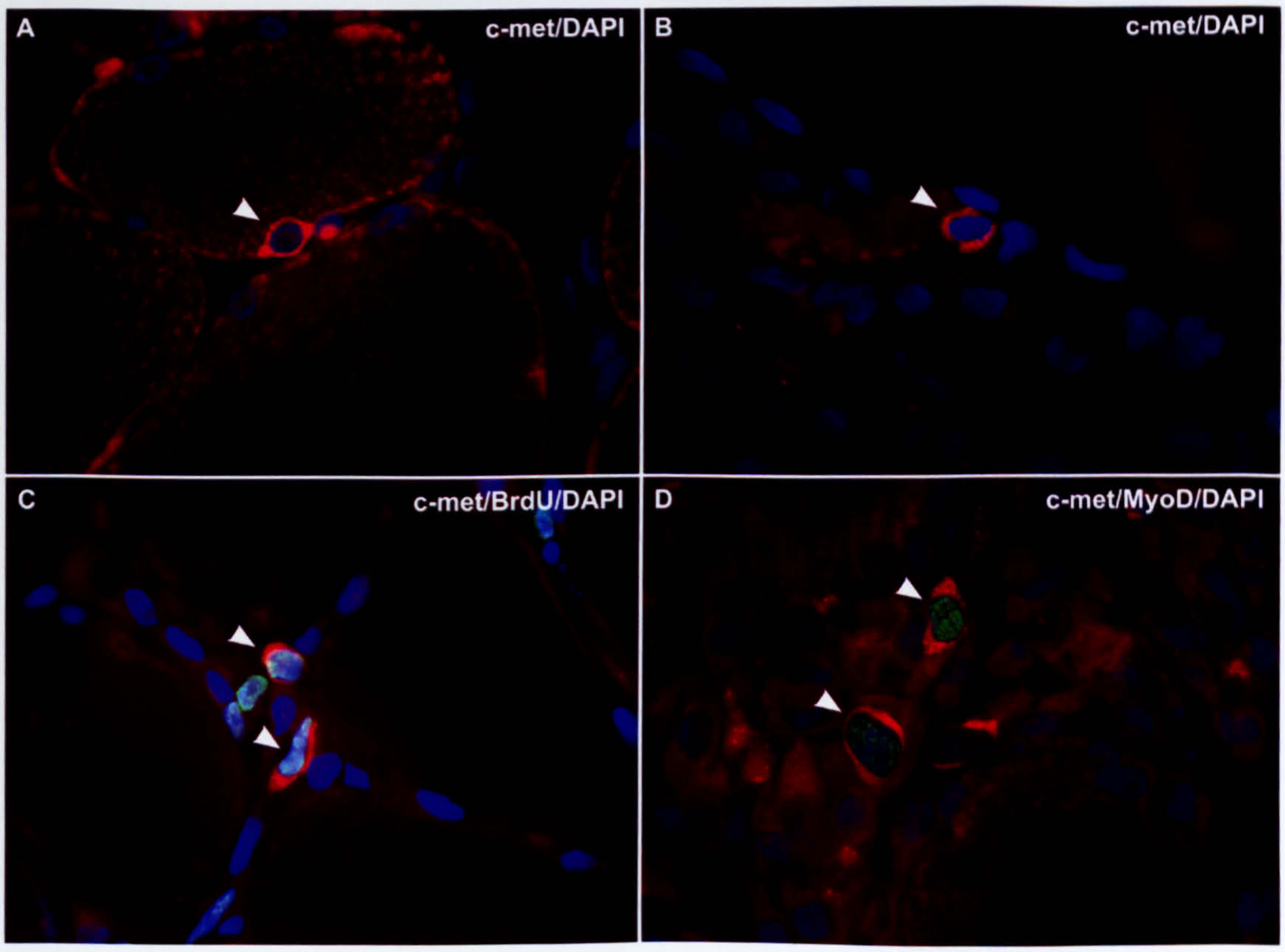

Figure 3.16 Satellite cells during regeneration of the soleus muscle.

Transverse sections were stained with c-met 1°Ab, and then with Texas red to show satellite cells (c-met labelled, A and B; arrowhead). Nuclei were identified using DAPI (blue). Double immunofluorescence staining showed that c-met positive cells had incorporated BrdU (green fluorescein stained, C; arrowheads), indicating their entry into the cell cycle. Also, some c-met labelled cells were positive for MyoD (green fluorescein stained, D; arrowheads) the myogenic transcription factor, indicating satellite cell proliferation and differentiation into the skeletal muscle lineage (all x1000 magnification).

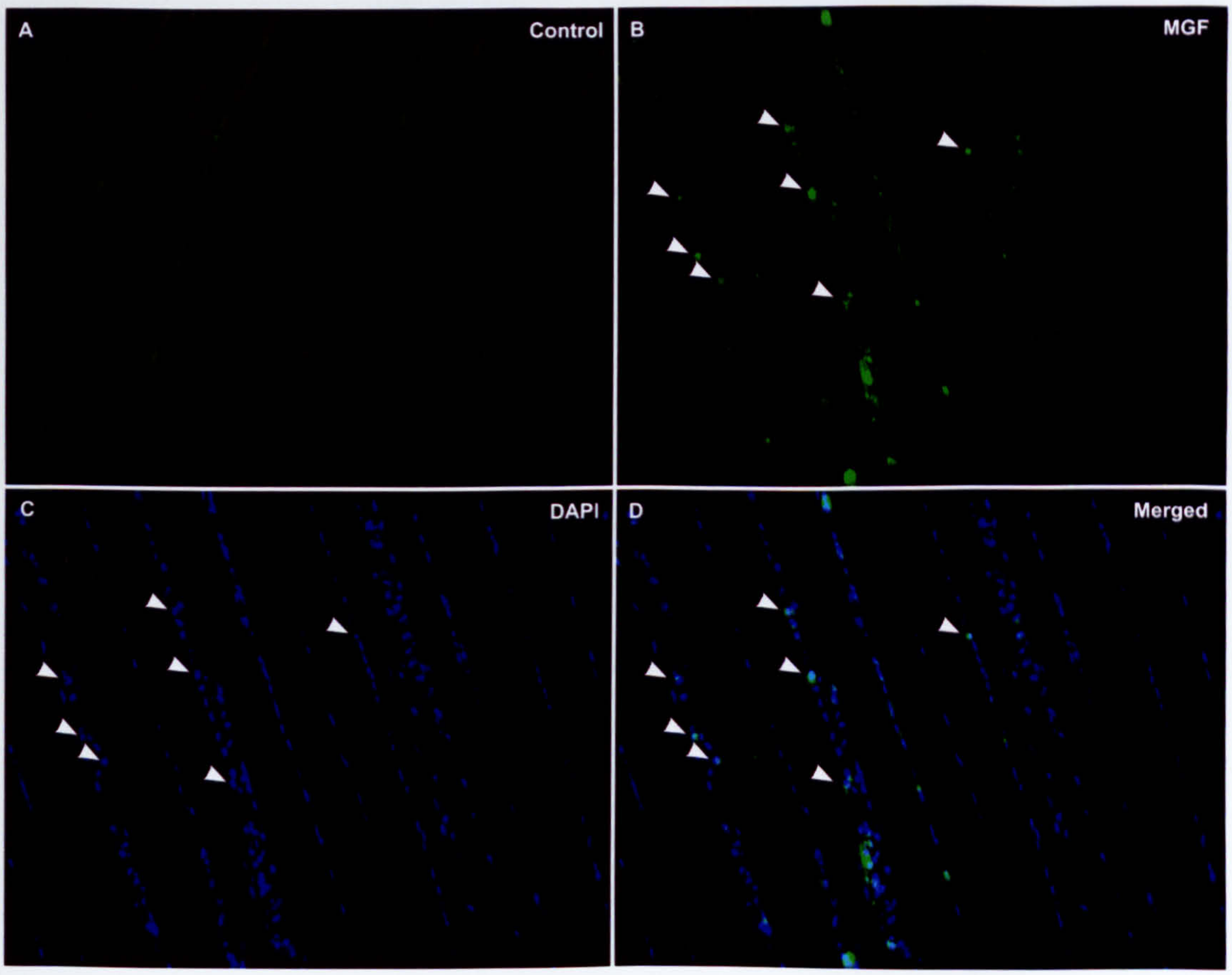

3.17 Mechano-growth factor (MGF) expression in the soleus muscle.

Longitudinal sections were stained with MGF 1°Ab and this was detected with fluorescein 2°Ab to show MGF positive nuclei. No MGF positive nuclei were found in the control muscle (A). In contrast, nuclei positive for MGF were detected after isoprenaline injection (green, B; arrowheads). Nuclei were identified using DAPI (blue, C; arrowheads). The localisation of MGF in the nuclei becomes apparent when the two images are merged (D; arrowheads) (all x200 magnification).

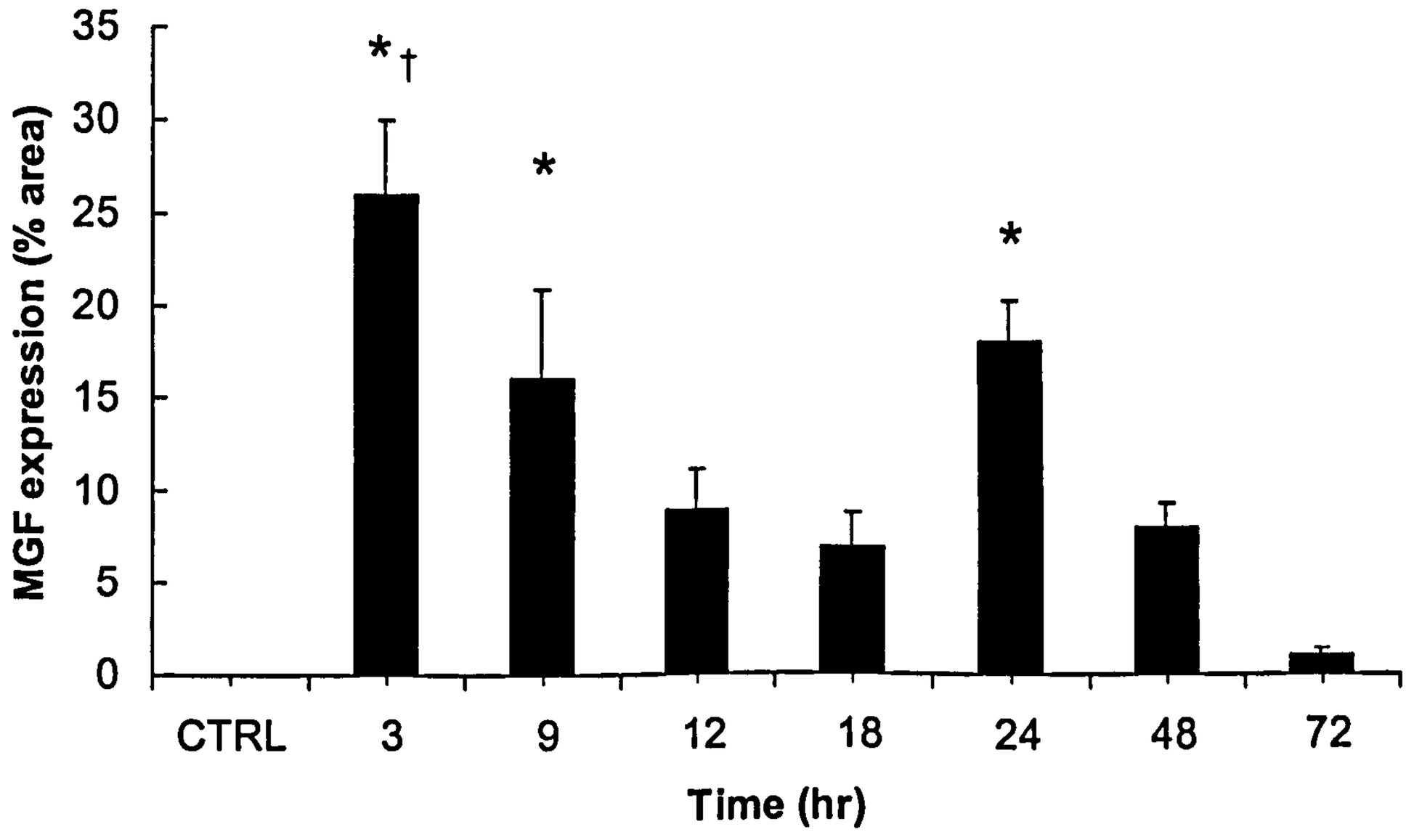

Figure 3.18 Time course of mechano-growth factor (MGF) expression in the soleus muscle.

Percent of MGF positive nuclei after a single injection (s.c.) of 20 mmol of isoprenaline kg^{-1}. While no MGF was found in the control muscles (CTRL) receiving saline vehicle only, detectable levels were observed between 3 and 72 hours after the isoprenaline. Results are Mean ± SEM for n=5 with *denoting significant differences ($P<0.01$) from CTRL. †denotes significant differences ($P<0.01$) compared with 12, 18, 48 and 72 hours.

MGF expression decreased with time and by 72 hours the amount of MGF positive nuclei was only 1%.

It was of interest that the hearts from the same isoprenaline-treated rats also had higher than normal expression levels of MGF (Figures 3.19; 3.20). MGF increased over time. At 24 hours MGF represented 1.6% of the field of view and it remained elevated up to 72 hours, following isoprenaline injection (Figure 3.20). The time course in the heart was a little different from that found in the soleus. It is however indicative of this growth factor's potential role in regeneration of the heart.

Key points:

1. Despite catecholamine-induced fibre death and loss, the soleus muscle repaired and replaced its full fibre complement by 28 days.

2. Muscle stem cells, satellite cells (c-met positive), were identified in the soleus muscle at the initiation of the fibre regeneration process.

3. Mechano-growth factor (MGF) expression in the soleus muscle and heart was significantly elevated up to 72 hours, following catecholamine-induced damage. This is in accordance with satellite cell activation and proliferation.

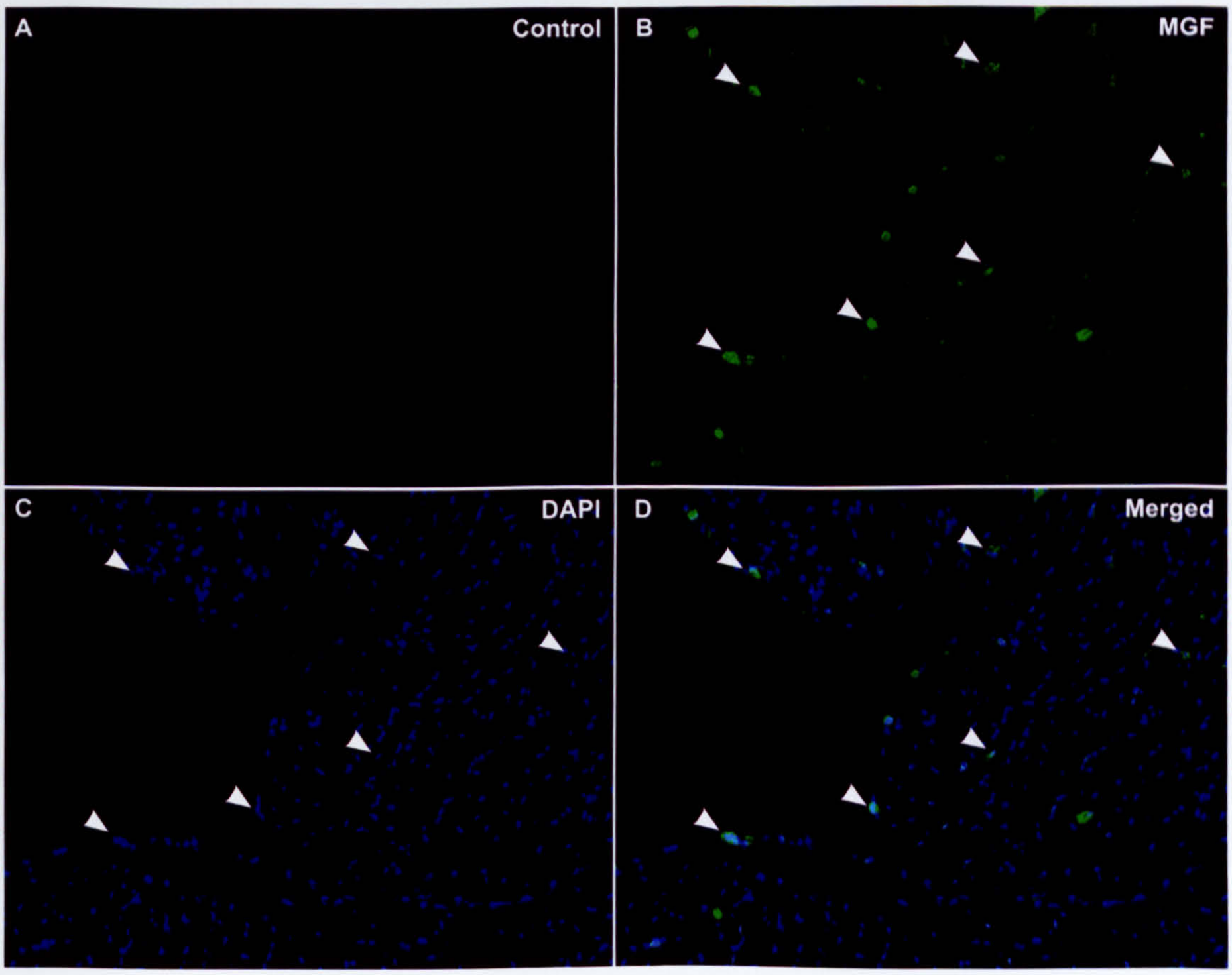

3.19 Mechano-growth factor (MGF) expression in the heart.

Transverse sections were stained with fluorescein to identify MGF positive staining in the heart. No MGF expression was detected in control hearts (A), but was apparent in the heart (B; arrowheads) after isoprenaline administration. Nuclei were identified using DAPI (blue, C; arrowheads). The localisation of MGF in the nuclei becomes apparent when the two images are merged (D; arrowheads) (x200 magnification).

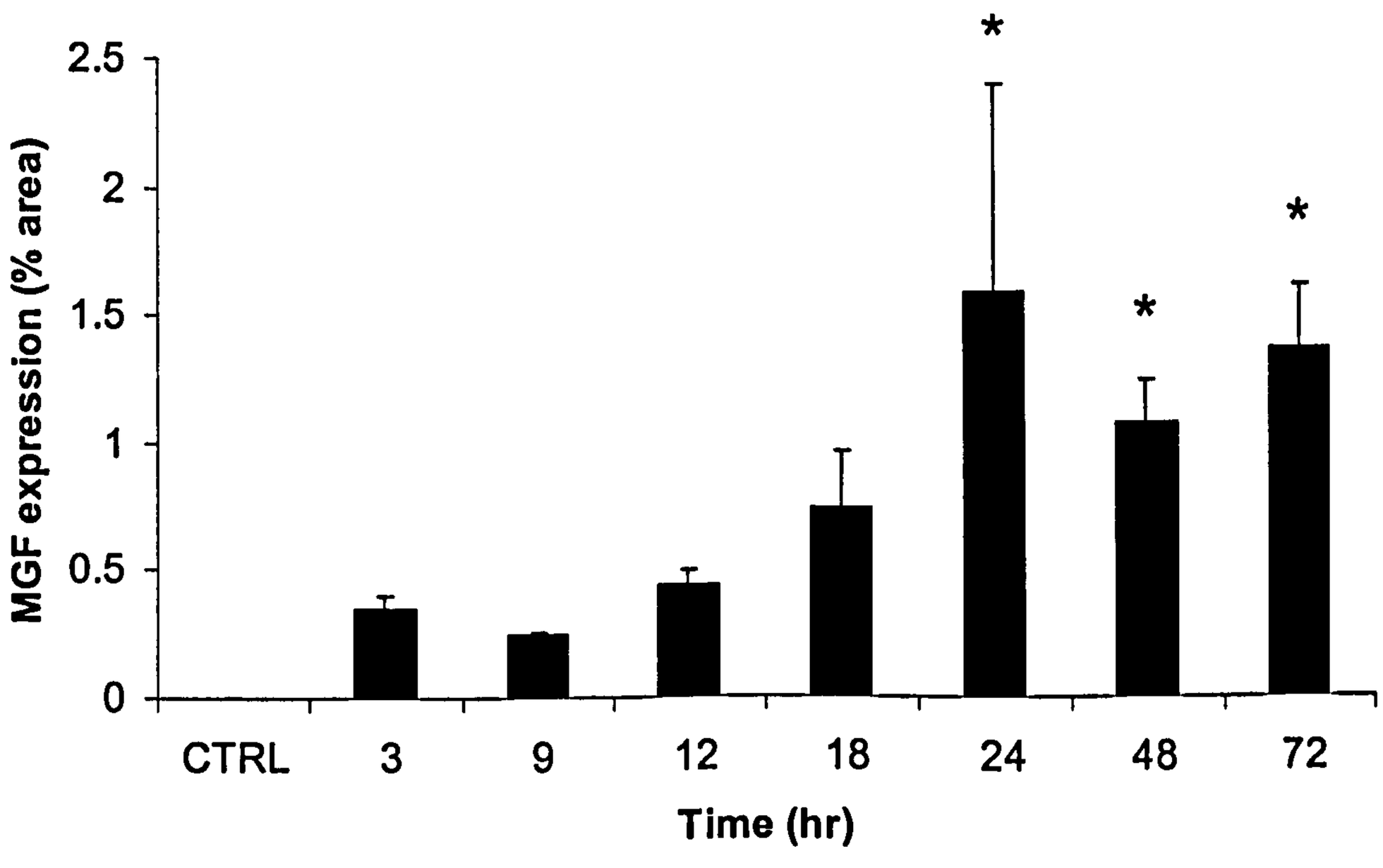

Figure 3.20 Time course of mechano-growth factor (MGF) expression in the heart.

Percent of MGF expression in response to a single injection (s.c.) of 20 mmol of isoprenaline kg^{-1}. No MGF was found in the control muscles (CTRL) receiving saline vehicle only. Results are Mean ± SEM for n=5 and *denotes significant differences ($P<0.01$) from CTRL.

3.4 Cardiomyocyte Death and Regeneration

3.4.1 Cardiac function

Evaluations of ventricular function showed that a single injection of isoprenaline (20 mmol kg^{-1}) caused marked changes in LV performance (Figure 3.21). When compared to control animals, at 1 day after injection, isoprenaline-treated animals exhibited a significantly ($P<0.05$) decreased LV developed pressure (LVDevP; CTRL, 88.5 ± 8.2; ISO, 64.3 ± 12.7 mmHg), $^{+}dP/dt$ (CTRL, 8124 ± 1027; ISO, 6546 ± 888 mmHg/s) and $^{-}dP/dt$ (CTRL, 7889 ± 1240; ISO 5730 ± 625 mmHg/s) and increased LV end-diastolic pressure (LVEDP; CTRL, 3.8 ± 1.5; ISO, 21.0 ± 4.2 mmHg), uncovering acute LV failure. Interestingly, these parameters started to improve after 3 days and all returned to control values by 14 days, indicating restored LV function.

3.4.2 Myocyte death, size and number

Gross characteristics of the heart are shown in Table 3.1. Briefly, isoprenaline injection caused significant ($P<0.05$) decreases in body weight, compared to control animals. Catecholamine exposure at the concentrations used here, caused both necrotic and apoptotic cardiomyocyte death in the rat heart in the presence of a patent coronary circulation, resulting in remodelling of the ventricular wall.

Morphometric analysis revealed considerable myocardial injury and focal necrosis to the LV, resulting in an increased area fraction of dead myocytes and interstitial cells and a decreased percentage area of viable myocytes, following bolus isoprenaline administration (Table 3.2). This cell damage occurred shortly after isoprenaline administration. The effect was most pronounced 1 day after injection, but for all time points (1, 3, 6 and 14 days), the myocardium showed significantly ($P<0.05$) less area occupied by viable myocytes, and a greater area occupied by dead and interstitial cells, compared to control animals. By 14 days, the area fraction of viable myocytes had increased slightly, so that it was now significantly ($P<0.05$) greater than at 1, 3 and 6 days. In parallel, the percentage of dead myocytes had significantly decreased ($P<0.05$) from 1 and 3 days.

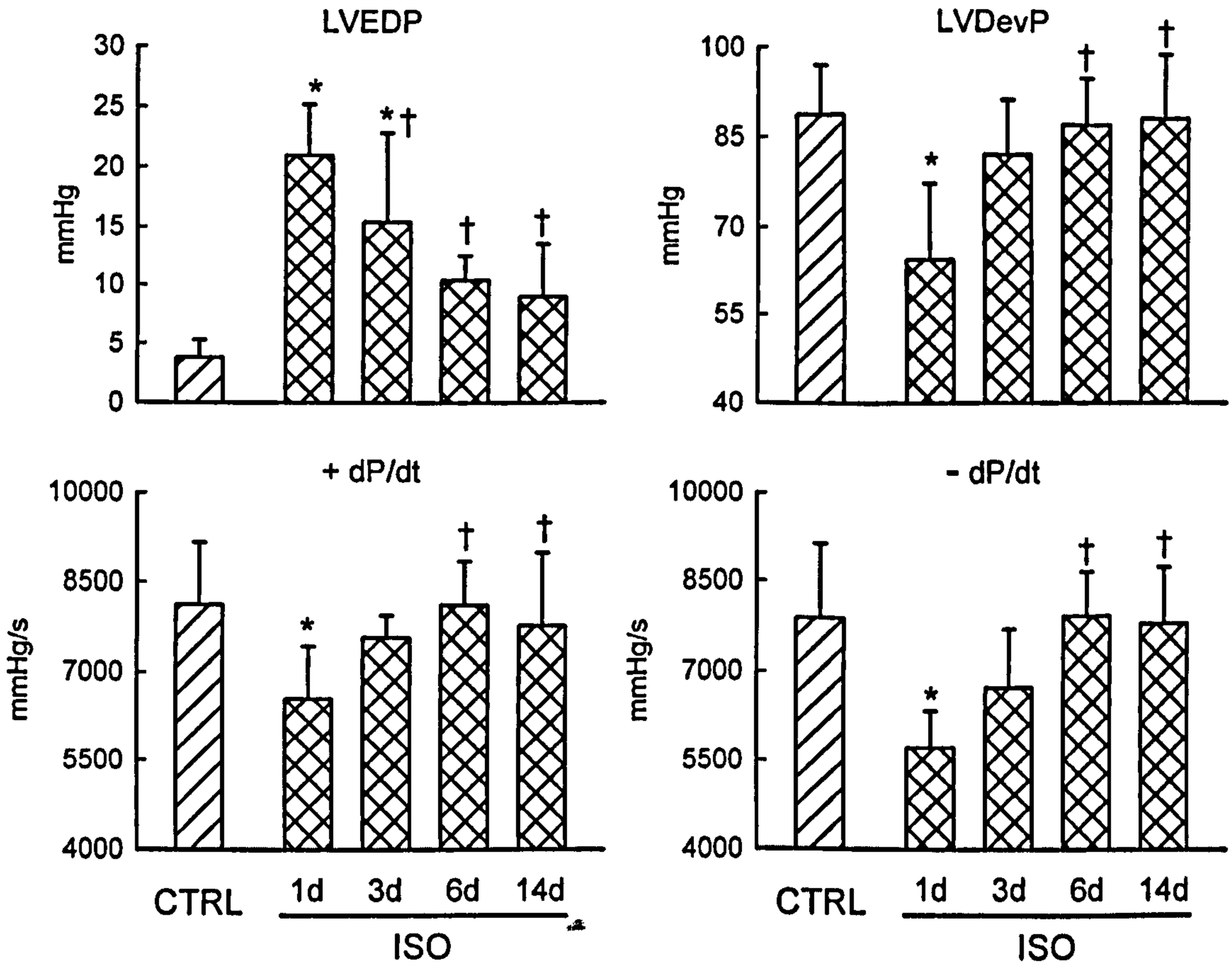

Figure 3.21 Left ventricular (LV) function.

Time course of changes in LV function in response to a single injection (s.c.) of 20 mmol of isoprenaline kg^{-1}. One group of animals (CTRL) received the saline vehicle. Haemodynamic measurements were taken by advancing a microtip pressure transducer into the LV cavity through the right carotid artery. Results are Mean ± SD for n=5. *denotes significant differences ($P<0.05$) from CTRL. †denotes significant differences ($P<0.05$) from 1 day. ISO indicates isoprenaline-treated animals; LVEDP, LV end-diastolic pressure; LVDevP, LV developed pressure; $^{+}$dP/dt, LV contraction; $^{-}$dP/dt, LV relaxation. ISO indicates isoprenaline-treated animals.

Table 3.1 Gross cardiac characteristics.

Changes in cardiac characteristics in response to a single injection (s.c.) of 20 mmol of isoprenaline kg^{-1}. One group of animals (CTRL) received the saline vehicle. Results are Mean ± SD for n=5. *denotes significant difference (P<0.05) from CTRL.

	BW (g)	Left ventricle (mg)	Chamber diameter (mm)	Chamber volume (mm^3)	Free wall thickness (mm)	Septum thickness (mm)	Wall thickness/ Chamber radius (mm)	LV mass/ Chamber volume (mg/mm^3)
CTRL	348 ± 8	790 ± 12	6.9 ± 0.8	315.6 ± 170.0	2.22 ± 0.2	1.9 ± 0.4	0.6 ± 0.1	2.5 ± 0.1
1 day	298 ± 11*	848 ± 54*	6.7 ± 0.7	336.1 ± 104.0	2.21 ± 0.2	1.6 ± 0.1	0.5 ± 0.1	2.6 ± 0.7
3 days	298 ± 5*	845 ± 75*	6.8 ± 0.4	374.6 ± 83.6	2.30 ± 0.1	2.0 ± 0.3	0.6 ± 0.1	2.2 ± 0.4
6 days	302 ± 17*	813 ± 26	7.4 ± 1.3	391.3 ± 145.2	2.13 ± 0.5	1.6 ± 0.2	0.5 ± 0.2	2.2 ± 0.9
14 days	298 ± 5*	724 ± 35	6.4 ± 1.4	381.5 ± 103.1	2.17 ± 0.2	1.6 ± 0.1	0.7 ± 0.2	2.0 ± 0.7

Table 3.2 Catecholamine-induced myocardial injury.

Percent number of viable myocytes, dead myocytes and interstitial cells were measured in the LV wall after a single injection (s.c.) of 20 mmol of isoprenaline kg^{-1}. One group of animals (CTRL) received the saline vehicle only. The percent area of myocytes, dead myocytes and interstitial cells was determined by using a 42 point morphometric reticle and counting the fraction of all points that lie over these cell profiles. At least 100 of each cell type were counted for each layer of the LV wall (sub-endocardium, mid-wall, sub-epicardium). But, if these numbers could not be achieved, then the entire region was measured (Anversa and Olivetti, 2002). Results are Mean ± SD for n=5. *denotes significant differences ($P<0.05$) from 1, 3, 6 and 14 days. $^{+}$denotes significant differences ($P<0.05$) from 1, 3 and 6 days and †denotes significant differences ($p<0.05$) from 1 and 3 days.

	Total Wall		
	Myocytes (%)	**Dead Cells (%)**	**Interstitium (%)**
CTRL	90 ± 0*	0 ± 0*	10 ± 0*
1d	69 ± 3	17 ± 4	15 ± 2
3d	67 ± 3	15 ± 2	19 ± 1
6d	70 ± 3	11 ± 3	19 ± 5
14d	76 ± 3^{+}	7 ± 1†	18 ± 2

Left ventricular weight was found to be significantly increased ($P<0.05$) at 1 and 3 days, when compared to controls. Notably, it had returned to normal values by 14 days after the isoprenaline injection (Figure 3.22). Comparable with the latter finding, myocyte volume was markedly increased ($P<0.05$) after 3 days, transiently decreased at 6 and 14 days, but consistently remained higher ($P<0.05$) than control values (Figure 3.22). Analysis of LV myocyte number revealed a significant and linear loss of myocytes from 1 to 3 days, (21 to 49 % decrease, $P<0.05$). Then, myocyte number increased slightly at 6 days becoming significantly ($P<0.05$) higher by 14 days compared to 3 days after isoprenaline injection. However, this value still remained lower than control animals (Figure 3.22).

Catecholamine-induced cardiomyocyte apoptosis, identified by labelling for caspase-3 (Figures 3.6; 3.7), was confirmed using the TdT (TUNEL) assay with dUTP (Figure 3.23). Table 3.3 describes the analytical process for assessing the effects of isoprenaline on dUTP labelled myocyte nuclei in the LV. The myocardium of control animals exhibited a low rate of myocyte apoptosis ($0.01 \pm 0.01\%$). In contrast, the amount of apoptotic myocyte nuclei was significantly ($P<0.05$) increased at 1, 3 and 14 days, compared to controls (Table 3.3).

The fraction of dUTP labelled myocyte nuclei in the LV was similar to the amount of caspase-3 labelled cardiomyocytes at 1 and 3 days (Figure 3.7), further confirming the specific identification of catecholamine-induced apoptosis in the heart. There were also clear distinctions between LV layers, in terms of myocyte death. The sub-endocardium was much more affected by isoprenaline than the mid-wall and sub-epicardium. The sub-endocardium exhibited a significantly ($P<0.05$) greater loss of myocytes, paralleled with more pronounced ($P<0.05$) areas of dead myocytes and interstitial cells, when compared to the mid-wall and sub-epicardium (Table 3.4). Similarly, the sub-endocardium and mid-wall displayed significantly ($P<0.05$) greater apoptotic myocyte nuclei 1 day after isoprenaline injection, when compared to sub-epicardium. By 3 days the number of apoptotic cells detected had

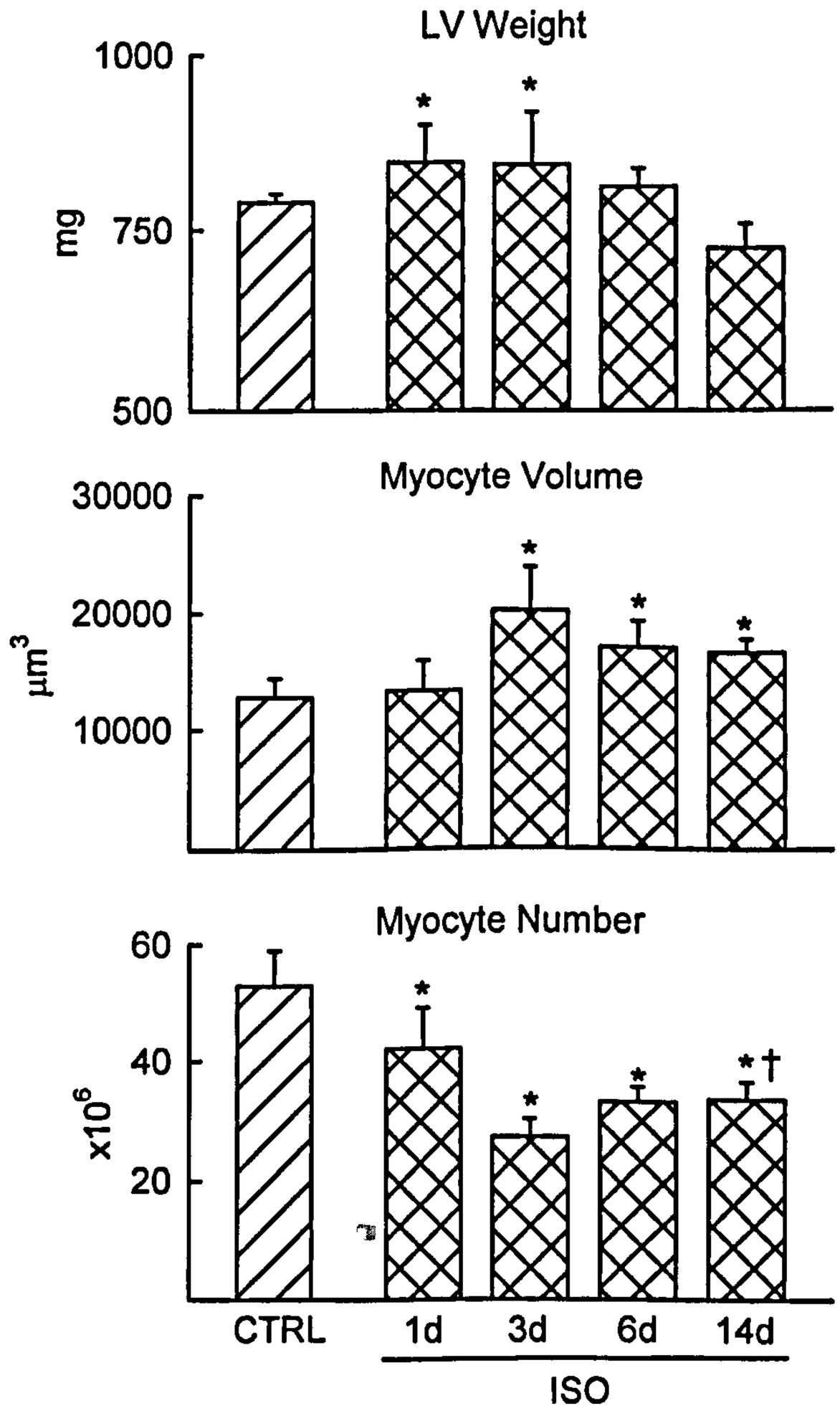

Figure 3.22 LV weight, myocyte volume and total myocyte number.

Time course of LV weight (top panel), myocyte cell volume (middle panel) and number (bottom panel), in response to a single injection (s.c.) of 20 mmol of isoprenaline kg^{-1}. One group of animals (CTRL) received the saline vehicle. Myocyte cell volume was calculated from the product of myocyte CSA and length. Myocyte number was determined from the total volume of myocytes and individual myocyte cell volume. Total volume of myocytes is the product of LV volume and percent area of viable myocytes (see methods). Results are Mean ± SD for n=5. *denotes significant differences ($P<0.05$) from CTRL. †denotes significant difference ($P<0.05$) from 3 days. ISO indicates isoprenaline-treated animals.

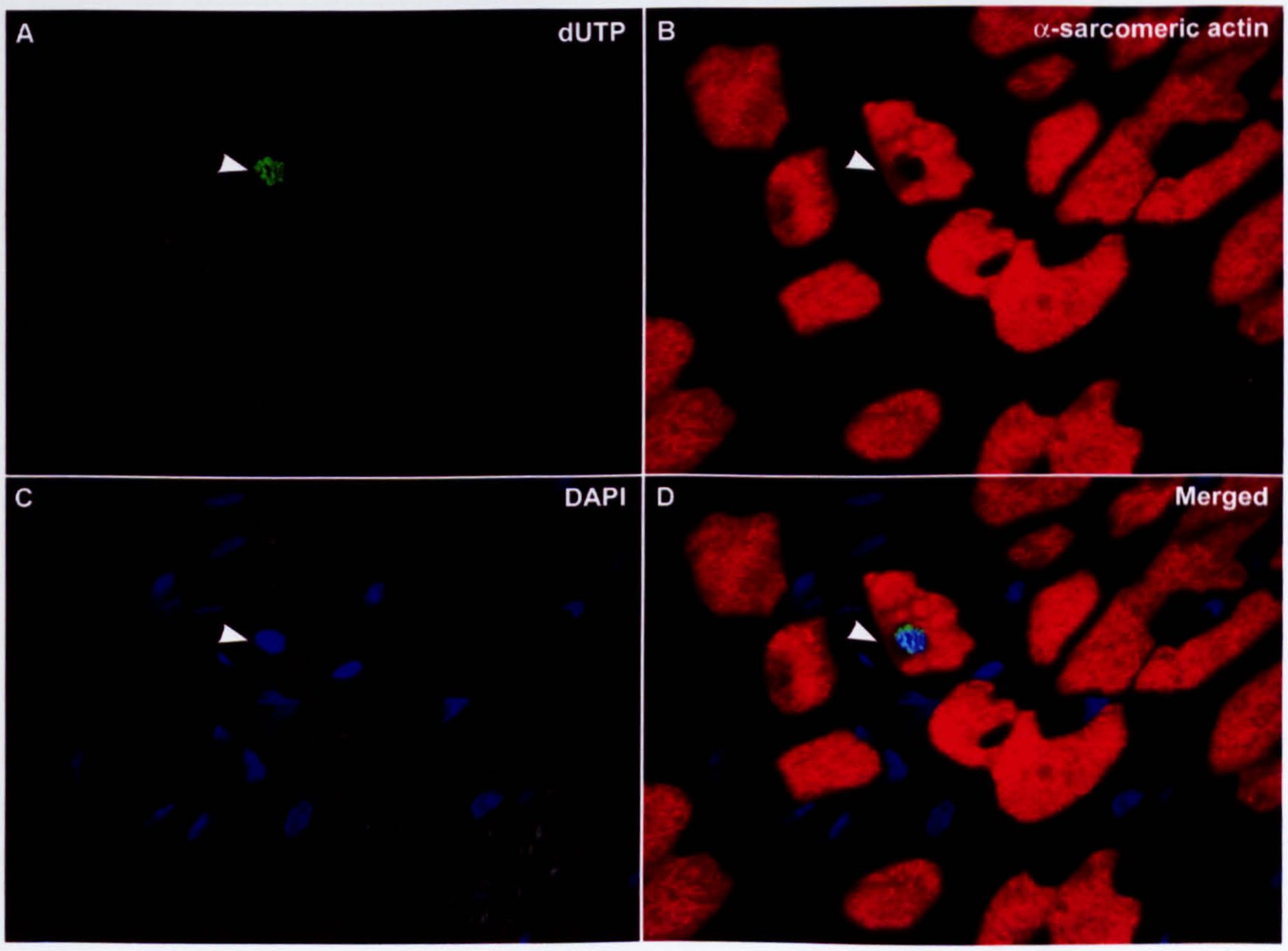

Figure 3.23 Isoprenaline-induced apoptosis in the LV.

Animals were injected (s.c.) with 20 mmol of isoprenaline kg^{-1}, killed at various time points up to 14 days, and 5μm cryo-sections of the heart cut transversely. DNA strand breaks in myocyte nuclei were immunohistochemically detected using the Terminal deoxynucleotidyl Transferase (TdT) assay with dUTP. dUTP positive nuclei (green, A; arrowhead) were detected in the myocardium. Myocyte cytoplasm was identified using an antibody against α-sarcomeric actin (red, B), and nuclei were counterstained with DAPI (blue, C). The dUTP labelled nuclei were confirmed as myocyte nuclei by merging the three images (D) (all x1000 magnification).

Table 3.3 Effects of isoprenaline on dUTP labelled myocyte nuclei in the LV. The fraction of apoptotic myocytes (dUTP positive) was determined by first obtaining the numerical density of myocyte nuclei in the myocardial area. This was done by counting the number of myocyte nuclei per unit area and multiplying by the total area of the myocardial tissue section. As the entire cross-section of myocardium was examined for apoptosis, the number of dUTP labelled myocytes divided by the numerical density of myocyte nuclei yields the percent apoptotic myocyte nuclei. Results are Mean ± SD for n=5. *denotes significant differences ($P<0.001$) from control animals. †denotes significant differences ($P<0.05$) from 1 day.

	CTRL	1 DAY	3 DAYS	14 DAYS
Myocardial area examined for apoptosis (mm^2)	35.8 ± 3.7	27.5 ± 2.1	34.5 ± 1.7	32.2 ± 1.7
Tdt labelled myocyte nuclei	3 ± 1	71 ± 11	33 ± 4	31 ± 10
Myocardial area examined for myocyte nuclear density (mm^2)	0.6 ± 0.01	0.6 ± 0.01	0.6 ± 0.01	0.6 ± 0.01
Myocyte nuclei	444 ± 89	376 ± 36	332 ± 37	380 ± 47
Myocyte nuclei/ mm^2	755 ± 151	639 ± 61	564 ± 62	646 ± 80
% Tdt labelled myocyte nuclei	0.01 ± 0.01	0.42 ± 0.09*	0.19 ± 0.04*†	0.15 ± 0.06*†

Table 3.4 Catecholamine-induced injury in the 3 layers of the LV wall.

Percent number of viable myocytes, dead myocytes and interstitial cells were measured in the each layer of the LV wall after a single injection (s.c.) of 20 mmol of isoprenaline kg^{-1}. One group of animals (CTRL) received the saline vehicle. The percent area of viable myocytes, dead myocytes and interstitial cells was determined using a 42 point morphometric reticle and counting the fraction of all points that lie over these cell profiles. At least 100 of each cell type were counted for each layer. Where this number of cells was not achieved, the entire layer was measured (Anversa and Olivetti, 2002). Results are Mean ± SD for n=5 and *denotes significant differences (P<0.05) from midwall and sub-epicardium.

	Sub-Endocardium			Mid-Wall			Sub-Epicardium		
	Myocytes (%)	*Dead Cells (%)*	*Interstitium (%)*	*Myocytes (%)*	*Dead Cells (%)*	*Interstitium (%)*	*Myocytes (%)*	*Dead Cells (%)*	*Interstitium (%)*
CTRL	90 ± 0	0 ± 0	10 ± 0	90 ± 1	0 ± 0	9 ± 1	90 ± 1	0 ± 0	10 ± 1
1d	50 ± 5*	32 ± 5*	18 ± 2	75 ± 4	12 ± 5	13 ± 2	80± 1	6 ± 3	13 ± 4
3d	45 ± 7*	29 ± 6*	26 ± 1*	74 ± 2	9 ± 1	17 ± 1	81 ± 2	5 ± 1	14 ± 1
6d	42 ±10*	26 ± 9*	33 ± 5*	84 ± 2	5 ± 0	12 ± 2	85 ± 2	2 ± 0	10 ± 1
14d	61 ± 4*	17 ± 3*	23 ± 1*	83 ± 3	3 ± 1	14 ± 3	83 ± 3	0 ± 0	16 ± 3

decreased so that there were no differences between myocardial layers (Figure 3.24).

As isoprenaline-treated animals exhibited a larger myocyte volume than their control counterparts (Figure 3.22), it was interesting to determine the distribution of myocyte sizes in the isoprenaline-treated animals. The frequency distribution of myocyte sizes showed that in control animals 85% were distributed between, 5000 to 22000 μm^3. In contrast, in isoprenaline-treated animals, only 66% of the myocytes were in this range. The remaining myocytes were both larger (range of 23000 to 39000: ISO 18%; CTRL, 12%), revealing myocyte hypertrophy and smaller (range of 1000 to 4000: ISO, 14%; CTRL, 0%), suggesting myocyte hyperplasia (Figure 3.25).

3.4.3 Myocyte regeneration

These interesting findings of smaller myocytes after isoprenaline injection pointed to the occurrence of cellular hyperplasia in the rat hearts following isoprenaline-induced acute and diffuse myocardial damage. To test this hypothesis, BrdU and Ki67 staining were used to assess myocyte-specific proliferation. Remarkably, BrdU-positive small myocytes (Figure 3.26) were detected as soon as 3 days after isoprenaline-injection.

This BrdU incorporation could reflect either new myocyte formation or reactive DNA synthesis in LV cardiomyocytes after catecholamine-induced myocardial damage. Ki-67 is somewhat preferable to BrdU for labelling proliferating cells because it is not involved in DNA repair. In fact, Ki-67 is a nuclear antigen expressed in all phases of the cell cycle, except G_0. All types of proliferating cells express Ki-67. On this basis, Ki67 labelling was used in conjunction with BrdU to confirm that these myocytes were 'true' replicating cells and not myocytes undergoing DNA repair.

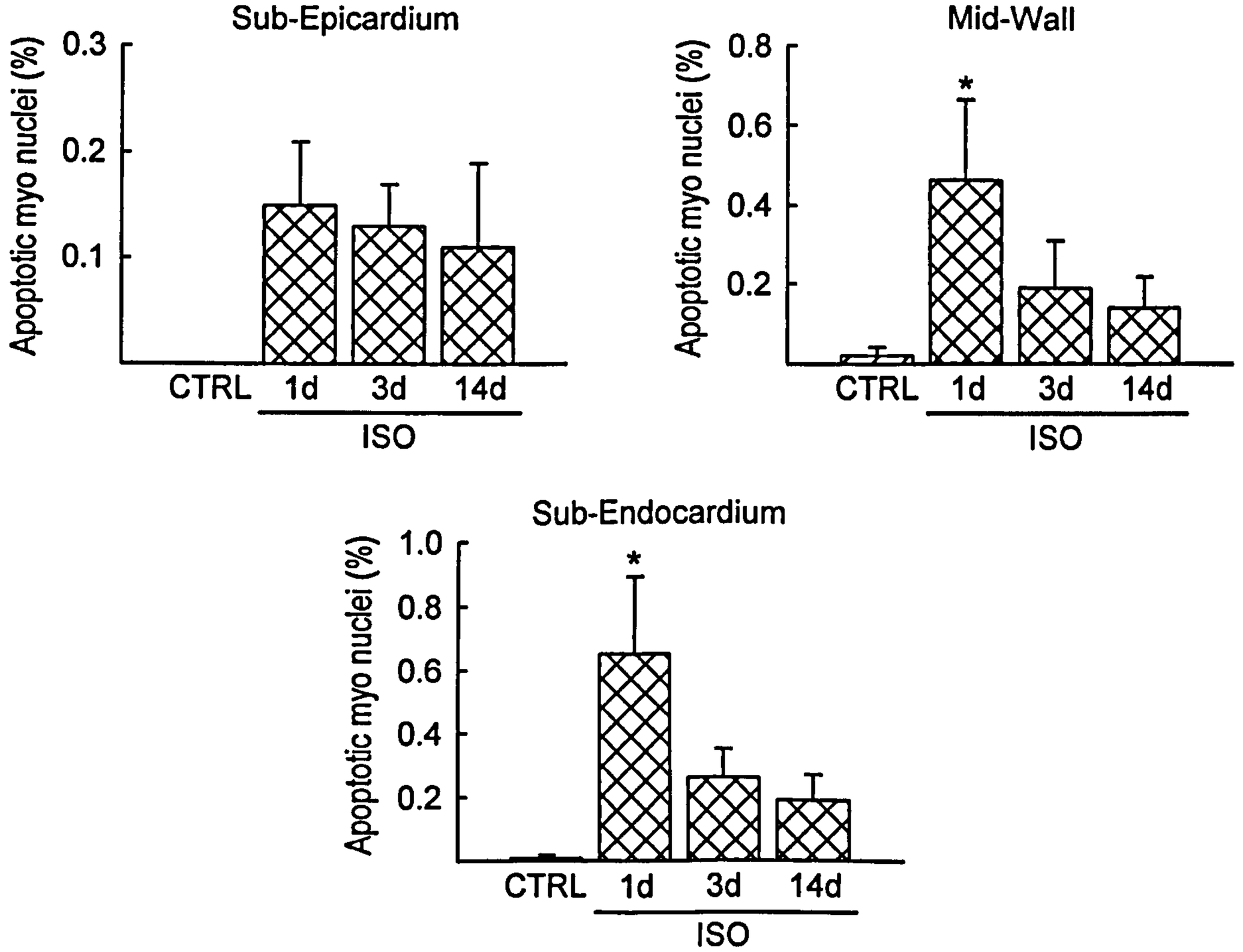

Figure 3.24 Apoptosis in the 3 layers of the LV wall.

Time course of percent apoptotic myocytes (dUTP positive) in the sub-endocardium, mid-wall and sub-epicardium layers of the LV wall, in response to a single injection (s.c.) of 20 mmol of isoprenaline kg^{-1}. One group of animals (CTRL) received the saline vehicle. The number of dUTP labelled myocyte nuclei per unit area of tissue were counted and by obtaining the numerical density of myocyte nuclei in each myocardial layer, the percentage of apoptotic myocyte nuclei was determined. Results are Mean ± SD for n=5 and *denotes significant differences ($P<0.05$) from sub-epicardium. ISO indicates isoprenaline-treated animals.

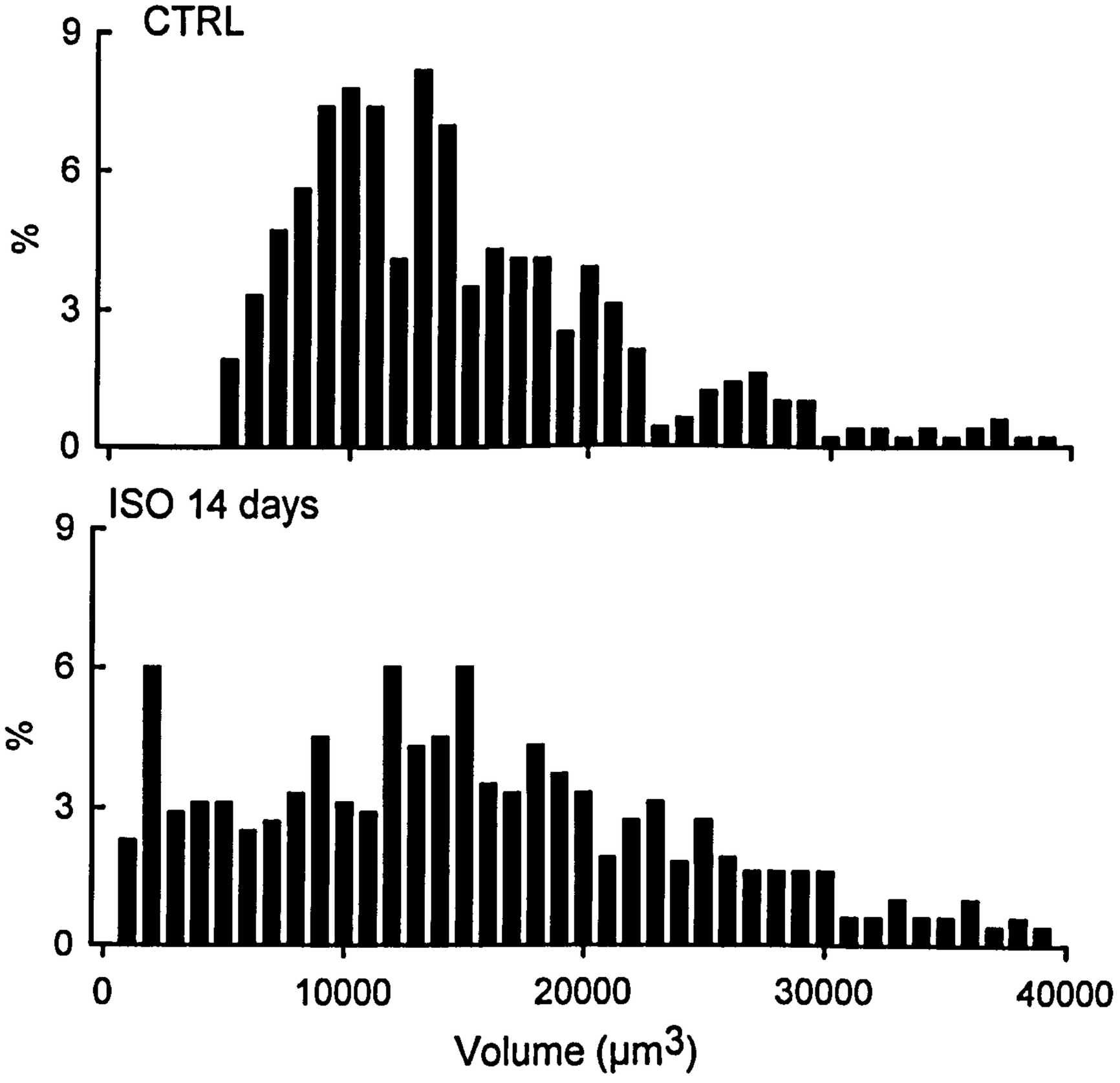

Figure 3.25 Distribution of myocyte sizes in the sub-endocardium.

Myocyte volume distribution in saline control animals (CTRL, top panel) and 14 days (bottom panel) after a single injection (s.c.) of 20 mmol of isoprenaline kg^{-1}. Myocyte cell volume was calculated from the product of myocyte cross-sectional area and length. ISO indicates isoprenaline-treated animals.

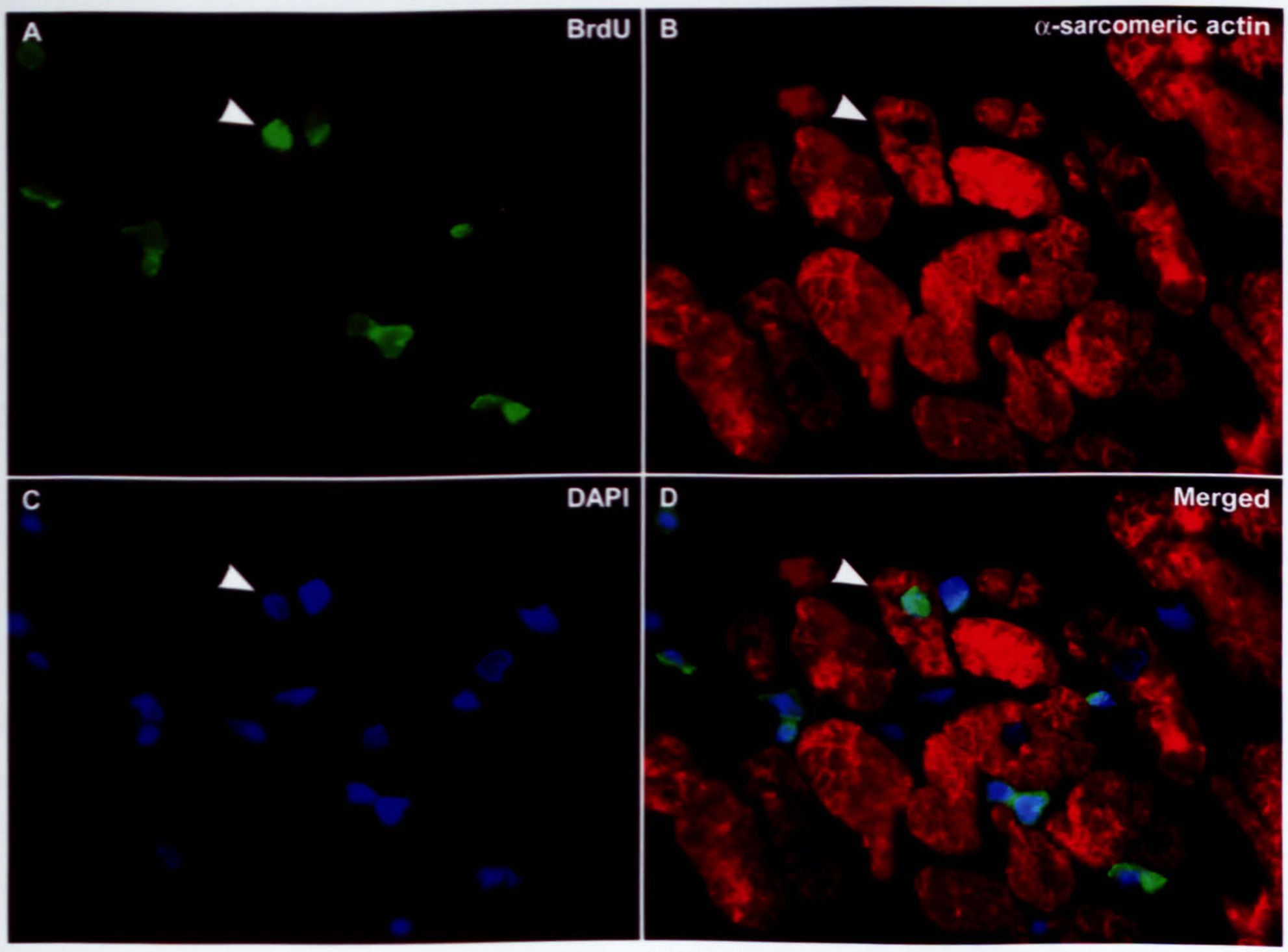

Figure 3.26 Newly formed myocyte in the myocardium (BrdU positive).

Newly formed myocytes were identified on transverse sections using antibodies against BrdU and α-sarcomeric actin, following isoprenaline-induced injury. A BrdU positive (green, A; arrowhead) myocyte (red, B) nuclei (blue, C) becomes clearly apparent when the three images are merged (D) (all x1000 magnification).

Accordingly, Ki67-positive myocyte nuclei were present in the LV myocardium following isoprenaline-injury, verifying the cycling nature of these cells (Figure 3.27). Consistent with myocyte death, regenerating myocytes were most evident in the sub-endocardium. At 6 days, there were 2 ± 1% BrdU positive myocytes ($P<0.05$) in the sub-endocardium, compared to only 0.3 ± 0.2% in the sub-epicardium. By 14 days, 4 ± 2% BrdU-positive myocyte nuclei ($P<0.05$) were present in the sub-endocardium, whereas only 2 ± 1% and 1 ± 1% were present in the mid-wall and sub-epicardium, respectively (Figure 3.28). In turn, the percentage of newly formed myocytes in the total LV wall increased in a linear time dependent manner, and by 6 days the number of BrdU positive myocytes were significantly ($P<0.05$) greater than 3 days and control animals. The peak amount of BrdU-positive myocytes (2%) was observed at 14 days (Figure 3.29). As described above, it should be noted that myocyte apoptosis decreased over time from 1 to 14 days after isoprenaline administration. This time dependent decrease in cardiac cell death was then simultaneously met by an increase in myocyte renewal over time (Figure 3.29). These findings suggest that myocyte regeneration is injury triggered, i.e. occurring as a response of the myocardium to replace the lost myocytes in a self-mediated attempt to repair the damage.

A subpopulation of small sized myocytes was identified in the hearts of isoprenaline-treated rats (Figure 3.25). To verify that this subset of cells corresponded to small developing myocytes, BrdU labelled myocyte sizes were measured at each time point after isoprenaline injection. Interestingly, the smallest myocytes were mainly BrdU-positive.

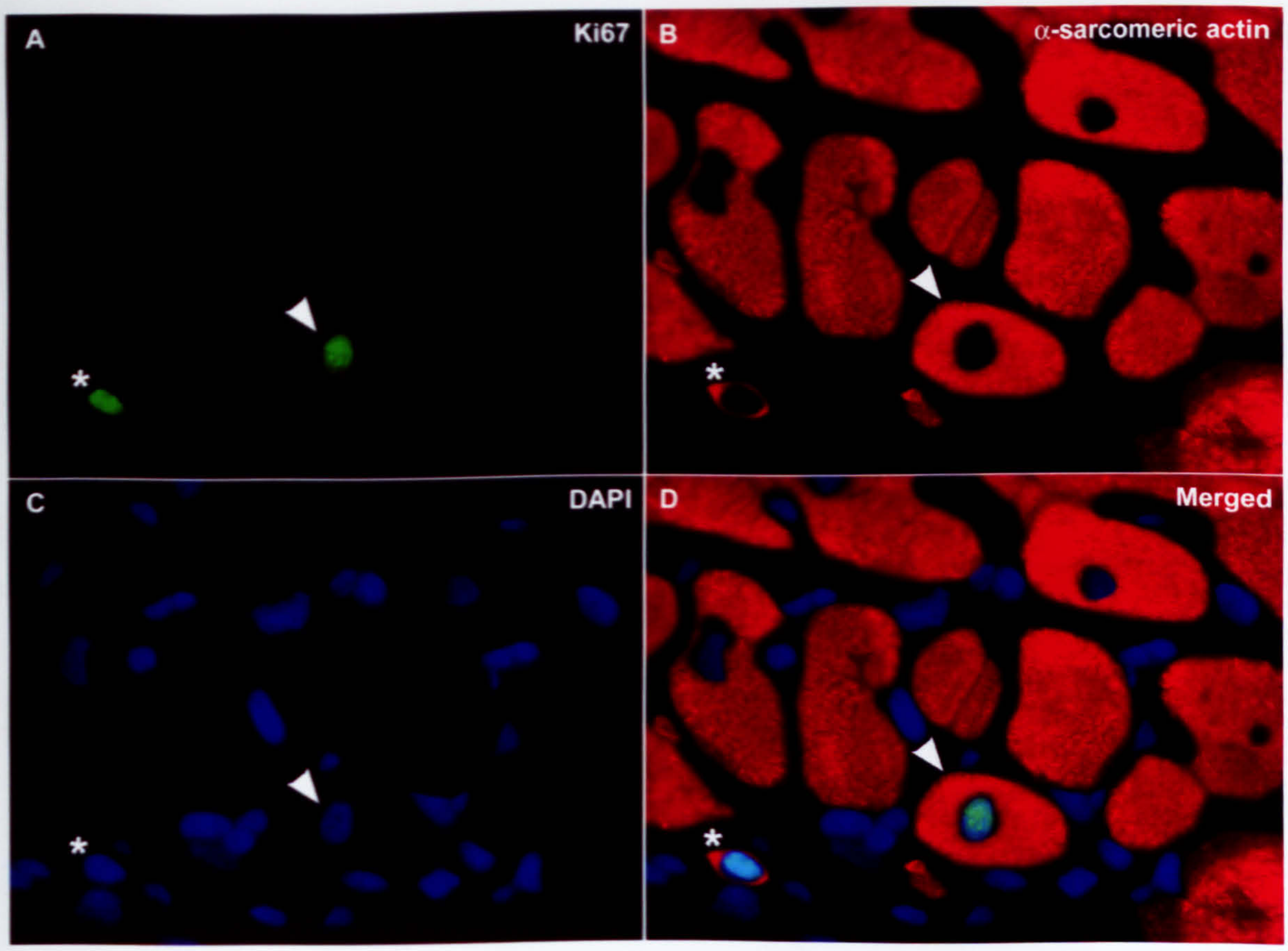

Figure 3.27 Newly formed myocytes in the myocardium (Ki67 positive).

Newly formed myocytes were confirmed by staining for Ki67 and α-sarcomeric actin. Ki67 positive nuclei (green, A; arrowhead) were identified in the myocardium as soon as 3 days after isoprenaline injection. The asterisk indicates a Ki67 positive nucleus of a small developing myocyte. Myocyte cytoplasm was detected by staining for α-sarcomeric actin (red, B). Nuclei were counterstained with DAPI (blue, C). The identification of a newly formed myocyte can be seen clearly when the three images are merged (D) (all x1000 magnification).

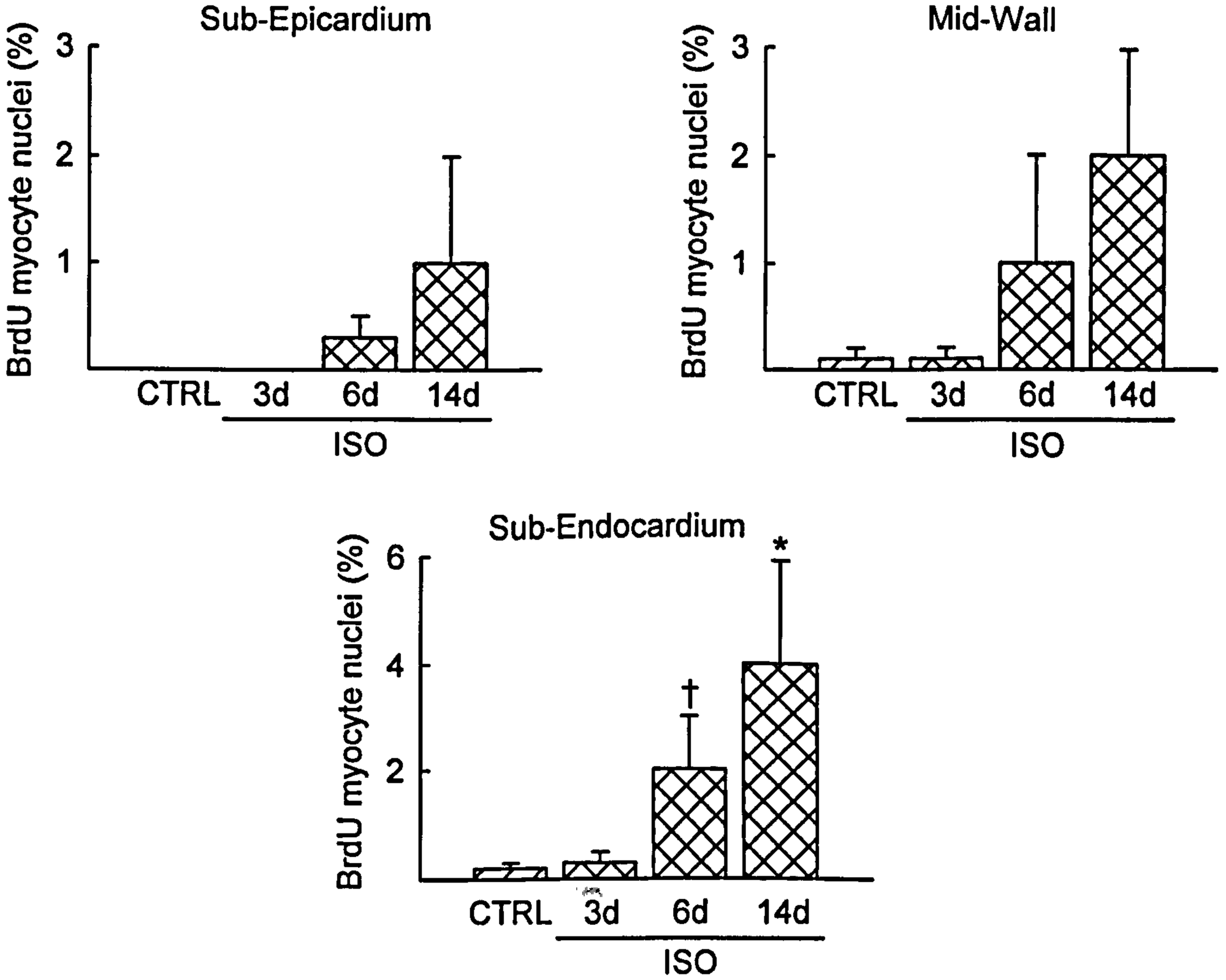

Figure 3.28 Newly formed myocytes in the 3 layers of the LV wall.

Time course of percent newly formed myocytes (BrdU positive) in the sub-endocardial, mid-wall and sub-epicardial layers of the LV wall, in response to a single injection (s.c.) of 20 mmol of isoprenaline kg^{-1}. One group of animals (CTRL) received the saline vehicle. All animals were injected (i.p.) with 50 mg of BrdU kg^{-1} twice daily until they were killed. The number of BrdU positive myocyte nuclei per 1500 myocytes were counted for each layer of the LV wall, across a total of 4 tissue sections, and expressed as a percent fraction. Results are Mean ± SD for n=5. *denotes significant difference ($P<0.05$) from mid-wall and sub-epicardium. †denotes significant difference ($P<0.05$) from sub-epicardium. ISO indicates isoprenaline-treated animals.

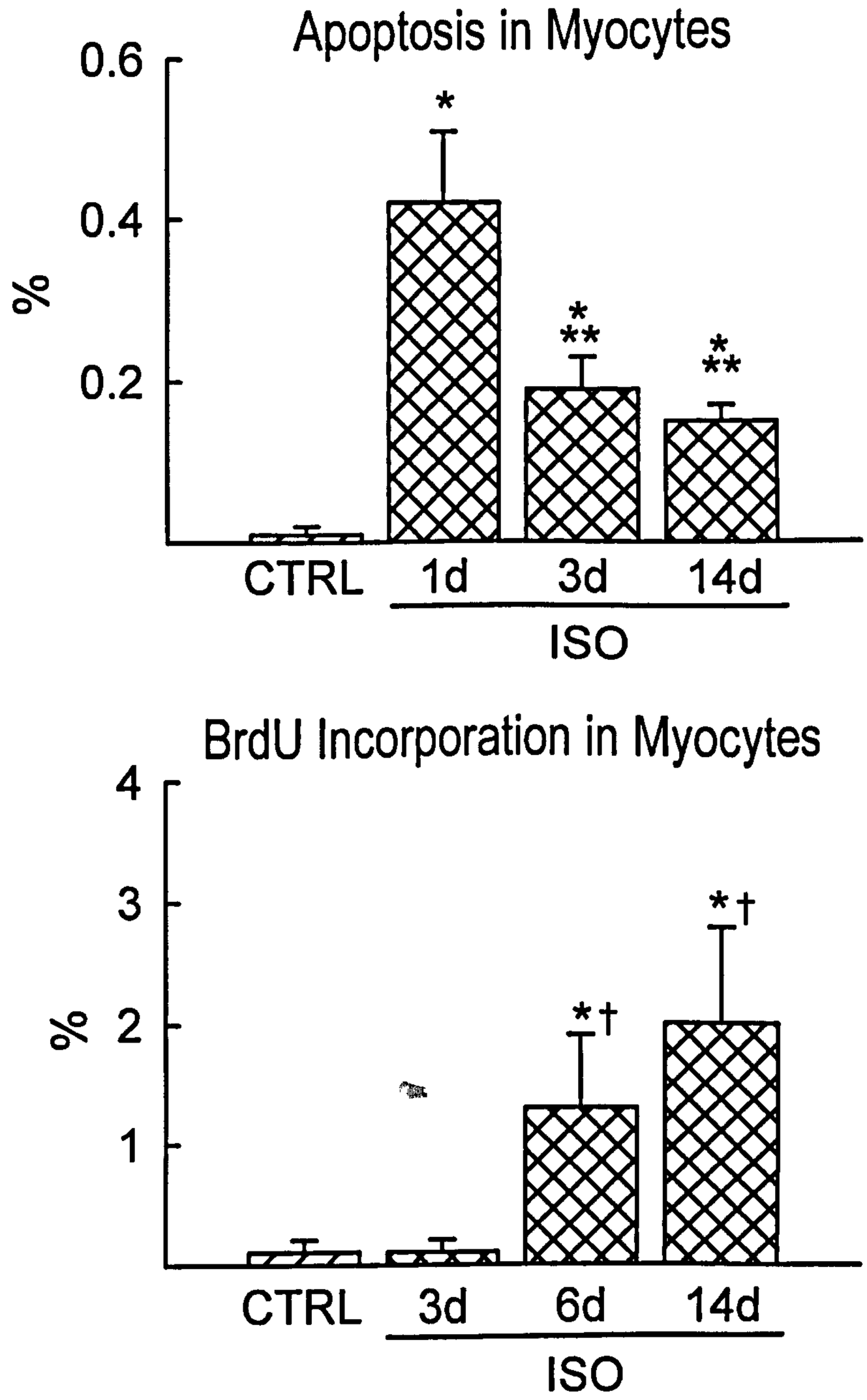

Figure 3.29 Cardiac cell death and regeneration.

Percent apoptotic (dUTP positive, top panel) and newly formed (BrdU positive, bottom panel) myocytes in the entire LV wall, in response to a single injection (s.c.) of 20 mmol of isoprenaline kg^{-1}. One group of animals (CTRL) received the saline vehicle. Results are Mean ± SD for n=5. *denotes significant differences ($P<0.001$) from CTRL. **denotes significant differences ($P<0.05$) from 1 day. †denotes significant differences ($P<0.05$) from 3 days. ISO indicates isoprenaline-treated animals.

Moreover, there were significant differences ($P<0.001$) in the sizes of the BrdU-positive cells over time, suggesting progressive maturation of these newly formed myocytes (Figures 3.30; 3.31). Indeed, beginning at 3 days, the average diameter of BrdU-positive myocytes was 3.5 ± 0.4μm. This had increased to 7.7 ± 0.8μm by 14 days (Figures 3.30; 3.31). More specifically, at 3 and 6 days after isoprenaline administration the sizes of BrdU-positive myocytes were significantly ($P<0.001$) smaller than BrdU-positive cells from control hearts. However, this difference was no longer apparent by 14 days (Figure 3.31). However, the BrdU-positive myocyte diameters of control and isoprenaline-treated animals were all significantly ($P<0.001$) smaller than BrdU-negative myocytes, indicating the immature phenotype of these cells.

3.4.4 Cardiac stem progenitor cells

In view of the recent identification of primitive and early-committed cells in the heart and their role in myocyte regeneration, the number of c-kit positive (c-kit^{POS}) cells in the myocardium was measured. Clusters of primitive and early committed cells expressing the stem cell antigen c-kit were found in the myocardium of control and isoprenaline-treated hearts (Figure 3.32). Interestingly, the number of cardiac c-kit^{POS} cells was found to be significantly ($P<0.01$) increased in isoprenaline-treated rats, when compared to controls. In fact, this value was 4-, 5-, 6- and 4-fold higher than controls at 1, 3, 6 and 14 days, respectively (Figure 3.33). Accordingly, the number of c-kit^{POS} cells increased 1 day after isoprenaline injection, compared to the control. Then, it peaked at 3 days remaining constant up to 6 days, being significantly ($P<0.05$) higher than at 1 day (Figure 3.33). By 14 days, c-kit^{POS} cell numbers started to decrease, but remained above control values (Figure 3.33). Many of these c-kit^{POS} cells were found to express ki67 in their nuclei, indicating activation and proliferation of these cells following the isoprenaline-injury (Figure 3.34). Consequently, some of the c-kit^{POS} cells expressed the transcription factor GATA4, which implicated cardiomyocyte differentiation (Figure 3.35). The recognition of cells positive for c-kit and GATA4 provided evidence of a link between primitive cells and early differentiating myocyte progenitors.

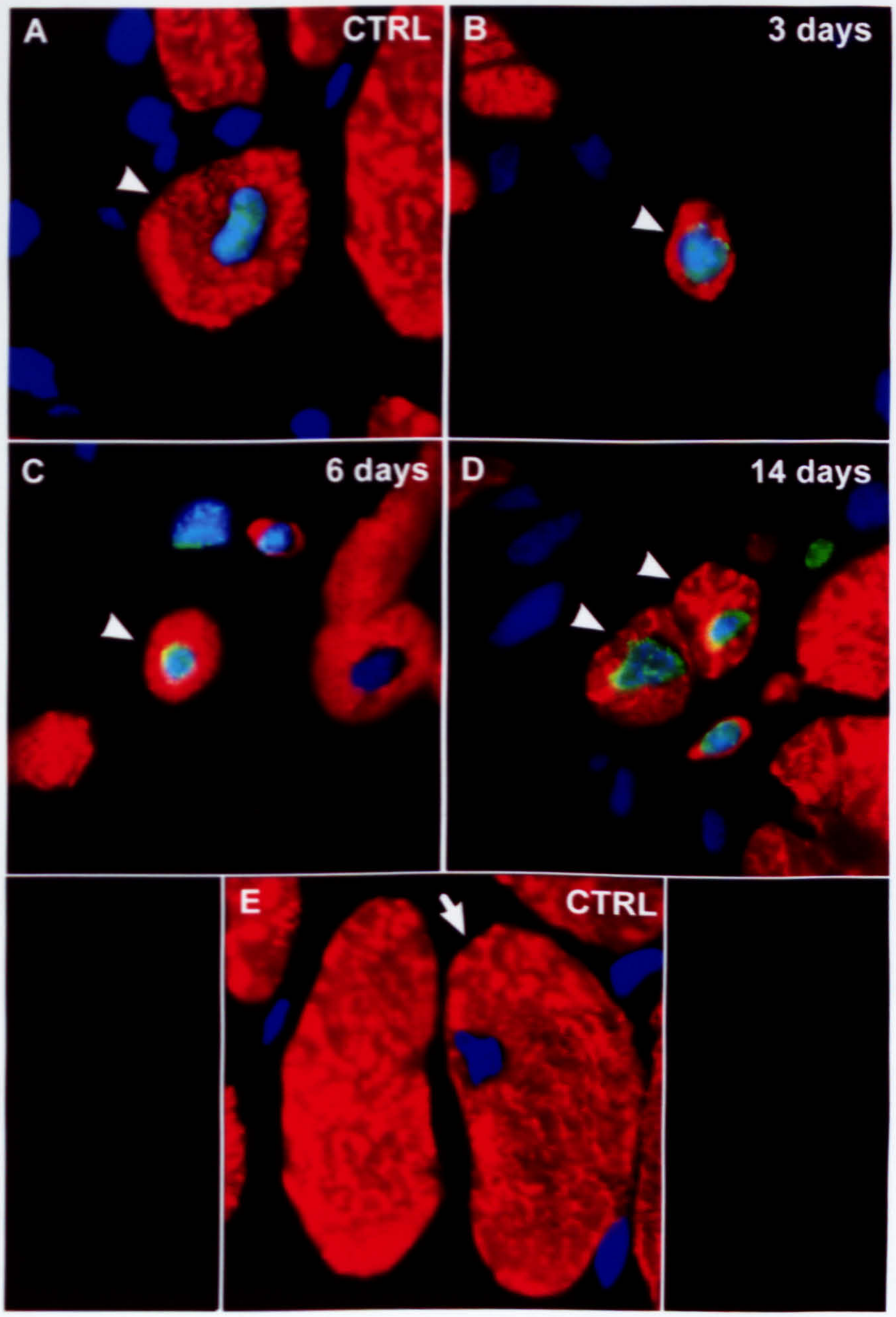

Figure 3.30 Newly-formed myocyte sizes.

The newly formed myocytes (arrowheads) increased in size from 3 days to 14 days, after isoprenaline bolus administration. BrdU positive (green) myocyte (red) nuclei (blue) in saline CTRL animals (A); and 3 (B), 6 (C) and 14 (D) days after isoprenaline injection. A differentiated myocyte (red; α-sarcomeric actin, blue; DAPI; arrow) (E) is larger than the all the BrdU positive myocytes (all x1000 magnification).

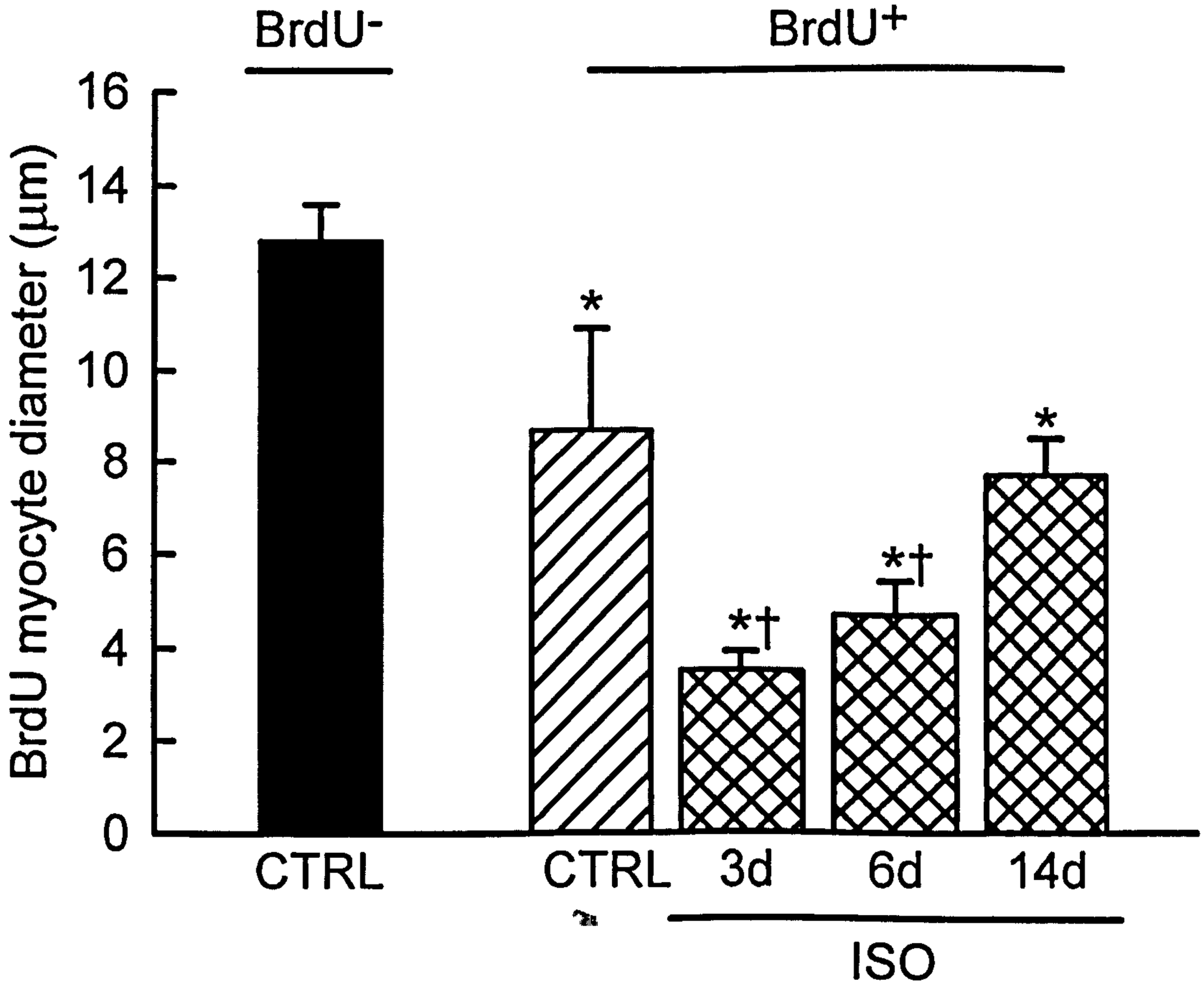

Figure 3.31 The size of newly formed myocytes

Time course of BrdU-positive myocyte diameter, in response to a single injection (s.c.) of 20 mmol of isoprenaline kg^{-1}. One group of animals (CTRL) received the saline vehicle. All animals were injected (i.p.) with 50 mg of BrdU kg^{-1} twice daily until they were killed. The myocyte diameters of BrdU-positive and BrdU-negative myocytes were measured across the cell nucleus in each sub-endocardium of the LV. Results are Mean ± SD for n=5. *denotes significant differences ($P<0.001$) from BrdU-negative myocytes in control animals. †denotes significant differences ($P<0.001$) from BrdU-positive myocytes in control animals. ISO indicates isoprenaline-treated animals.

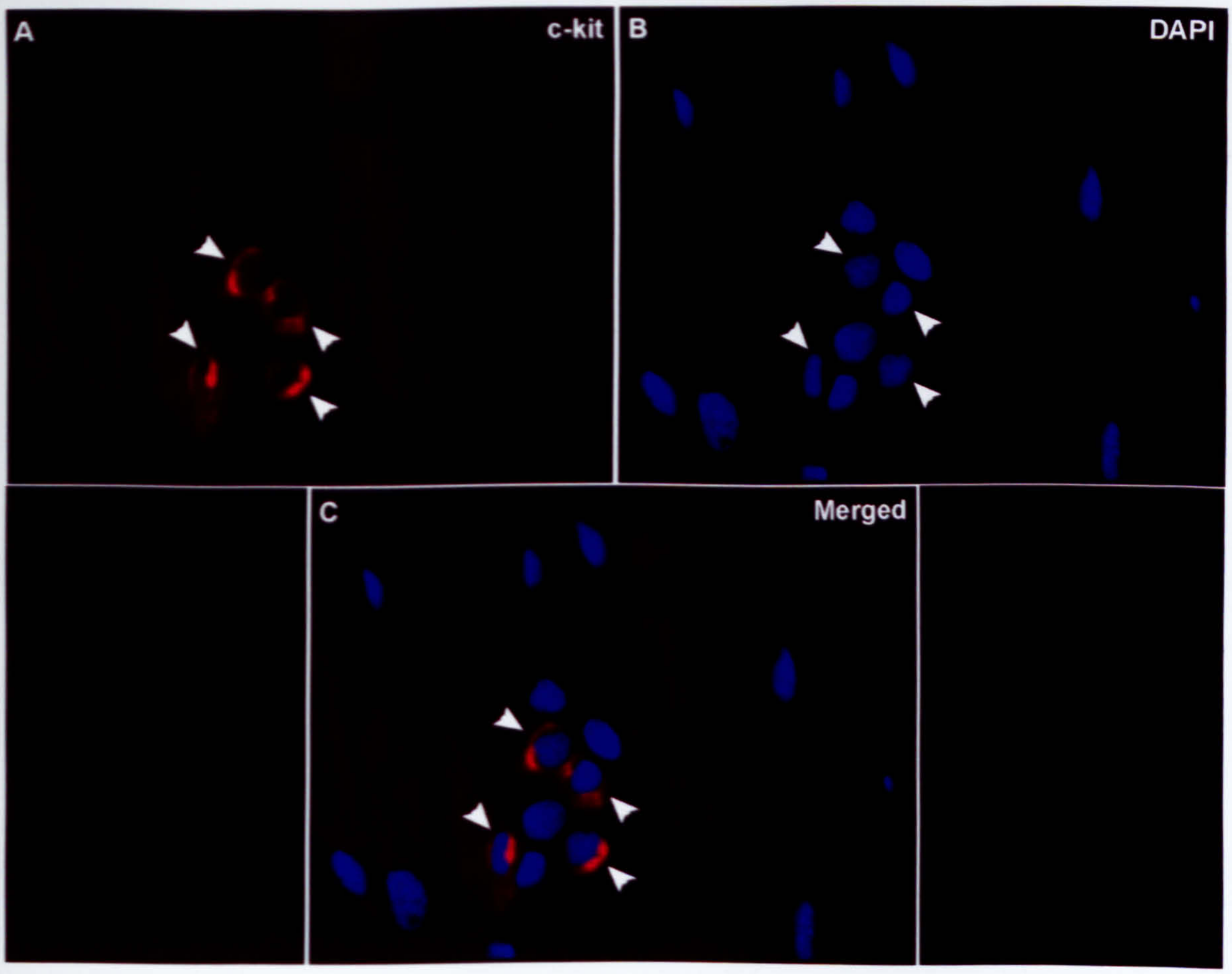

Figure 3.32 Cardiac stem progenitor cells in the rat myocardium.

Transverse sections were stained with c-kit 1°Ab and this was detected with TRITC 2°Ab to show c-kit positive cells (red, A; arrowheads) in the myocardium. Nuclei were stained with DAPI (blue, B). The localisation of the c-kit receptor on the surface of the nuclei is apparent when the two images are merged (C) (all x1000 magnification).

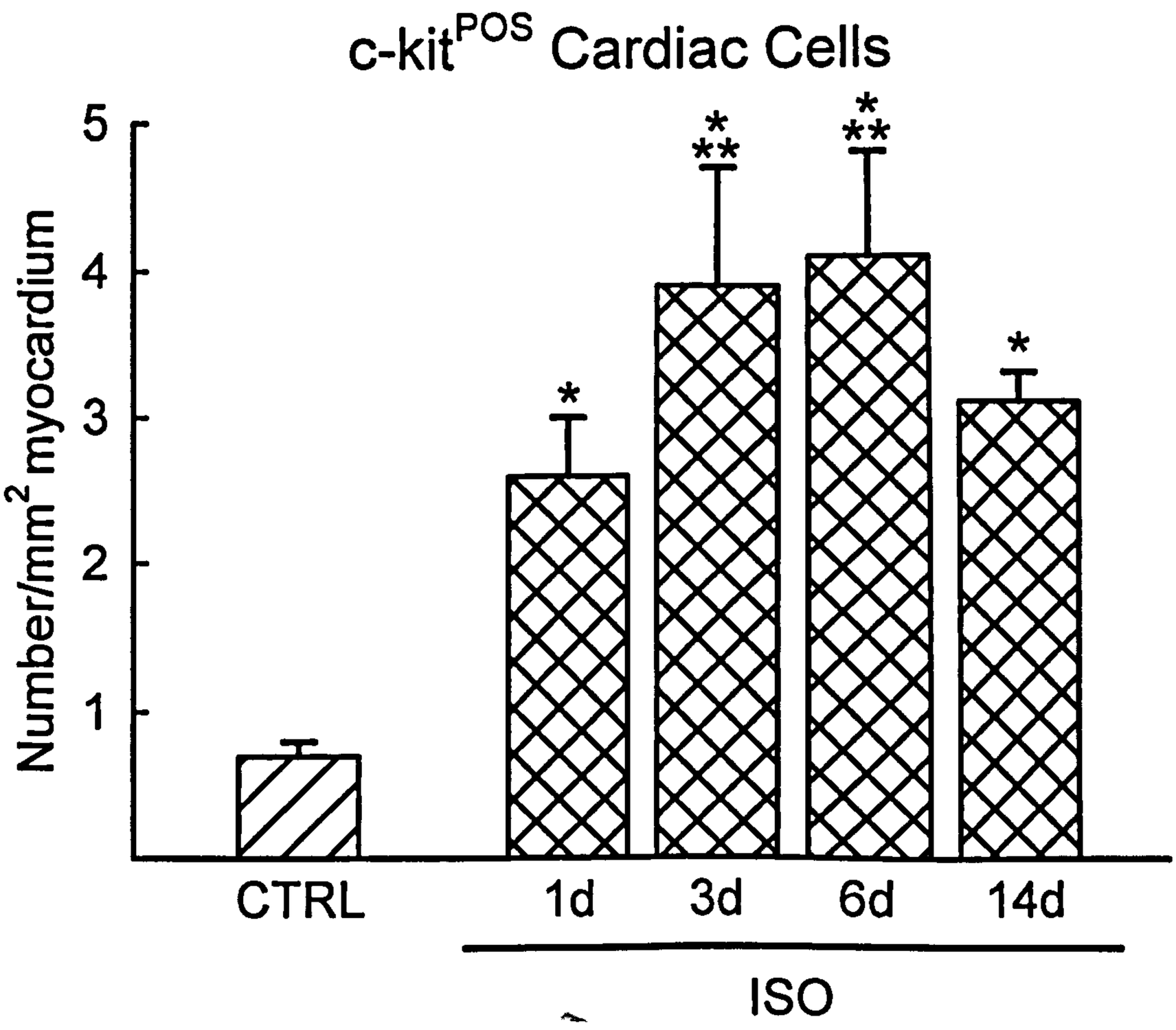

Figure 3.33 Cardiac stem progenitor cells.

Time course of c-kit^{POS} cardiac cells, in response to a single injection (s.c.) of 20 mmol of isoprenaline kg^{-1}. One group of animals (CTRL) received the saline vehicle. The number of c-kit^{POS} cells in a total of 3 myocardial cross-sections was counted and by measuring the area of each myocardial cross section, the number of c-kit^{+} cells per unit area of myocardial tissue determined. Results are Mean ± SD for n=5. *denotes significant differences ($P<0.01$) from CTRL. **denotes significant differences ($P<0.05$) from 1 day. ISO indicates isoprenaline-treated animals.

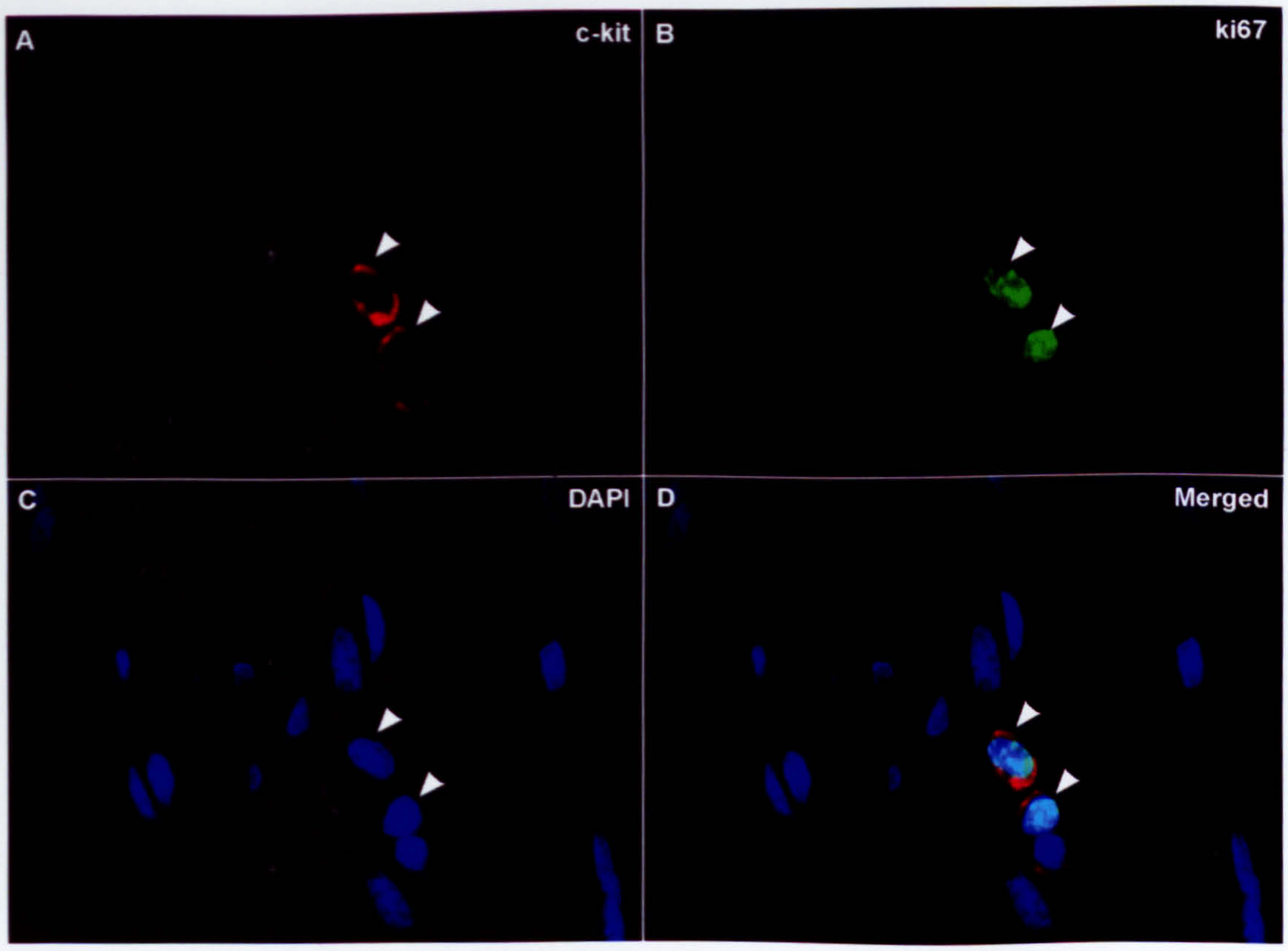

Figure 3.34 Proliferating cardiac stem progenitor cells in the rat myocardium.

Transverse sections were double stained for c-kit and Ki67 to identify cycling stem cells, following isoprenaline-induced myocardial damage. Two c-kit positive cells (red, A; arrowheads) are also positive for Ki67 (green, B; arrowheads), indicating their activated state. Nuclei were counterstained with DAPI (blue, C). The cycling stem cells can be seen more clearly when the three images are merged (D) (all x1000 magnification).

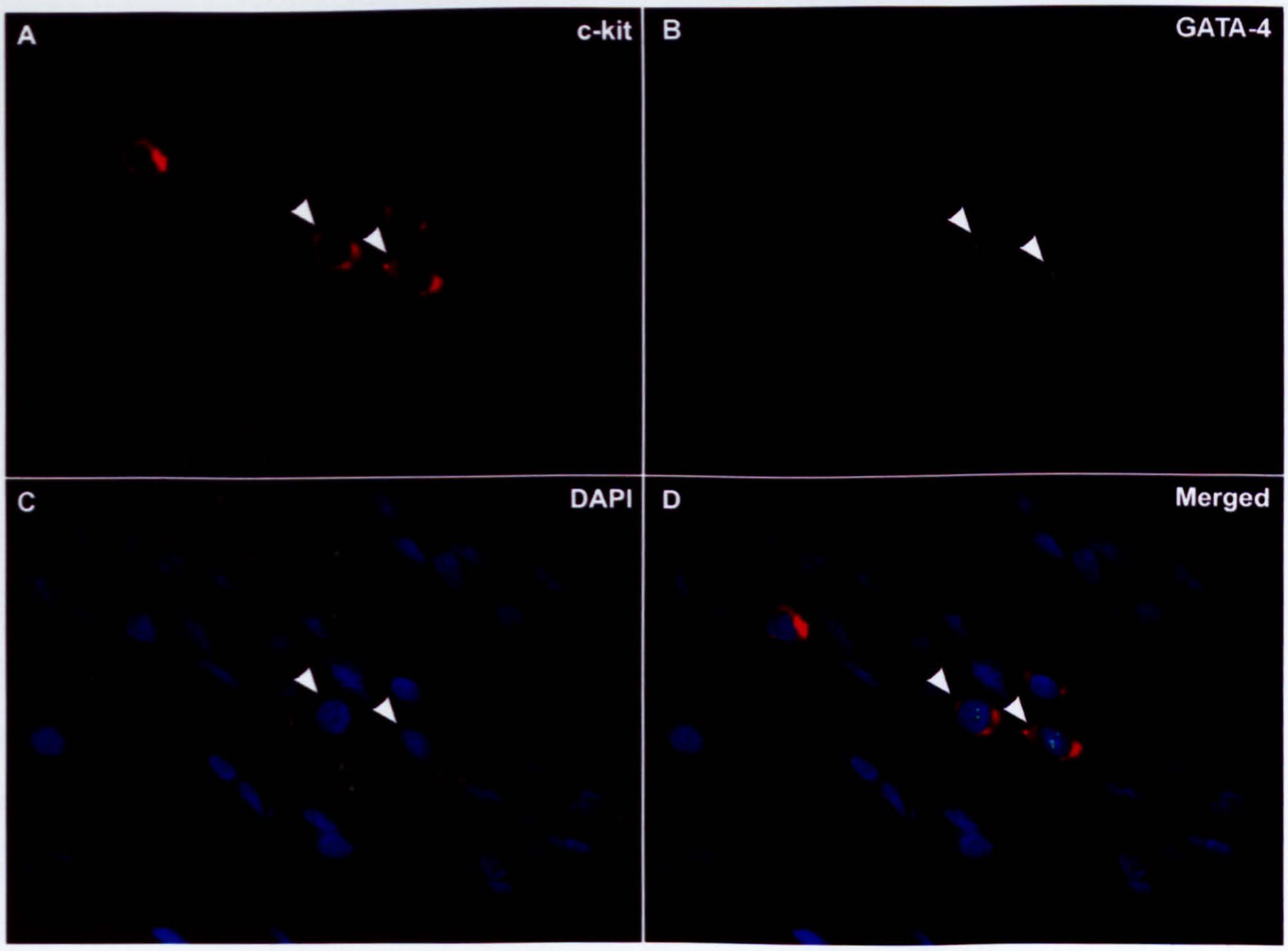

Figure 3.35 Commitment of cardiac stem progenitor cells in the rat myocardium.

Transverse sections were double stained for c-kit and GATA4 to recognize the committed progeny of cardiac stem cells during the regeneration process, after isoprenaline-injury. Two c-kit positive cells (red, A; arrowheads) express GATA4 (green dots, B; arrowheads) in their nuclei (blue, C). This becomes more apparent when the three images are merged (D) (all x1000 magnification).

Notably, these myocyte progenitors (c-kit^{POS}/GATA4^{POS}) were constantly identified between 3 and 14 days after isoprenaline-induced myocardial damage (Figure 3.35).

Key points:

1. Cardiac function was depressed at 1 day after isoprenaline injection, exhibiting acute cardiac failure. However, by 6 days it started to improve and this persisted through to 14 days.

2. Acute isoprenaline exposure caused significant cardiomyocyte necrosis and apoptosis. This was most prominent in the sub-endocardial layer.

3. Acute isoprenaline exposure caused increases in LV weight, which returned to control values by 14 days.

4. Acute isoprenaline exposure resulted in a decreased LV myocyte number and an increased myocyte volume.

5. Isoprenaline-treated animals exhibited a change in the frequency distribution of cardiomyocyte size, with a greater number of larger and smaller myocytes when compared to control animals.

6. Isoprenaline-treated hearts responded to the extensive cardiomyocyte damage and loss caused by isoprenaline, in part through myocyte hyperplasia. This was evident through the generation of newly formed myocytes which were positive for BrdU and ki67. These myocytes were all smaller than the other myocytes and most prominent in the sub-endocardial layer.

7. Resident cardiac progenitor cells expressing the stem cell antigen, c-kit, were identified in the myocardium. Isoprenaline-induced damage caused these cells to increase in number up to 6 days and many expressed ki67, exhibiting their cycling nature. Also many of these c-kit positive cells expressed GATA4, indicative of early differentiating myocyte progenitors.

3.5 Continuous Infusion of Catecholamines

To more faithfully reflect the sustained higher than normal levels of catecholamines in heart failure patients, a continuous infusion, rather than a bolus injection, of catecholamines was studied. This was achieved using osmotic mini pumps.

3.5.1 Growth and hypertrophy

Continuous infusion of catecholamines over 28 days resulted in marked increases in bodyweight and the individual weights of the heart and various skeletal muscles. Since rats continue to grow throughout most of their adult life, all groups showed a significant increase ($P<0.05$) in body weight over time (Figure 3.36). However, the isoprenaline group showed the greatest increase of 38% over the 28 day period, compared with 17% for the adrenaline group and 26% for the sham-operated controls. The fact that the adrenaline treated rats gained less weight than the placebo controls meant that by 28 days the isoprenaline group were significantly ($P<0.05$) 16% heavier than the adrenaline group (Figure 3.36). Over 28 days, no differences were found for body weight between the experimental groups and the placebo group (Figure 3.36).

To determine whether continuous infusions of the catecholamines affected the animals' appetite and consequently their food and water consumptions, these variables were monitored over the course of the 28 day experimental period. Both isoprenaline and adrenaline-treated groups showed initial significant decreases ($P<0.05$) in their appetites and total food consumptions at 3 days, when compared to the saline placebo group (Figures 3.37; 3.38). However, these returned to values above those of the placebo group by 7 days and remained stable up to 28 days (Figure 3.37; 3.38).

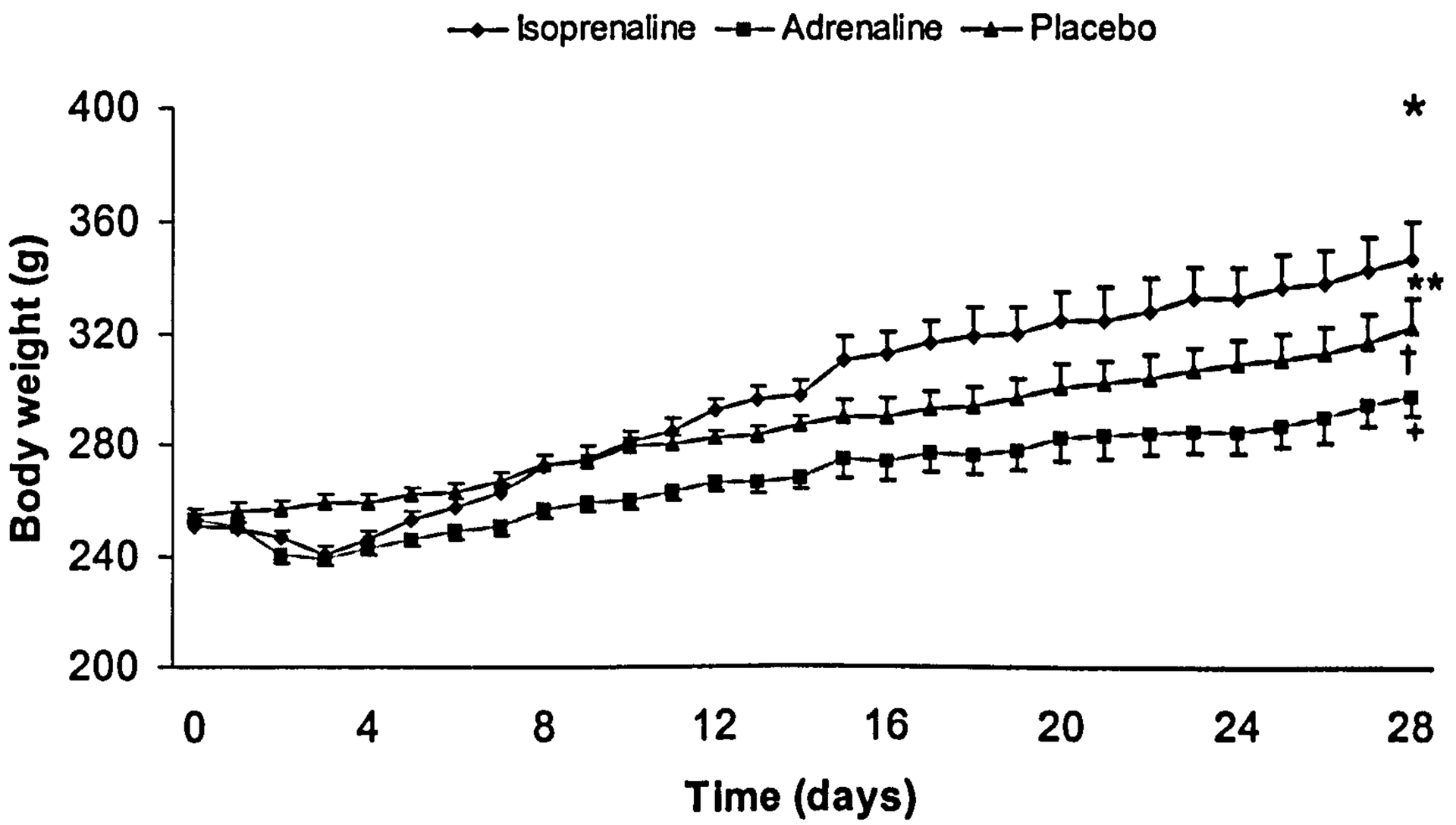

Figure 3.36 Rat body weights during chronic exposure to catecholamines.
All animals were weighed daily during 28 days of continuous infusion with either 20 mmol $kg^{-1}d^{-1}$ of isoprenaline, adrenaline or saline (placebo) only, delivered via osmotic mini pumps. Results are Mean ± SEM for n=5-20. $^{+}$denotes significant differences ($P<0.05$) within the placebo controls, between 28 days and 0, 3 and 7 days. **denotes significant difference ($P<0.05$) within the isoprenaline group, between 28 days and 0, 3 and 7 days. †denotes significant difference ($P<0.05$) within the adrenaline group, between 28 days and 0, 3 and 7 days. *denotes significant difference ($P<0.05$) between isoprenaline vs. adrenaline groups.

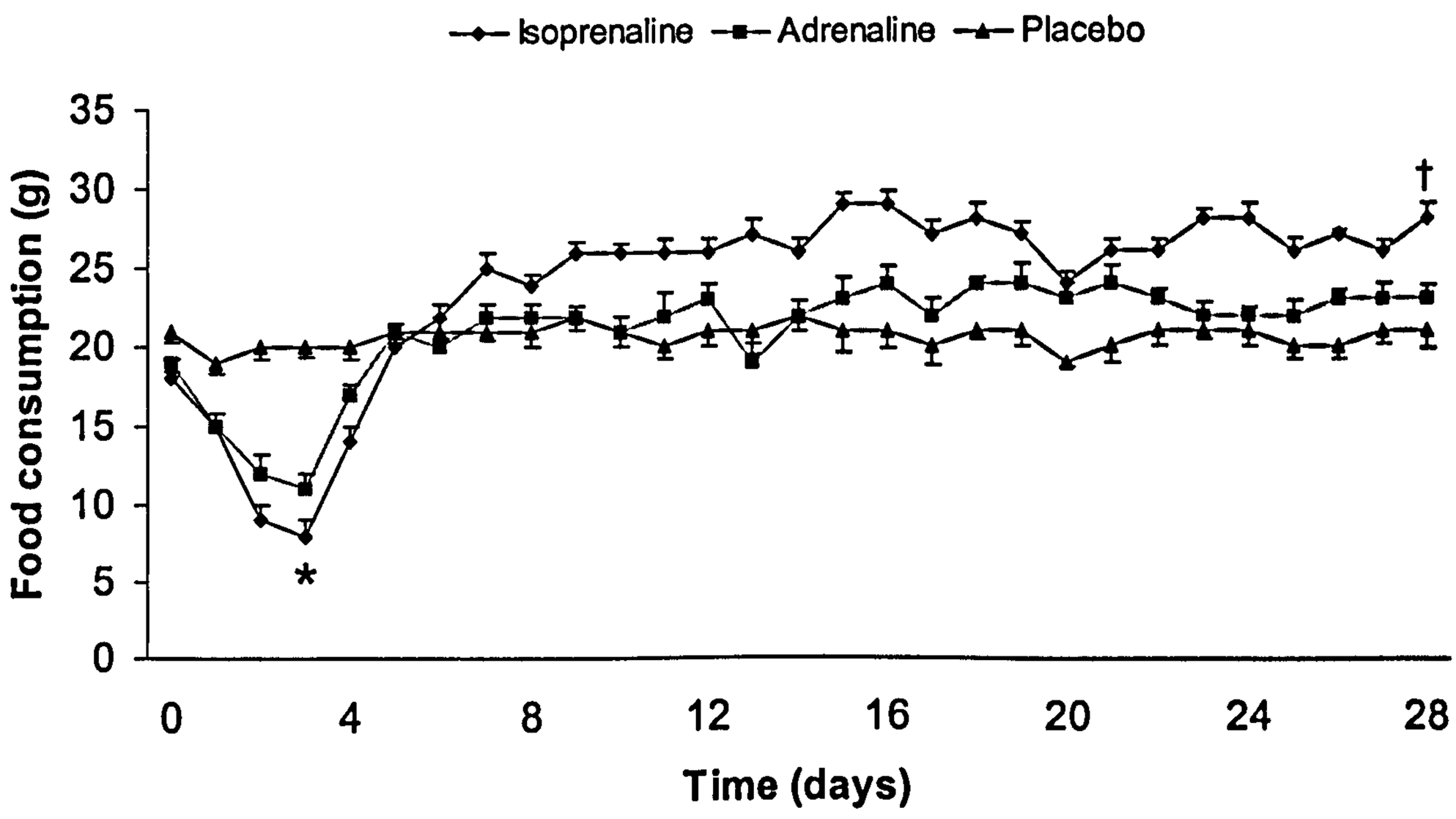

Figure 3.37 Food consumption during chronic exposure to catecholamines.

The food consumptions were measured daily during the continuous infusion of either 20 mmol $kg^{-1}d^{-1}$ of isoprenaline, adrenaline or saline (placebo) only and delivered via osmotic mini pumps. Results are Mean ± SEM for n=5-20. No differences were found over time for the saline placebo controls. *denotes significant differences ($P<0.05$) between isoprenaline and adrenaline groups vs. placebo controls. †denotes significant difference ($P<0.05$) between isoprenaline group vs. placebo controls.

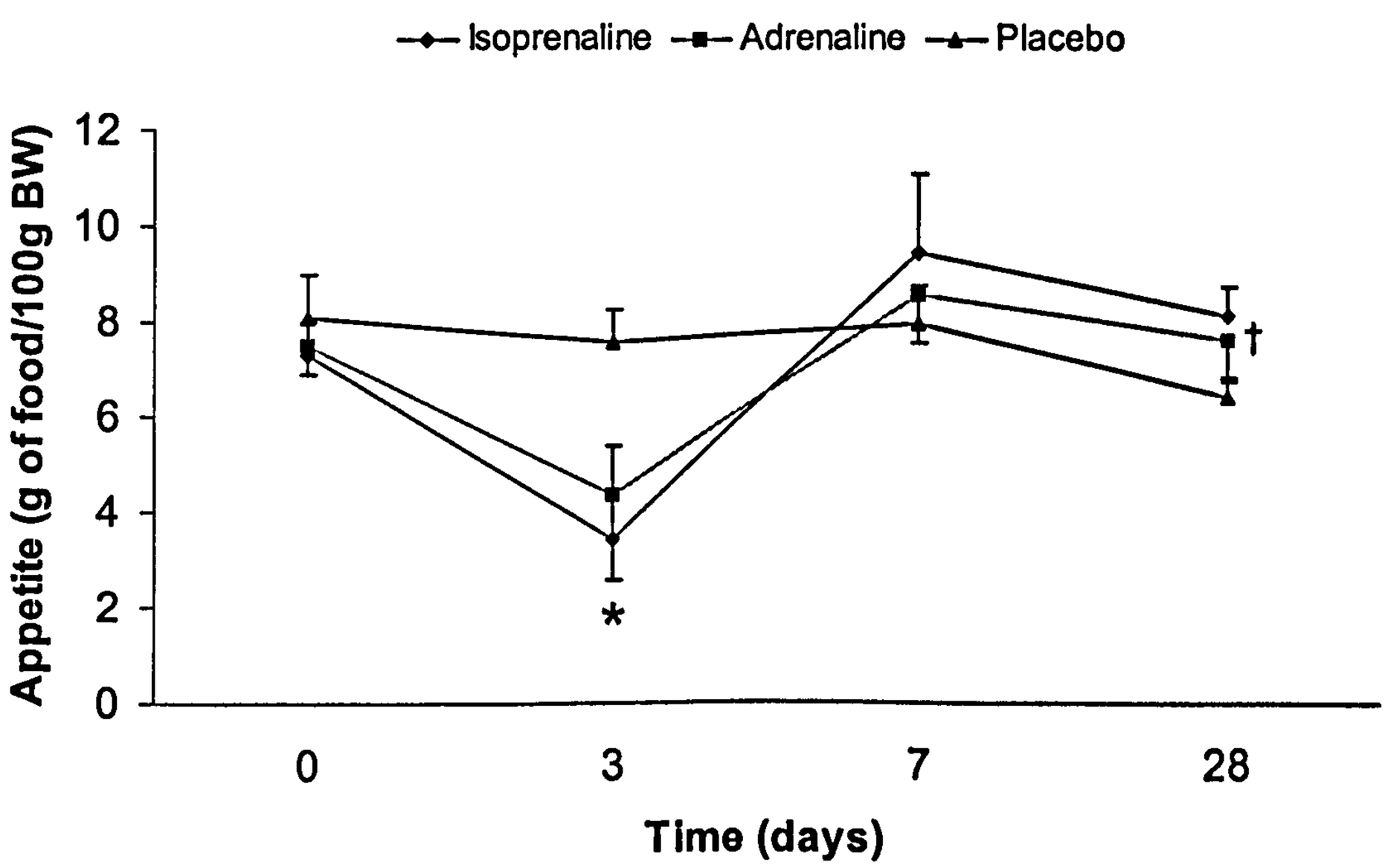

Figure 3.38 Changes in appetite during chronic exposure to catecholamines. Animals' appetites were measured during continuous infusion with either 20 mmol $kg^{-1}d^{-1}$ of isoprenaline, adrenaline or saline (placebo) only, delivered via osmotic mini pumps. Results are Mean ± SEM for n=5-20. No differences were found over time for the saline placebo controls. † denotes significant differences ($P<0.05$) over time, specifically 3 day vs. all other time points in the isoprenaline and adrenaline groups. *denotes significant difference ($P<0.05$) between isoprenaline and adrenaline groups vs. placebo controls.

By 28 days the amount of food consumed by the isoprenaline group was significantly greater ($P<0.05$) than that consumed by the placebo rats (Figure 3.37). There were no statistical differences between groups in terms of their water consumptions, over the 28 day infusion period (Figure 3.39). However, comparable to their appetite and food consumptions, the isoprenaline and adrenaline-treated animals did show an initial decrease in their water consumptions at 2 days. Thereafter, it remained slightly but consistently higher than in the control animals (Figure 3.39).

In keeping with the growth of the whole animal, the hearts of the placebo group increased by 15% over time (Figure 3.40). However, no significant differences were seen in heart weight between the zero day control and the placebo groups at any of the time points. Both the continuous infusions of isoprenaline and adrenaline caused the weight of the heart to increase over time (Figure 3.40). In the isoprenaline group, the weight of the heart increased by 43% ($P<0.05$ versus zero day control) by 28 days of infusion. However, most of this increase over the controls had occurred by just 5 days (Figure 3.40). In the adrenaline group, the weight of the heart increased, but not as quickly or to the same extent as the isoprenaline group, this being 16% heavier ($P<0.05$ versus zero day control) after 28 days of infusion (Figure 3.40).

It was found that continuous infusion of 20 mmol isoprenaline $kg^{-1}d^{-1}$ caused ~35% increase ($P<0.05$) in heart weight, when compared to the placebo group at every time point analysed over 28 days infusion (Figure 3.40). Also the increase in heart weight over 28 days seen in the isoprenaline group was significantly different ($P<0.05$) from the adrenaline group (26, 18, 16 and 23% greater at 5, 7, 14 and 28 days, respectively). Although the adrenaline animals displayed an increase in heart weight over 28 days, these increases were not found to be significant, when compared to the saline placebo group (Figure 3.40).

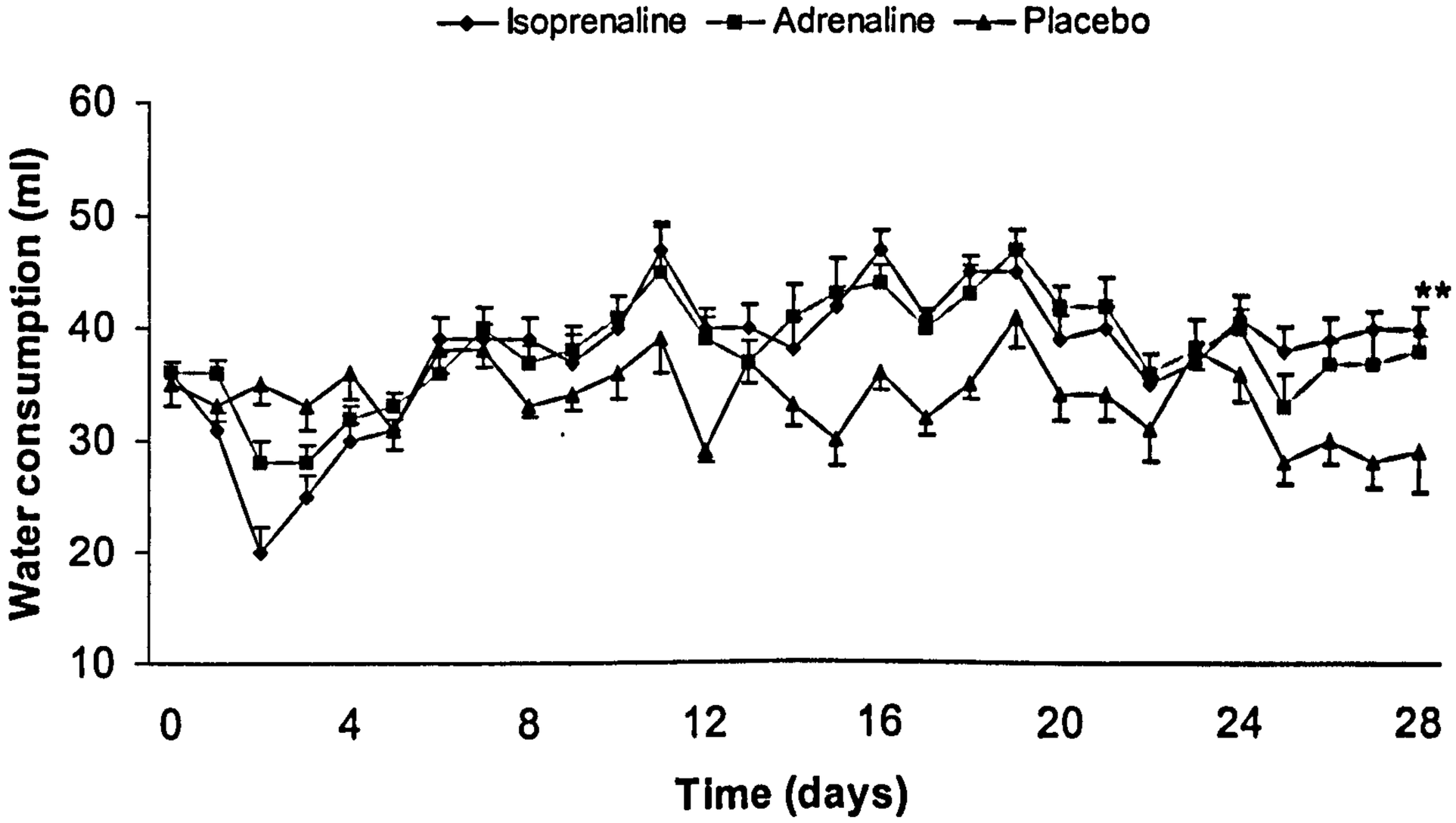

Figure 3.39 Water consumption during chronic exposure to catecholamines. Water intake was measured daily during the continuous infusion of either 20 mmol $kg^{-1}d^{-1}$ of isoprenaline, adrenaline or saline (placebo) only, delivered via osmotic mini pumps. Results are Mean ± SEM for n=5-20. No differences were found over time for the saline placebo controls. **denotes significant difference ($P<0.05$) within in the isoprenaline group, between 2 days and 0, 7 and 28 days. No differences were found over time for the adrenaline group.

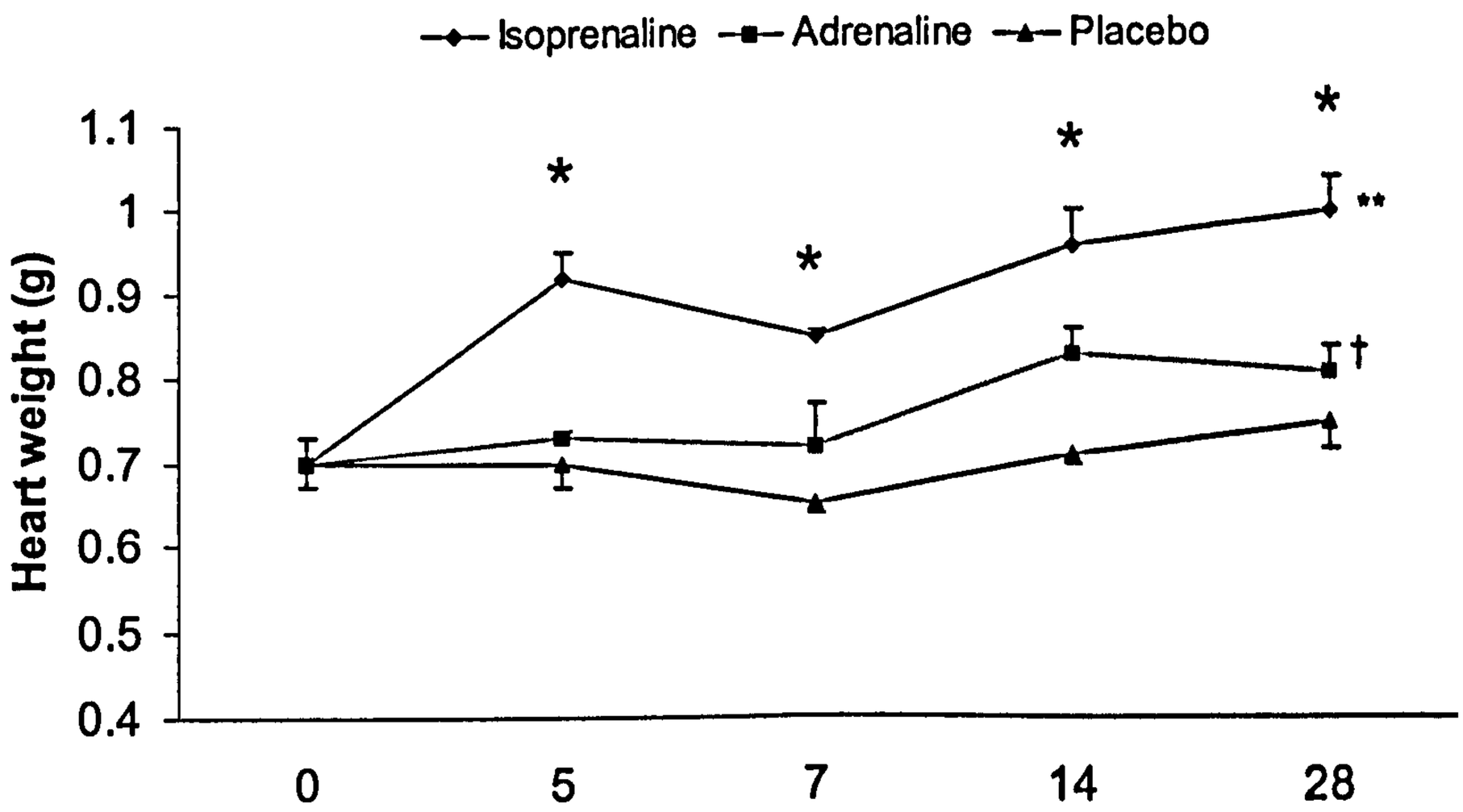

Figure 3.40 Heart weight after chronic exposure to catecholamines.

The weight of the heart was measured in response to continuous infusion with either 20mmol $kg^{-1}d^{-1}$ of isoprenaline, adrenaline or saline (placebo) only, as delivered via osmotic mini pumps. Results are Mean ± SEM for n=5. No significant differences were found between zero day control and placebo controls at any time points. **denotes significant differences ($P<0.05$) in heart weights within the isoprenaline group, compared with zero day control. † denotes significant differences ($P<0.05$) in heart weights within the adrenaline group, compared with zero day control. *denotes significant differences ($P<0.05$) between isoprenaline vs. adrenaline groups and placebo controls.

A similar sequence of events emerged with the soleus muscle. Muscles in the placebo group increased gradually over time, even though these increases in weight were not significantly different from the zero day control muscles (Figure 3.41). The isoprenaline and adrenaline-treated groups, both showed significant increases ($P<0.05$) over time, being 42% and 28% heavier at 28 days respectively, compared to zero day control (Figure 3.41). Although not always significantly greater, the muscles exposed to the two catecholamines were always larger than those of the sham-operated saline placebo group (Figure 3.41).

To establish whether these increases in muscle mass represented true hypertrophy, after 28 days soleus muscles were sectioned and fibre cross-sectional areas determined (Figure 3.42). The isoprenaline and adrenaline infused groups exhibited significant ($P<0.05$) increases in the fibre cross-sectional areas of their soleus muscles, when compared to the placebo group (Figure 3.42). These findings, combined with the increases in muscle weight, indicate that significant muscle hypertrophy had occurred in the soleus following 28 days of catecholamine infusion.

Two predominantly fast twitch muscles, the tibialis anterior and the plantaris muscles were also studied. These too showed increases in their weights over 28 days of either isoprenaline or adrenaline infusion (Figures 3.43; 3.44). Following 28 days of isoprenaline infusion, both muscles were significantly heavier ($P<0.05$) than the zero time control and placebo control groups, with the tibialis anterior 68% heavier than zero day control and 28% heavier than the placebo group (Figure 3.43). Changes in the plantaris were similar, i.e. 72% and 33% heavier than zero time and placebo controls, respectively (Figure 3.44). The adrenaline group showed similar increases in muscle weight ($P<0.05$) over time, but generally not as great as in the isoprenaline group (Figures 3.43; 3.44).

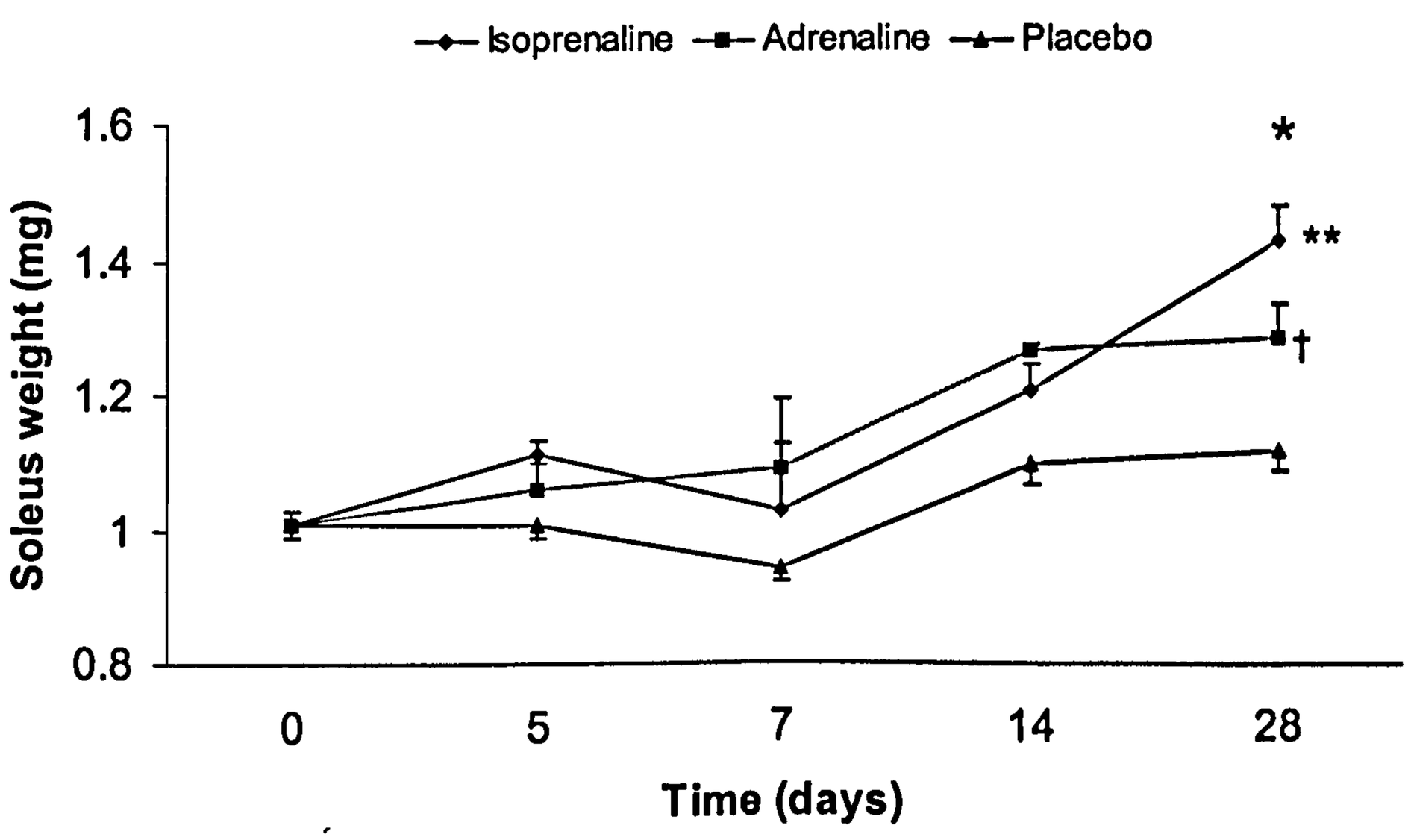

Figure 3.41 Soleus weights after chronic exposure to catecholamines.

Wet weights of the soleus muscle were measured in response to continuous infusion with either 20 mmol $kg^{-1}d^{-1}$ of isoprenaline, adrenaline or saline (placebo) only and delivered via osmotic mini pumps. Results are Mean ± SEM for n=5. No significant differences were found between zero day control and placebo controls at any time points. **denotes significant differences ($P<0.05$) in soleus weights within the isoprenaline group, compared with zero day control. †denotes significant differences ($P<0.05$) in soleus weights within the adrenaline group, compared with zero day control. *denotes significant difference ($P<0.05$) between isoprenaline group vs. placebo controls.

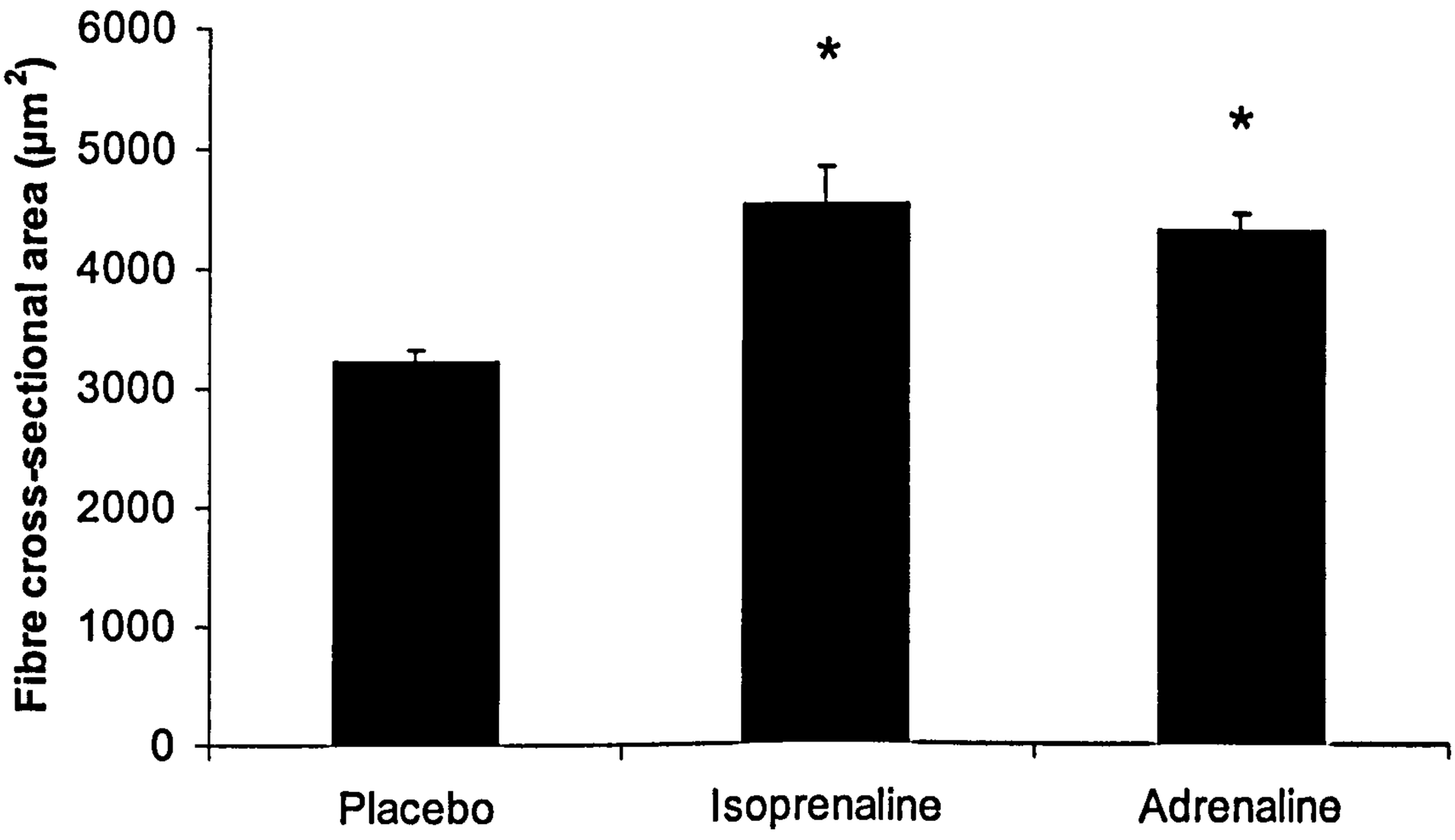

Figure 3.42 Cross-sectional areas of fibres in the soleus muscle after chronic exposure to catecholamines.

Muscles were isolated 28 days after continuous infusion with either 20 mmol $kg^{-1}d^{-1}$ of isoprenaline, adrenaline or saline (placebo) only, delivered via osmotic mini pumps. These were sectioned (5µm) and stained for myosin ATPase. Regardless of fibre type the cross-sectional area of at least 100 fibres were measured for each muscle. Results are Mean ± SEM for n=5. *denotes significant differences ($P<0.05$) from saline placebo controls.

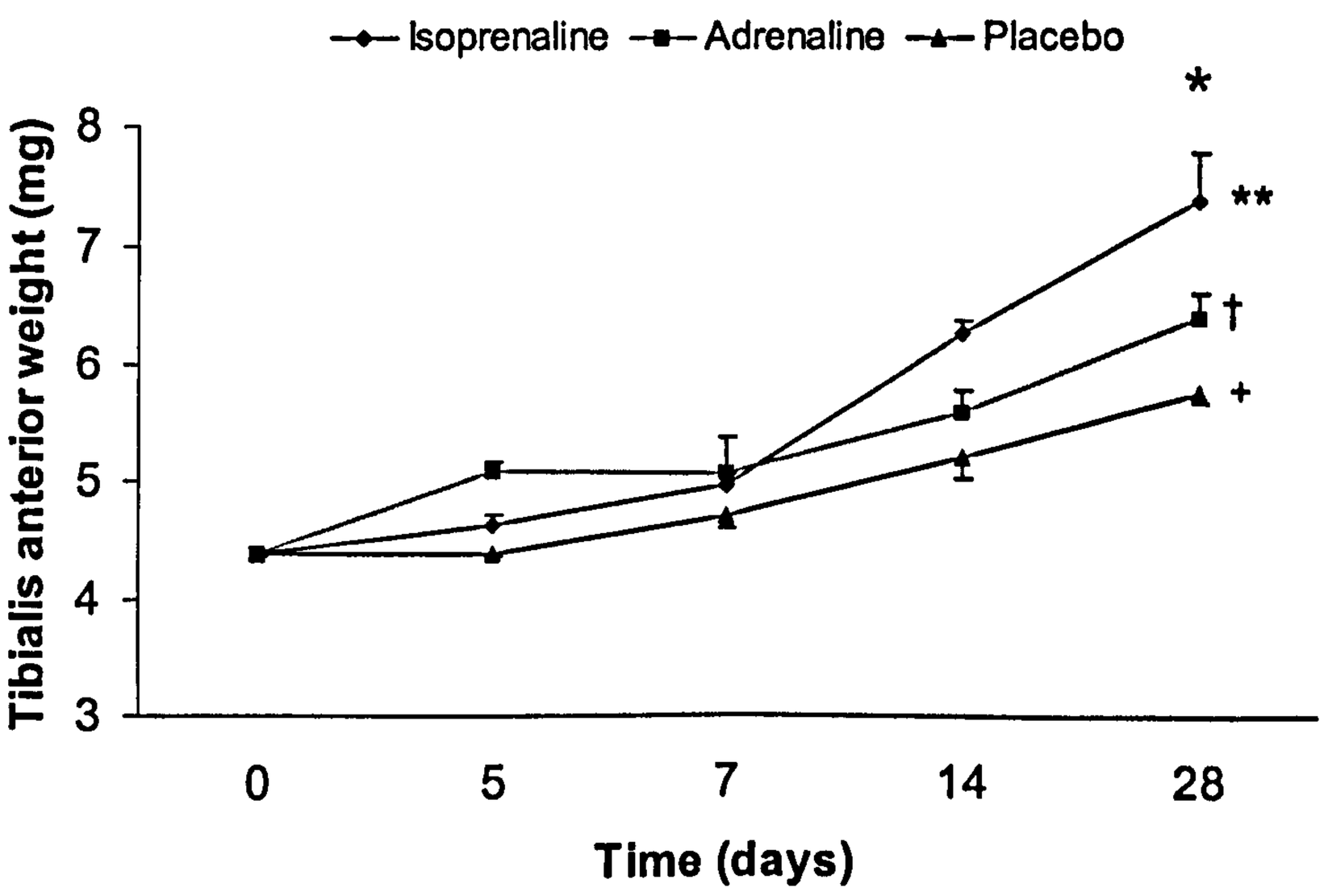

Figure 3.43 Tibialis anterior weights after chronic exposure to catecholamines.

Wet weights of the tibialis anterior muscle were taken in response to continuous infusion with either 20 mmol $kg^{-1}d^{-1}$ of isoprenaline, adrenaline or saline (placebo) only, delivered via osmotic mini pumps. Results are Mean ± SEM for n=5. $^{+}$denotes significant differences ($P<0.05$) in tibialis anterior weights within the placebo controls, compared with zero day control. **denotes significant differences ($P<0.05$) in tibialis anterior weights within the isoprenaline group, compared with zero day control. †denotes significant differences ($P<0.05$) in tibialis anterior weights within the adrenaline group, compared with zero day control. *denotes significant difference ($P<0.05$) between isoprenaline group vs. placebo controls.

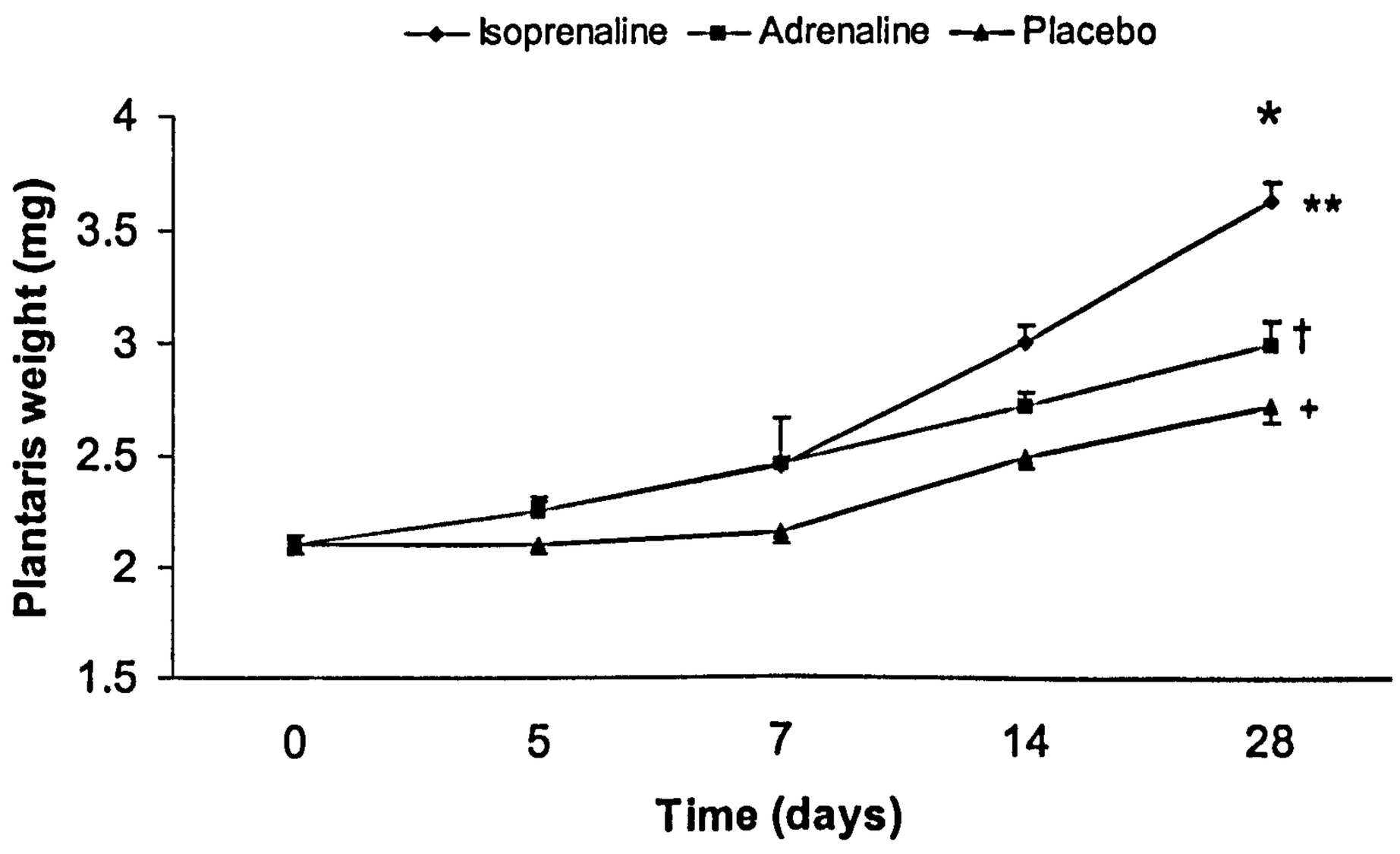

Figure 3.44 Plantaris weights after chronic exposure to catecholamines.

Wet weights of the plantaris muscle were measured in response to continuous infusion with either 20 mmol $kg^{-1}d^{-1}$ of isoprenaline, adrenaline or saline (placebo) only, delivered via osmotic mini pumps. Results are Mean ± SEM for n=5. $^{+}$denotes significant differences ($P<0.05$) in plantaris weights within the placebo controls, compared with zero day control. **denotes significant differences ($P<0.05$) in plantaris weights within the isoprenaline group, compared with zero day control. † denotes significant differences ($P<0.05$) in plantaris weights within the adrenaline group, compared with zero day control. *denotes significant difference ($P<0.05$) between isoprenaline group vs. placebo controls.

Overall, both natural and synthetic catecholamines induced a larger heart and skeletal muscles, with isoprenaline being more potent than the adrenaline. The effect on the skeletal muscles was greater for fast-twitch muscles, with isoprenaline infusion resulting in higher percent increases in muscle mass of the tibialis anterior and plantaris (72% and 68%, respectively), than the soleus muscle (42%).

3.5.2 Necrotic and apoptotic cell death

The sham-operated saline placebo rats showed no necrosis or apoptosis in any of the muscles analysed, i.e. heart, tibialis anterior, soleus, plantaris, diaphragm, over the 28 day experimental period. Similarly neither necrotic nor apoptotic fibres were found in the plantaris or diaphragm muscles, following 28 days of continuous infusion with either 20 mmol of isoprenaline or adrenaline $kg^{-1}d^{-1}$. Also, only a single necrotic fibre was found in one tibialis anterior muscle from the isoprenaline-treated group (n=5).

In marked contrast, continuous infusion of catecholamines resulted in both necrotic and apoptotic myocyte death in the heart and soleus muscles from the same animals. Fourteen days exposure to 20 mmol isoprenaline $kg^{-1}d^{-1}$ lead to 0.6% ($P<0.05$, versus placebo sham) cardiomyocyte necrosis (Table 3.5), approximately 15-fold higher than the levels of apoptosis. Although small, the amount of apoptosis increased in a time-dependent manner (Table 3.5) and by 28 days was almost 0.1%, which was significantly greater ($P<0.05$) than the sham-operated controls, but remained approximately 10-15-fold less than the amount of necrosis.

Seven days exposure to 20 mmol of adrenaline $kg^{-1}d^{-1}$ also caused significant ($P<0.05$, versus placebo sham) cardiomyocyte necrosis (Table 3.5). However, the amount of necrotic damage seen in the adrenaline group was not as great (~10%) as that found in the isoprenaline group. Despite this, the apoptotic death was similar between the 2 groups, i.e. adrenaline vs. isoprenaline.

Table 3.5 Myocyte death in the heart after chronic exposure to catecholamines. Necrotic (anti-myosin labelled) and apoptotic (caspase-3 labelled) cardiomyocytes were quantified (% area) after continuous infusion of either 20 mmol $kg^{-1}d^{-1}$ of isoprenaline, adrenaline or saline (placebo) only, delivered via osmotic mini pumps. Results are Mean ± SEM for n=5. *denotes significant differences ($P<0.05$) from placebo controls. ND denotes not determined.

% AREA	PLACEBO		
	7 days	14 days	28 days
Necrosis	0 ± 0	0 ± 0	ND
Apoptosis	0 ± 0	0 ± 0	0 ± 0
	Isoprenaline		
Necrosis	0.3 ± 0.09	0.6 ± 0.29*	ND
Apoptosis	0.03 ± 0.01	0.04 ± 0.02	0.07 ± 0.02*
	Adrenaline		
Necrosis	0.03 ± 0.00*	ND	ND
Apoptosis	0.02 ± 0.01	0.04 ± 0.01*	0.07 ± 0.01*

In the adrenaline group, the amount of apoptosis progressively increased over time (Table 3.5) and was significantly greater ($P<0.05$) than found in the saline placebo group (Table 3.5).

In the soleus muscle, continuous infusion of 20 mmol isoprenaline $kg^{-1}d^{-1}$ caused a significant increase ($P<0.05$) in the number of necrotic fibres at 14 days (6 ± 1 fibres; 0.3%), compared with no necrotic fibres in the soleus muscles of the placebo control animals (Table 3.6). Twenty mmol of adrenaline $kg^{-1}d^{-1}$ also caused significant ($P<0.05$, versus saline placebo) necrotic fibre damage after 7 days (0.1%).

In a similar manner to the heart, apoptotic fibres increased over time in the soleus muscle for both isoprenaline and adrenaline groups; these being significantly different ($P<0.05$) from placebo at 14 and 28 days (Table 3.6). Also, the amounts of apoptosis and necrosis were similar within and between these groups, over the 28 day experimental period (Table 3.6).

3.5.3 Fibre regeneration in the soleus

As predicted, from the above results for the placebo muscles, no differences were found in the total number of fibres in the soleus muscle between placebo groups at 7, 14 and 28 days. Also, only a total of five regenerating fibres were found in all of the 15 soleus muscle samples from placebo controls. Hence, all placebo data were pooled to create just one saline sham-operated group.

In contrast, 7 days of continuous infusion with isoprenaline had a marked effect on the number of viable fibres in the soleus muscle (Figure 3.45). The total number of fibres decreased by 28% ($P<0.05$) from 2653 ± 111 to 1923 ± 84. The number of viable fibres present at 14 days was still 20% lower than in the controls.

Table 3.6 Fibre death in the soleus muscle after chronic exposure to catecholamines.

Necrotic (anti-myosin labelled) and apoptotic (caspase-3 labelled) fibres were measured in the soleus muscle after continuous infusion of either 20 mmol $kg^{-1}d^{-1}$ of isoprenaline, adrenaline or saline (placebo) only, delivered via osmotic mini pumps. Results are Mean ± SEM and expressed as total number of necrotic or apoptotic fibres in the entire soleus muscle, with percentage cell death shown in parentheses for n=5. *denotes significant differences ($P<0.05$) from placebo controls. ND denotes not determined.

NUMBER OF FIBRES (%)	7 DAYS	14 DAYS	28 DAYS
	Placebo		
Necrosis	0 ± 0 (0)	0 ± 0 (0)	ND
Apoptosis	0 ± 0 (0)	0 ± 0 (0)	0 ± 0 (0)
	Isoprenaline		
Necrosis	2 ± 1 (0.1)	6 ± 1 (0.3)*	ND
Apoptosis	2 ± 1 (0.1)	5 ± 2 (0.2)*	7 ± 1 (0.2)*
	Adrenaline		
Necrosis	3 ± 1 (0.1)*	ND	ND
Apoptosis	3 ± 2 (0.2)	5 ± 2 (0.3)*	6 ± 1 (0.2)*

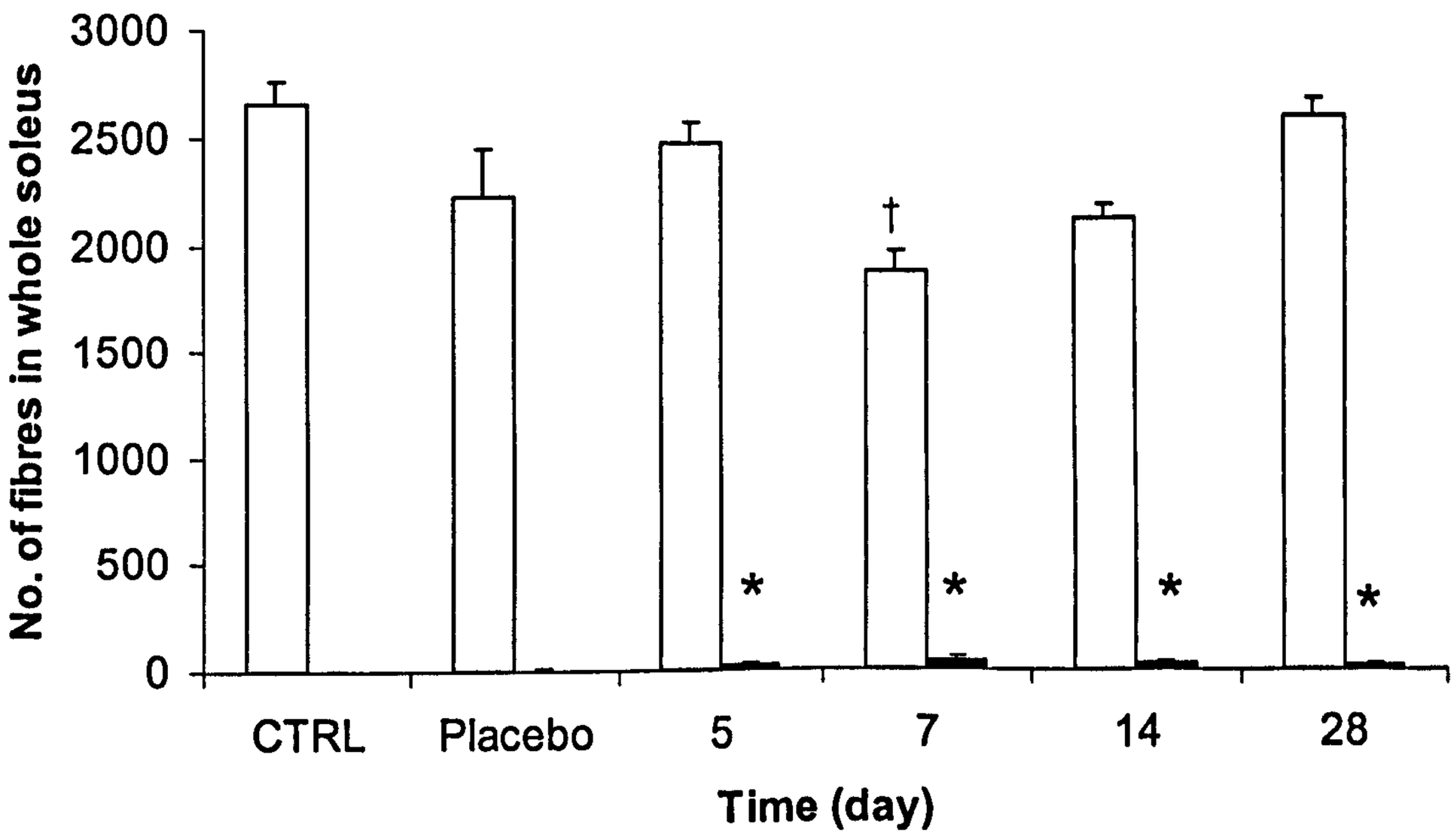

Figure 3.45 Fibre loss and regeneration in the soleus muscle after chronic exposure to isoprenaline.

Number of normal (□) and newly-formed regenerating fibres (■) following continuous infusion with 20 mmol of isoprenaline $kg^{-1}d^{-1}$, delivered via osmotic mini pumps. Results are Mean ± SEM for n=5. *denotes significant differences ($P<0.05$) from zero day control (CTRL) and placebo control animals. †denotes significant differences ($P<0.05$) from zero day control, 5 and 28 days.

However, by 28 days the total number (2602 ± 87) had almost returned to normal (Figure 3.45). The number of regenerating fibres, as detected by labelling with embryonic/neonatal myosin Ab, represented 1, 2, 2 and 1% of the total number of fibres in the entire soleus at 5, 7, 14 and 28 days, respectively. Although low, these numbers of regenerating fibres at all time points were significantly greater ($P<0.05$) than in either the muscles from zero day control or saline placebo animals (Figure 3.45).

Continuous infusion of equimolar adrenaline resulted in a similar pattern of fibre loss and regeneration in the soleus muscle. That is, seven days of adrenaline exposure caused a significant ($P<0.01$) 23% loss of fibres (Figure 3.46). After 14 days the total number of fibres increased to 2217, and by 28 days to 2360. Comparable with the events after the isoprenaline infusion, the number of regenerating fibres was significantly ($P<0.05$) increased following 5, 7, 14 and 28 days of continuous adrenaline (compared to zero day control and saline placebo animals). Similarly, the number of regenerating fibres represented 2, 1, 1 and 1% of the total number of fibres present at 5, 7, 14 and 28 days, respectively (Figure 3.46).

To compare the differences, in terms of fibre loss and regeneration, induced by the acute bolus injection and continuous infusion of catecholamines data were analysed using 2-way ANOVA. With isoprenaline the number of normal fibres 5 days following the single injection was significantly lower ($P<0.05$) than that seen after 5 days following its daily infusion. In contrast, this was reversed at 7 days, with the total number of fibres following continuous infusion significantly lower ($P<0.05$) than compared to that at 7 days after the single injection. These findings suggest a shifting of fibre loss to the right of the time spectrum, with continuous infusion. However, the number of regenerating fibres following a single injection was significantly ($P<0.05$) greater at 5 and 7 days, compared to the number following continuous infusion.

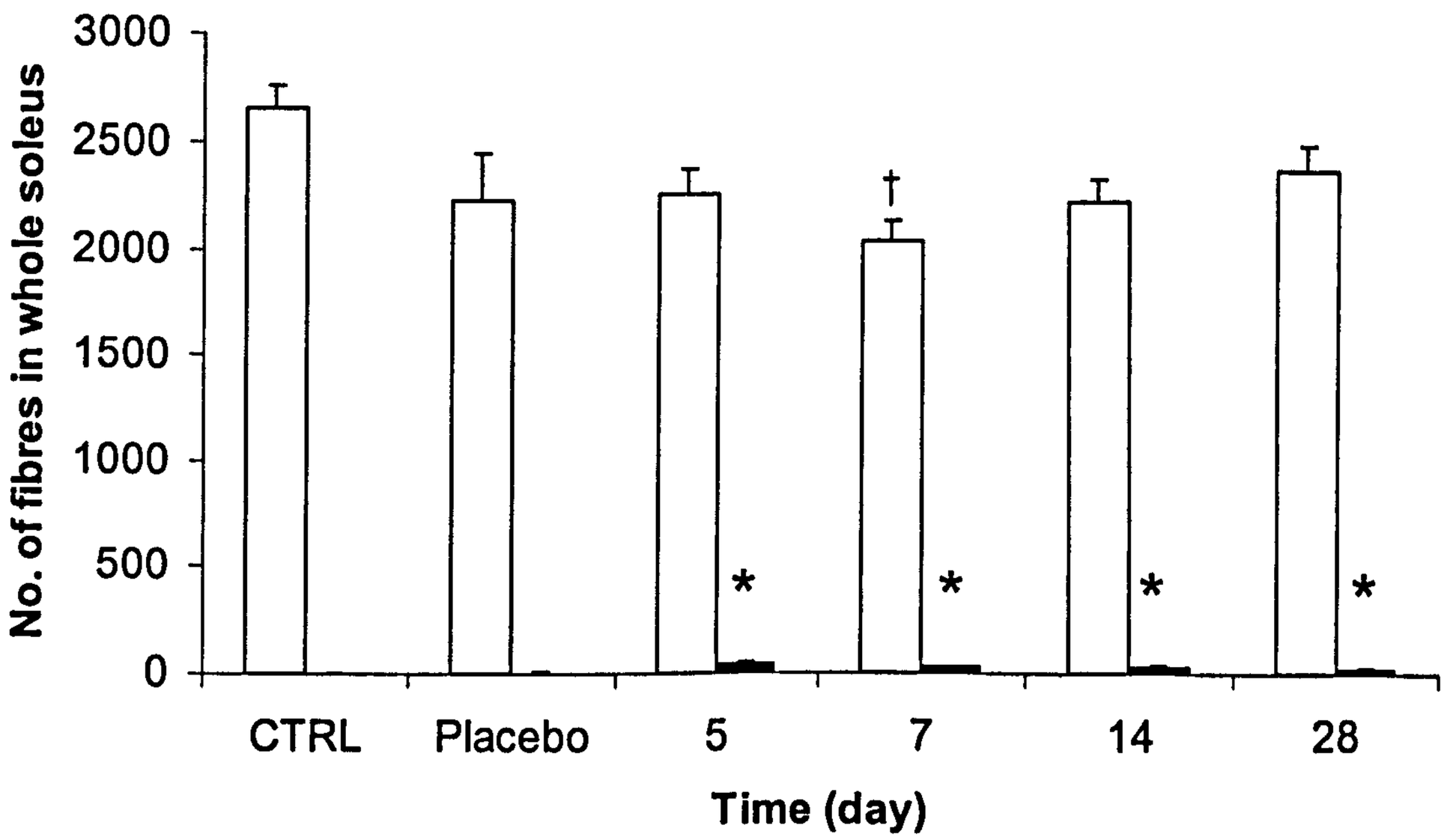

Figure 3.46 Fibre loss and regeneration in the soleus muscle after chronic exposure to adrenaline.

Number of normal (□) and newly-formed regenerating fibres (■) following continuous infusion with 20 mmol of adrenaline $kg^{-1}d^{-1}$, delivered via osmotic mini pumps. Results are Mean ± SEM for n=5. *denotes significant differences ($P< 0.05$) from zero day control and placebo control animals. †denotes significant difference ($P<0.01$) from zero day control.

These findings suggest that a single injection of isoprenaline resulted in a greater regenerative response at 5 and 7 days than that solicited when administered as a daily infusion. No differences were seen between acute and continuous adrenaline exposures concerning the total numbers of viable or regenerating fibres.

3.5.4 Fibrosis

The collagen content of control and all catecholamine-treated soleus muscles were not different at 2% each. This could reflect the rapid and extensive regenerative capacity of this skeletal muscle, without any fibrosis. However in the heart significant changes in fibrosis were observed. Here, in contrast to skeletal muscle, continuous infusion of catecholamines caused marked increases in the collagen content (Figures 3.47; 3.48). Examples of collagen staining in sections of the soleus and heart muscle can be seen in Figure 3.47. By 14 days, the percent collagen in the hearts taken from the isoprenaline and adrenaline-treated groups was 12 and 7%, respectively (Figure 3.48). This was ~9 and ~4% higher than that found in zero time control and saline placebo control hearts. The increase in cardiac collagen in the isoprenaline group was found to be significantly different ($P<0.05$) from all other groups (Figure 3.48). The greater fibrosis in response to the more potent isoprenaline is consistent with the higher levels of necrotic cell death that this synthetic catecholamine induces.

Key points:

1. Continuous infusion of catecholamines over 28 days caused significant increases in body weight and individual weights of the heart and slow and fast skeletal muscles.

2. Continuous infusion of catecholamines resulted in fibre hypertrophy, as exemplified by increases in fibre CSA in the soleus muscle.

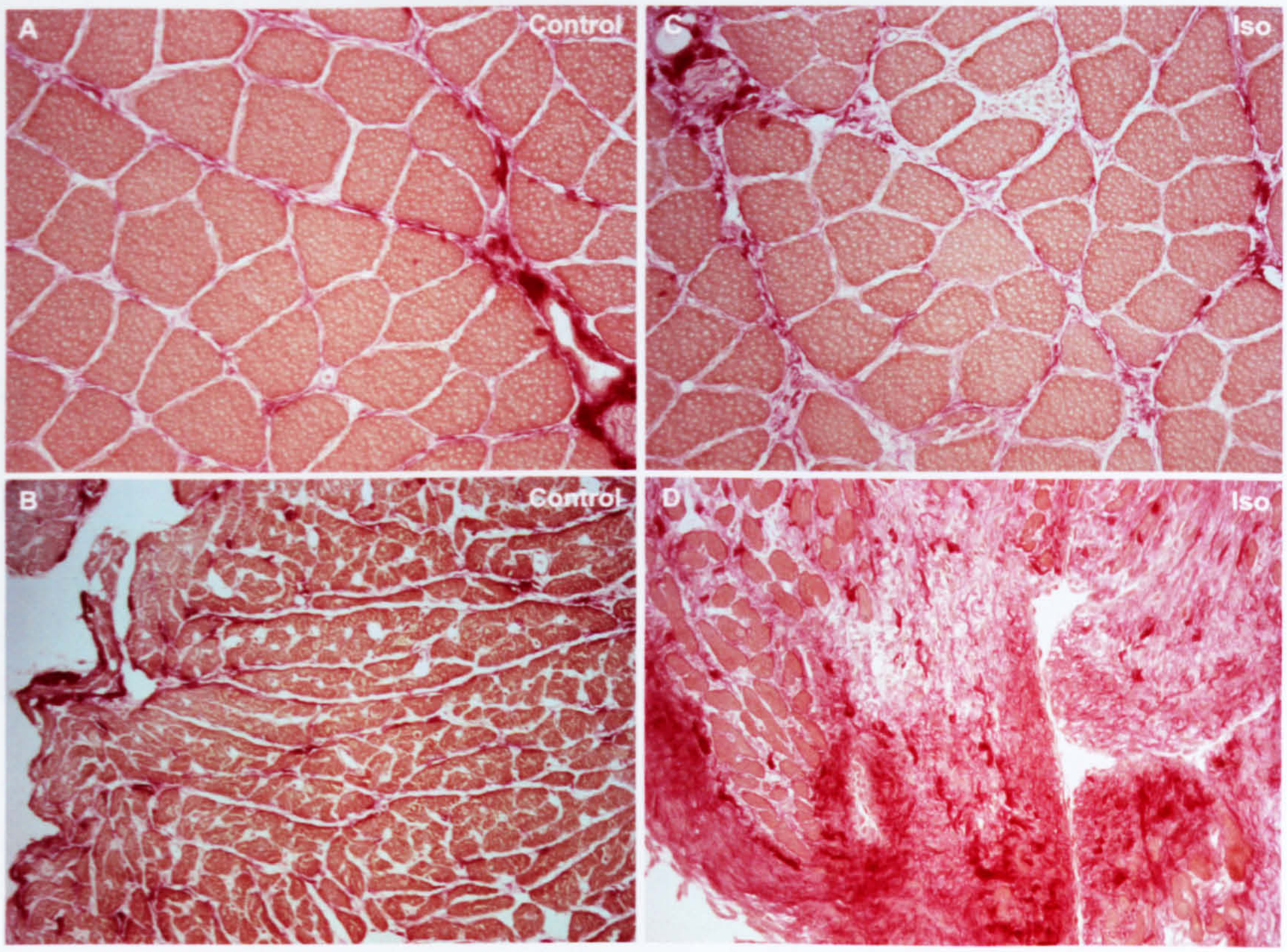

Figure 3.47 Collagen content in the heart and soleus muscle.

Transverse sections were stained with Sirius Red to identify connective tissue (mostly collagen) in the heart and soleus muscle (collagen, red; myocytes, yellow/orange). No changes in collagen content were present in the soleus muscle (control, A; isoprenaline-treated, B). In contrast, the heart exhibited increased collagen content after 14 days of continuous catecholamine infusion (control, C; isoprenaline-treated, D) (all x200 magnification).

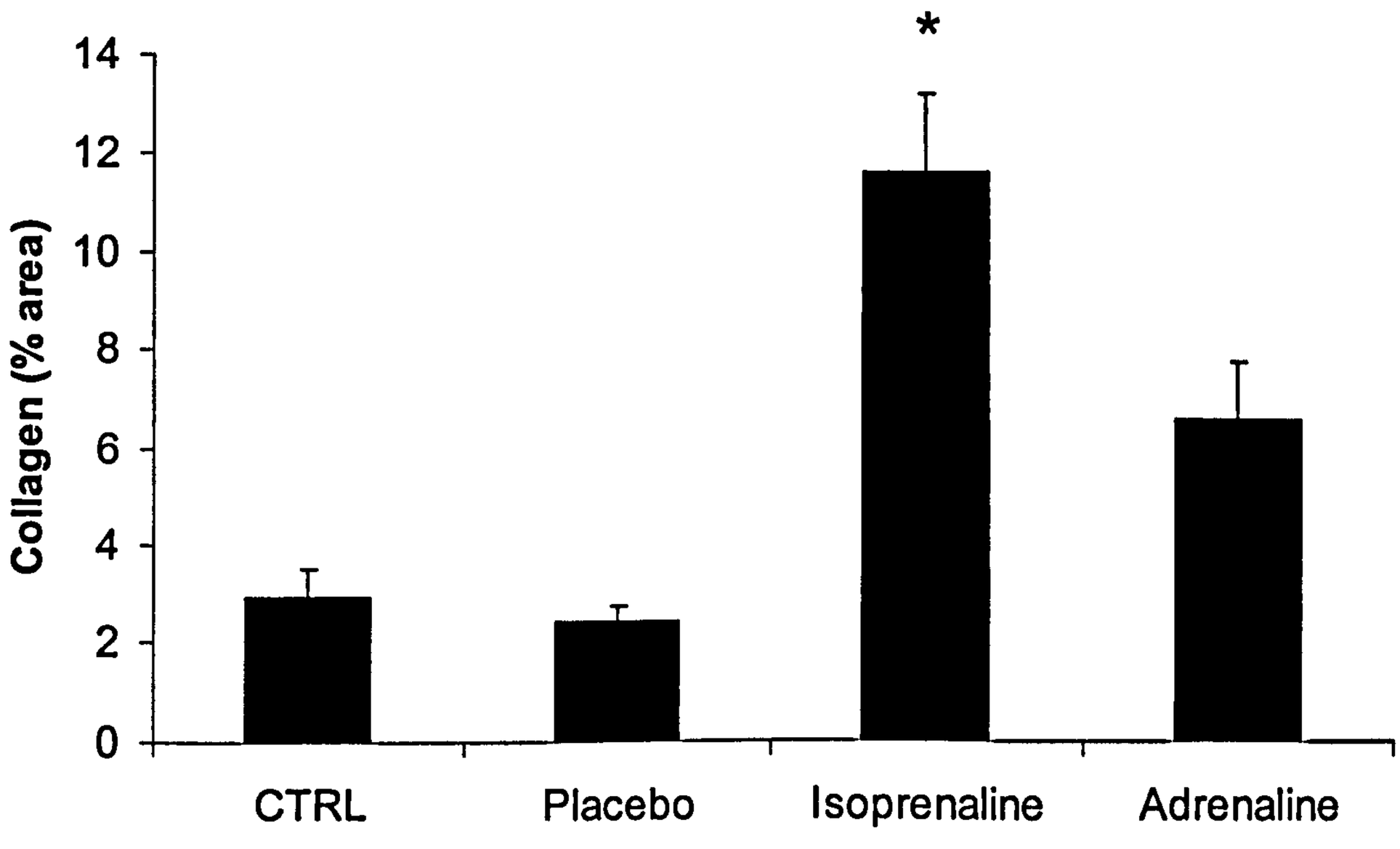

Figure 3.48 Collagen content in the heart after chronic exposure to catecholamines.

Percent area of collagen was measured in the heart following 14 days of continuous infusion with either 20 mmol $kg^{-1}d^{-1}$ of isoprenaline, adrenaline or saline (placebo) only, delivered via osmotic mini pumps. Results are Mean ± SEM for n=5. *denotes significant difference ($P<0.05$) from zero day control (CTRL), placebo controls and adrenaline groups.

3. Continuous infusion of catecholamines caused necrotic and apoptotic cell death in both the heart and soleus muscles. This was met by a continual process of fibre regeneration in the soleus muscle.

4. Continuous infusion of catecholamines resulted in extensive fibrosis (increased collagen content) in the heart, but not the soleus muscle.

4.0 DISCUSSION

Three main findings emanate from this study. First, whether administered acutely or chronically catecholamines induce both necrotic and apoptotic fibre death in the soleus muscle. Chronic exposure also caused muscle hypertrophy, against a background of continual fibre death and regeneration. The latter could lead to detrimental consequences, with a net loss of muscle fibres, due to a compromised skeletal muscle regenerative capacity. Second, acute and chronic exposure to catecholamines is also detrimental for the heart causing significant cell death, hypertrophy and fibrosis. Third, the heart compensated for the acute damage caused by excessive catecholamines through both cardiomyocyte hypertrophy and hyperplasia.

4.1 Fibre Death and Skeletal Muscle Regeneration

4.1.1 Catecholamine-induced damage

A single injection of the natural catecholamines adrenaline or noradrenaline, or the synthetic derivative, isoprenaline, induced fibre necrosis and apoptosis in the soleus muscle of the rat. These findings are highly significant as no damage was found in any of the control muscles from those animals that received the saline vehicle, but no catecholamine. Previous findings from our laboratory have shown that the amount of damage depends on the dose administered and the time course defining optimal necrotic and apoptotic damage (Ng et al., 2002; Goldspink et al., 2004). Interestingly, significant damage to skeletal muscle in response to excess catecholamines is a novel finding. This study shows for the first time that acute exposure to adrenaline or noradrenaline, as well as isoprenaline, results in significant necrosis and apoptosis in the skeletal myocytes of otherwise normal rats.

The time course of apoptosis in the soleus muscle in the present study are also novel. Previously, Ng et al. (2002) reported the injurious effects of isoprenaline, causing severe fibre necrosis, in the rat soleus muscle. Ng et al. (2002) found that this toxic damage was initiated at lower doses than that in the myocardium (1μg vs. 10μg kg^{-1}) and peaked earlier at 12 vs. 18 hr post injection. While the present findings of significant necrosis in the soleus muscle following acute catecholamine

exposure confirm these earlier observations in our laboratory, apoptosis increased in a time dependent manner, being greatest at about 18-24 hours. This provides evidence of the similarities in the onset and time course of apoptosis and necrosis in the soleus muscle, when comparing with the study by Ng et al. (2002). Interestingly, these data could suggest that the two processes may be one and the same, rather than 2 separate independent pathways. Recently, our laboratory suggested that catecholamine-induced apoptosis and necrosis either originate from common initial pathways, or that they maybe one and the same process, i.e. a continuum of events. This was a result of finding close similarities in the dose-responses, spatial distributions and receptor sub-type mediation for apoptosis and necrosis after a single injection of isoprenaline (Goldspink et al., 2004). Through the immunohistochemical technique of double immunofluorescence, both necrosis and apoptosis could be visualised on the same section of the soleus muscle. Interestingly, the present findings revealed that apoptosis (caspase-3 labelled) and necrosis (myosin antibody incorporated) co-localised within the same muscle fibres (Figure 3.10). More specifically, the number of fibres that were apoptotic alone was zero. Therefore, all fibres that were initially detected as apoptotic also became labelled as necrotic, suggesting at the least a process of secondary necrosis. That is, apoptotic fibres initially with intact membranes were not phagocytosed rapidly enough, such that their sarcolemmal membranes subsequently became disrupted (i.e. secondary necrosis) allowing the large anti-myosin Ab to enter. Caspase-3 positive fibres with disrupted sarcolemmal membranes after the isoprenaline administration, confirm this secondary necrosis (Figure 3.10). Hence all apoptotic fibres appear to undergo this secondary phase before being removed from the muscle. Conceivably, this could occur before, or after, the formation of apoptotic bodies (Goldspink et al., 2003). In contrast, some fibres were necrotic only, with no signs of apoptosis. A possible explanation for these findings may be that once a fibre becomes necrotic and its membrane becomes disrupted and leaky, its intracellular contents leak out and cause inflammatory responses such that neighbouring viable fibres become damaged and subsequently necrotic. Alternatively, a completely different mechanistic pathway, independent of apoptosis and any inflammation caused by

secondary necrosis, may have initiated this small portion of the injured and necrotic fibres.

The current findings could also be explained by taking into account the role of the mitochondria in cell death. Permeabilisation of the outer membrane of mitochondria is a feature of both apoptosis and necrosis, and this process of simultaneous induction of apoptotic and necrotic death has been termed 'necrapoptosis' (Lemasters et al., 2002). Following permeabilisation of the outer mitochondrial membrane, the availability of ATP could determine which type of cell death predominates, in that cells rapidly depleted of ATP undergo necrosis as opposed to apoptosis (Leist and Jaattela, 2001). This process of simultaneous induction of both types of cell death could also explain the present findings. Regardless, of how distinctive the two cell death pathways may actually be, or whether they share common initial pathways, the present findings highlight the importance of examining both types of cell death following a common insult. This is an area which many investigators have previously ignored, examining either one or the other cell death phenotype, and in particular the more 'fashionable' apoptosis.

The present findings of necrotic fibre death in the soleus muscle after acute catecholamine exposure, also agrees with the previous findings of Heap et al. (1996). The workers (Heap et al., 1996) reported isoprenaline-induced necrosis in the soleus muscle of the rat. Although the same dose of isoprenaline was used (i.e. 5mg kg^{-1}) in both studies, the amount of necrosis reported here was significantly greater than that found by Heap et al. (1996), i.e. 8.0 ± 1.8% fibres vs.1.8 ± 0.3% volume. The reason for this discrepancy could be due to differences in the detection of necrotic fibre damage. In the present study, a highly sensitive method (*in vivo*) which is specific for detecting damaged myocytes was used. However, Heap et al. (1996) assessed the extent of necrosis by the size of interstitial space and connective tissue using standard haematoxylin and eosin (H&E) staining, and did not specifically detect necrotic fibres. Another β_2-agonist, clenbuterol, has also been found to cause a similar amount of necrotic fibre damage to the soleus muscle, examined 18 hours after a single 5mg kg^{-1} injection (Burniston et al., 2002).

Furthermore, the necrotic damage was reduced by 89% by the prior administration of the β_2-AR antagonist, ICI 118,551. It was reported by Ng et al. (2002) that isoprenaline myotoxicity was mediated via β_2-AR in the soleus and β_1-AR in the heart (Ng et al., 2002). Also, it has been shown that β_2-AR blockade before isoprenaline injection, significantly decreased the amount of myocyte death in the soleus, whereas β_1-AR blockade was ineffective (Goldspink et al., 2004). These findings prove that the damaging effects of catecholamines on the soleus muscle are mediated through the β_2-AR pathway. These findings agree with the present findings demonstrating further the detrimental effects of β-AR stimulation on the soleus muscle.

Interestingly, the present study revealed that only the soleus muscle out of the 4 skeletal muscles examined was damaged by catecholamine administration. That is the tibialis anterior, plantaris and diaphragm muscles showed no necrotic or apoptotic fibres following catecholamine injection. All of these muscles were isolated from the same animals, clearly demonstrating different sensitivity levels to the catecholamines. The soleus muscle is composed of predominantly slow-twitch oxidative (Type I) muscle fibres (Figure 3.15), and is highly active due to its involvement in the control of posture and gait. It is suggested that slow-twitch postural muscles have a higher incidence of fibre degeneration and consequent regeneration, and a higher number of satellite cells (Schmalbruch and Hellhammer, 1977), than fast- twitch muscles. This is due to more frequent and chronic recruitment of postural muscles in maintaining stance and gait. Therefore, these characteristics make it increasingly more susceptible to injury (Wanek and Snow, 2000).

As catecholamines also cause significant damage to the heart, it is thought that because the soleus muscle is close to the metabolic pattern (oxidative) and characteristics of contractile proteins (i.e. slow MHC) in the cardiac muscle, this could explain why it is damaged, when compared to the other faster contracting and glycolytic skeletal muscles. They are predominantly oxidative muscles relying on their many mitochondria to generate their ATP and due to the role the mitochondria

plays in cell death this could partially explain why these myocytes are more vulnerable to the injurious effects of catecholamines (Primeau et al., 2002). Another explanation is that the soleus muscle has a ~3-fold greater number of β-ARs than fast glycolytic muscles, e.g. vastus lateralis and gastrocnemius (Martin et al., 1989; Jensen et al., 1995). Also, it has been suggested that type I fibres have ~4.5-fold greater β-AR density than that found in type IIb fibres and 2-fold greater than type IIa. Hence, the overall β-AR density will be directly proportional to the percentage of the different fibre types present in any muscle (Martin et al., 1989). Although Martin et al. (1989) did not specify which sub-type of β-AR was upregulated in these different skeletal muscles, it has previously been shown that skeletal muscles predominantly express β_2-ARs (Yang and McElligott, 1989; Jensen et al., 1995). As it has previously been shown that the damaging effects of isoprenaline on the soleus muscle are mediated through the β_2-AR pathway (Goldspink et al., 2004), then the higher proportion of β-ARs in this muscle could explain the different effects of catecholamines between the different muscle types, with their different fibre type compositions, in the present study. In contrast to these logical differences in β-AR density between slow and fast skeletal muscle, the heart contains more β-ARs than the soleus and could explain the extensive cell death and myocyte loss in the heart in the present study.

Interestingly, unlike fast fibres, it is noted that both slow skeletal muscle fibres and cardiac muscle cells contain phospholamban (PLB), the principal inhibitor of SR Ca^{2+} uptake by SERCA2 (Simmerman and Jones, 1998). In fact, over-expression of the β_1-ARs in PLB -/- knockout mice have an enhanced survival, decreased cardiac hypertrophy, fibrosis and improved cardiac function, due to a faster decay of intracellular calcium transients and decreased diastolic calcium levels and loads (Engelhardt et al., 2004; Iwanaga et al., 2004). Therefore, these data suggest a protective role for deleting PLB in over β-AR stimulation. The mechanism of cell death from catecholamines will be discussed later in this section. However, when taking all these explanations into account the present findings are still unclear, as it cannot be explained why the slow fibres present in the faster glycolytic (tibialis

anterior, plantaris) and mixed diaphragm muscles were not damaged by the catecholamines and so needs further investigation.

In the present study, isoprenaline was found to cause greater damage to the soleus muscle than did adrenaline or noradrenaline. Noradrenaline is selective for β_1-ARs and displays a 10 to 30-fold higher binding affinity to β_1 receptors, compared to β_2 receptors (Bristow, 2000). Therefore, noradrenaline is an exceptionally cardiotoxic substance, producing significant myocyte damage in the heart, as cardiac muscle predominantly possesses β_1-ARs (Katz, 2001). However, as it is β_1-AR selective, its effects on skeletal muscle would be expected to be much less (Figure 3.9). In contrast, isoprenaline and adrenaline are both β_1 and β_2-AR agonists with very similar affinities for both β-AR subtypes. Therefore, one might anticipate that on a molar equivalent basis they would cause similar significant amounts of damage to both the heart and skeletal muscle. However, from the present study is it clear that isoprenaline was more potent than both adrenaline and noradrenaline.

Pharmacologically the 3 catecholamines differ. The half-life of isoprenaline was designed to be greater than adrenaline and noradrenaline, so therefore adrenaline and noradrenaline are removed from the blood faster than isoprenaline ($t_{1/2}$ ISO: 5 minutes; Conolly et al., 1972; $t_{1/2}$ Ad and NAd: 2 minutes; www.anaesthesiauk.com). Furthermore, adrenaline and noradrenaline have moderately high affinities for neuronal reuptake, which means that the majority of the administered hormone may not reach β-adrenergic receptors (Bristow et al., 2001). These findings could offer an explanation as to why isoprenaline is more potent and induces significantly greater damage to the soleus muscle. However, these findings are interesting and warrant further investigation.

4.1.2 Fibre regeneration and time course of the regenerative process

Regardless of whether significant fibre degeneration occurred through necrosis and/or apoptosis as a consequence of a single injection of catecholamine, the present findings confirm the ability of skeletal muscle to regenerate fibres following injury. Indeed, the soleus muscle was able to regenerate these fibres with complete

restoration of the full fibre complement by 28 days. The process of regeneration and sequence of events described in the present study agrees with previous data from studies assessing the regenerative capacity of the extensor digitorum longus (EDL) and soleus muscles after very severe toxic damage induced by snake venom (Harris et al., 1975; Whalen et al., 1990; Davis et al., 1991). The time course of regeneration in the present study was similar to those in previous studies, with respect to phagocytotic clearance of damaged fibres, the appearance of immature myotubes, their subsequent development into small regenerating fibres and the total restoration of functional fibres by 28 days. This rapid process of regeneration indicates the existence of an intact nervous system, microcirculation and viable satellite cells in this damage model. These variables are crucial for successful regeneration to take place (Whalen et al., 1990; Irintchev et al., 1997; Pavlath et al., 1998).

The peak time of detecting regenerating fibres was 7 days following isoprenaline administration, with 8 ± 2.6% of the fibres in the whole soleus undergoing regeneration (Figure 3.11). These findings correlate exactly with the amount of damage (i.e. 8.0 ± 1.8%) found in the soleus muscle within 18 hours of the isoprenaline administration. The findings were similar for adrenaline, but with only 1.7 ± 0.7% of the fibres in the entire soleus regenerating at 7 days, reflecting the low level of damage at 1.0 ± 0.5%. This confirms that there was complete regeneration of the fibres that were initially damaged by the 2 catecholamines. The extent of the injury will govern the time course of regeneration (Whalen et al., 1990). It is clear that following adrenaline there was less damage, and therefore the time to repair these damaged fibres and replace them was quicker, exhibited by complete restoration occurring earlier at about 14 days (Figure 3.12).

Interestingly, the present study found the appearance of some small individual fibres regenerating within the basement membrane of another fibre 10 days following catecholamine injection (Figure 3.13, F). Fibre splitting or branching is a characteristic feature of muscle regeneration, and it is probably due to the incomplete fusion of myofibres regenerating within the same basal lamina (Bourke

and Ontell, 1984; Blaivas and Carlson, 1991). Furthermore, fibre splitting is commonly observed in patients with neuromuscular diseases, hypertrophied muscles and aging muscles (Alnaqeeb and Goldspink, 1986), all of which are associated with abnormal regenerative capacity. The latter was clearly not the case in the present study. The evidence of fibre branching in the present study shows smaller fibres that appear to have their own individual basement membranes, but are growing within another fibre, suggesting the appearance of 3 fibres within 1. This phenomenon is not commonly reported and morphologically different from standard described fibre branching and splitting. Collectively these findings suggest that there would be full restoration of fibres following injury (i.e. one for one), and possibly a few additional fibres (e.g. 3 for 1 here: Figure 3.13, F). The present study found that after 28 days there was full restoration of muscle fibres in the soleus muscle, i.e. 2653 ± 111 at zero time, compared with 2544 ± 69 at 28 days. After 28 days only a very small numbers of regenerating fibres were present, suggesting that the degeneration/regeneration process was complete. It is possible that the appearance of any additional fibres (arising from 3 for 1) was balanced by some fibres that were damaged and irreversibly lost, without any regeneration at all. However, to keep this matter in perspective the number of '3 in 1' fibres seen within the entire soleus muscle was very small, and hence the impact of such additional fibres on the overall fibre number would be small.

In order to provide a sufficient source of new myonuclei for muscle repair, successful skeletal muscle regeneration relies on a source of myoblast cells (Charge and Rudnicki, 2004). In the present study satellite cells were marked using an antibody against c-met, the tyrosine kinase receptor. C-met is present on quiescent, activated and proliferating satellite cells (Cornelison and Wold, 1997). C-met positive cells were identified in sections of the soleus muscle following catecholamine-induced damage. Furthermore, the present study also demonstrated the existence of proliferating c-met positive cells, shown by the co-expression with BrdU. Also, transcription of the myogenic factor, MyoD, indicated the muscle tissue specific expression of these cells (Figure 3.16). Although not quantified, these cells were most abundant 1-3 days after catecholamine injection. The earlier phase of

muscle injury was accompanied by the activation of inflammatory cells and myogenic cells. In the present study, both inflammatory and myogenic cells infiltrated and were most evident in the damaged regions of the muscle at 2 days (Figure 3.13, B). As immature myotubes were present at 3 days (Figure 3.13, C), the differentiation of these cells and consequent fusion into myotubes must have occurred here. These findings strongly suggest that these c-met, BrdU, MyoD positive cells identified after isoprenaline injection could potentially be satellite cells or myoblasts, activating the repair process and giving rise to new fibres.

The splice variant of IGF-1, MGF, has been implicated in the activation of satellite cells, following muscle injury (Hill and Goldspink, 2003; Hill et al., 2003). The present findings provide strong evidence of a role played by MGF in the activation of satellite cells and consequent regeneration of skeletal muscle. MGF positive nuclei were present in the isoprenaline-treated soleus muscles from 3 to 72 hours. In contrast, no MGF-labelled nuclei were present in the control muscles (Figures 3.17; 3.18). MGF mRNA transcripts are elevated before the splice variant IGF-1Ea, and peaked at 24 hours and 4 days after stretch-stimulation and bupivacaine induced-injury, respectively. Furthermore, this was before the development of peak damage (Hill et al., 2003). In agreement with the present findings, this suggests that there is a rapid autocrine 'surge' effect when degeneration begins (3 hours in the present study). The levels of MGF remained elevated and surged again 24 hours after catecholamine injection (Figure 3.18). MGF mRNA levels increase prior, or at similar time points, to M-cadherin and MyoD mRNA and proteins, suggesting a role for MGF in initiating the proliferation and differentiation of satellite cells (Hill et al., 2003; Hill and Goldspink, 2003). These findings agree with the present study, in that c-met-MyoD positive cells (predicted as activated satellite cells), were identified in the soleus muscle 24 hours after treatment. These data are supported further as the levels of MGF had decreased by 72 hours, once these cells had fused to form myotubes and regeneration had begun. These observations were similar to the findings of Hill et al. (2003).

Certain discrepancies do however exist between the present study and that of Hill et al. (2003). Where the present study assessed the protein expression of MGF in muscle sections, Hill et al. (2003) reported MGF at the level of mRNA and this would be expected to appear before the protein end product. However, 24 hours and 4 days were the first time points to be analysed by Hill et al. (2003) after stretch stimulation and bupivacaine induced-injury, respectively, so it's entirely possible that MGF expression could have been apparent sooner had they looked for it. Interestingly, the present study found MGF to be present within the nuclei of cells, but due to technical problems the present study failed to exhibit the co-expression of MGF with satellite cell markers. However, these findings may provide first evidence of MGF's possible status as a transcription factor.

The present study reveals that 14 days after catecholamine administration, the soleus muscle fibres were predominantly composed of the slow MHC isoform (Figure 3.14). These findings confirm those reported by Whalen et al. (1990), who found that the slow phenotype was homogeneously expressed in the regenerated fibres of the soleus 21 days after snake toxin-induced injury. These findings were also supported by Davis et al. (1991), but 56 days after venom injury. The present findings could be interpreted as suggesting that the relatively few type IIa fibres were targeted specifically and destroyed by the catecholamines. However, this does not seem likely considering no catecholamine-induced damage was present in any of the predominantly faster muscles, containing an even greater proportion of IIa fibres. Further support for rejecting this view is that by 28 days, the fibre proportions were the same as in the control muscle (Figure 3.14).

The accumulation of the slow MHC isoform is largely dependent upon the activity pattern delivered by the motor neuronal innervation restored to regenerating muscle fibres. In the absence of innervation such fibres are inactive and accumulate adult fast myosin (Whalen et al., 1990; Davis et al., 1991). As fibres become re-innervated, there is a suppression of the production of the developmental and fast MHC, and activation of the neurally-regulated expression of slow MHCs (Davis et al., 1991). These findings agree with the present study, as it was shown that at 14

days after the catecholamine injection there was a suppression of the embryonic/neonatal MHC, with an increased proportion of newly regenerated fibres with centralised nuclei (a characteristic prior to re-innervation) and expression of slow MHCs.

Alternatively, the accumulation of the slow phenotype in the regenerated fibres could arise from either the slow motor neurones being more resistant to the effects of the catecholamines or fast neurones transforming to slow ones during the course of the regeneration (Whalen et al., 1990). Because the full fibre complement and the fibre proportions were the same as controls by 28 days, the latter hypothesis is rejected. It may seem plausible in the present study, that the slow neurones are more resistant to the catecholamines. In that, the fast neurones simply require a longer period to be put back and re-innervate the muscle fibres once again and therefore the production of the type IIa and intermediate phenotype. However, this hypothesis is also rejected as no fibre death was found in faster muscles, therefore the present findings would perhaps suggest that faster neurones are more resistant to the catecholamines, and slow neurones are more susceptible.

4.1.3 Continuous infusion of catecholamines

As CHF patients exhibit sustained high levels of catecholamines and these have been implicated in the severe muscle wasting seen in some of these patients (Anker et al., 1997a,b), it was important to investigate the effects of chronic, as well as acute, exposure to the catecholamines.

Continuous infusion of the catecholamines (20 mmol $kg^{-1}d^{-1}$) caused significant increases in body weight, muscle mass and fibre cross-sectional area (CSA), with these being most dramatic in the isoprenaline-treated animals. The increase in body weight could be a result of oedema, exemplified by the development of heart failure with continuous catecholamine exposure. The present findings confirm the work of Ryall et al. (2003), who found that continuous infusion of 1.4 mg $kg^{-1}d^{-1}$ of the β_2-agonist, fenoterol, resulted in a significantly greater body mass, EDL and soleus muscle weights. This was accompanied by increased fibre CSA, as well as improved

muscle function. The present study found that after 28 days of catecholamine exposure, the soleus, tibialis anterior and plantaris muscles had increased their masses over time and were all heavier, when compared to the placebo controls. The increase in muscle mass was explained directly by the increase in fibre CSA, measured in the soleus muscle. In keeping with their greater size, the isoprenaline-treated animals consumed a greater amount of food over the 28 day experimental period, but their appetites (food/100g rat) remained the same. In the first 3 days, both experimental groups displayed a decreased appetite, food and water consumptions most probably due to the initial acute stress effects of the catecholamines. After this brief period, everything returned to placebo control values, illustrating the adaptation and desensitisation of these animals, with respect to hunger and thirst, to the chronic exposure to the catecholamines.

Despite their anabolic effects, the continuous infusions of the catecholamines still caused small but significant amounts of fibre necrosis and apoptosis in the soleus over the 28 day experimental period (Table 3.6). As in acute exposure, there was resultant muscle regeneration in the soleus demonstrated by the presence of small myofibres positive for neonatal and embryonic MHC. However, the incidence of cell death and the resultant regeneration was not as great as that caused by a single, bolus injection. These findings could be explained by the fact that a single bolus injection would have a much greater immediate impact and higher plasma levels for a few minutes, than a daily dose infused over 24 hours. Also, although not measured, these findings suggest the down-regulation and/or impaired coupling of the β-ARs in the soleus muscle, with chronic β-AR stimulation (Ryall et al., 2003). It is interesting to note that this down regulation and desensitisation of the β-ARs did not affect the physiological response, i.e. muscle hypertrophy. These findings would suggest that catecholamines *per se* may not be responsible for the anabolic effects seen in skeletal muscle. Interestingly, in the present study only the anabolic, and not myotoxic effects were apparent in the other muscles. These findings could suggest that the signalling pathway mediating cell death is different from the pathway mediating muscle hypertrophy with exposure to catecholamines.

As stated, the soleus muscle showed small regenerating fibres positive for embryonic/neonatal MHC, and these were present from 5 days. These were constant in number up to 28 days. These findings could be interpreted as a retardation of the development of the regenerating fibres by the sustained presence of the circulating catecholamines. However, the total number of fibres continued to increase over 28 days, suggesting that these fibres did mature into the adult phenotype (Figure 3.45; Figure 3.46). Alternatively, the present findings could indicate that, although small, there is a continuous process of fibre death and regeneration occurring in the soleus muscle, throughout the continuous infusion of the catecholamines. If continued for long enough, several cycles of degeneration-regeneration could compromise the ability of the resident muscle satellite cells to proliferate and replace the damaged fibres, due to a decreased telomeric length with consequent satellite cell senescence (Reimann et al., 2000; Decary et al., 2000). Furthermore, in muscular dystrophies the failure to regenerate fibres has been attributed to exhaustion of the proliferative potential of the satellite cell pool because of the continual need for satellite cell proliferation and fibre repair. This results in massive muscle atrophy, infiltration of collagen and fat and muscle weakness (Reimann et al., 2000). In the present investigation, the effects of chronic catecholamine exposure were not studied beyond 28 days. However, it would be interesting to investigate whether similar muscle wasting through fibre loss would occur if the muscles were exposed for a greater period, i.e. creating further cycles of degeneration and regeneration. This could be the case in CHF, with the sustained high levels of catecholamines compromising satellite cells and a progressive loss of fibres resulting in the dramatic fall in muscle mass and weakness. Reduced activity levels would exacerbate the situation as well as causing physiological atrophy of the remaining viable fibres.

In light of recent advances with cellular therapy (Torrente et al., 2001), it is questionable whether the pool of muscle stem cells is limiting and can be reasonably attributed to the progression of muscle wasting. This is because of the ability of other cells e.g. BMDCs to give rise to satellite cells and consequently muscle fibres (Ferrari et al., 1998; LeBarge and Blau, 2002), as well as the existence of a side population of muscle stem cells possibly originating in the vasculature (Asakura et

al., 2001). Furthermore, it would be interesting to investigate whether there could be an optimal dose of catecholamines, which induces muscle hypertrophy but does not cause cell death.

Insulin-like growth factor-1 and MGF increases the rate of protein synthesis, thereby increasing muscle hypertrophy and mass (Musaro et al., 2001; Goldspink, 2001), as well as promoting the activation and subsequent proliferation and differentiation of muscle satellite (stem) cells (Allen and Boxhorn, 1989; Chakravarthy et al., 2000; Rabinovsky et al., 2003; Hill et al., 2003). Therefore, muscle repair and hypertrophy appear to involve at least some of the same signalling pathways. Accordingly, it has been questioned whether local muscle damage is a pre-requisite for muscle hypertrophy (Hill and Goldspink, 2003). In the present study catecholamine-induced damage to the soleus muscle caused an upregulation of MGF expression, in order to activate the satellite cell pool to ensure the regeneration of muscle fibres (Figure 3.18). Due to its role in muscle regeneration it is conceivable, yet speculative, that local IGF-1 is also elevated following catecholamine damage. Therefore, the anabolic effects of catecholamines could be attributed to an autocrine/paracrine elevation in IGF-1 and its splice variant MGF. These factors would serve to activate the satellite cell pool and ensure the regenerative process, while simultaneously causing muscle hypertrophy by mediating part of their effects directly through the differentiated muscle fibres. Hence, the muscle adaptation seen following catecholamine exposure is a manifestation of repeated injury and repair resulting in over-expression of the two growth factors. Furthermore, it has been reported that satellite cells play a critical role in the hypertrophic response, giving rise to new myonuclei (Barton-Davis et al., 1999). It has been reported that in trained human subjects with fibre hypertrophy there is a significant increase in the number of fibres which are stained for embryonic and fetal MHCs (Kadi and Thornell, 2000). Therefore, the muscle may adapt to training through hypertrophy and hyperplasia (Kadi and Thornell, 2000). In the present study, at 28 days there was a slight elevation for fibre number above control in the soleus, possibly suggesting an adaptive response involving both hypertrophy and hyperplasia, caused by IGF-1 and MGF expression.

These mechanisms could possibly explain the hypertrophic response in the soleus muscle. However, it may not be as straightforward for the other muscles, as they were not damaged as a result of the catecholamines, but still exhibited a considerable increase in muscle mass. A possible explanation is that due to signalling of damage from the soleus muscle there is a paracrine (systemic effect) effect of IGF-1, resulting in significant hypertrophy to the other muscles in the body. This concept seems particularly warranted due to the findings that chronic β_2-AR stimulation by clenbuterol caused increased soleus muscle mass (16%) mediated by the local production of IGF-1 by myocytes, which subsequently had an autocrine or paracrine effect in eliciting muscle hypertrophy (Awede et al., 2002). Alternatively, another mechanism not involving IGF-1 or its splice variants, could explain the anabolic effects of catecholamines. Therefore, the possible direct and indirect mechanisms of the anabolic effects of catecholamines warrant further investigation. Like their β_2-AR counterpart, clenbuterol, catecholamines could potentially be considered for clinical application in ameliorating muscle wasting, e.g. as seen with ageing and disease states such as heart failure and cancer. However, the potential beneficial effects of exposure to catecholamines are counteracted by the severe damaging effects to the heart.

4.2 Cardiomyocyte Death and Regeneration

The accepted paradigm considers the adult mammalian heart as a post-mitotic organ, which possesses a relatively constant number of myocytes from shortly after birth to adulthood and senescence, dismissing the occurrence of new myocyte formation. On this basis, pathologic remodelling of the cardiac left ventricle has been so far described as the product of different on-going processes which include: myocyte slippage and chamber dilation; fibrosis and scar formation; excessive accumulation of interstitial matrix; increased wall stress; myocyte hypertrophy; neurohormonal activation; cytokine release; progressive myocyte hypertrophy; cell apoptosis and necrosis. The results of the present study shed new light on the pathophysiology of ventricular remodelling. Indeed, it has demonstrated that myocyte cellular hyperplasia through activation and differentiation of cardiac stem cells is a significant phenomenon that participates in the wall repair after diffuse

myocardial injury in the presence of a patent coronary circulation. This reinforces a new view that considers the heart as a self-renewing organ, able to heal itself (Nadal-Ginard et al., 2003).

4.2.1 Cardiomyocyte death and loss

Cardiovascular disease in both the human myocardium and animal models have demonstrated that a variety of pathological states of the heart are associated with myocyte apoptosis, including myocarditis (Blankenberg et al., 1999), transplant rejection (Koglin et al., 1999), myocardial ischemic injury (Olivetti et al., 1996) and heart failure (Olivetti et al., 1997). Late in heart disease myocyte death exceeds regeneration resulting in the reduction in the total number of LV myocytes (Kajstura et al., 1995). The imbalance between cell death and cell multiplication in favour of the former might be critical in the development of cardiac failure. Since it is known that heart failure patients exhibit an elevated circulating level of catecholamines, and as the use of β-AR antagonists have a dramatic impact on both clinical outcomes and the progression of the underlying myocardial failure (Bristow, 2000), it has been suggested that increased sympathetic activity may play an important role in the pathophysiology of myocardial failure, via the stimulation of β-ARs.

It is well documented that catecholamines are cardiotoxic (Rona et al., 1959; Todd et al., 1980; Teerlink et al., 1994; Heap et al., 1996), causing myocyte necrosis (Benjamin et al., 1989) and apoptosis *in vitro* (Communal et al., 1998) and *in vivo* (Shizukuda et al., 1998; Xi et al., 2000). Catecholamine-induced cardiomyocyte apoptosis is mediated through β-ARs, specifically through the β_1-AR subtype (Zaugg et al., 2000; Goldspink et al., 2004). This involves increases in cAMP and PKA-mediated increase in Ca^{2+} influx (Communal et al., 1998). Increased cytosolic Ca^{2+} affects mitochondrial membrane permeability and triggers the release of apoptogenic factors, including the initiator caspase-9 from the damaged mitochondria (Zaugg et al., 2000). This in turn activates the effector caspases -3, -6 and -7 which act downstream in the common pathway to carry out the final biochemical changes seen in apoptosis (Kang and Izumo, 2003). Additionally, myocardial apoptosis mediated through β-AR signalling appears to involve both the

activation of the MAPKs (i.e. JNK, c-Jun, N-terminal kinase and p38) and increased production of reactive oxygen species (Sugden and Clerk, 1998; Siwik et al., 1999).

In the present study, extensive focal cell death was found in the LV after isoprenaline injection, occupying 17 ± 4% of the myocardial area after 1 day. Furthermore, the present findings describe caspase-3 positive cardiomyocytes in the hearts of isoprenaline-treated rats. These were most evident just 3 hours following the single 20 mmol kg^{-1} injection (Figure 3.7), and decreased thereafter. These findings were similar for dUTP labelled myocytes, showing only 0.4% at 24 hours and decreasing to 0.15% by 72 hours (Table 3.3). Therefore, through the certified use of both techniques, isoprenaline caused myocardial apoptosis, which was evident in a time-dependent manner. The resultant effect of isoprenaline-induced necrotic and apoptotic death was the significant loss of myocytes in the LV (Figure 3.22).

Continuous infusion of catecholamines in the rat caused significant cardiomyocyte necrosis and apoptosis, although this was not as severe as that following a single injection. This further supports the notion of desensitisation and/or downregulation of β-receptors with chronic sympathetic activation; a protective mechanism that is found in heart failure (Vatner et al., 1999). Despite the reduced levels of cell death reported in the present study, continuous exposure to the catecholamines resulted in a marked hypertrophic response in the heart. This was apparent as an increase in ventricular mass occurring rapidly within 5 days and increasing further with time (Figure 3.40). This was more severe in the isoprenaline-treated animals, clearly demonstrating the synthetic catecholamines greater potency on hypertrophy as well as cell death. This cardiac hypertrophy was coupled with increased myocardial collagen content (Figure 3.47; 3.48), possibly due to cardiomyocyte death (necrosis) and reparative fibrosis. The effects of chronic sympathetic stimulation on the heart are mainly mediated through the β-ARs, as β-AR blockade significantly prevented these deleterious adaptations (Asai et al., 1999; Karoor et al., 2004). The mechanisms responsible for these changes have been attributed to abnormal cardiomyocyte Ca^{2+} transients related to decreased expression of the SR protein,

junctin (Engelhardt et al., 2001; 2004), the cardiac Na^+-H^+ exchanger 1 (NHE1) and increased sodium load (Engelhardt et al., 2002), and phospholamban (Iwanaga et al., 2004). Increased circulating catecholamines have been implicated as a primary causative factor in the development of cardiomyopathy and early mortality (Dash et al., 2001). Although no measurement of function was obtained here, the present findings exhibit the development of a cardiomyopathy with chronic β-AR stimulation, confirming the studies of others (Benjamin et al., 1989; Kudej et al., 1997; Morisco et al., 2001; Engelhardt et al., 1999; 2001; 2002; Geng et al., 1999).

The SR calcium-release channel is a key component in muscle excitation-contraction (EC) coupling (Wehrens and Marks, 2003). The release of calcium from the SR through ryanodine receptor (RyR) channels initiates contraction of the muscle fibre. After depolarization of the myocyte membrane, voltage-gated L-type Ca^{2+} channels are activated in the sarcolemmal membrane encompassing the transverse T-tubule. The ensuing Ca^{2+} influx triggers a much greater Ca^{2+} efflux through RyRs on the SR via a process termed Ca^{2+}-induced Ca^{2+} release, inducing cell contraction. The increase in cytosolic Ca^{2+} concentration during a contraction is immediately followed by Ca^{2+} removal, resulting in deactivation of the contractile machinery and muscle relaxation. Cytosolic Ca^{2+} is pumped back into the SR by SR Ca^{2+}-ATPase (SERCA2), which is regulated by PLB (Simmerman and Jones, 1998).

Increased levels of circulating catecholamines activate β-ARs, elevate intracellular cAMP, and activate PKA. PKA phosphorylation modulates RyR and PLB, function both *in vitro* and *in vivo* (Marx et al., 2000), inducing in the short term, myocyte contractility. In contrast, in the long term, mal-adaptation of this classic physiological pathway plays an important role in the pathophysiology of heart failure, which is a chronic hyper-adrenergic state. Indeed, it has been previously found that the RyR is PKA-hyperphosphorylated in end-stage heart failure (Marx et al., 2000). Defective Ca^{2+} handling has been implicated in many pathological conditions and the spatial organisation of the RyRs appear to be of key importance in determining cell fate. Notably, hyperphosphorylation of RyR induces myocyte apoptosis (Jayaraman and Marks, 1997; George et al., 2003). Infusion of

isoproterenol results in PKA phosphorylation of RyR in the rat, indicating that systemic catecholamines can activate phosphorylation of RyR *in vivo* (Reiken et al., 2004). Therefore, it is highly tempting to speculate that the same mechanism has been operating to induce cell death in cardiac myocyte and soleus muscle fibres following catecholamine administration and exposure, in the present study.

A universal characteristic of end-stage failing myocardium is depressed SR Ca^{2+} cycling, caused by decreased expression of the cardiac SR Ca^{2+} ATPase (SERCA2a), and/or a relative overabundance of the SERCA2 inhibitory protein PLB. Furthermore, increased PLB expression in slow-twitch skeletal muscle is associated with impaired contractile function and muscle remodelling (Song et al., 2004). More importantly, SERCA2a over-expression and PLB depletion have been shown to have beneficial effects on contractility in heart failure (Chaudhri et al., 2002; Del Monte et al., 2002). Interestingly, in cardiac and slow skeletal muscle SR, but not in fast skeletal muscle SR, the Ca^{2+}-ATPase (SERCA2) is subject to regulation by PLB (Simmerman and Jones, 1998). It is widely recognized that dephospho-PLB inhibits SERCA2 function through physical interaction with the enzyme, and dissociation of the two proteins upon phosphorylation of PLB by PKA relieves the inhibition. On this basis, one of the possible mechanisms of isoprenaline-induced apoptosis and necrosis selectively in the rat heart and soleus muscles could relay on the presence of PLB only in cardiomyocytes and slow twitch skeletal fibres (abundant in the soleus), opposed to the absence of this protein in the fast fibres (Simmerman and Jones, 1998). Reiken et al. (2004) examined hearts from a rat model in which heart failure develops 6-month post-myocardial infarction (PMI). Six months PMI, these hearts showed PKA hyperphosphorylation of RyR and PKA hypophosphorylation of PLB resulting in Ca^{2+} myocyte cytoplasmic overload (Reiken et al., 2004). This provides evidence that RyR and PLB are differentially regulated with respect to PKA-dependent phosphorylation during hyper-adrenergic state of heart failure (Reiken et al., 2004). Therefore, the same mechanism could partially explain why catecholamines cause significant necrosis and apoptosis to cardiomyocytes and the predominantly slow soleus skeletal muscle, while not affecting faster muscles.

4.2.2 Myocyte regeneration

Diffuse myocardial injury in the presence of a patent coronary circulation, was associated with an increase in the number of myocyte nuclei in the LV synthesizing DNA. At 6 and 14 days after injury, this response involved 1 and 2% of the LV myocyte nuclei, respectively. Since the LV possesses 33 x 10^6 and 34 x 10^6 myocytes by 6 and 14 days, then 330 000 and 680 000 nuclei were undergoing DNA synthesis, respectively. Importantly, a small fraction of myocyte nuclei (0.01% in the LV), showed BrdU labelling in control rats, implying that DNA replication was occurring in ~5300 myocyte nuclei under control conditions. Therefore, DNA synthesis is normally present in a population of differentiated myocytes and this process is greatly potentiated by isoprenaline-induced injury.

The observations arising from this investigation are in contrast with a previous study carried out by Soonpaa and Field (1994) who found that in response to isoprenaline-induced cardiac hypertrophy, cardiomyocytes isolated from adult mice did not synthesise DNA. There are however certain methodological discrepancies between the present study and that of Soonpaa and Field (1994). First, in the latter study the isolation procedure yielded only big, fully mature cardiomyocytes making it impossible to analyse the entire, heterogeneous myocyte population. In the present study the majority of BrdU labelled myocytes were of small size. By using immunohistochemistry on tissue sections, the analysis of all myocytes could be achieved, including those which were discarded or missed by Soonpaa and Field (1994) during their isolation procedure. Second, Soonpaa and Field (1994) intentionally induced hypertrophy through continuous infusion of isoprenaline for 7 days delivered via osmotic mini pumps. But this occurred in the absence of necrosis, which could prove significant for new myocyte formation. Also, chronic catecholamine administration could have minimised the detection of DNA replicating myocytes by progressively killing these myocytes. It is somewhat surprising that Soonpaa and Field (1994) failed to find any 3H-thymidine labelling of myocyte nuclei in an animal model, that under physiologic conditions has a mitotic index of 47 myocyte nuclei/million (Oh et al., 2003). If it is assumed that the

cell cycle last ~24 hours then the percentage of thymidine labelled nuclei should be 0.1%. Therefore, these data can be questioned.

These findings are in direct disagreement with the present study and also that described by Rumyanstev (1991). Rumyanstev (1991) reported reactive DNA synthesis after bolus isoprenaline administration which induced focal necrosis within the myocardium. These findings, and that from the present study, raise the possibility that DNA replication is injury mediated. In fact, it has been shown by Kajstura et al. (1998) that human hearts with ischaemic or idiopathic dilated cardiomyopathies had a greater number of myocytes undergoing mitosis, than control hearts. Also, proliferating human myocytes (ki67-positive) and events characteristic of cell division (i.e. the formation of mitotic spindles and contractile rings, karyokinesis and cytokinesis) were found in regions adjacent to, and distant from, the infarcted area (Beltrami et al., 2001). Together these findings lend support for an injury mediated response for new myocyte formation, as these processes exist more in the viable myocardium after a myocardial infarction, than in control hearts.

It has recently been postulated that the heart is not a post-mitotic organ, and that myocyte death and regeneration are part of the normal homeostasis of the heart. In addition to hypertrophy, new myocyte generation predominates over cell death and contributes significantly to organ growth during normal cardiac growth to adulthood in both animals and humans (Nadal-Ginard et al., 2003). This is supported by the detection of myocytes undergoing mitosis in normal, control rat (Overy and Priest, 1966), mice (Anversa and Kajstura, 1998) and human hearts (Kajstura et al., 1998). Subsequently, DNA synthesis persists in the adult heart (Kajstura et al., 1994; Anversa and Kajstura, 1998) and even though at a low frequency, this could potentially be sufficient to sustain cardiac function in a non-diseased heart during adulthood. Also, the increase in myocyte numbers in the adult heart is an under estimation due to concurrent cell death seen with maturation (Anversa et al., 1990; Kajstura et al., 1996; Anversa and Olivetti, 2002). The finding of myocyte cell death in the adult heart again supports the concept of cardiac regeneration, because if

myocyte renewal did not take place then the heart would simply disappear within a few decades of life (Nadal-Ginard et al., 2003).

In the present study, BrdU immunofluorescence localisation in nuclei cannot in principle discriminate whether the DNA synthetic activity is coupled with nuclear hyperplasia or polyploidy formation. It has previously been reported that 3 months after coronary constriction myocyte growth was not accompanied by a change in the distribution of ploidy, and DNA replication was at most minimally involved in the polyploidisation of ventricular muscle cells (Kajstura et al., 1994). In support for this, there is no increase in the number of multinucleated myocytes after puberty in both animals and man (Alder and Friedburg, 1986; Anversa and Olivetti, 2002). Therefore, if the DNA-replicating myocytes underwent karyokinesis without cytokinesis, there would be an increase in the number of multi-nucleated myocytes with age, which is not the case. However, despite these findings it cannot be excluded that this phenomenon may be a significant incident in the present study.

Furthermore, it could be argued that the finding of BrdU positive myocytes represent DNA repair and not actual new myocyte formation. However, the concept of BrdU labelled myocytes representing significant DNA repair occurring in these myocytes is refuted due to the detection of ki67 in the nuclei of myocytes, following isoprenaline injury. Ki67, a nuclear protein expressed in all stages of the cell cycle (except G_o) and not involved in DNA repair, has also been detected in myocytes by others investigating the adaptation of the heart in various pathological states (Beltrami et al., 2001; Anversa et al., 2002; Quaini et al., 2002; Urbanek et al., 2003).

Interestingly, the present study identified that all BrdU and ki67 positive myocytes were small. This altered the distribution of myocyte size in the LV, so that a higher number of smaller myocytes were present 14 days after injection, when compared to control hearts. Previously it has been shown that young adult rats which have been subjected to a myocardial infarction possess small replicating myocytes, similar in appearance to those identified in the present study, 7 days after infarction (Nadal-

Ginard et al., 2003). In the present study, these small BrdU labelled myocytes increased in size over time following isoprenaline injection (Figures 3.30; 3.31), but they never reached the size of a BrdU negative myocyte in 14 days. These findings are highly significant. First, importantly they show the generation of new myocytes, and secondly they demonstrate the progressive maturation of these myocytes into the adult phenotype, with time.

It should be noted that the presence of a patent coronary circulation could have dramatically and positively contributed to the generation and progressive maturation of these newly formed myocytes. In contrast, myocardial damage produced by coronary occlusion with consequent reduced or absent blood flow could explain the little evidence of myocyte regeneration in ischemic cardiac disease. Furthermore, the presence of smaller BrdU positive myocytes, strongly demonstrates that this DNA synthesis is actual evidence of new myocyte generation after bolus administration of isoprenaline. If they were involved in DNA repair or ploidy formation, these cells would be expected to be the same size as the adult BrdU negative myocytes, not small and increasing in size over time. In parallel, the present study found a significant increase in myocyte number after 14 days, compared to the loss seen at 3 days (Figure 3.22). These findings support the notion that the heart is able to repair itself, replacing a proportion of lost myocytes following isoprenaline-induced cell death and loss, and resulting in a compensatory increase in myocyte number. This correlates with the restored ventricular function 14 days after isoprenaline administration, as demonstrated by the normalisation of LVEDP (Figure 3.21).

Isoprenaline-induced injury altered the distribution of myocyte size in the LV, shifting the curve to the left (Figure 3.25). These findings add further support for the generation of new myocytes which are smaller than existing myocytes, but also imply that larger and perhaps older myocytes are more susceptible to the toxic effects of isoprenaline. Their loss would also leave less large cells in the myocardium after isoprenaline injection. Cell death has been shown to correlate with the size of the cell and the level of cellular senescence (Brenner et al., 1998). It

has been shown that large myocytes are older, do not react to growth stimuli and are prone to activate the cell death pathway. In contrast, smaller cells are younger, possess the ability to undergo hypertrophy, cell division and are less susceptible to cell death.

In the present study the small, newly formed myocytes were most abundant in the severely damaged sub-endocardial layer of the LV wall. Due to the transmural distribution of myocardial blood flow across the ventricular wall, the subendocardium is more vulnerable to reduced coronary perfusion than the rest of the myocardium. Isoprenaline injection causes an elevated LVEDP (Figure 3.21) and reduced endocardial-to-epicardial flow ratio. These haemodynamic changes superimposed on the primary myotoxic effect of isoprenaline creates greater cell death and loss in the sub-endocardium, compared to the other layers. These findings suggest that cell death could provide the signalling mechanism for initiating new myocyte formation. This is supported by a simultaneous decrease in myocyte apoptosis and an increase in the number and growth of BrdU labelled myocyte nuclei with time. Indeed, Bischoff (1986) showed that skeletal muscle regeneration is initiated by the release of an endogenous mitogen from traumatised, crushed adult muscle. Furthermore, it is worth noting that tissue-specific micro-environmental cues delivered by stromal components influence the fate of both adult stem cells and their progeny (Spradling et al., 2003).

The question now is where do these newly formed myocytes come from? There are two potential sources; cells which are resident within the heart, i.e. cardiac stem cells (Beltrami et al., 2003; Oh et al., 2003; Matsuura et al., 2003), or systemic cells, i.e. BMDCs which continuously colonise the myocardium and contribute to myocyte renewal (Nadal-Ginard et al., 2003). It has previously been shown that BMDCs can give rise to new myocytes either when injected into or stimulated to 'home to' the heart by cytokine administration, following a myocardial infarction (Orlic et al., 2001a; 2001b). Supporting these findings, Eisenberg et al. (2003) reported the differentiation of hematopoietic progenitor cells into cardiomyocytes *in vitro*. Interestingly, blood cells that are normally recruited to damaged tissue, i.e.

macrophages, also demonstrated an ability to integrate into contractile heart tissue and underwent cardiac differentiation (Eisenberg et al., 2003). This concept in skeletal muscle regeneration is supported by the work of Camargo et al. (2003). In the present study, the regeneration of new cardiomyocytes by myeloid cells (Eisenberg et al., 2003; Camargo et al., 2003) cannot be neglected. Considering the number of interstitium cells in the myocardium increased with time (Table 3.2), and immunostaining showed many cells positive for CD68 in isoprenaline-treated hearts (data not shown) this prospect seems conceivable and warrants further investigation.

The present study identified clusters of c-kit positive (c-kit^{POS}) cells in the myocardium of both control and isoprenaline-treated rats. These primitive cells have been identified by others in the hearts of humans (Quaini et al., 2002; Urbanek et al., 2003), rats (Beltrami et al., 2003) and mice (Oh et al., 2003; Matsuura et al., 2003; Torella et al., 2004) and have been termed cardiac stem cells (CSCs). These cells were found to be lineage negative (Beltrami et al., 2003) and represented approximately 0.6 per mm^2 myocardium (Torella et al., 2004), agreeing with the present findings of 0.7 per mm^2 myocardium in control rat hearts (Figure 3.33). As a result of the isoprenaline-injury, these cells became activated and proliferated, as evidenced through the expression of ki67 in the nuclei of c-kit^{POS} cells (Figure 3.34). So after 3 and 6 days they were significantly elevated above control values. Since the appearance of small BrdU labelled myocytes began at 3 days, and reached their peak by 14 days, while the number of c-kit^{POS} cells decreased from 6 days, these findings suggest that these newly formed myocytes were derived from cardiac progenitor cells.

In the present study, many of the cardiac progenitor cells (c-kit^{POS}) expressed the transcription factor, GATA4, indicative of early stage cardiac myogenic differentiation (Figure 3.35), and small amounts of sarcomeric proteins in the cytoplasm (Figure 3.27). This phenotype strongly suggests that these cells represent amplifying myogenic precursors and/or progenitors derived from the activation of a more primitive stem cell. The expression of transcription factors associated with early cardiac development, such as GATA4 and particularly the expression of

cardiac specific sarcomeric proteins, by some cells is evidence of their cardiac myogenic potential and fate. That cells with similar characteristics have been identified in the human (Quaini et al., 2002; Urbanek et al., 2003), rat (Beltrami et al., 2003) and mouse (Torella et al., 2004) lends support for the present findings. Urbanek et al. (2003) identified myocyte precursors in human cardiac hypertrophy, which were very small cells positive for c-kit on the surface membrane, MEF2 in the nuclei and a thin cytoplasmic layer positive for cardiac myosin. These were confirmed by Torella et al. (2004) in the hearts of 4 month old mice. In the present study, the appearance of cells positive for a thin layer of α-sarcomeric actin and ki67 in the nuclei were evident (Figure 3.27, asterisk), suggesting an extremely immature cardiomyocyte phenotype. Unfortunately, these cells were not stained for c-kit, so precise conclusions cannot be made on their exact status and origin.

The present study revealed increased MGF, the splice variant of IGF-1, expression in the myocardium. This was most pronounced 24 hours after the isoprenaline injection and remained elevated thereafter (Figure 3.20). These findings could have implications for the role of MGF in the local control and regulation of both myocyte cellular hypertrophy and hyperplasia, perhaps similar to the previous described effects of IGF-1 in the heart (Donohue et al., 1994; Ito et al., 1993; Reiss et al., 1996). Donohue et al. (1994) suggested that IGF-1 may participate in initiating ventricular hypertrophy. Similarly but in neonatal myocytes in culture, Ito et al. (1993) found IGF-1 increased the mRNA levels of myosin light chain-2 and troponin I as early as 60 minutes, with maximum levels after 6 hours. These were then maintained for as long as 24 hours. Furthermore, the cell size as evaluated morphometrically was almost doubled after 48-hour treatment with IGF-1 (Ito et al., 1993). In contrast to these data, Reiss et al. (1996) reported that transgenic mice in which the cDNA for the human insulin-like growth factor 1B (IGF-1B) was placed under the control of a rat α-MHC promoter, significantly increased myocyte number and BrdU labelled myocytes after a period of 45 days. However, myocyte cell volume was comparable in both transgenic and control mice at all ages. These findings were confirmed by Torella et al. (2004) who showed increased BrdU incorporation in cardiomyocytes of IGF-1 transgenic mice with increasing age.

Therefore, IGF-1 over-expression increased the extent of myocyte formation in the heart, and this adaptation was consistent with the mitogenic effect of this growth factor in several cell types, e.g. skeletal muscle.

As MGF has been shown to stimulate satellite cell activation and proliferation (Yang and Goldspink, 2002; Hill et al., 2003), as well as muscle hypertrophy (Goldspink, 2001), it is plausible that given the time course of MGF expression in the heart, MGF had a significant mechanistic effect initiating cardiomyocyte hypertrophy and formation. Interestingly, Goldspink and Goldspink (2003) reported the protective effects of MGF against apoptosis, through Akt phosphorylation in cardiac myocytes. In addition, MGF may play a role similar to its effects in skeletal muscle (Hill et al., 2003) in the activation of the CSC pool. Indeed, HGF (c-met) and IGF-1 receptors have been described on the surface of CSCs (Chimenti et al., 2002). Moreover, local injections of HGF and IGF-1 aid the repair of infarcted hearts in mice, with the numbers of viable cardiac stem cells increasing in the border zone, the infarcted region and the remote surviving portion of the wall. This results in myocyte regeneration two weeks later, with the new myocardium containing parenchymal cells and coronary vessels consisting of resistance arterioles and capillaries (Chimenti et al., 2002). Notably, MGF and other growth factors, elevated after isoprenaline-induced injury could be significant underlying factors involved both in CSC proliferation and CSC-mediated myocyte renewal, thereby promoting the reparative process in the heart. However, these suggestions are purely speculative and further investigations are necessary.

4.2.3 Myocyte hypertrophy

Findings in this investigation indicate that myocyte hypertrophy occurred in the LV after isoprenaline-induced diffuse myocardial damage. A 58% increase in myocyte cell volume in the sub-endocardial layer was observed 3 days after isoprenaline injection. Although this decreased after 6 and 14 days (30%), it still remained greater than myocyte cell volume in control hearts. When the distribution of myocyte size was studied 14 days after isoprenaline injection, the distribution pattern changed to indicate an increase in number of both smaller and larger

myocytes (Figure 3.25). These findings are supported by Rumyanstev (1991) who reported cardiomyocyte hypertrophy following two 85mg injections of isoprenaline kg^{-1}. Chronic β-AR stimulation results in myocardial hypertrophy (Benjamin et al., 1989; Engelhardt et al., 1999; 2002) and the present study shows that with chronic exposure of catecholamines there is an increase in heart weight. Therefore, the hypertrophic myocyte response seen in the present study with bolus isoprenaline administration could be mediated through the β-receptor pathway. Karoor et al. (2004) found that β-blockade administration to $G_{s\alpha}$ over-expressed mice significantly reduced the phospho-kinase levels of p38 MAP kinase, $p70^{S6K}$, ERK, Akt and JNK, which were related to the growth and death of cardiomyocytes in these mice. Furthermore, Asai et al. (1999) showed that β-AR blockade with propranolol in $G_{s\alpha}$ over-expressed mice arrested myocyte hypertrophy, fibrosis and apoptosis and decreased mortality rates.

However, the cellular hypertrophy reported here is most likely to be reactive, being a compensatory response for the extensive loss of myocytes. The exact mechanism of this isoprenaline-induced myocyte hypertrophy in the present study needs further investigation. Particularly as the elevated levels of MGF could exert a hypertrophic effect on cardiomyocytes similar to that shown in skeletal muscle (Goldspink, 2001). Interestingly, it has recently been proposed that clenbuterol, a selective β_2-AR agonist, causes increased levels of IGF-1 in cardiomyocytes (Yacoub, 2004; personal communications) as well as in skeletal muscle (Awede et al., 2002), implicating a process of β-AR stimulation and the local production of these growth factors.

Similar to that observed after discrete myocardial infarction, Teerlink et al. (1994) showed myocardial hypertrophy and ventricular dilation that was out of proportion to LV mass, when rats were treated with two massive doses of isoprenaline. In the present study LV weight was also significantly increased 1 and 3 days after the bolus administration of isoprenaline. It then returned to normal levels after 14 days (Figure 3.22). These findings could be explained by oedema being present 1 and 3 days after injection. A disproportion existed between the increases in LV weight

(7%) and the expansions in myocyte cell volume after the acute exposure to isoprenaline. This apparent inconsistency reflects the impact of myocyte loss, myocyte hyperplasia and myocyte cellular hypertrophy on the overall response of the myocardium to this diffuse injury.

In functional terms the present study showed an increased LVEDP and decreased $^{+}$dP/dt and $^{-}$dP/dt 1 day after the isoprenaline injection. These haemodynamic responses are indicative of acute overt heart failure. However, interestingly these parameters started to improve after 3 days and had almost returned to normal values by 14 days (Figure 3.21). This subsequent recovery of cardiac function was due to the regenerative capacity of the ventricle, which through myocyte hypertrophy (Teerlink et al., 1994) and formation (Urbanek et al., 2003), reconstitutes the myocardial mass and restores normal cardiac haemodynamics. However, it could be possible that this improved function may not be preserved beyond 14 days. The analysis of a later time point, e.g. 28 days, would enable greater insight into whether these improvements in cardiac performance persist, or not, due to further myocyte hyperplasia and hypertrophy.

These findings are the first of their kind to report reactive DNA synthesis and new myocyte formation following isoprenaline-induced myocardial damage. Most importantly, this is the first evidence of successful myocardial repair without the need for any treatment. Thus reinforcing the concept of the heart as a self-renewing organ. Indeed, previous reports which have examined human hearts (Kajstura et al., 1998; Beltrami et al., 2001; Urbanek et al., 2003) and animal models (Beltrami et al., 2003) injured by myocardial infarction or aortic constriction and in heart failure have shown myocyte regeneration in the myocardium, but without maintenance of cardiac function. The difference could relate to the presence of a patent normal coronary circulation in the present model, which envisions the absolute need of a normal blood flow for an effective myocardial repair through CSC activation. Therefore, this model could offer further valuable insight into the process and control of myocyte cellular renewal.

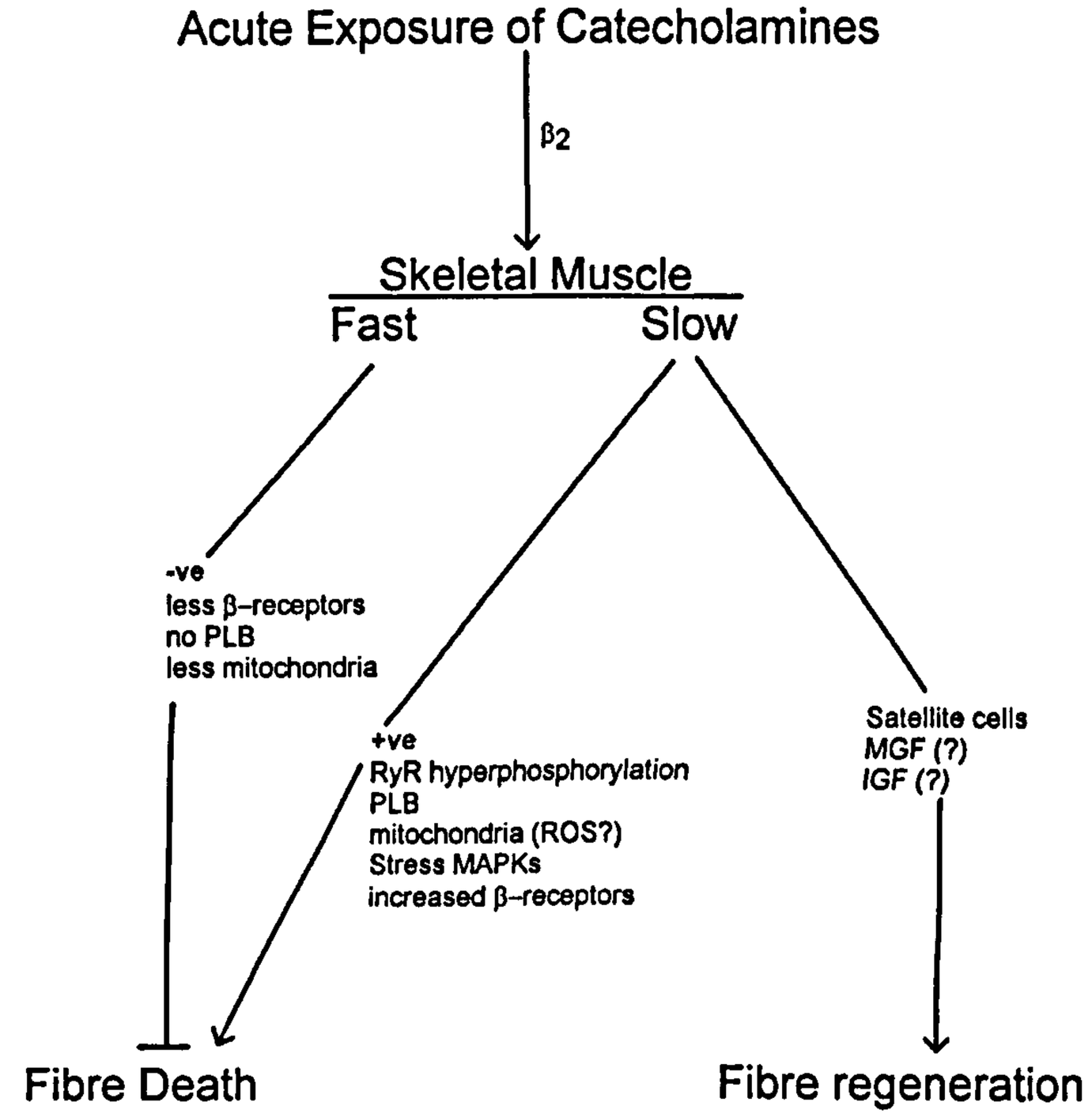

Figure 4.1 Schematic representation of the effects of acute catecholamine exposure on skeletal muscle.

In the skeletal muscle the effects of catecholamine exposure are mediated through the β_2 receptors. A single 20 mmol injection of either isoprenaline or adrenaline kg^{-1} induced fibre death, via necrosis and apoptosis, in the soleus muscles of the rat. It is speculated that the underlying mechanism of fibre death could relate to hyperphosphorylation of the RyR. In marked contrast, the faster glycolytic muscles (tibialis anterior, plantaris and diaphragm) were not damaged by catecholamines. This phenomenon could relate to the absence of PLB, involved in SR Ca^{2+} re-uptake, less β-receptors and/or less mitochondria in fast twitch fibres. The soleus muscle replaced its lost fibres with new fibres through activation and subsequent proliferation of its satellite stem cell pool. These processes are most probably governed by paracrine/autocrine regulatory mechanisms of growth factors, IGF and its splice variant MGF.

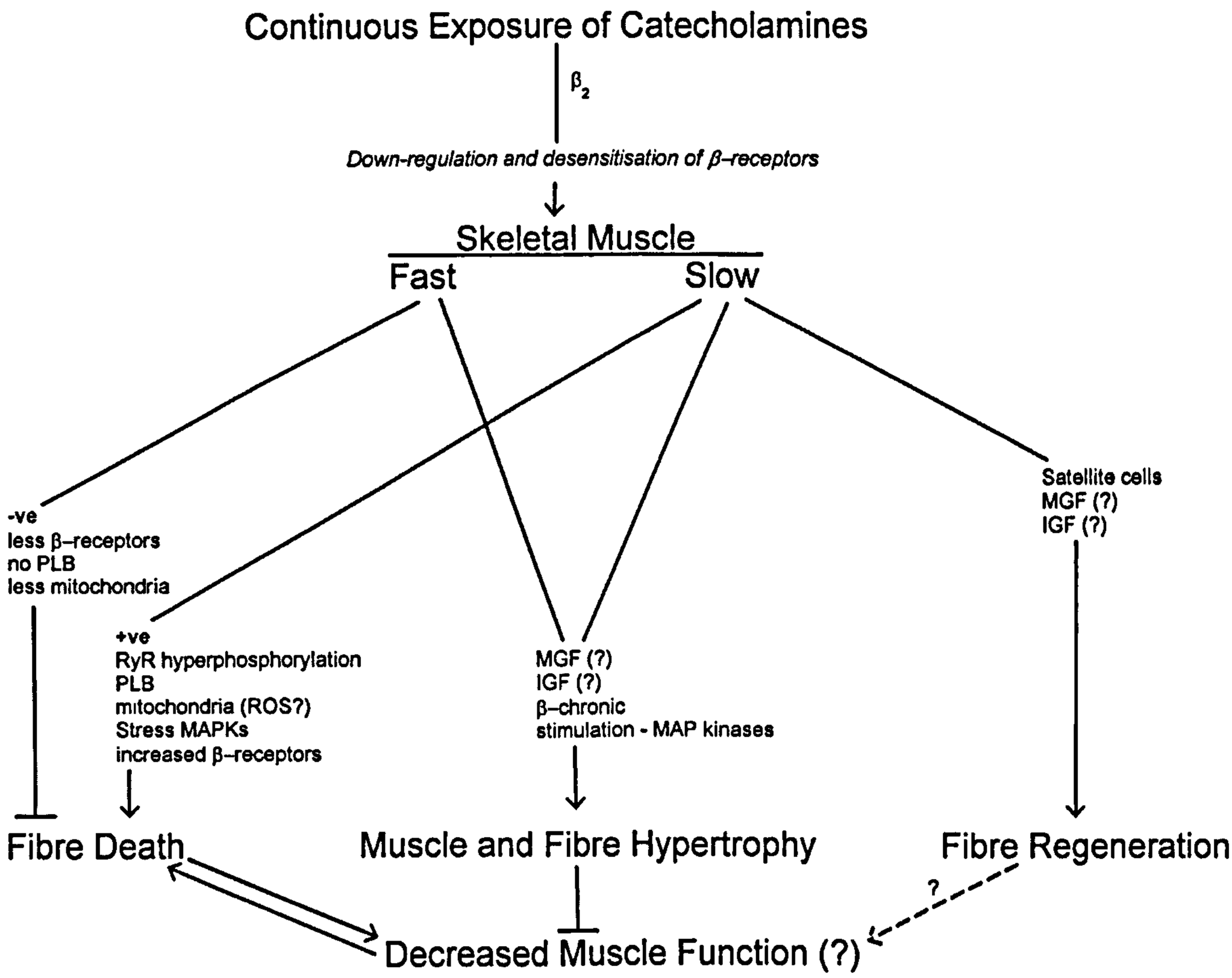

Figure 4.2 Schematic representation of the effects of continuous exposure of catecholamines on skeletal muscle.

Continuous exposure of catecholamines caused a down-regulation and/or desensitisation of the β-receptors. Continuous exposure resulted in fibre death in the soleus muscles, but not the faster muscles. There was significant hypertrophy to both slow and fast skeletal muscles, and this effect was probably mediated through the MAP kinase pathways activated through chronic β-AR stimulation and/or the growth factors IGF and MGF. Continuous exposure of catecholamines caused a continual process of fibre death and regeneration in the soleus muscle. In the longer term, this could result in muscle wasting due to the limited capacity of the skeletal muscle stem cell pool, and therefore a compromised muscle function (blue dotted line).

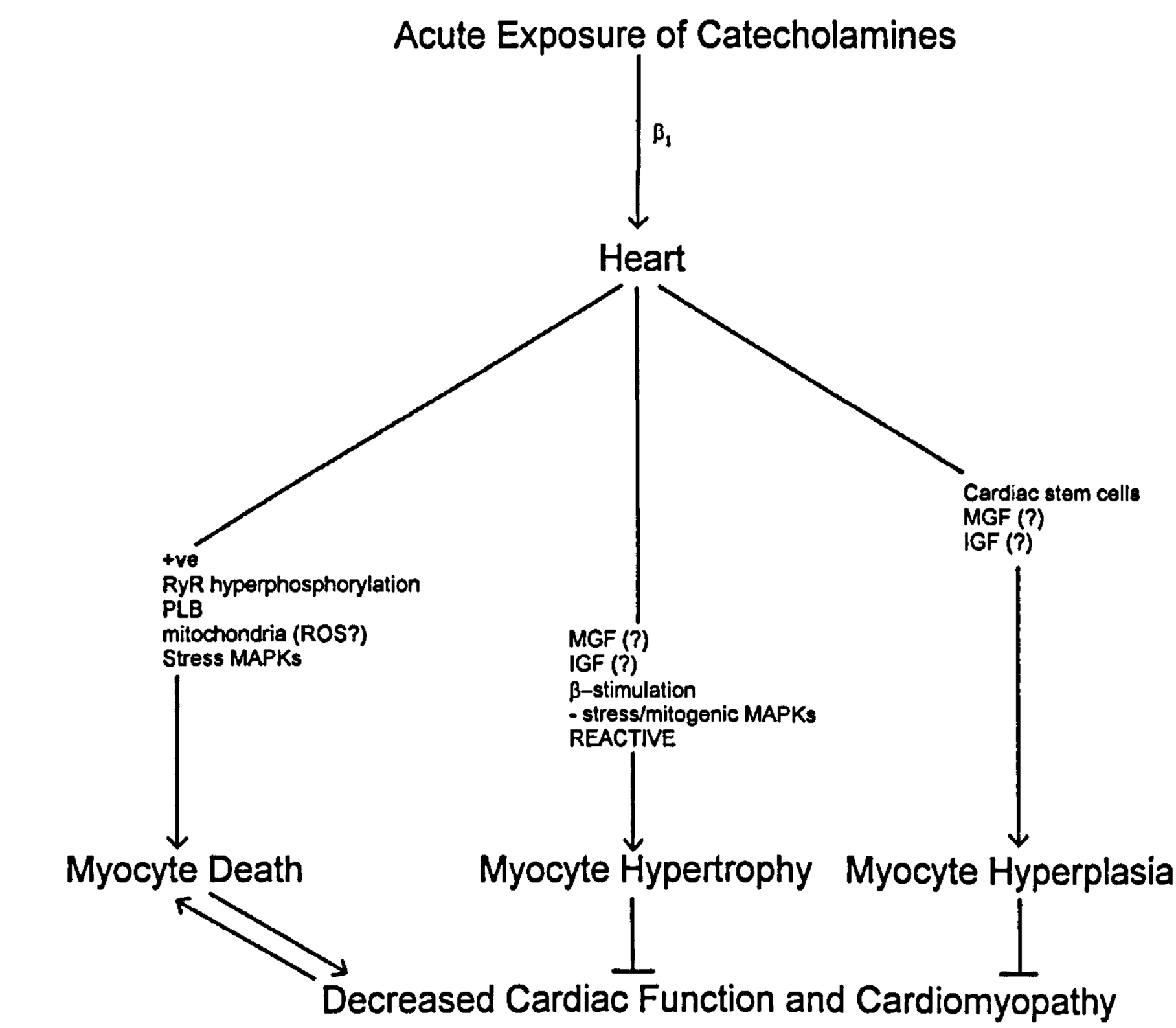

Figure 4.3 Schematic representation of the effects of acute catecholamine exposure on the heart.

In the heart the effects of catecholamine exposure are mediated through the β_1 receptors and possibly by the 'non-classical' pathway involving the β_2 receptors. A single 20 mmol injection of isoprenaline kg^{-1} induced extensive cardiomyocyte death, via necrosis and apoptosis. It is speculated that the underlying mechanism of myocyte death could relate to hyperphosphorylation of the RyR, leading to Ca^{2+} myocyte cytoplasmic overload and cardiac dysfunction. The heart compensated and adapted to the dramatic loss of cardiomyocytes through both myocyte hypertrophy and hyperplasia, in order to restore cardiac performance. New myocyte formation was produced through the activation and ensuring proliferation and differentiation of the cardiac stem cell pool. These processes were most probably governed by the growth factors IGF and MGF.

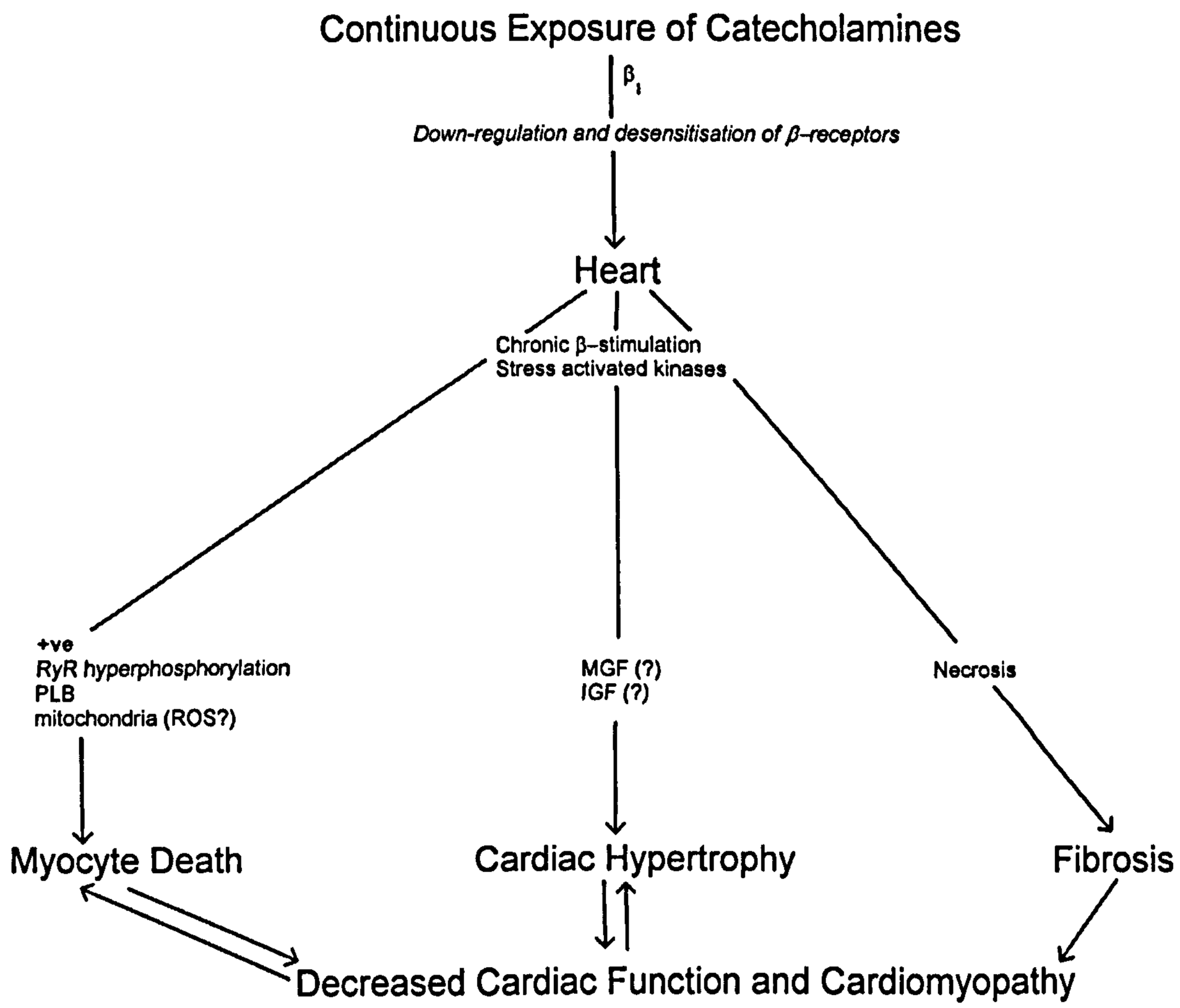

Figure 4.4 Schematic representation of the effects of continuous catecholamine exposure on the heart.

In the heart continuous catecholamine exposure caused a desensitisation and/or down-regulation of β-receptors. Chronic exposure of catecholamines caused cardiomyocyte death, reparative fibrosis and hypertrophy, resulting in decreased cardiac function and the development of cardiomyopathy. These effects were most probably governed by the hyperphosphorylation of the RyR, stress-activated MAP kinase pathway and possibly the growth factors IGF and MGF.

In summary, the present study shows for the first time the toxic effects of catecholamines to the soleus muscle, causing significant fibre apoptosis as well as necrosis. Regardless of the nature of the death and loss of fibres, this skeletal muscle has the ability to regenerate, with full restoration of fibre number and fibre type proportions by 28 days, following acute catecholamine exposure. Chronic catecholamine exposure leads to repeated cycles of degeneration-regeneration within the soleus muscle of the rat. Over a prolonged period of time, this could lead to consequent net loss of muscle fibres and hence muscle wasting, due to the limited proliferative potential of the muscle stem cell pool. On the other hand, catecholamines could potentially be beneficial in promoting skeletal muscle hypertrophy and growth. However, it may not be the effects of the catecholamines *per se* on the adaptive response of the muscle. These mechanisms need to be investigated further before any clinical applications are proposed. Furthermore, the undesirable effects of chronic β-AR stimulation on the heart render the use of such hormones impractical in attempting to ameliorate muscle wasting. The use of IGF-1 or MGF may offer attractive alternatives considering their roles in regulating the satellite cell pool and stimulating protein synthesis, and consequent muscle hypertrophy and growth. Therapeutic strategies should focus on promoting the expression of these growth factors and rescuing skeletal muscle wasting.

In the heart, a single bolus injection of isoprenaline produces severe myocardial damage, resulting in a loss of myocytes and an acute impairment of cardiac performance. The heart compensates initially by myocyte hypertrophy and secondary by myocyte hyperplasia. This myocyte hyperplasia is produced by the activation and differentiation of the cardiac stem cell pool. In the presence of a patent coronary circulation these processes significantly repair the acute damage, restoring normal ventricular function.

5.0 CONCLUSIONS

The chronic hyper-adrenergic state plays an important role in the pathophysiology of heart failure. Impaired contractile function and skeletal muscle wasting have been observed in CHF patients (Anker et al., 1997a). It is possible that the increased sympathetic drive seen in this population is linked to this functional deterioration of the skeletal muscles as well as the heart. This thesis has tested the hypothesis that cardiac and skeletal muscles respond in a similar manner when exposed to excess catecholamines. Acute exposure of catecholamines caused significant necrotic and apoptotic cell death and resultant myocyte loss to both the heart and soleus muscles. The catecholamine-induced myocyte necrosis and apoptosis in the soleus muscle is a novel finding. The damaging effects of catecholamines on both striated muscles were specific for mature, differentiated myocytes. Upon injury, stem-progenitor cells present within cardiac and skeletal tissues became activated and through the ensuring proliferation and differentiation of these cells, new myocytes were formed and functional capacity was restored.

The present findings raise many questions which remain unanswered. It is postulated that the mechanism underlying cell death from catecholamine exposure in both muscles relates to the ryanodine receptor (RyR), which is of key importance in determining cell fate. Increased protein kinase A (PKA), activated through elevated intracellular cAMP from β-AR stimulation, causes PKA hyperphosphorylation of RyR. This results in defective channel function and excitation coupling, leading to consequent Ca^{2+} myocyte cytoplasmic overload and cardiac dysfunction (Reiken et al., 2003). In principle, fast-twitch muscle fibres could also be exposed to hyperphosphorylation of RyR. Therefore, something other this mechanism could account for the damage by catecholamines. As phospholamban (PLB) plays a regulatory role in inhibiting Ca^{2+} reuptake by the SR through SERCA2, the finding that the faster glycolytic muscles were not damaged by the catecholamines, could be related to the absence of PLB in these muscle fibre types. However, other distinctive characteristics of these faster muscle fibres, e.g. decreased number of β-ARs and fewer mitochondria, when compared to their slower contracting counterparts could also explain this phenomenon. But the reason for this discrepancy still

remains unclear, considering that the faster muscles examined, even contain slow-twitch muscle fibres.

Sustained high levels of catecholamines caused significant hypertrophy to both the heart and skeletal muscles, including the fast-twitch muscles. It may not be the effects of catecholamines *per se* that are responsible for this muscle hypertrophy. As the β_2-agonist, clenbuterol, has a paracrine and autocrine effect on IGF-1 levels (Awede et al., 2002), it is speculated that these anabolic effects maybe due to the increased local and systemic expression of IGF-1 and its splice variant, MGF, after the catecholamine administration. However, further investigations are required to clarify the mechanisms involved. Chronic exposure to catecholamines leads to repeated cycles of degeneration-regeneration within the soleus muscle. In the long term, this could have detrimental consequences through the resultant net loss of muscle fibres and wasting, due to the limited proliferative capacity of the muscle stem cell pool. Further analysis of the potential of muscle stem cells to contribute to this process is warranted, especially in the light of the rapid and dramatic loss of muscle mass in HF patients with cachexia.

Through the continuous infusion of catecholamines the heart was significantly damaged, exhibiting reparative fibrosis and undergoing hypertrophy. This could lead to considerable deleterious consequences, and further outlines the toxic effects of catecholamines. Following acute damage from isoprenaline, the heart compensated and adapted to the dramatic loss of cardiomyocytes through both myocyte hypertrophy and hyperplasia. Notably, the present study is the first to report the ability of the heart to spontaneously initiate repair mechanisms and bring about new myocyte formation and restore cardiac function in the absence of any exogenous treatment. Due to the significant amount of myocyte regeneration found in this damage model, when compared to models of coronary occlusion or constriction, a patent coronary circulation may be crucial in regulating the regenerative process in the heart. Furthermore, by confirming the presence of stem progenitor cells in the adult heart, this finding could help to answer the question to why these cells do not mobilise and divide in response to an ischemic injury and regenerate the damaged myocardium.

6.0 FUTURE DIRECTIONS

- Following acute isoprenaline exposure, does the improved cardiac function remain stable after 14 days, and if so, can this be attributed in part due to further new myocyte formation?
- What is the impervious factor associated with the predominantly fast muscles that protects them from the injurious effects of catecholamines? Could it reside in the elimination of PLB in fast twitch fibres, fewer β-receptors, less mitochondria, less capillarisation, when compared to their slower counterparts?
- Is the mechanism underlying cell death from catecholamine exposure in both the heart and slow soleus muscles due to hyperphosphorylation of the RyR? This could be specifically investigated through immunoprecipitation and back-phosphorylation of RyRs and immunohistochemistry techniques (Marx et al., 2000).
- In order to ascertain whether IGF-1 is implicated in the regenerative and hypertrophic response of the heart and skeletal muscles, mRNA and protein levels should be measured, following catecholamine exposure.
- If catecholamines are administered continuously over a longer period (i.e. 56 days), does the process of continual fibre death and regeneration seen in the soleus muscle result in muscle wasting? Is this due a compromised capacity of the satellite cell pool? Therefore, can catecholamine exposure be seriously linked to the impaired muscle endurance found in some CHF patients?
- Does new cardiomyocyte formation play a significant role in the remodelling of the heart following continuous catecholamine exposure?
- Is a patent coronary circulation crucial in regulating the regenerative process in the heart? This could be examined by comparing the effects of isoprenaline exposure with a model of coronary occlusion of constriction (TAC).

7.0 REFERENCES

Adler, C. P. and Friedburg, H. (1986). Myocardial DNA content, ploidy level and cell number in geriatric hearts: post mortem examination of human myocardium in old age. *Journal of Molecular and Cellular Cardiology*, **18**, 39-53.

Allen, R. E. and Boxhorn, L. K. (1989). Regulation of skeletal muscle satellite cell proliferation and differentiation by transforming growth factor-beta, insulin-like growth factor I, and fibroblast growth factor. *Journal of Cell Physiology*, **138**, 311-315.

Alnaqueeb, M. A. and Goldspink, G. (1986). Changes in fibre type, number and diameter in developing and ageing skeletal muscle. *Journal of Anatomy*, **153**, 31-45.

Altman, D. G. (1991). *Practical statistics for medical research*. London: Chapman and Hall

Anker, S. D., Chua, T. P., Ponikowski, P., Harrington, D., Swan, J. W., Kox, W. J., Poole-Wilson, P. A. and Coats, A. J. S. (1997a). Hormonal changes and catabolic/anabolic imbalance in chronic heart failure and their importance for cardiac cachexia. *Circulation,* **96,** 526-534.

Anker, S. D., Ponikowski, P., Varney, S., Chua, T. P., Clark, A. L., Webb-Peploe, K. M., Harrington, Kox, W. J., Poole-Wilson, P. A. and Coats, A. J. S. (1997b). Wasting as independent risk factor for mortality in chronic heart failure. *The Lancet,* **349,** 1050-1053.

Anversa, P., Loud, A. V., Giacomelli, F. and Wiener, J, (1978). Absolute morphometric study of myocardial hypertrophy in experimental hypertension. II. Ultrastructure of myocytes and interstitium. *Laboratory Investigation*, **38**, 597-609.

Anversa, P., Palackal, T., Sonnenblick, E. H., Olivetti, G. and Capasso, J. M. (1990). Hypertensive cardiomyopathy: Myocyte nuclei hyperplasia in the mammalian rat heart. *Journal of Clinical Investigation*, **85**, 994-997.

Anversa, P. and Kajstura, J. (1998). Ventricular myocytes are not terminally differentiated in the adult mammalian heart. *Circulation Research*, **83**, 1-14.

Anversa, P. (2000). Myocyte death in the pathological heart. *Circulation Research*, **86**, 121–124.

Anversa, P., Leri, A., Kajstura, J. and Nadal-Ginard, B. (2002). Myocyte growth and cardiac repair. *Journal of Molecular and Cellular Cardiology*, **34**, 91-105.

Anversa, P. and Olivetti, G. (2002). Cellular basis of physiological and pathological myocardial growth. In *Handbook of Physiology. Section 2. The Cardiovascular System. Volume I. The Heart* (Eds. E. Page, H. A. Fozzard, R. J. Solaro), pp 75-144. New York: Oxford University Press.

Anversa, P. and Nadal-Ginard, B. (2002). Myocyte renewal and ventricular remodelling. *Nature*, **415**, 240-243.

Asai, K., Yang, G-P., Geng, Y-J., Takagi, G., Bishop, S., Ishikawa, Y., Shannon, R. P., Wagner, T. E., Vatner, D. E., Homcy, C. J. and Vatner, S. F. (1999). β-Adrenergic receptor blockade arrests myocyte damage and preserves cardiac function in the transgenic $G_{s\alpha}$ mouse. *Journal of Clinical Investigation*, **104**, 551-558.

Asakura, A., Seale, P., Girgis-Gabardo, A. and Rudnicki, M. A. (2002). Myogenic specification of side population cells in skeletal muscle. *Journal of Cell Biology*, **159**, 123-134.

Awede, B. L., Thissen, J-P. and Lebacq, J. (2002). Role of IGF-1 and IGFBPs in the changes in mass and phenotype induced in rat soleus muscle by clenbuterol. *American Journal of Physiology*, **282**, E31-E37.

Balsam, L. B., Wagers, A. J., Christensen, J. L., Kofidis, T., Weissman, I. L. and Robbins, R. C. (2004). Haematopoietic stem cells adopt mature haematopoietic fates in ischaemic myocardium. *Nature*, **428**, 668-673.

Barton-Davis, E. R., Shoturma, D. I. and Sweeney, H. L. (1999). Contribution of satellite cells to IGF-1 induced hypertrophy of skeletal muscle. *Acta Physiologica Scandinavica*, **167**, 301-305.

Behfar, A., Zingman, L. V., Hodgson, D. M., Rauzier, J-M., Kane, G. C., Terzic, A. and Puceat, M. (2002). Stem cell differentiation requires a paracrine pathway in the heart. *FASEB Journal*, **16**, 1558-1566.

Beltrami, A. P., Urbanek, K., Kajstura, J., Yan, S. M., Finato, N., Bussani, R., Nadal-Ginard, B., Silvestri, F., Leri, A., Beltrami, C. A., Anversa, P. (2001). Evidence that human cardiac myocytes divide after myocardial infarction. *New England Journal of Medicine*, **344**, 1750-1757.

Beltrami, A. P., Barlucchi, L., Torella, D., Baker, M., Limana, F., Chimenti, S., Kasahara, H., Rota, M., Musso, E., Urbanek, K., Leri, A., Kajstura, J., Nadal-Ginard, B. and Anversa, P. (2003). Adult cardiac stem cells are multipotent and support myocardial regeneration. *Cell*, **114**, 763-76.

Benjamin, I. J., Jalil, J. E., Tan, L. B., Cho, K., Weber, K. T. and Clark, W. A. (1989). Isoproterenol-induced myocardial fibrosis in relation to myocyte necrosis. *Circulation,* **65,** 657-670.

Bischoff, R. (1986). A satellite cell mitogen from crushed adult muscle. *Developmental Biology,* **115,** 140-147.

Bischoff, R. (1997). Chemotaxis of skeletal muscle satellite cells. *Development Dynamics*, **208,** 505-515.

Black, S. C., Huang, J. Q., Rezaiefar, P., Radinovic, S., Eberhart, A., Nicholson, D. W. and Rodger I. W. (1998). Co-localization of the cysteine protease caspase-3 with apoptotic myocytes after in vivo myocardial ischemia and reperfusion in the rat. *Journal of Molecular and Cellular Cardiology*, **30,** 733–742.

Blaivas, M. and Carlson, B. M. (1991). Muscle fiber branching – Difference between grafts in old and young rats. *Mechanisms of Ageing and Development*, **60,** 43-53.

Blankenberg, F., Narula, J. and Strauss H. W. (1999). In vivo detection of apoptotic cell death: a necessary measurement for evaluating therapy for myocarditis, ischemia, and heart failure. *Journal of Nuclear Cardiology*, **6,** 531-9.

Blaveri, K., Heslop, L., Yu, D. S., Rosenblatt, J. D., Gross, J. G., Partridge, T. A. and Morgan, J. E. (1999). Patterns of repair of dystrophic mouse muscle: studies on isolated fibers. *Developmental Dynamics*, **216,** 244-256.

Blough, E. R. and Lindermann, J. K. (2000). Lack of skeletal muscle hypertrophy in very aged male Fischer 344 x Brown Norway rats. *Journal of Applied Physiology*, **88,** 1265-1270.

Boatwright, K. M. and Salvesen, G. S. (2003). Mechanisms of caspase activation. *Current Opinion in Cell Biology*, **15,** 725-731.

Bodine-Fowler, S. (1994). Skeletal muscle regeneration after injury: An Overview. *Journal of Voice,* **8,** 53-62.

Bottaro, D. P., Rubin, J. S., Faletto, D. L., Chan, A. M-L., Kmiecik, T. E., Vande Woude, G. F. and Aaronson, S. A. (1991). Identification of the hepatocyte growth factor receptor as the c-met proto-oncogene product. *Science*, **251,** 802-804.

Bourke, D. L. and Ontell, M. (1984). Branched myofibers in long-term whole muscle transplants: A quantitative study. *The Anatomical Record*, **209,** 281-288.

Brazelton, T. R., Nystrom, M. and Blau, H. M. (2003). Significant differences among skeletal muscles in the incorporation of bone marrow-derived cells. *Developmental Biology*, **262**, 64-74.

Brenner, A., Stampfer, M. R., Aldac, M. C. (1998). Increased p16 expression with first senescence arrest in human mammary epithelial cells and extended growth capacity with p16 inactivation. *Oncogene*, **17**, 199-205.

Bristow, M. R. (2000). β-adrenergic receptor blockade in Chronic Heart Failure. *Circulation*, **101**, 558-569.

Bristow, M. R., Port, J. D. and Kelly, R. A. (2001). Treatment of heart failure: Pharmacological methods. In *Heart Disease: A Textbook of Cardiovascular Medicine, Volume 1* (Eds. E. Braunwald, D. P. Zipes, P. Libby), pp 562-599. London: W. Saunders Company.

Brooke, M. H. and Kaiser, K. K. (1974). The use and abuse of muscle histochemistry. *Annals of the New York Academy of Sciences*, **228**, 121-144.

Burniston, J. G., Ng, Y., Clark, W. A., Colyer, J., Tan L-B. and Goldspink, D. F. (2002). Myotoxic effects of clenbuterol in the rat heart and soleus muscle. *Journal of Applied Physiology*, **93**, 1824-1832.

Caccia, M. R., Harris, J. B. and Johnson, M. A. (1979). Morphology and physiology of skeletal muscle in aging rodents. *Muscle Nerve*, **2**, 202-212.

Camargo, F. D., Green, R., Capetenaki, Y., Jackson, K. A. and Goodell, M. A. (2003). Single hematopoietic stem cells generate skeletal muscle through myeloid intermediates. Nature Medicine, 9, 1520-1527.

Carlson, B. M. and Faulkner, J. A. (1983). The regeneration of skeletal muscle fibers following injury: A review. *Medicine and Science in Sports and Exercise*, **15**, 187-198.

Chakravarthy, M. V., Davis, B. S. and Booth, F. W. (2000). IGF-I restores satellite cell proliferative potential in immobilized old skeletal muscle. *Journal of Applied Physiology*, **89**, 1365-1379.

Charge, S. B. P. and Rudnicki, M. A. (2004). Cellular and molecular regulation of muscle regeneration. *Physiological Reviews*, **84**, 209-238.

Chaudhri, B., Del Monte, F., Hajjar, R. J. and Harding, S. E. (2002). Interaction between increased SERCA2a activity and β-adrenoceptor stimulation in adult rabbit myocytes. *American Journal of Physiology*, **283**, H2450-H2457.

Chimenti, S., Barlucchi, L., Limana, F., Jakoniuk, I., Cesselli, D., Beltrami, A. P., Mancarella, S., Castaldo, C., Nadal-Ginard, B., Leri, A., Kajstura, J. and Anversa, P. (2002). Local mobilization of resident cardiac primitive cells by growth factors repairs the infarcted heart. *Circulation*, **106 (Suppl. II)**, II14.

Choo, J. J., Horan, M. A., Little, R. A. and Rothwell, N. J. (1992). Anabolic effects of clenbuterol in skeletal muscle are mediated by β_2-adrenoreceptor activation. *American Journal of Physiology*, **263**, E50-E56.

Chou, J. J., Matsuo, H., Duan, H. and Wagner, G. (1998). Solution structure of the RAIDD CARD and model for CARD/CARD interaction in caspase-2 and caspase-9 recruitment. *Cell*, **94**, 171–180.

Clarke, A. R., Purdie, C. A., Harrison, D. J., Morris, R. G., Bird, C. C., Hooper, M. L. and Wyllie A. H. (1993). Thymocyte apoptosis induced by p53-dependent and independent pathways. *Nature*, **362**, 849–852.

Communal, C., Singh, K., Pimental, D. R. and Colucci, W. S. (1998). Norepinephrine stimulates apoptosis in adult rat ventricular myocytes by activation of the β-adrenergic pathway. *Circulation*, **98**, 1329-1334.

Conolly, M. E., Davies, D. S., Dollery, C. T., Morgan, C. D., Paterson, J. W. and Sandler, M. (1972). Metabolism of isoprenaline in dog and man. *British Journal of Pharmacology*, **46**, 458-472.

Cornelison, D. D. W. and Wold, B. J. (1997). Single-cell analysis of regulatory gene expression in quiescent and activated mouse skeletal muscle satellite cells. *Developmental Biology*, **1997**, 270-283.

Counter, C. M., Avilion, A. A., LeFeuvre, C. E., Stewart, N. G., Greider, C. W., Harley, C. B. and Bacchetti, S. (1992). Telomere shortening associated with chromosome instability is arrested in immortal cells which express telomerase activity. *EMBO Journal*, **11**, 1921-1929.

Cui, Y., Shen, Y-T., Kalthof, B., Iwase, M., Sato, N., Uechi, M., Vatner, S. F. and Vatner, D. E. (1996). Identification and functional role of β-adrenergic receptor subtypes in primate and rodent: In vivo versus isolated myocytes. *Journal of Molecular and Cellular Cardiology*, **28**, 1307-1317.

Cusella-De Angelis, M. G., Lyons, G., Sonnino, C., De Angelis, L., Vivarelli, E., Farmer, K., Wright, W. E., Molinaro, M., Bouche, M., Buckingham, M. and Cossu, G. (1992). MyoD, myogenin independent differentiation of primordial myoblasts in mouse somites. *The Journal of Cell Biology*, **116**, 1243-1255.

Darzynkiewicz, Z., Juan, G., Li, X., Gorczyca, W., Murakami, T. and Traganos, F. (1997). Cytometry in cell necrobiology: Analysis of apoptosis and accidental cell death (necrosis). *Cytometry,* **27,** 1-20.

Dash, R., Kadambi, V. J., Schmidt, A. G., Tepe, N. M., Biniakiewicz, D., Gerst, M. J., Canning, A. M., Abraham, W. T., Hoit, B. D., Liggett, S. B., Lorenz, J. N., Dorn, G. W. II. and Kranias, E. G. (2001). Interactions between phospholamban and β-adrenergic drive may lead to cardiomyopathy and early mortality. *Circulation*, **103,** 889-896.

Davis, C. E., Harris, J. B. and Nicholson, L. V. B. (1991). Myosin isoform transitions and physiological properties of regenerated and re-innervated soleus muscles of the rat. *Neuromuscular Disorders*, **1,** 411-421.

DeAngelis, L., Berghella, L., Coletta, M., Lattanzi, L., Zanchi, M., Cusella-DeAngelis, M. G., Ponzetto, C. and Cossu, G. (1999). Skeletal myogenic progenitors originating from the embryonic dorsal aorta coexpress endothelial and myogenic markers and contribute to postnatal muscle growth and regeneration. *Journal of Cell Biology*, **147,** 869-877.

Decary, S., Mouly, V., Hamida, C. B., Sautet, A., Barbet, J. P. and Butler-Browne, G. S. (1997). Replicative potential and telomere length in human skeletal muscle: Implications for satellite cell-mediated therapy. *Human Gene Therapy*, **8,** 1429-1438.

Decary, S., Hamida, C. B., Mouly, V., Barbet, J. P., Hentati, F. and Butler-Browne, G. S. (2000). Shorter telomeres in dystrophic muscle consistent with extensive regeneration in young children. *Neuromuscular Disorders*, **10,** 113-120.

Deb, A., Wang, S., Skelding, K. A., Miller, D., Simper, D. and Caplice, N. M. (2003). Bone marrow-derived cardiomyocytes are present in the adult human heart: a study of gender mismatched bone marrow transplantation patients. *Circulation*, **107,** 1247-1249.

Del Monte, F., Harding, S. E., Dec, G. W., Gwathmey, J. K. and Hajjar, R. J. (2002). Targeting phospholamban by gene transfer in human heart failure. *Circulation*, **105,** 904-907.

Deveraux, Q. L., Takahashi, R., Salvesen, G. S. and Reed, J. C. (1997). X-linked IAP is a direct inhibitor of cell-death proteases. *Nature*, **388,** 300–304.

Didenko, V.V. and Hornsby, P.J. (1996). Presence of double-strand breaks with single-base 3′ overhangs in cells undergoing apoptosis but not necrosis. *Journal of Cell Biology*, **135,** 1369–1376

Didenko, V. (2003). In situ detection of DNA damage – methods and protocols. New York: Humana Press.

Donohue, T. J., Dworkin, L. D., Lango, M. N., Fliegner, K., Lango, R. P., Benstein, J. A., Slater, W. R. and Catanese, V. M. (1994). Induction of myocardial insulin-like growth factor-I gene expression in left ventricular hypertrophy. *Circulation*, **89**, 799-809.

Dorn, G. W. II., Tepe, N. M., Lorenz, J. N., Koch, W. J., Liggett, S. B. (1999). Low- and high-level transgenic expression of β_2-adrenergic receptors differentially affect cardiac hypertrophy and function in $G_{s\alpha}$ overexpressing mice. *Proceedings of the National Academy of Sciences*, **96**, 6400-6405.

Drexler, H., Reide, U., Munzel, T., Konig, H., Funke, E. and Just, H. (1992). Alterations of skeletal muscle in Chronic Heart Failure. *Circulation*, **85**, 1751-1759.

Dupont-Versteegden, E. E., Houle, J. D., Gurley, C. M. and Peterson, C. A. (1998). Early changes in muscle cell fiber size and gene expression in response to spinal cord transection and exercise. *Journal of Cell Biology*, **274**, C1124-1140.

Ecob-Prince, M., Hill, M. and Brown, W. (1989). Immunocytochemical demonstration of myosin heavy chain expression in human muscle. *Journal of Neurological Sciences*, **91**, 71-78.

Eisenberg, L. M., Burns, L. and Eisenberg, C. A. (2003). Hematopoietic cells from bone marrow have the potential to differentiate into cardiomyocytes *in vitro*. *Anatomical Record*, **274A**, 870-82.

Ellison, G., Cox, H., Goldspink, D. F., Burniston, J., Clark, W. and Tan, L. B. (2002). The synthetic catecholamine, isoprenaline, induces apoptosis and necrosis in the soleus muscle of the rat. *Journal of Physiology*, **543.P**, 100P.

Ellison, G. Tan, L-B and Goldspink, D.F. (2003). Injury and repair of skeletal muscle exposed to excess catecholamines. *Journal of Muscle Research and Cell Motility*, **24**, 367.

Engelhardt, S., Bohm, M., Erdmann, E. and Lohse M. J. (1996). Analysis of beta-adrenergic receptor mRNA levels in human ventricular biopsy specimens by quantitative polymerase chain reactions: progressive reduction of beta 1-adrenergic receptor mRNA in heart failure. *Journal of the American College of Cardiology*, **27**, 146-54.

Engelhardt, S., Hein, L., Wiesmann, F. and Lohse, M. J. (1999). Progressive hypertrophy and heart failure in β_1-adrenergic receptor transgenic mice. *Proceedings of the National Academy of Sciences. USA*, **96**, 7059-7064.

Engelhardt, S., Boknik, P., Keller, U., Neumann, J., Lohse, M. J. and Hein, L. (2001). Early impairment of calcium handling and altered expression of junctin in hearts of mice overexpressing the β_1-adrenergic receptor. *FASEB*, **15**, 2718-2720.

Engelhardt, S., Hein, L., Keller, U., Klambt, K. and Lohse, M. J. (2002). Inhibition of Na^+-H^+ exchange prevents hypertrophy, fibrosis and heart failure in β_1-adrenergic receptor transgenic mice. *Circulation Research*, **90**, 814-819.

Engelhardt, S., Hein, L., Dyachenkow, V., Kranias, E. G., Isenberg, G. and Lohse, M. J. (2004). Altered calcium handling is critically involved in the cardiotoxic effects of chronic β-adrenergic stimulation. *Circulation*, **109**, 1-7.

Ferrari, G., Cusella-De Angelis, G., Coletta, M., Paolucci, E., Stornaiuolo, A., Cossu, G. and Mavilio, F. (1998). Muscle regeneration by bone marrow-derived myogenic progenitors. *Science*, **279**, 1528-1530.

Francis, G. S., Benedict, C., Johnstone, D. E., Kirlin, P. C., Nicklas, J., Liang, C., Kubo, S. H., Rudin-Toretsky, E. and Yusuf, S. (1990). Comparison of neuroendocrine activation in patients with left ventricular dysfunction with and without congestive heart failure. *Circulation,* **82,** 1724-1729.

Freedman, N. J. and Lefkowitz, R. J. (2004). Anti-beta(1)-adrenergic receptor antibodies and heart failure: causation, not just correlation. *Journal of Clinical Investigation*, **113**, 1379-82.

Garry, D. J., Yang, Q., Bassel-Duby, R. and Sanders Williams, R. (1997). Persistent expression of MNF identifies myogenic stem cells in postnatal muscles. *Developmental Biology,* **188,** 280-294.

Gaussin, V., Tomlinson, J. E., Depre, C., Engelhardt, S., Antos, C. L., Takagi, G., Hein, L., Topper, J. N., Liggett, S. B., Olsen, E. N., Lohse, M. J., Vatner, S. F. and Vatner, D. E. (2003). Common genomic response in different mouse models of β-adrenergic-induced cardiomyopathy. *Circulation*, **108**, 2926-2933.

Gavrieli, Y., Sherman, Y. and Ben-Sasson, S. A. (1992). Identification of programmed cell death in situ via specific labeling of nuclear DNA fragmentation. *Journal of Cell Biology*, **119**, 493-501.

Geng, Y-J., Ishikawa, Y., Vatner, D. E., Wagner, T. E., Bishop, S. P., Vatner, S. F. and Homcy, C. J. (1999). Apoptosis of cardiac myocytes in $G_{s\alpha}$ transgenic mice. *Circulation Research*, **84**, 34-42.

George, C. H., Higgs, G. V., Mackrill, J. J. and Lai, F. A. (2003). Dysregulated Ryanodine Receptors Mediate Cellular Toxicity. *Journal of Biological Chemistry*, **278**, 28856-28864.

Goldspink, D. F. and Cox, V. M. (1997). Skeletal Muscle. In *Anaesthetic Physiology and Pharmacology* (Eds. W. McCaughey, R. S. J. Clarke, J. P. H. Fee, W. F. M. Wallace), pp 263-280. Edinburgh: Churchill Livingstone.

Goldspink, D. F., Burniston, J. G. and Tan, L-B. (2003) Cardiomyocyte death and the ageing and failing heart. *Experimental Physiology*, **88**, 447-58.

Goldspink, D. F., Burniston, J. B., Ellison, G. M., Clark, W. A., Tan, L-B. (2004). Catecholamine-induced apoptosis and necrosis in cardiac and skeletal myocytes of the rat in vivo: the same or separate pathways? *Experimental Physiology*, **89**, 407-416.

Goldspink, G., Scutt, A., Loughna, P., Wells, D., Jaenicke, T. Gerlach, G-F. (1992). Gene expression in skeletal muscle in response to mechanical signals. *American Journal of Physiology*, **262**, R326-363.

Goldspink, G. (2001). Method of treating muscular disorders. United States Patent No. US 6,221,842 B1.

Goldspink, P. H. and Goldspink, G. (2003). The expression and role of the IGF-1 splice variant (MGF) in cardiac muscle. *Journal of Muscle Research and Cell Motility*, **24**, 341.

Grounds, M. D., Garrett, K. L., Lai, M. C., Wright, W. E. and Beilharz, M. W. (1992). Identification of skeletal muscle precursor cells in vivo by use of MyoD1 and myogenin probes, *Cell and Tissue Research*, **267**, 99-104.

Grounds, M. D. (1998). Age-associated changes in the response of skeletal muscle cells to exercise and regeneration. *Annual New York Academy of Sciences*, **854**, 78-91.

Gussoni, E., Soneoka, Y., Strickland, C. D., Buzney, E. A., Khan, M. K., Flint, A. F., Kunkel, L. M. and Mulligan, R, C. (1999). Dystrophin expression in the *mdx* mouse restored by stem cell transplantation. *Nature*, **401**, 390-394.

Guth, L. and Samaha, F. J. (1970). Procedure for histochemical demonstration of actomyosin ATPase. *Experimental Neurology*, **28**, 365-367.

Handsforth, D. P. (1962). Isoproterenol-induced myocardial infarction in animals. *Archives of Pathology*, **73**, 161-165.

Harris, J. B., Johnson, M. A. and Karlsson, E. (1975). Pathological responses of rat skeletal muscle to a single subcutaneous injection of a toxin isolated from the venom of the Australian tiger snake, *Notechis scutatus scutatus*. *Clinical and Experimental Pharmacology and Physiology*, **2**, 383-404.

Hawke, T. J. and Garry, D. J. (2001). Myogenic satellite cells: Physiology to molecular biology. *Journal of Applied Physiology,* **91,** 534-551.

Heap, S. J., Hudlicka, O. and Okyayuz-Baklouti, I. (1996). Isoprenaline-induced damage in cardiac and skeletal muscle: Interaction with methylxanthines. *Drug Development Research*, **37**, 249-258.

Hill, M. and Goldspink, G. (2003). Expression and splicing of the insulin-like growth factor gene in rodent muscle is associated with muscle satellite cell (stem) cell activation following local tissue damage. *Journal of Physiology*, **549**, 409-418.

Hill, M., Wernig, A. and Goldspink, G. (2003). Muscle satellite (stem) cell activation during local tissue injury and repair. *Journal of Anatomy*, **203**, 89-99.

Hiraoka, M. (2002). Modulation of electrical properties by ions, hormones and drugs. In *Handbook of Physiology. Section 2. The Cardiovascular System. Volume I. The Heart* (Eds. E. Page, H. A. Fozzard, R. J. Solaro), pp 595-653. New York: Oxford University Press.

Hoak, J. C., Warner, E. D. and Connor, W. E. (1969). New concept of levarterenol-induced acute myocardial necrosis. *Archives of Pathology*, **87**, 332-338.

Holly, T. A., Drincic, A., Byun, Y., Nakamura, S., Harris, K., Klocke, F. J. and Cryns, V. L. (1999). Caspase inhibition reduces myocyte cell death induced by myocardial ischemia and reperfusion *in vivo*. *Journal of Molecular and Cellular Cardiology*, **31**, 1709–1715.

Horak, A. R. and Opie, L. H. (1983). Energy metabolism of the heart in catecholamine-induced myocardial injury. In *Advances in Myocardiology, Volume 4* (Eds. E. Chazov, V. Saks, G, Rona), pp 23-43.

Hughes, S. M., Cho, M., Karsch-Mizrachi, I., Travis, M., Silberstein, L., Leinwand, L. A. and Blau, H. M. (1993). Three slow myosin heavy chains sequentially expressed in developing mammalian skeletal muscle. *Developmental Biology,* **158,** 183-199.

Hunt, S. A., Baker, D. W., Chin, M. H., Cinquegrani, M. P., Feldmanmd, A. M., Francis, G. S., Ganiats, T. G., Goldstein, S., Gregoratos, G., Jessup, M. L., Noble, R. J., Packer, M., Silver, M. A., Stevenson, L. W., Gibbons, R. J., Antman, E. M., Alpert, J. S., Faxon, D. P., Fuster, V., Gregoratos, G., Jacobs, A. K., Hiratzka, L. F., Russell, R. O. and Smith, S. C. Jr. (2001). ACC/AHA Guidelines for the Evaluation and Management of Chronic Heart Failure in the Adult: Executive Summary A Report of the American College of Cardiology/American Heart Association Task Force on Practice Guidelines: Developed in Collaboration With the International Society for Heart and Lung Transplantation; Endorsed by the Heart Failure Society of America. *Circulation*, **104**, 2996-3007.

Irintchev, A., Zeschnigk, M., Starzinski-Powitz, A. and Wernig, A. (1994). Expression pattern of M-cadherin in normal, denervated and regenerating mouse muscles. *Developmental Dynamics,* **199,** 326-337.

Ishii, K., Zhai, W. G., Akita, M. (1998). Effects of isoproterenol on the orbicularis oculi and stapedius muscles. *Journal of Otorhinolaryngol Relat Spec*, **60**, 98-102.

Ito, H., Hiroe, M., Hirata, Y., Tsujino, M., Adachi, S., Schichiri, M., Koike, A., Nogami, A. and Marumo, F. (1993). Insulin-like growth factor-I induces hypertrophy with enhanced expression of muscle specific genes in cultured rat cardiomyocytes. *Circulation*, **87**, 1715-1721.

Iwanaga, Y., Hoshijima, M., Gu, Y., Iwatate, M., Dieterie, T., Ikeda, Y., Date, M., Chrast, J., Matsuzaki, M., Peterson, K. L., Chien, K. R. and Ross, J. Jr. (2004). Chronic phospholamban inhibition prevents progressive cardiac dysfunction and pathological remodeling after infarction in rats. *The Journal of Clinical Investigation*, **113**, 727-736.

Iwase, M., Uechi, M., Vatner, D. E., Asia, K., Shannon, R. P., Kudej, R. K., Wagner, T. E., Wight, D. C., Patrick, T. A., Ishikawa, Y., Homcy, C. J. and Vatner, S. F. (1997). Cardiomyopathy induced by cardiac $G_{s\alpha}$ overexpression. *American Journal of Physiology*, **272**, H585-589.

Jahns, R., Boivin, V., Hein, L., Triebel, S., Angermann, C. E., Ertl, G. and Lohse, M. J. (2004). Direct evidence for a β_1-adrenergic receptor–directed autoimmune attack as a cause of idiopathic dilated cardiomyopathy. *Journal of Clinical Investigation*, **113**, 1419-1429.

Jankowski, R. J., Deasy, B. M., Cao, B., Gates, C. and Huard, J. (2002). The role of CD34 expression and cellular fusion in the regeneration capacity of myogenic progenitor cells. *Journal of Cell Science*, **115**, 4361-4374.

Jayaraman, T and Marks, A. R. (1997). T cells deficient in inositol 1,4,5-trisphosphate receptor are resistant to apoptosis. *Molecular and Cellular Biology*, **17**, 3005-3012.

Jensen, J., Brors, O. and Dahl, H. A. (1995). Different β-adrenergic receptor density in different rat skeletal muscle fibre types. *Pharmacology and Toxicology,* **76,** 380-385.

Jones, D. A. and Round, J. M. (1990). *Skeletal muscle in health and disease.* Manchester: Manchester University Press.

Kadi, F. and Thornell, L. E. (2000). Concomitant increases in myonuclear and satellite cell content in female trapezius muscle following strength training. *Histochemistry and Cell Biology*, 113, 99-103.

Kajstura, J., Zhang, X., Reiss, K., Szoke, E., Li, P., Lgrasta, C., Cheng, W., Darzynkiewicz, Z., Olivetti, G. and Anversa, P. (1994). Myocyte cellular hyperplasia and myocyte cellular hypertrophy contribute to chronic ventricular remodeling in coronary artery narrowing-induced cardiomyopathy in rats. *Circulation Research*, **74**, 383-400.

Kajstura, J., Zhang, X., Liu, Y., Szoke, E., Cheng, W., Olivetti, G., Hintze, T. H. and Anversa, P. (1995). The cellular basis of pacing-induced dilated cardiomyopathy. Myocyte cell loss and myocyte cellular reactive hypertrophy. *Circulation*, **92**, 2306-17.

Kajstura, J., Cheng, W., Sarangarajan, R., Baosheng, P. L., Li, B., Nitahara, J. A., Chapnick, S., Reiss, K., Olivetti, G. and Anversa, P. (1996). Necrotic and apoptotic myocyte death in the aging heart of Fischer 344 rats. American Journal of Physiology, 40, H1215-H1228.

Kajstura, J., Leri, A., Finato, N., Di Loreto, C., Beltrami, C. A. and Anversa, P. (1998). Myocyte proliferation in end-stage cardiac failure in humans. *Proceedings of the National Academy of Sciences USA*, **95**, 8801-8805.

Kang, H-J., Kim, H-S., Zhang, S-Y., Park, K-W., Cho, H-J., Koo, B-K., Kim, Y-J., Lee, D. S., Sohn, D-W., Han, K-S., Oh, B-H., Lee, M-M. and Park, Y-B. (2004). *Effects of intracoronary* infusion of peripheral blood stem cells mobilized with granulocyte-colony stimulating factor *on left ventricular* systolic function and restenosis after coronary stenting in myocardial infarction: *the magic cell* randomized clinical trail. *The Lancet*, **363**, 751-756.

Kang, P. M. and Izumo, S. (2003). Apoptosis in heart: basic mechanisms and implications in cardiovascular disease. *Trends in Molecular Medicine*, **9**, 177 - 182.

Kanoh, M., Takemura, G., Misao, J., Hayakawa, Y., Aoyama, T., Nishikagi, K., Noda, T., Fujiwara, T., Fukuda, K., Minatogutchi S. and Fujiwara, H. (1999). Significance of myocytes with positive DNA in situ nick end-labeling (TUNEL) in hearts with dilated cardiomyopathy. Not apoptosis but DNA repair. *Circulation*, **99**, 2757–2764

Karoor, V., Vatner, S. F., Takagi, G., Yang, G., Thaisz, J., Sadoshima, J. and Vatner, D. E. (2004). Propanolol prevents enhanced stress signalling in $G_{s\alpha}$ cardiomyopathy: Potential mechanism for β-blockade in heart failure. *Journal of Molecular and Cellular Cardiology*, **36**, 305-312.

Katz, A. M. (2001). *Physiology of the Heart*. London: Lippincott Williams & Wilkins.

Kerr, F. R., Winterford, C. M. and Harmon, B. V. (1994). Apoptosis: its significance in cancer and cancer therapy. *Cancer*, **73**, 2013–2026.

Kjekshus, J. K. (1975). The role of free fatty acid (FFA) in catecholamine-induced cardiac necrosis. In *Recent advances in studies on cardiac structure and metabolism. Pathophysiology and morphology of myocardial cell alterations, Volume 6* (Eds. A. Fleckenstein, G. Rona), pp 183-191. Baltimore: University Park Press.

Koglin, J., Granville, D. J., Glysing-Jensen, T., Mudgett, J. S., Carthy, C. M., McManus, B. M. and Russell, M. E. (1999). Attenuated acute cardiac rejection in NOS2 -/- recipients correlates with reduced apoptosis. *Circulation*, **99**, 836-42.

Koishi, K., Zhang, M., McLennan, I. S. and Harris, A. J. (1995). MyoD protein accumulates in satellite cells and is neurally regulated in regenerating myotubes and skeletal muscle fibers. *Developmental Dynamics,* **202,** 244-254.

Koizumi, S. Lipp, P., Berridge, M. J. and Bootman, M. D. (1999). Regulation of Ryanodine Receptor Opening by Lumenal Ca2+ Underlies Quantal Ca2+ Release in PC12 Cells. *Journal of Biological Chemistry*, **274**, 33327-33333.

Kudej, R. K., Iwase, M., Uechi, M., Vatner, D. E., Oka, N., Ishikawa, Y., Shannon, R. P., Bishop, S. P. and Vatner, S. E. (1997). Effects of chronic β-adrenergic receptor stimulation in mice. *Journal of Molecular and Cellular Cardiology*, **29**, 2735-2746.

Kumar, S., Sharma, S. and Katoch, S. S. (2003). Early onset of the maximum protein anabolic effect induced by isoproterenol in chick skeletal and cardiac muscle. *Acta Physiol Hung*, **90**, 57-67.

LaBarge, M. A and Blau, H. M. (2002). Biological progression from adult bone marrow to mononucleate muscle stem cell to multinucleate muscle fiber in response to injury. *Cell*, **111**, 589-601.

LaFlamme, M. A., Myerson, D., Saffitz, J. E. and Murry, C. E. (2002). Evidence for cardiomyocyte repopulation by extracardiac progenitors in transplanted human hearts. *Circulation Research*, **90**, 634-640.

Leist, M. and Jaattela, M. (2001). Four deaths and a funeral: from caspases to alternative mechanisms. *Nature Reviews: Molecular and cellular biology*, **2**, 589-598.

Lemasters, J. J., Qian, T., He, L., Kim, J-S, Elmore, S. P., Cascio, W. E. and Brenner, D. A. (2002). Role of mitochondrial inner membrane permeabilisation in necrotic cell death, apoptosis and autophagy. *Anti-oxidant Redox Signal*, **4**, 769-781.

Lohse, M. J., Engelhardt, S. and Eschenhagen, T. (2003). What is the role of β-adrenergic signaling in heart failure? *Circulation Research*, **93**, 896-906.

Lowes, B. D., Gilbert, E. M., Abraham, W. T., Minobe, W. A., Larrabee, P., Ferguson, D., Wolfel, E. E., Lindenfeld, J., Tsvetkova, T., Robertson, A. D., Quaife, R. A. and Bristow, M. R. (2002). Myocardial gene expression in dilated cardiomyopathy treated with β-blocking agents. *New England Journal of Medicine*, **346**, 1357–1365.

Mann, D. L., Kent, R. L., Parsons, B. and Cooper, G. (1992). Adrenergic effects on the biology of the adult mammalian cardiocyte. *Circulation*, **85**, 790-804.

Manjo, G. and Joris, I. (1995). Apoptosis, Oncosis, and Necrosis: An overview of cell death. *American Journal of Pathology*, **146**, 3-15.

Martin, W. H., Murphree, S. S. and Saffitz, J. E. (1989). β-Adrenergic receptor distribution among muscle fibre types and resistance arterioles of white, red and intermediate skeletal muscle. *Circulation Research*, **64**, 1096-1105.

Matsuura, K., Nagai, T., Nishigaki, N., Oyama, T., Nishi, J., Wada, H., Sano, M., Toko, H., Akazawa, H., Sato, T., Nakaya, H., Kasanuki, H. and Komuro, I. (2004). Adult cardiac Sca-1-positive cells differentiate into beating cardiomyocytes. *Journal of Biological Chemistry*, **279**, 11384-11391.

Marx, S. O., Reiken, S., Hisamatsu, Y., Jayaraman, T., Burkhoff, D., Rosemblit, N., Marks, A. R. (2000). PKA phosphorylation dissociates FKBP12.6 from the calcium release channel (ryanodine receptor): Defective regulation in failing hearts. *Cell*, **101**, 365-376.

Mauro, A. (1961) Satellite cell of skeletal muscle fibers. *Journal of Biophysics, Biochemistry and Cytology*, **9**, 493-495.

McArdle, A., Vasilaki, A. and Jackson, M. (2002). Exercise and skeletal muscle ageing: Cellular and molecular mechanisms. *Ageing Research Reviews*, **1**, 79-93.

McKinney-Freeman, S. L., Jackson, K. A., Camargo, F. D., Ferrari, G., Mavilio, F. and Goodell, M. A. (2002). Muscle-derived hematopoietic stem cells are hematopoietic in origin. *Proceedings of the National Academy of Sciences*, **99**, 1341-1346.

Menasche, P., Hagege, A. A., Vilquin, J-T., Desnos, M., Abergel, E., Pouzet, B., Bel, A., Sarateanu, S., Scorsin, M., Schwartz, K., Bruneval, P., Benbunan, M., Marolleau, J-P. and Duboc, D. (2003). Autologous skeletal myoblast transplantation for severe postinfarction left ventricular dysfunction. *Journal of American College of Cardiology*, **41**, 1078-83.

Mendez, J. and Keys, A. (1960). Density and composition of mammalian muscle. *Metabolism*, **9**, 184-188.

Miller, K. J., Thaloor, D., Matteson, S. and Pavlath, G. K. (2000). Hepatocyte growth factor affects satellite cell activation and differentiation in regenerating skeletal muscle. *American Journal of Physiology*, **278**, C174-C181.

Minotti, J. R., Christoph, I., Oka, R., Weiner, M. W., Wells, L. and Massie, B. M. (1991). Impaired skeletal muscle function in patients with congestive heart failure. *The Journal of Clinical Investigation,* **88,** 2077-2082.

Morisco, C., Zebrowski, D. C., Vatner, D. E., Vatner, S. F. and Sadoshima, J. (2001). β-Adrenergic cardiac hypertrophy is mediated primarily by the β_1-subtype in the rat heart. *Journal of Molecular and Cellular Cardiology*. **33**, 561-573.

Mosinger, B., Stejskal, J. and Mosinger, B. Jr. (1977). Heart infarction-like effect induced by natural catecholamines *in vitro*. *Experimental Pathology*, **14**, 157-161.

Mummery, C., Ward-Van Oostwaard, D., Doevendans, P., Spijker, R., van den Brink, S., Hassink, R., van der Heyden, M., Opthof, T., Pera, M., Brutel de la Riviere, A., Passier, R. and Tertoolen, L. (2003). Differentiation of human embryonic stem cells to cardiomyocytes: Role of co-culture with visceral endoderm-like cells. *Circulation*, **107**, 2733-2740.

Murry, C. E., Soonpaa, M. H., Reinecke, H., Nakajima, H., Nakajima, H. O., Rubart, M., Pasumarthi, K. B. S., Virag, J. I., Bartelmez, S. H., Poppa, V., Bradford, G., Dowell, J. D., Williams, D. A. and Field, L. J. (2004). Haematopoietic stem cells do not transdifferentiate into cardiac myocytes in myocardial infarcts. *Nature*, **428**, 664-8

Musaro, A., McCullagh, K., Paul, A., Houghton, L., Dobrowolny, G., Molinaro, M., Barton, E. R., Sweeney, H. L. and Rosenthal, N. (2001). Localized IGF-1 transgene expression sustains hypertrophy and regeneration in senescent skeletal muscle. *Nature Genetics*, **27**, 195-200.

Nachlas, M., Tsou, K. C., Desouza, E., Cheung, C. C. and Seligman, A. M. (1957). Cytochemical demonstration of SDH by the use of a new p-Nitrophenyl substituted dietrazole. *Journal of Histochemistry and Cytochemistry,* **5,** 420-436.

Nadal-Ginard, B., Kajstura, J., Leri, A., Anversa, P. (2003). Myocyte death, growth, and regeneration in cardiac hypertrophy and failure. *Circulation Research*, **92**, 139-50.

Narusawa, M., Fitzsimons, R. B., Izumo, S., Nadal-Ginard, B., Rubinstein, N. A. and Kelly, A. M. (1987). Slow myosin in developing rat skeletal muscle. *The Journal of Cell Biology,* **104,** 447-459.

Nemeth, P. and Pette, D. (1981). Succinate dehydrogenase activity in fibres classified by myosin ATPase in three hind limb muscles of the rat. *Journal of Physiology,* **320,** 73-80.

Ng, Y., Goldspink, D. F., Burniston, J. G., Clark, W. A., Colyer, J. C. and Tan, L. B. (2002). Characterisation of isoprenaline myotoxicity on slow-twitch skeletal versus cardiac muscle. *International Journal of Cardiology,* **86,** 299-309.

Nicholson, D. W, and Thornberry, N. A. (1997). Caspases, killer proteases. *Trends in Biochemical Science*, **22**, 299–306.

Nolan, A. C., Clark, W. A. Jr., Karwoski, T. and Zak, R. (1983). Patterns of cellular injury in myocardial ischemia determined by monoclonal antimyosin. *Proceedings of the National Academy of Sciences USA*, **80**, 6046-50.

Nygren, J. M., Jovinge, S., Breitbach, M., Sawen, p., Roll, W., Hescheler, J., Taneera, J., Fleischmann, B. K. and Jacobsen, S. E. W. (2004). Bone marrow-derived hematopoietic cells can generate cardiomyocytes at a low frequency through cell fusion but not transdifferentiation. *Nature Medicine*, **10**, 494-501.

Oh, H., Bradfute, S. B., Gallardo, T. D., Nakamura, T., Gaussin, V., Mishina, Y., Pocius, J., Michael, L. H., Behringer, R. R., Garry, D. J., Entman, M. L. and Schneider, M. D. (2003). Cardiac progenitor cells from adult myocardium: Homing, differentiation, and fusion after infarction. *Proceedings of the National Academy of Sciences U S A*, **100**, 12313-12318.

Olivetti, G., Quaini, F., Sala, R., Lagrasta, C., Corradi, D., Bonacina, E., Gambert, S. R., Cigola, E. and Anversa P. (1996). Acute myocardial infarction in humans is associated with activation of programmed myocyte cell death in the surviving portion of the heart. *Journal of Molecular Cell Cardiology*, **28**, 2005-16.

Olivetti, G., Abbi, R., Quaini, F., Kajstura, J., Cheng, W., Nitahara, J. A., Quaini, E., Di Loreto, C., Beltrami, C. A., Krajewski, S., Reed, J. C. and Anversa, P. (1997). Apoptosis in the failing human heart. *New England Journal of Medicine*, **336**, 1131-41.

Opasich, C., Ambrosino, N., Felicetti, G., Aquilani, R., Pasini, E., Bergitto, D., Mazza, A., Cobelli, F. and Tavazzi, L. (1999). Heart-failure related myopathy: Clinical and physiological insights. *European Heart Journal,* **20,** 1191-1200.

Opie, L. H. (2001). Mechanisms of cardiac contraction and relaxation. In *Heart Disease: A Textbook of Cardiovascular Medicine, Volume 1* (Eds. E. Braunwald, D. P. Zipes, P. Libby), pp 443-478. London: W. Saunders Company.

Orlic, D., Kajstura, J., Chimenti, S., Jakoniuk, I., Anderson, S. M., Li, B., Pickel, J., McKay, R., Nadal-Ginard, B., Bodine, D. M., Leri, A. and Anversa, P. (2001a). Bone marrow cells regenerate infarcted myocardium. *Nature*, **410**, 701-705.

Orlic, D., Kajstura, J., Chimenti, S., Limana, F., Jakoniuk, I., Quaini, F., Nadal-Ginard, B., Bodine, D. M., Leri, A. and Anversa, P. (2001b). Mobilized bone marrow cells repair the infarcted heart, improving function and survival. *Proceedings of the National Academy of Sciences*, **98**, 10344-10349.

Overy, H. R. and Priest, R. E. (1966). Mitotic cell division in postnatal cardiac growth. *Laboratory Investigation*, **15**, 1100-1103.

Packer, M. (1992). The neurohormonal hypothesis: a theory to explain the mechanism of disease progression in heart failure. *Journal of the American College of Cardiology*, **20**, 248-254.

Pavlath, G. K., Thaloor, D., Rando, T. A., Cheong, M., English, A. W. and Zheng, B. (1998). Heterogeneity among muscle precursor cells in adult skeletal muscles with differing regenerative capacities. *Developmental Dynamics*, **212**, 495-508.

Perin, E. C., Dohmann, H. F. R., Borojevic, R., Silva, S. A., Sousa, A. L. S., Mesquita, C. T., Rossi, M. I. D., Carvalho, A. C., Dutra, H. S., Dohmann, H. J. F., Silva, G. V., Belem, L., Vivacqua, R., Rangel, F. O. D., Esporcatte, R., Geng, Y. J., Vaughn, W. K., Assad, J. A. R., Mesquita, E. T. and Willerson, J. T. (2003). Transendocardial autologous bone marrow cell transplantation for severe chronic ischemic heart failure. *Circulation*, **107**, 2294-2302.

Primeau, A. J., Adhihetty, P. J. and Hood, D. A. (2002). Apoptosis in heart and skeletal muscle. *Canadian Journal of Applied Physiology*, **27**, 349-95.

Putman, C. T., Sultan, K. R., Wassmer, T., Bamford, J. A., Skorjanc, D. and Pette, D. (2001). Fiber-type transitions and satellite cell activation in low-frequency-stimulated muscles of young and aging rats. *Journal of Gerontology*, **56A**, B510-B519.

Quaini, F., Urbanek, K., Beltrami, A. P., Finato, N., Beltrami, C. A., Nadal-Ginard, B., Kajstura, J., Leri, A. and Anversa, P. (2002). Chimerism of the transplanted heart. *New England Journal of Medicine*, **346**, 5-15.

Qu-Petersen, Z., Deasy, B., Jankowski, R., Ikezawa, M., Cummins, J., Pruchnic, R., Mytinger, J., Cao, B., Gates, C., Wernig, A. and Huard, J. (2002). Identification of a novel population of muscle stem cells in mice: Potential for muscle regeneration. *Journal of Cell Biology*, **157**, 851-864.

Rabinovsky, E. D., Gelir, E., Gelir, S., Lui, H., Kattash, M., Demayo, F. J., Shenaq, S. M. and Schwartz, R. J. (2003). Targeted expression of IGF-1 transgene to skeletal muscle accelerates muscle and motor neuron regeneration. *FASEB*, **17**, 53-55.

Ranatunga, K. W. and Thomas, P. E. (1990). Correlation between shortening velocity, force-velocity relation and histochemical fibre-type composition in rat muscles. *Journal of Muscle Research and Cell Motility*, **11**, 240-250.

Reiken, S., Gaburjakova, M., Guatimosim, S., Gomez, A. M., D'Armiento, J., Burkhoff, D., Wang, J., Vassort, G., Lederer, W. J., Marks, A. R. (2003). Protein kinase A phosphorylation of the cardiac calcium release channel (ryanodine receptor) in normal and failing hearts. *Journal of Biological Chemistry*, **278**, 444-453.

Reimann, J., Irintchev, A. and Wernig, A. (2000). Regenerative capacity and number of satellite cells in soleus muscles of normal and *mdx* mice. *Neuromuscular Disorders*, **10**, 276-282.

Reiss, K., Cheng, W., Ferber, A., Kajstura, J., Li, P., Li, B., Olivetti, G., Homcy, C. J., Baserga, R. and Anversa, P. (1996). Overexpression of insulin-like growth factor-1 in the heart is coupled with myocyte proliferation in transgenic mice. *Proceedings of the National Academy of Sciences USA*, **93**, 8630-8635.

Renault, V., Thorne, L. E., Eriksson, P. O., Butler-Browne, G. and Mouly, V. (2002). Regenerative potential of human skeletal muscle during aging. *Aging Cell*, **1**, 132-139.

Rona, G. (1985). Catecholamine Cardiotoxity. *Journal of Molecular and Cellular Cardiology*, **17**, 291-306.

Rona, G., Chappel, C. I., Balazs, T. and Gaudry, R. (1959). An infarct-like myocardial lesion and other toxic manifestations produced by isoproterenol in the rat. *A. M. A. Archives of Pathology*, **67**, 99-111.

Ruest, L. B., Khalyfa, A. and Wang, E. (2002). Development-dependent disappearance of caspase-3 in skeletal muscle is post-transcriptionally regulated. *Journal of Cellular Biochemistry*, **86**, 21-28.

Rumyanstev, P. P. (1991). Replicative behaviour of different types of cardiomyocytes in terms of experimental conditions, age and systemic position of animals. In *The Development and Regenerative Potential of Cardiac Muscle* (Eds J. O. Oberpriller, J. C. Oberpriller, A. Mauro), pp 81 – 92. New York: Harwood Academy.

Rupp, H., Dhalla, K. S. and Dhalla, N. S. (1994). Mechanisms of cardiac cell damage due to catecholamines: significance of drugs regulating central sympathetic outflow. *Journal of Cardiovascular Pharmacology,* **24,** S16-24.

Ryall, J. G., Plant, D. R., Gregorevic, P., Sillence, M. N. and Lynch, G. S. (2003). β_2-agonist administration reverses muscle wasting and improves muscle function in aged rats. *Journal of Physiology*, **555,** 175-188.

Sadeh, M., Czyzewski, K. and Stern, L. Z. (1985). Chronic myopathy induced by repeated bupivacaine injections. *Journal of Neurological Sciences,* **67,** 229-238.

Saraste, A. and Pulkki, K. (2000). Morphologic and biochemical hallmarks of apoptosis. *Cardiovascular Research*, **45,** 528-537.

Sattler, M., Liang, H., Nettesheim, D., Meadows, R. P., Harlan, J. E., Eberstadt, M., Yoon, H. S., Shuker, S. B., Chang, B. S., Minn, A. J., Thompson, C. B. and Fesik, S. W. (1997). Structure of Bcl-xL-Bak peptide complex: recognition between regulators of apoptosis. *Science*, **275,** 983–986.

Schiaffino, S., Gorza, l., Sartore, S., Saggin, l., Ausoni, S., Vianello, M., Gundersen, K. and Lomo, T. (1989). Three myosin heavy chain isoforms in type 2 skeletal muscle fibres. *Journal of Muscle Research and Cell Motility,* **10,** 197-205.

Schlaich, M. P., Kaye, D. M., Lambert, E., Sommerville, M., Socratous, F. and Esler, M. D. (2003). Relation between cardiac sympathetic activity and hypertensive left ventricular hypertrophy. *Circulation*, **108,** 560-565.

Schlutz, E. (1996). Satellite cell proliferative compartments in growing skeletal muscles. *Developmental Biology*, **175,** 84-94.

Schlutz, E. and Lipton, B. H. (1982). Skeletal muscle satellite cells: Changes in proliferation potential with age. *Mechanical Ageing Development*, **20,** 377-383.

Schmalbruch, H. and Hellhammer, U. (1977). The number of nuclei in adult rat muscles with special reference to satellite cells. *Anatomical Record*, **189,** 169-175.

Schmalbruch, H. and Lewis, D. M. (2000). Dynamics of nuclei of muscle fibers and connective tissue cells in normal and denervated rat muscles. *Muscle Nerve*, **23,** 617-626.

Seale, P., Sabourin, L. A., Girgis-Gabardo, A., Mansouri, A., Gruss, P. and Rudnicki, M. A. (2000). *Pax7 is* required for the specification of myogenic satellite cells. *Cell*, **102,** 777-786.

Shizukuda, Y., Buttrick, P. M., Geenen, D. L., Borczuk, A. C., Kitsis, R. N. and Sonnenblick, E. H. (1998). β-Adrenergic stimulation causes apoptosis: Influence of tachycardia and hypertrophy. *American Journal of Physiology*, **275**, H961-H968.

Simmerman, H. K. and Jones, L. R. (1998). Phospholamban: protein structure, mechanism of action, and role in cardiac function. *Physiological Reviews*, **78**, 921-947.

Siwik, D. A., Tzortzis, J. D., Pimental, D. R., Chang, D. L., Pagano, P. J., Singh, K., Sawyer, D. B. and Colucci W. S. (1999). Inhibition of copper-zinc superoxide dismutase induces cell growth, hypertrophic phenotype, and apoptosis in neonatal rat cardiac myocytes in vitro. *Circulation Research*, **85**, 147-53.

Song, Q., Young, K. B., Chu, G., Gulick, J., Gerst, M., Grupp, I. L., Robbins, J. and Kranias, E. G. (2004). Overexpression of phospholamban in slow-twitch skeletal muscle is associated with depressed contractile function and muscle remodeling. *FASEB Journal*, **18**, 974-976.

Soonpaa, M. H. and Field, L. J. (1994). Assessment of cardiomyocyte DNA synthesis during hypertrophy in adult mice. *American Journal of Physiology*, **266**, H1439-H1445.

Spradling, A., Drummond-Barbosa, D. and Kai, T. (2001). Stem cells find their niche. *Nature*, **414**, 98–104.

Sugden, P.H. and Clerk, A. (1998). "Stress-responsive" mitogen-activated protein kinases (c-Jun N-terminal kinases and p38 mitogen-activated protein kinases) in the myocardium. *Circulation Research*, **83**, 345-52.

Sweat, F., Puchtler, H., Rosenthal, S. I. (1964). Sirius Red F3BA as a stain for connective tissue. *Archives of Pathology*, **78**, 69-72.

Syntichaki, P. and Tavernarakis, N. (2002). Death by necrosis: Uncontrollable catastrophe, or is there order behind the chaos. *EMBO reports*, **3**, 604-609.

Tambara, K., Sakakibara, Y., Sakaguchi, G., Lu, F., Premaratne, G. U., Lin, X., Nishimura, K. and Komeda, M. (2003). Transplanted skeletal myoblasts can fully regenerate the infarcted myocardium when they survive in the host in large numbers. *Circulation*, **108 (Suppl II)**, II-259-II-263.

Tatsumi, R., Anderson, J. E., Nevoret, C. J., Halevy, O. and Allen, R. E. (1998). HGF/SF is present in normal adult skeletal muscle and is capable of activating satellite cells. *Developmental Biology*, **194**, 114-128.

Teerlink, J. R., Pfeffer, J. M. and Pfeffer, M. A. (1994). Progressive ventricular remodelling in response to diffuse isoproterenol-induced myocardial necrosis in rats. *Circulation Research,* **75**, 105-113.

Thompson, R. B., Emani, S. M., Davis, B. H., Van den Bos, E. J., Morimoto, Y., Craig, D., Glower, D. and Taylor, D. A. (2003). Comparison of intracardiac transplantation: Autologous skeletal myoblasts versus bone marrow cells. *Circulation*, **108 (Suppl II)**, II-262-II-271.

Tidball, J. G. (1995). Inflammatory cell response to acute muscle injury. *Medicine and Science in Sport and Exercise*, **27**, 1022-1032.

Todd, G. L., Cullan, G. E. and Cullan, G. M. (1980). Isoproterenol-induced myocardial necrosis and membrane permeability alterations in the isolated perfused rabbit heart. *Experimental and Molecular Pathology*, **33**, 43-54.

Torella, D., Rota, M., Nurzynska, D., Musso, E., Monsen, A., Shiraishi, I., Zias, E., Walsh, K., Rosenzweig, A., Sussman, M. A., Urbanek, K., Nadal-Ginard, B., Kajstura, J., Anversa, P., Leri, A. (2004). Cardiac stem cell and myocyte aging, heart failure, and insulin-like growth factor-1 overexpression. *Circulation Research*, **94**, 514-24.

Torrente, Y., Tremblay, J-P., Pisati, F., Belicchi, M., Rossi, B., Sironi, M., Fortunato, F., El Fahime, M., Grazia D'Angelo, M., Caron, N. J., Constantin, G., Paulin, D., Scarlato, G. and Bresolin, N. (2001). Intraarterial injection of muscle-derived $CD34^{+}Sca\text{-}1^{+}$ stem cells restores dystrophin in *mdx* mice. *Journal of Cell Biology*, **152**, 335-348.

Ungerer, M., Bohm, M., Elce, J. S., Erdmann, E., Lohse, M. J. (1993). Altered expression of β-adrenergic receptor kinase and β_1-adrenergic receptors in the failing human heart. *Circulation*, **87**, 454–463.

Urbanek, K., Quaini, F., Tasca, G., Torella, D., Castaldo, C., Nadal-Ginard, B., Leri, A., Kajstura, J., Quaini, E., Anversa, P. (2003). Intense myocyte formation from cardiac stem cells in human cardiac hypertrophy. *Proceedings of the National Academy of Sciences U S A*, **100**, 10440-5.

Vatner, D. E., Asai, K., Iwase, M., Ishikawa, Y., Wagner, T. E., Shannon, R. P., Homcy, C. J. and Vatner, S. F. (1998). Overexpression of myocardial $G_{s\alpha}$ prevents full expression of catecholamine desensitization despite increased β-adrenergic receptor kinase. *Journal of Clinical Investigation*, **101**, 1916-1922.

Vatner, D. E., Asai, K., Iwase, M., Ishikawa, Y., Shannon, R. P., Homcy, C. J. and Vatner, S. F. (1999). Beta-adrenergic receptor-G protein-adenylyl cyclase signal transduction in the failing heart. *American Journal of Cardiology*, **83**, 80H-85H.

Waagstein, F., Hjalmarson, A., Varnauskas, E. and Wallentin, I. (1975). Effect of chronic β-adrenergic receptor blockade in congestive cardiomyopathy. *British Heart Journal*, **37**, 1022–1036.

Wanek, L. J. and Snow, M. H. (2000). Activity-induced fiber regeneration in rat soleus muscle. *The Anatomical Record,* **258,** 176-185.

Wehrens, X. H. T. and Marks, A. R. (2003). Altered function and regulation of cardiac ryanodine receptors in cardiac disease. *Trends in Biochemical Sciences*, **28,** 671-678.

Whalen, R. G., Harris, J. B., Butler-Browne, G. S. and Sesodia, S. (1990). Expression of myosin isoforms during notexin-induced regeneration of rat soleus muscle. *Developmental Biology,* **141,** 24-40.

Williams, P., Simpson, H., Kenwright, J., Goldspink, G (2001). Muscle fibre damage and regeneration resulting from surgical limb distraction. *Cells Tissues Organs*, **169,** 395-400.

Wokke, J. H., Van Den Oord, C. J., Leppink, G. J. and Jennekens, F. G. (1989). Perisynaptic satellite cells in human external intercostals muscle: A quantitative and qualitative study. *Anatomical Record*, **223**, 174-180.

www.bhf.org.uk

www.anaesthesiauk.com

Xi, H., Shin, W. S., Suzuki, J-I., Nakajima, T., Kawada, T., Uehara, Y., Nakazawa, M. and Toyo-oka, T. (2000). Dystrophin disruption might be related to myocardial cell apoptosis caused by isoproterenol. *Journal of Cardiovascular Pharmacology*, **36,** S25-S29.

Xu, L and Meissner, G. (1998). Regulation of Cardiac Muscle Ca2+ Release Channel by Sarcoplasmic Reticulum Lumenal Ca2+. *Biophysical Journal*, **75**, 2302-2312.

Yang, S. Y. and Goldspink, G. (2002). Different roles of the IGF-IEc peptide (MGF) and mature IGF-1 in myoblast proliferation and differentiation. *FEBS Letters*, **522,** 156-160.

Yang, Y.-T. and McElligott, M. A. (1989). Multiple actions of β-adrenergic agonists on skeletal muscle and adipose tissue. *Biochemical Journal,* **261,** 1-10.

Yeh, E. T. H., Zhang, S., Wu, H. D., Korbling, M., Willerson, J. T. and Estrov, Z. (2003). Transdifferentiation of human peripheral blood $CD34^{+}$-enriched cell population into cardiomyocytes, endothelial cells, and smooth muscle cells *in vivo*. *Circulation*, **108,** 2070-2073.

Yunge, L., Bruneval, P., Cokay, M. S., Berry, B., Peters, H., Poulsen, R. and Huttner, I. (1989). Perturbation of the sarcolemmal membrane in isoproterenol-induced myocardial injury of the rat. *American Journal of Pathology,* **134,** 171-185.

Zarnegar, R. and Michalopoulos, G. K. (1995). The many faces of hepatocyte growth factor: from hepatopoiesis to hematopoiesis. *Journal of Cell Biology*, **129**, 1177-1180.

Zaugg, M., Xu, W., Lucchinetti, E., Shafiq, S. A., Jamali, N. Z. and Siddiqui, M. A. (2000). Beta-adrenergic receptor sub-types differentially affect apoptosis in adult rat ventricular myocytes. *Circulation*, **102**, 344-50.